University of Southampton

Engineered antibodies in the treatment of B cell lymphoma

Jamie Honeychurch, BSc. (Hons)

Doctor of Philosophy

Department of Immunochemistry
Faculty of Medicine, Health and Biological Sciences

December 2000

UNIVERSITY OF SOUTHAMPTON

ABSTRACT

FACULTY OF MEDICINE, HEALTH AND BIOLOGICAL SCIENCES
DEPARTMENT OF IMMUNOCHEMISTRY

Doctor of Philosophy

Engineered antibodies in the treatment of B cell lymphoma

Jamie Honeychurch BSc. (Hons)

The incidence of lymphoma is rising, now representing 3 % of cancers in the UK alone. Current treatments include chemotherapy and radiotherapy, but whilst significant remission is often observed, responses frequently prove not to be durable. Thus, alternative treatments are sought.

One such alternative is the use of bispecific antibodies (BsAb), which show dual specificity for both a target antigen on the tumor cell, and a cytotoxic trigger molecule on an effector cell. In this way, BsAb are able to directly bridge the two together, and focus an attack against tumor. Which tumor antigens make the most suitable targets, and which immune cells the most effective killers is still being determined.

To further investigate these issues, we have designed a panel of $F(ab')_2$ BsAb against a range of murine B cell lymphoma antigens (idiotype, MHC class II, CD19, CD22 and CD40). We have assessed the relative merits in targeting both T cells and neutrophils against these antigens. In the first case, BsAb were directed towards the CD3 and CD2 molecules of the T cell receptor. In the second, a transgenic mouse was utilised, to investigate the therapeutic potential of targeting G-CSF primed neutrophils via human FcγRI. Extensive analysis of these derivatives both in vitro and in vivo has revealed that it is the nature of the tumor antigen itself that has most bearing on therapy.

This work indicates that effector mechanisms such as antibody-dependent cellular cytotoxicity, whilst certainly contributing to tumor removal, are not sufficient to eradicate the malignant clone. Instead, it appears likely that a combination of growth inhibitory signals, and generation of T cell immunity are more important to successful therapy. In light of this, Ab dimers were produced in an effort to increase the signaling potential of mAb. Following dimerisation, mAb were able to induce growth arrest and cell death in human lymphoma lines, as well as showing increased complement activation. Dimers were also able to protect against in vivo tumor challenge.

The data represented here points to some important considerations for the future design and development of BsAb therapy, and indicates that the nature of the target antigen is critical to therapeutic outcome.

Contents

List of Tables

CHAPTER 1

CHAPTER 3

CHAPTER 4

CHAPTER 7

List of Figures

CHAPTER 1

CHAPTER 3

CHAPTER 4

CHAPTER 6

CHAPTER 7

CHAPTER 8

Acknowledgements

Firstly I would like to thank Martin and Alison, for their excellent supervision and assistance during the course of my study. I would also like to thank all other members of the Tenovus research laboratory who have helped me over this time. In particular, Maureen for the mAb preps, Ruth for help with the FACS, and all the animal technicians, especially Richard, for help with the mice! In addition, I must thank Ingmar and Jan for providing the transgenic mice, and also for their input and advice during the course of the work. Also, Dr Thomas Valerius, not only for helpful advice, but for supplying copious amounts of G-CSF.

Funding was provided by Tenovus Solentside and Tenovus Cardiff.

Special thanks must also go to Mark and Smudge, for all their assistance, and for providing entertainment to brighten up the day!

I must also thank my parents for their encouragement and support, not only through this, but throughout the whole of my education. And, to Tina, a special thank you for always being there, and for making my life complete.

Lastly, to all @ Metalheadz, in particular Goldie, Groove, Fabio, Storm and Kemi (RIP 1999). Much love and respect to you all. Peace through universal beats. Headz for life.

Abbreviations

Ab	Antibody
ADCC	Antibody-dependent cellular cytotoxicity
AML	Acute myelogenous leukaemia
APC	Antigen presenting cell
BCR	B cell receptor
BsAb	Bispecific antibody
C	Constant region
Ca^{2+}	Calcium ion
CC	Cell cycle
CCA	Cell cycle arrest
CDR	Complementarity determining region
CLL	Chronic lymphocytic leukaemia
CTL	Cytotoxic T lymphocyte
DC	Dendritic cell
EGF	Epidermal growth factor
Fab	Fragment antigen binding
Fc	Fragment crystallisable
FcR	Fc receptor
FcRn	Neonatal Fc receptor
FcγR	Fc gamma receptor
G-CSF	Granulocyte colony-stimulating factor
GPI	Glycosyl phosphatidylinositol
H chain	Immunoglobulin heavy chain
H_2O_2	Hydrogen peroxidase
HAMA	Human anti-mouse antibody response
HD	Homodimer
HOCL	Hypochlorous acid
HV	Hypervariable region

Id	Idiotype
IFN-γ	Interferon gamma
Ig	Immunoglobulin
IL	Interleukin
ITAM	Immunoreceptor tyrosine based activation motif
ITIM	Immunoreceptor tyrosine based inhibitory motif
J chain	Joining chain
κ	Kappa (light chain)
L chain	Immunoglobulin light chain
λ	Lambda (light chain)
LTS	Long-term survival
mAb	Monoclonal antibody
MAC	Membrane attack complex
MHC	Major histocompatibility complex
MPO	Myeloid peroxidase
MuG-CSF	Murine G-CSF
NHL	Non-Hogkin's Lymphoma
NK	Natural Killer cell
PAGE	Polyacrylamide gel electrophoresis
PI	Propidium Iodide
pIgR	Polyclonal Ig receptor
PKC	Protein kinase C
PLC	Phospholipase C
PMN	Neutrophil
PTK	Protein tyrosine kinases
RCC	Redirected cellular cytotoxicity
RhG-CSF	Recombinant human G-CSF
RIP	Ribosome inactivating protein
SDS	Sodium dodecyl sulphate
SH2 domain	Src homology-2 domain
TCR	T cell receptor

TNF	Tumor necrosis factor
TRAF	TNF-receptor associated factor
V	Variable region

Chapter 1
Introduction

1.1 General Introduction

Cancer prevalence as a whole has risen over the past few decades, and in the UK alone, Non-Hodgkin's lymphoma (NHL) now represents 3 % of the total cancer incidence, with over 4000 deaths annually (1). Although the pathobiology of NHL is well understood, progress in curative intervention remains slow. Therapeutic strategies for the treatment of lymphoma have traditionally focused on a combination of radio- or chemotherapy, coupled to bone marrow transplantation. These regimens can result in significant disease remission, but responses often prove not to be durable, as tumor cells develop resistance to therapeutic reagents (2). Moreover, clinical application is limited by non-specific toxicity. An alternative approach, and one that is gaining in support, is that of antibody (Ab) therapy.

First described by Kohler and Milstein in 1975 (3), monoclonal antibodies (mAb) are highly specific reagents which can serve as tools to re-direct immune defence mechanisms against malignant cells, potentially triggering processes of antibody-dependent cellular cytotoxicity (ADCC), complement activation, or apoptosis, as a result of effector cell recruitment and activation of various cellular signaling pathways. Alternatively, mAb can function as vehicles to transport immunotoxins or radioisotopes to tumor in a highly selective manner.

However, despite their great potential, the expectations surrounding these Ab have generally not been fulfilled, with only a handful of mAb proving to be clinically effective against lymphoma (4). Much of this failure has been attributed to poor effector recruitment *in vivo*. As an attempt to combat this inefficiency mAb can be engineered into bispecific derivatives. Such bispecific antibodies (BsAb) simultaneously recognise both a target antigen on the tumor cell and a cytotoxic trigger molecule on an effector cell, thus activating and focusing a specific immune response against the malignancy (5).

Whether utilising mAb or BsAb as therapeutic reagents the basic premise remains the same – destruction of tumor through activation of immune mechanisms. Such an approach is not new and has foundations in the theory of immune surveillance first proposed nearly a century ago.

1.2 Immune-surveillance – natural tumor immunity?

The concept of immune-surveillance, in which tumor cells are recognised and eradicated by a natural immune response, was first conceived in the 1900s by Paul Ehrlich. His hypothesis was built on the observation that transplanted tumors were often rejected. However, such experiments were conducted prior to the development of inbred rodent lines, and we now know this rejection not to be an indication of tumor immunity, but rather major histocompatibility complex (MHC) incompatibility. The theory that the immune system can detect and eliminate malignant cells remains. In the 1940's, Thomas and Burnet surmised that tumor eradication was dependent on malignant cells bearing exclusive antigenic determinants that could be recognised by T cells, initiating an immune response (6). Whilst evidence for immune-surveillance against, for example, melanoma exists, many such responses are not tumor immune-surveillance in the purest sense. For example, development of lymphoid tumor in transplant patients frequently correlates to viral transformation, thus, immune responses here are most likely developed to prevent the spread of oncogenic virus, rather than tumor *per se* (7)

It is clear that natural recognition and elimination of malignancy can, and does, take place. However, such processes are often evaded by tumor cells through down-regulation of MHC class I (MHC I) expression, and disruption of peptide processing pathways (8). Macrophages, neutrophils (PMN), and natural killer (NK) cells have all been shown to infiltrate and destroy tumor, but such responses are often too late, or too weak to prevent the progression of disease. Nethertheless, natural effector mechanisms provide a solid basis for immunotherapeutic approaches, which aim to supplement and augment these defence systems.

1.3. Immunotherapy

Strategies for immunotherapy of cancer can be divided in to three broad categories - cellular approaches (such as bone marrow transplant), gene therapy, or the use of protein agents (such as Ab) (discussed in 9). Whilst all merit investigation, our attention shall be turned towards the application of Ab therapeutics.

The development of mAb, first described in the seminal paper by Milstein and Kohler (3) paved the way for Ab-based therapies allowing production of well-defined, highly specific Ab in almost limitless quantities. In the last decade numerous trials have been conducted with mAb either in their native form, modified to carry drugs, toxins and radioisotopes, or engineered to be bispecific (with one arm recognising a tumor antigen and the other an immune effector cell or toxin). A timeline of the major developments in Ab-based immunotherapy is given in Table.1.1. More recently, developments in Ab engineering techniques have been further able to extend their application (10). Many clinical trials were originally conducted with murine Ab, which suffer from problems of immunogenicity. Modern, recombinant technology, allowing production of chimerised (murine variable region, human constant region) or humanised (murine hypervariable regions and human framework regions) Ab to reduce immunogenicity and extend serum half-life are distinctly advantageous. Evolution of such technologies, coupled with an increasing understanding of Ab-effector interactions, and the role that tumor antigens contribute to the immune response allows constant improvement of immunotherapeutic strategies. With several advanced clinical trials now in operation and approval of the IDEC-C2B8 mAb as an agent for cancer therapy in the US (4), it seems that Ab mediated immunotherapy is finally on the way to being recognised as a useful treatment modality.

Central to these developments, and to the future improval of Ab engineering, and application, is our knowledge of immunoglobulin (Ig) structure and function. Before discussing the relative merits and failures of both mAb and BsAb, it is logical therefore that we introduce the basic building block for Ab therapy: the Ig molecule.

Table 1.1 A timeline of antibody based immunotherapy: major developments and landmarks.

A Timeline of Antibody Based Immunotherapy		
1895	Hericourt and Richet	Treated cancer patients with anti-sera raised in dogs and donkeys
1953	Pressman and Korngold	Demonstrated antibodies could be used specifically to target cancer cells
1962	Mandy and Nisonoff	First bispecific $F(ab)_2$ conjugates from rabbit IgG
1975	Kohler and Milstein	Developed monoclonal antibody technology
1979	Nadler et al.	Conducted the first immunotherapy trials with a mAb
1984	Milstein and Cuello	Developed hybrid-hybridoma technology to produce bispecific IgG
1985	Staerz et al.	Demonstrated T cell targeting by heteroconjugates
1988	Reischmann et al.	First therapeutic mAb to be humanised (CAMPATH-1)
1989	Brown et al.	First successful results from clinical trials conducted in patients using anti-Id mAb
1993	Holliger et al.	Recombinant technology for BsAb – Diabodies
1997	Anderson et al.	First mAb to be approved for treatment of cancer in U.S. (IDEC-C2B8; anti-CD20)

1.4 Immunoglobulin Structure

Porter and Edelman deduced the basic structural composition of Ig during the 1950/60s. Working independently, they conceptualised Ig chain structure to be an association of two heavy (H) chains and two light (L) chains, linked by both disulphide and non-covalent bonding. X-ray crystallography and electron microscopy studies have expounded these initial findings, and a cartoon representation of the structure is illustrated overleaf (Figure 1.1).

The Ig molecule is comprised of distinct regions – two identical Fab (fragment antigen binding) arms, and an Fc (fragment crystallisable) tail. IgA, IgE and IgG molecules contain an additional, highly flexible hinge that joins these regions together. Segregation of the antigen and effector binding regions can be achieved through limited enzymatic proteolysis. Digestion with pepsin, which essentially cleaves C terminal to the hinge, yields a $F(ab')_2$ and pFc', the pFc' being the CH3 domain. It is from such $F(ab')_2$ molecules that BsAb can be produced, following reduction and chemical linkage of two heterologous Fab' fragments. Alternatively, papain digestion, cleaving N terminal of the hinge, yields two Fab fragments and Fc, although due to the non-specific activity of the enzyme, given time it will digest the entire Ig molecule.

Fab and Fc fragments represent the two functionally distinct components of an Ig molecule. The Fab arms provide antigen specificity and the Fc imparts biological function through recruitment of effector cells, or complement, in a class/ isotype dependent fashion. However, to fully understand how an Ab's physical make-up relates to its functional activity we must consider its structure in finer detail.

As mentioned, Ig consists of two L chains and two H chains. Sequence analysis of L chains reveal their structure to be composed of distinct homology regions, or domains, of approximately 110 amino acids in size, classified as being variable (V) or constant (C). L chains can be one of two basic types, kappa (κ) or lambda (λ), present in different proportions for different species. In man for example, approximately 40 % of L chains are λ, and 60 % are κ, while in mice this ratio is 5 %: 95 % (11).

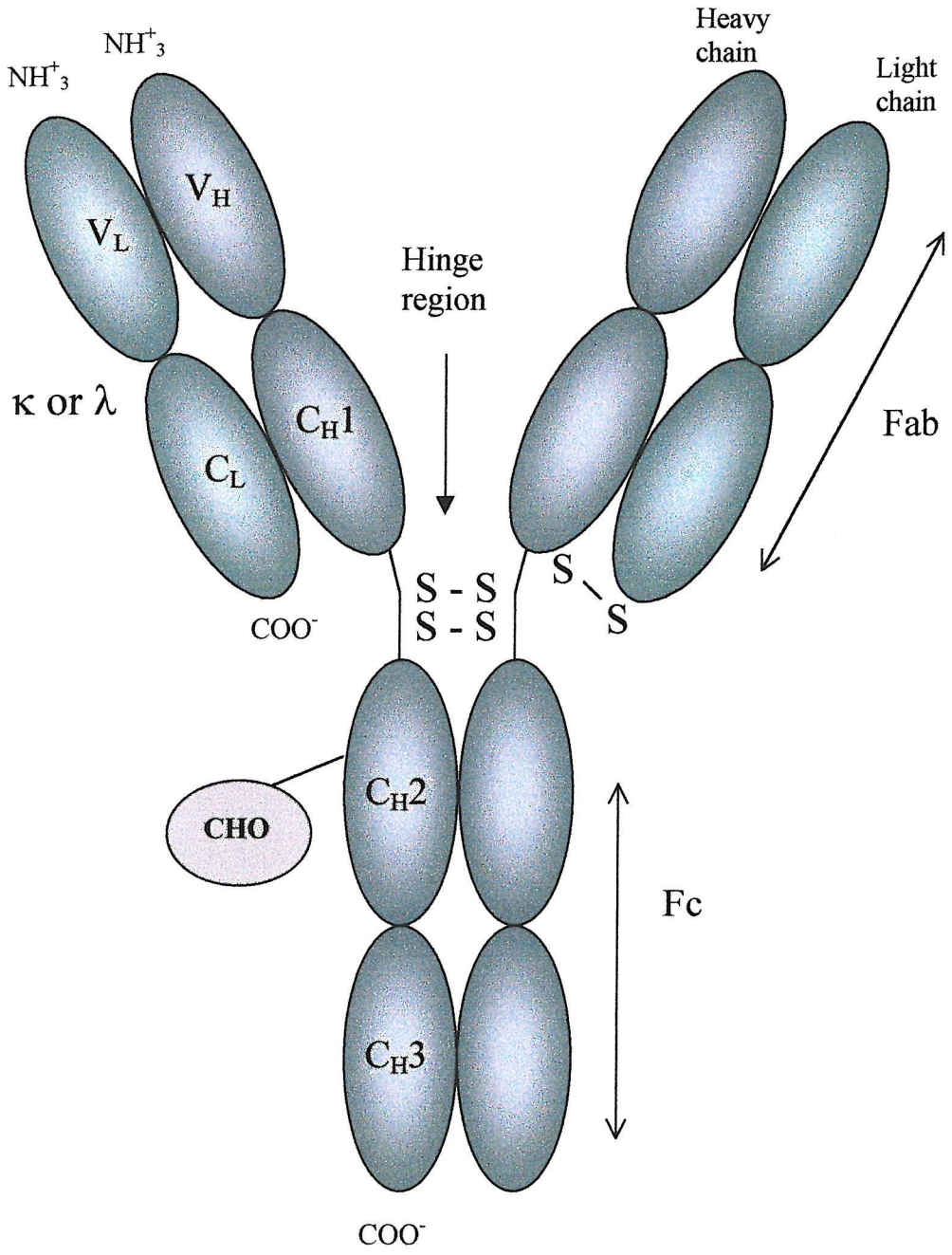

Fig.1.1 The immunoglobulin molecule. Shown is a schematic of the basic IgG molecule, composed of two H and two L chains. It should be noted that IgM, and IgE have five H-chain domains, whereas IgG, IgD and IgA have four.

H chains show a similar composition, consisting of a VH region and a differing number of CH regions depending on Ig class. For example, IgG has three C domains, whereas IgM has four. Indeed, it is the composition of these CH domains that determine the class and isotype of an Ab. There are five heavy chain isotypes, α, δ, ε, γ and μ, corresponding to the five Ig classes IgA, IgD, IgE, IgG, and IgM. Any given heavy chain can associate with either a κ or λ light chain, but a single Ig molecule will only express one or the other, never a mixture of both.

Ig domains are folded into compact globular structures consisting of two anti-parallel β-pleated sheets, linked by an intrachain disulphide bridge. The VL and VH domains, which provide antigen binding specificity, can be further sub-divided into framework regions and hypervariable (HV) regions, the former being more conserved sequences, and the latter showing high levels of sequence variability. The hypervariable regions or complementarity determining regions (CDRs) comprise the physical antigen-binding site of the molecule.

Variability is achieved at a genetic level, by random rearrangements of the gene segments composing the multi-gene families that encode the L and H chains. V and J gene rearrangements in the L chain and VDJ rearrangements in the H chain confer V region hypervariability, and lead to generation of mature, immunocompetent B cells, expressing a variety of surface antigens (see Figure 1.2). The intricacies of these rearrangements will not be discussed here, but a full review can be found in (12, 13).

The C domains that form the Fc tail dictate the biological activity of the Ig molecule. As mentioned, this varies with class, and a brief description of each is given below, and summarised in Table 1.2

Fig.1.2 Overview of B cell development and antigen expression. Shown is a cartoon depicting the main developmental stages in the life of a B cell, from the earliest stem cell phase through to the generation of a fully activated plasma cell. Listed are the major antigens expressed during each stage of the life-cycle, with particular reference to those that may serve as targets for immunotherapy

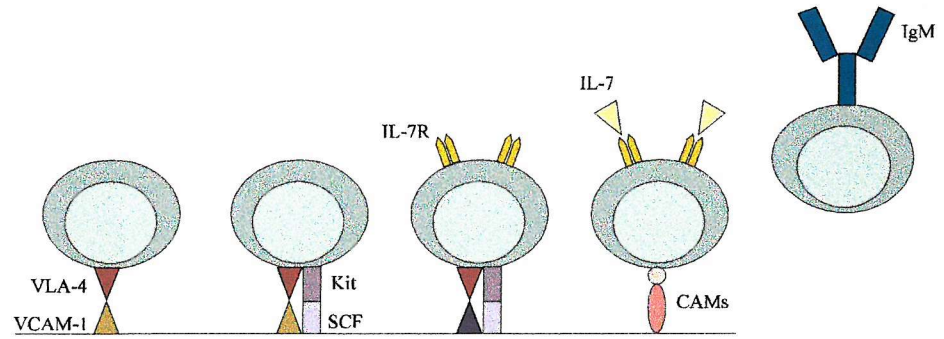

BONE MARROW STROMAL CELL

Stem cell	**Early Pro-B**	**Late Pro-B**	**Pre-B**	**Immature B**
		D-J rearrangement H chain	***V-DJ rearrangement H chain***	***D-J rearrangement L chain***
Class II CD38	Class II CD19 CD20 CD38	Class II CD19 CD20 CD38	Class II μ CD19 CD20 CD38 CD40	Class II IgM CD19 CD20 CD40

Antigen Independent

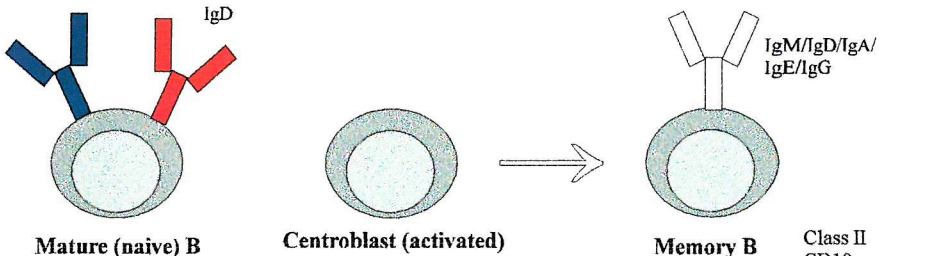

Mature (naive) B

MHC II
IgM
IgD
CD19
CD20
CD22
CD40

Centroblast (activated)

Somatic hypermutation

Memory B

Class switching

Class II
CD19
CD20
CD40

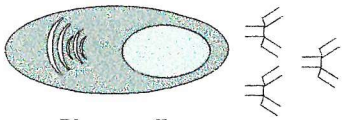

Plasma cell

Class switching

IgM/IgA/
IgE/IgG

CD38
CD40

Antigen Dependent

1.5 Immunoglobulin classes

1.5.1 IgM

IgM constitutes approximately 5-10 % of total serum Ig. It is present as a surface bound molecule on B cells, in a monomeric 180 kDa form, or secreted by plasma cells as a disulphide linked pentamer, with polymerisation aided by an additional polypeptide, joining (J) chain of 15 kDa.
IgM is superior to IgG in terms of complement activation, correlating with the multiple Fc regions present, and also has a higher valency, making it extremely efficient at binding multivalent antigens such as bacterial surfaces. It is the initial Ab class to be produced in the primary immune response to antigen and generally has low affinity, relying on its multivalency for high avidity.

1.5.2 IgA

IgA is present in a monomeric form at relatively low levels in serum, or as a dimer in external secretions such as saliva, tears, and mucus, where it is the predominant Ig class. Secretory IgA is also linked to a J chain (like IgM), together with a further 70 kDa secretory component – a remnant of the poly-Ig receptor responsible for the transport of IgA across epithelial cells. Functionally, the secretory component confers immunity from proteolytic degradation in the mucosal environment, where IgA serves to block pathogen adhesion by cross-linking bacterial/viral surface antigens.

1.5.3 IgE

IgE is present at only very low levels in serum, but has potent biological activity. Existing as a 190 kDa monomer, IgE binds with high avidity to Fcε receptors on mast cells and basophils, initiating subsequent degranulation when cross-linked by antigen. The active mediators released (eg.histamine) can lead to the hypersensitivity reactions symptomatic of hay fever, and asthma.

1.5.4 IgD

IgD is expressed in a membrane bound form on mature B cells, where it serves to co-operate in B cell activation following antigen binding. A biological effector function for IgD remains elusive.

1.5.5 IgG

IgG represents 80 % of total serum Ig. In man, four different sub-classes exist, designated γ1, γ2, γ3 and γ4. All are based on a common 146 kDa monomeric structure comprising two heavy (γ) chains, and two light (κ/ λ) chains, but distinguishable by the size of the hinge region and number of inter-γ chain disulphide bonds. IgG is the only class capable of crossing the placental barrier, and thus confers protection to the foetus and neonate. It is also the major Ig class involved in the secondary immune response.

Table 1.2 Biological and physiochemical differences of Ig classes.

	IgG1	IgG2	IgG3	IgG4	IgA1	IgA2	IgD	IgE	IgM
Heavy chain	γ1	γ2	γ3	γ4	α1	α2	δ	ε	μ
Mean serum conc (mg/ml)	9	3	1	0.5	3	0.5	0.03	0.0003	1.5
Mol.wt (x 10^3)	146	146	170	146	160	160	150	190	900
Half-life (days)	23	23	8	23	6	6	3	2.5	5
Complement fixation (classical)	++	+	+++	-	-	-	-	-	+++
Cross placenta	++	+/-	++	++	-	-	-	-	-
Mast cell binding	-	-	-	-	-	-	-	+++	-
Monocyte/ Macrophage binding	+++	+	+++	+/-	+	-	-	+	-

Adapted from Kuby (2000), Immunology 4th Edition. (Ref. 14)

1.6. Antigenic Targets for Immunotherapy

The highly specific nature of mAb allows the precise targeting of a wide range of tumor-associated antigens. These include oncofetal antigens, growth factor receptors, and a variety of differentiation markers (CD antigens). Ideally, a given target antigen should be confined purely to tumor cells so as not to deplete normal cells or tissue, but in reality, the opportunity for this rarely occurs. Indeed, for B cell lymphoma, the only truly tumor specific antigen is the B cell receptor (BCR) idiotype (Id). Instead, tumor selectivity through lineage-specific mAb with high affinity and minimal cross-reactivity is a more realistic goal. In addition, where targeting of host effector mechanisms is the goal, the antigen of choice should ideally be present at high density, homogeneously expressed, and not be modulated, or shed from the cell surface (15).

A number of antigens expressed by malignant B cells (as well as normal B and other cellular populations) have been selected as targets for therapeutic strategies. Those that are of particular relevance to this thesis will now be discussed briefly.

1.6.1. Idiotype

As discussed previously, Abs display incredible heterogeneity in their antigen binding V regions. Subtle variations in protein sequence within the hypervariable domains of the V regions produce determinants, or idiotopes, unique to each Ab molecule. The collection of idiotopes on an Abs V regions forms the Id. Clonally derived tumor cells expressing identical surface Ig molecules will thus exhibit identical idiotypic determinants. Anti-Id mAb raised against these determinants can therefore discriminate between malignant and normal cells, and positively select them for immunological attack. In the case of B cell lymphoma, anti-Id mAb are directed towards components displayed by membrane IgM (and IgD), part of the BCR complex.

1.6.2. BCR Complex

Whilst Ig of any isotype can be expressed on the B cell surface, the classes

preferentially displayed during B cell development are IgM and IgD. Whilst IgD expression is confined to certain developmental stages (see Figure 1.2), the μH chain is expressed throughout B cell development. Thus, we shall consider the BCR complex in terms of IgM. The BCR can essentially be described as surface Ig (composed of two membrane bound μH chains and two μL chains), non-covalently associated with a heterodimer of CD79α (Igα; mb-1) and CD79β (Igβ; B29) (16, 17). Sodium dodecyl sulphate (SDS) Polyacrylamide gel electrophoresis (PAGE) analysis reveals the murine CD79 α/ β proteins to migrate with an approximate molecular weight of 34 kDa and 39 kDa respectively, whereas in man they are 47 and 37 kDa (reviewed in 18). Size differences between murine and human proteins are due to additional glycosylation.

The disulphide-linked CD79 heterodimer is responsible for transport of the BCR complex to the plasma membrane. Partially assembled BCR is retained in the endoplasmic reticulum until associated with CD79α, which is both necessary and sufficient to permit the exit of the BCR complex from this compartment, and effect its transport to the cell surface (19).

The cytoplasmic tail of the IgM molecule itself is incredibly short (only 3 amino acids in length), and so consequently lacks the capacity to activate major intracellular signaling processes. Instead, this role is fulfilled by the α/β heterodimer. In this way the IgM μ chains are able to direct a variety of functions including proliferation, differentiation, anergy, and deletion. Aggregation of surface IgM leads to phosphorylation of the α/β heterodimer (20) at specific consensus sequences known as ITAM (immunoreceptor tyrosine based activation motifs) (21) by Src-family kinases constitutively associated with the resting BCR. This leads to association and phosphorylation of other Src homology-2 (SH2) domain containing protein tyrosine kinases (PTK) such as Syk, and subsequent triggering of downstream signaling cascades that ultimately result in changes in intracellular calcium levels and activation of nuclear transcription factors. BCR mediated signaling pathways are reviewed in (22).

Signaling through the BCR is regulated both positively and negatively by co-receptors

such as CD19 and CD22, which can themselves serve as targets for mAb based immunotherapy.

1.6.3. CD19/CD21/TAPA-1 complex

CD19 is a 95 kDa glycoprotein, expressed on B cells from early stages of development through to plasma cell differentiation. It is a member of the Ig super-family, and forms part of a multimolecular signal complex on the surface of B cells, together with CD21 (complement receptor 2, CR2); CD81 (TAPA-1); and Leu-13 (23).

CD19 exerts its effects on B cell activation and proliferation through a 243 amino acid intracellular tail. Ligation of CD19 and/or BCR by antigen, initiates rapid phosphorylation of tyrosine residues in the cytoplasmic tail of the molecule, which then serve to amplify BCR signaling events. Activation of src-family PTK and interaction with other downstream signaling molecules effectively lowers by two orders of magnitude the number of BCR complexes requiring antigen ligation in order to activate B cells (reviewed in 24).

That CD19 is the dominant signaling member in the 19/21/TAPA-1 complex has been demonstrated by Sato et al (25) using mice carrying a transgene encoding the extracellular and transmembrane portions of CD19, but with the cytoplasmic region deleted. These were compared to CD19 knockout mice and found to have an identical phenotype, presenting abnormal B cell development and reduced levels of signaling through the BCR.

1.6.4. CD22

CD22 is a 135 kDa phosphoglycoprotein, whose surface expression is limited to IgD positive mature B cells (26). It functions not only as an intercellular adhesion molecule binding ligands expressing sialic acid, but also has a role in modulation of BCR signaling thresholds. Whilst initial observations pointed to a positive regulatory role for CD22 in this capacity, growing evidence now supports a role for negative regulation of BCR-signaling. This includes association of CD22 with SHP-1, a

protein tyrosine phosphatase known to be involved in negative regulation of BCR signaling (27), evidence that dissociation of CD22 from the BCR complex serves to increase BCR signaling responses (28), and the finding that CD22-deficient mice display increased levels of stimulation and autoantibody production (29).

Such regulatory pathways may function by reciprocal interactions between CD19 and CD22. Recent observations indicate that CD19 expression is required for initiation of CD22 negative regulatory functions, and that CD22 in turn may also target CD19 itself for inhibition (30).

1.6.5. CD40

CD40 is a 48 kDa transmembrane glycoprotein belonging to the tumor necrosis factor (TNF) receptor family. Its expression was initially believed to be restricted to cells of the B lineage, but in recent years it has been identified on a broad spectrum of antigen presenting cells, endothelial/ epithelial cells, and hematopoietic precursors (31).

Binding of CD40 to its ligand, CD154 (CD40L), is thought to induce CD40 trimerisation and activation of signal transduction pathways operating via a network of TNF-receptor associated factors (TRAF), including CD40 receptor associated factor 1 (CRAF1, TRAF-3), TRAF-2 and TRAF-5 (32, and reviewed in 33). Signaling can result in a range of both positive and negative responses. *In vitro*, CD40 ligation on B cells can result in proliferation, activation of resting B cells, skewing of B cell maturation towards a memory cell phenotype, induction of homotypic adhesion, and induction of Fas expression (reviewed in 34). *In vivo*, CD40-CD40L interactions are critical in germinal centre formation (35) and class switching, regulation of immune responses and have roles in resistance to infection and autoimmune disorders (34).

Anti-CD40 mAb have also proved to be particularly effective at eradicating murine lymphoma cells *in vivo* (36). Recent studies in this laboratory have demonstrated that anti-CD40 therapy results in a rapid expansion of cytotoxic CD8 T cells, that not only give protection against initial tumor dose, but also provide immunity to subsequent tumor re-challenge. This activity is independent of CD4 cells and is most likely functioning by activating antigen presenting cells (APC) (of an as yet undetermined

nature) to enhance presentation of tumor antigen to CD8 cells, probably by cross-priming mechanisms.

Given the key roles played by molecules such as CD19, CD22 and CD40 in regulating B cell activity, and other immune cell functions, it seems logical that they be considered as targets for immunotherapy of NHL. Other Ab applied in this thesis have been targeted to MHC class II (MHC II), CD38 and CD20, and these antigens will be discussed at the appropriate point in the text.

1.7. Mechanisms of Antibody Induced Tumor Regression

There are a number of potential mechanisms by which mAb can eliminate tumor. These include recruitment and activation of immune effector cells, complement fixation, or direct signaling of cell cycle arrest and apoptosis to the target cell.

1.7.1. ADCC

Ab bound to its specific antigen leaves its Fc portion free to engage Fc receptors (FcR), thus triggering the cytotoxic activity of an assortment of effector cells such as macrophages, PMN, eosinophils and NK cells. There are three main classes of receptor for IgG on human leukocytes: FcγRI (CD64), FcγRII (CD32), and FcγRIII (CD16). All three are capable of triggering ADCC of tumor both *in vitro* and *in vivo*, providing they are engaged by IgG of an appropriate isotype (reviewed in 37). The exact structure and function of the IgG receptors will be discussed in some detail later in this chapter. That Ab isotype is critical to processes such as ADCC has been clearly demonstrated using matched sets of Ab with identical antigen specificity but differing isotype (38, 39). Such experiments indicate that human IgG1 and IgG3, rat IgG2b and murine IgG2a are the most potent isotypes.

1.7.2. Complement Activation

The complement system comprises a number of plasma proteins involved primarily in destruction of infectious microorganisms. There are three main pathways of

complement activation: classical, alternate and lectin based. Of these, the Ab triggered classical pathway appears the most relevant to immunotherapy. The complement system operates as a tightly regulated cascade, with all three pathways converging round a pivotal C3 molecule. C3 is central to instigating a number of complement based effects including opsonisation, production of an inflammatory response, and formation of the cytolytic membrane attack complex (MAC), as outlined below.

The first component in the complement cascade, C1, becomes activated on binding of at least two Fc portions of antigen-bound IgM or IgG (40). This induces a conformational change within part of C1 called C1q, triggering innate serine esterase activity and production of a C1s component, which acts on downstream targets C4 and C2. The cleavage products of these two proteins combine to form the enzyme C3 convertase, which cleaves C3.

C3 convertase proteolytically cleaves C3 into two fragments: C3a and C3b. C3a is an anaphylatoxin able to trigger histamine release from mast cells, leukocytes and platelets, whereas C3b, once bound to the target cell, can potentiate that cell's destruction by engaging phagocytes through their C1 and C3 receptors (CR1 and CR3) (41). C3b also catalyses subsequent complement cascade reactions by complexing with the C3 convertase to produce C5 convertase. C5 convertase cleaves C5 into two molecules, C5a (again, an extremely potent anaphylatoxin), and C5b, which becomes membrane bound. This in turn binds C6 and C7 forming a high affinity receptor for C8, and finally up to 15 C9 molecules to produce the transmembrane pore-forming MAC (42). Resultant death is either by osmotic lysis or toxicity induced by the influx of large concentrations of calcium ions (43).

The destructive power of complement warrants protective armoury to be displayed by host cells, preventing their destruction by activated complement components. Several molecules such as Decay Accelerating Factor (DAF, CD55), Membrane Cofactor Protein (MCP, CD46), Factor H, and Factor I (44), are involved in the regulation of C3 activity, either by its cleavage into inactive products, or causing its dissociation from enzyme complexes. These complement resistance factors are often exploited by tumors, with over expression of molecules such as DAF and MCP contributing to the poor levels of complement activation mediated by mAb (45).

1.7.3. Cell Death and Apoptosis

There are two forms of cell death: necrosis and apoptosis. Prior to the discovery of apoptosis, necrosis was considered the major death process. Necrosis arises from severe molecular or structural damage, and is characterised by loss of membrane integrity, swelling, lysis and release of cellular contents into the extracellular environment. However, the inflammatory reactions associated with this type of death are disruptive to normal tissue homeostasis, and so it became evident that a more physiological death mechanism must exist (46).

First described by Kerr et al in 1972 (47), apoptosis is a morphologically and biochemically distinct form of cell death, separate from necrosis. It is crucial for deletion of cells in a variety of processes, including positive and negative selection of B and T cells, and has been demonstrated to arise spontaneously in the majority of malignancies (48). The possibilities of enhancing tumor apoptosis through irradiation, chemotherapy, and Ab therapy are therefore appealing.

Morphologically, apoptosis is characterised by chromatin compaction and margination, cytoplasmic condensation, cell shrinkage, nuclear fragmentation and formation of membrane bound apoptotic bodies which are released and rapidly ingested by neighbouring phagocytic cells, thus reducing the likelihood of inflammation (reviewed in 49). Biochemically, apoptosis is defined by enzymatic internucleosomal DNA fragmentation. This cleavage results in production of DNA fragments of between 180-200 base pairs, which are clearly detectable as a ladder using agarose gel electrophoresis.

The classical features of apoptosis arise through the activation of a number of enzymes. Central to this death mechanism are the cysteine proteases, of which the caspase family is the best characterised. These are responsible for cleavage of a number of crucial repair enzymes, and cellular substrates such as lamins, thus producing the cytoskeletal breakdown observed during apoptosis (50). Cleavage of nuclear DNA is conducted by nucleases, which are activated prior to the morphological changes observed during apoptosis, and irreversibly confine a cell to

deletion. Although the exact nature of the proteins involved remains questionable, the most probable candidate is CAD (caspase activated Dnase) and its receptor ICAD (inhibitor of CAD) (51). Cleavage of nuclear DNA may serve a protective function, preventing the passage of active genetic material to neighbouring cells (52).

Transglutaminase activity occurs relatively late in the apoptotic cascade and is linked to the formation of apoptotic bodies which are phagocytosed by surrounding cells. These enzymes are responsible for cross-linking intracellular proteins, which serves to provide a rigid framework within the bodies, helping maintain their integrity, and preventing leakage of cellular contents, thus reducing the risk of inflammation (53).

1.7.4. Cell Cycle Arrest

The cell cycle (CC) is a defined course of events taken by a replicating cell, as it passes from a non-dividing state, through DNA synthesis and mitosis. Progression through this cycle is governed by the cyclin family of proteins, and their associated kinases (cdks) (54). The cycle begins when a cell receives a stimulatory signal driving it from G0 to G1, a process that is associated with changes in intracellular calcium (55). It then progresses into a DNA synthesis stage, termed S phase. This results in generation of a tetraploid cell, which remains in G2 until mitosis, M, where the cell divides to form two daughter cells of diploid chromosome content.

On receiving certain stimuli a cell may arrest its passage through the CC, halting at defined check points at the border of G1 and G2/M. Here, damaged cells may either undergo genomic repair or be deleted by apoptosis. G1 arrest is associated with the oncoprotein p53 (56), induced by DNA damage following, for example, ionising radiation. The status of p53 has an important bearing on tumor therapy, such that tumors expressing wild type p53 (such as Acute Lymphoblastic Leukaemia) have good prognosis, whereas those with mutated p53 are more resistant to therapy (57). As human tumors are frequently associated with mutated or non-functional p53, treatments relying on induction of CCA or apoptosis may face difficulty. However, in the case of B cell malignancy, where apoptosis triggered through the BCR is independent of p53 (58), mAb directed against the BCR may provide an effective means of deleting malignant cells.

1.8. mAb: The not-so Magic Bullets.

Despite all the promise monoclonal technology has to offer, little of the potential has been translated into therapeutic success. Several Phase I and Phase II clinical trials using unmodified Ab have been conducted, with only a handful of mAb providing a number of partial and complete responses. Whilst virtually no durable remissions have been obtained against solid tumors, a limited number of responses have been achieved against B cell malignancies. Ab to three antigens in particular – Id, CD52 and CD20 – have proven most effective (reviewed in 2 and 4).

The human chimeric anti-CD20 mAb, (IDEC-C2B8, Rituximab) is the most extensively studied, and most therapeutically active mAb thus produced. Phase II trials conducted in over 200 patients produced a response rate of nearly 50%, with minimal toxicity and human anti-mouse Ab (HAMA) response (59). It has since become the first mAb to gain FDA approval as an agent for cancer therapy.

The humanised anti-CD52 mAb, CAMPATH-1, has been tested against a range of B malignancies, but proven most effective against CLL. Responses range from 40 – 80%, with one trial conducted producing 5 CR, and 2 PR from 8 assessable patients (60). However, application of the mAb was associated with severe toxicity and approval remains to be granted.

Anti-Id mAb have also been used to treat NHL, showing favourable responses, with a number of long lasting responses (61). Treatment with anti-Id mAb is hampered by circulating Id shed from tumor, escape of Id negative variants and the requirement of customising mAb for each individual patient. Thus, wide-scale clinical application is not practical.

In general, the limited clinical responses observed following mAb treatment can be attributed to a number of factors, as detailed in Table 1.3, and discussed below.

Table 1.3 Problems associated with mAb based therapy

Barriers to mAb Therapy
Inaccessibility of tumor cells
Non-specific binding of mAb
Extracellular antigen
Antigenic modulation
Inadequate effector recruitment
Phenotypic changes in tumor
Immune response to Ab

Adapted from Stevenson G. T. (1993) (Ref. 15).

Antigenic modulation is a mechanism by which tumor can escape Ab-mediated attack, mainly when that Ab is required to recruit natural effectors. Ab binding to, and cross-linking its target antigen can result in the lateral movement of the Ab-antigen complex, polarising in patches or caps. These lattice works can subsequently either be internalised or shed from the cell surface, thus reducing target antigen expression. This greatly impairs recruitment of FcγR bearing effector cells, or complement proteins.

Modulation can be influenced by a number of factors including the nature of the target antigen molecule, its density, Ab affinity, Ab concentration, cell type, and temperature (62). The route of internalisation is also variable, as is the fate of the internalised protein, with some receptor molecules being recycled back to the cell surface, whilst others are degraded internally.

Modulation can be overcome by using univalent mAb derivatives such as FabFc which are incapable of cross-linking their target antigens, but can still recruit effector cells via the Fc portion (63). Although *in vitro* these derivatives do not induce modulation, *in vivo* significant modulation can still occur due to indirect cross-linking of surface antigen to FcγR bearing cells (64). However, the rate of modulation is

slower than that seen with bivalent derivatives. Whilst modulation may impede the recruitment of endogenous effectors and complement, it can be used to an advantage in the delivery of immunotoxins to tumors. MAb targeted against antigens such as CD22, which strongly modulates, provide an effective route of delivering cytotoxic compounds to neoplastic cells (65).

Antigens shed from the cell surface may also limit the efficacy of a derivative by acting as a biological sink. Hence, Ab can be consumed before it even has an opportunity to arrive at its target destination (15). Antigens may become cleaved from the cell surface enzymatically, or else secreted. Increasing the dose of infused mAb may combat this phenomenon to some extent, but such a strategy is highly wasteful. Also multiple doses of an Ab may elicit an immune reaction against the Ab. Many mAb are derived from rodent sources and so can generate HAMA responses. This can be overcome to some degree by use of immunosuppressants to dampen the immune response, but as the intention is to utilise immune resources to treat the tumor this approach is somewhat contradictory. Alternatively, chimeric or humanised mAb are now being employed much more routinely. As discussed previously, protein engineering techniques allow the transplantation of the rodent Ab variable domains or CDR loops onto human Ab, thus retaining antigen specificity, but decreasing immunogenicity (10).

Ideally, a target antigen should be present at a high density on the cell surface. Density can be affected by the processes of modulation and antigenic shedding, and also by mutational loss. Spontaneous genetic mutation of a malignant cell may severely reduce the therapeutic potential of an Ab. A classic example of this is in anti-Id therapy of B cell lymphoma. Tumors may escape anti-Id mAb either by altering the structure of their idiotypes, usually by point mutation (66), or by undergoing mutational loss resulting in the complete loss of expression of idiotype on the cell surface.

Tumor inaccessibility is another factor affecting Ab therapy. The relatively high molecular weight of IgG means that it may have difficulty in reaching tumors that have poor vascular or lymphatic penetration. Ab can be engineered either chemically or genetically to be of reduced size, for example by removal of the Fc portion to leave

$F(ab')_2$. Although this may confer some advantage in terms of tumor penetration, it will be unable to recruit natural effectors through FcR. Recombinant technology and the production of increasingly smaller Ab fragments can improve biodistribution (67), but at the cost of reduced serum half—life.

The most significant failure of most mAb is their apparent inability to engage effector mechanisms *in vivo* (15). Selection of the most appropriate Ab class and isotype is critical, as the nature of the Ab used affects its capacity to effectively activate endogenous cytotoxic processes. However, one way to specifically improve recruitment, is through the use of BsAb.

1.9. Bispecific Antibodies

BsAb display dual specificity, with one arm chosen to recognise either a tumor restricted marker, or a molecule whose expression is dramatically increased on malignant cells, and the other arm directed towards a toxin or molecule present on an effector cell population (68). On engagement, a recruited effector cell not only displays direct cytotoxicity (Figure 1.3), but can also release cytokines into the immediate environment. These can have a direct growth inhibitory effect on the tumor (69), as well as stimulating further effector cell recruitment and activation, leading to an enriched population of immune effector cells at the tumor site. This specific activation is limited to the tumor, as univalent binding of the effector specific arm of the BsAb alone is not sufficient to trigger cellular activation (70). Hence, only on cross-linking to the tumor do effector cells become appropriately stimulated.

1.9.1. BsAb Production

There are two basic techniques for BsAb production – hybrid-hybridoma fusion, and chemical conjugation. The first produces whole IgG molecules with dual specificity, whereas the second can be employed to manufacture both intact IgG and $F(ab')_2$ derivatives.

Hybrid-hybridoma formation of BsAb involves the somatic fusion of two hybridoma cells, a methodology first described by Milstein and Cuello in 1983 (71). Each parent

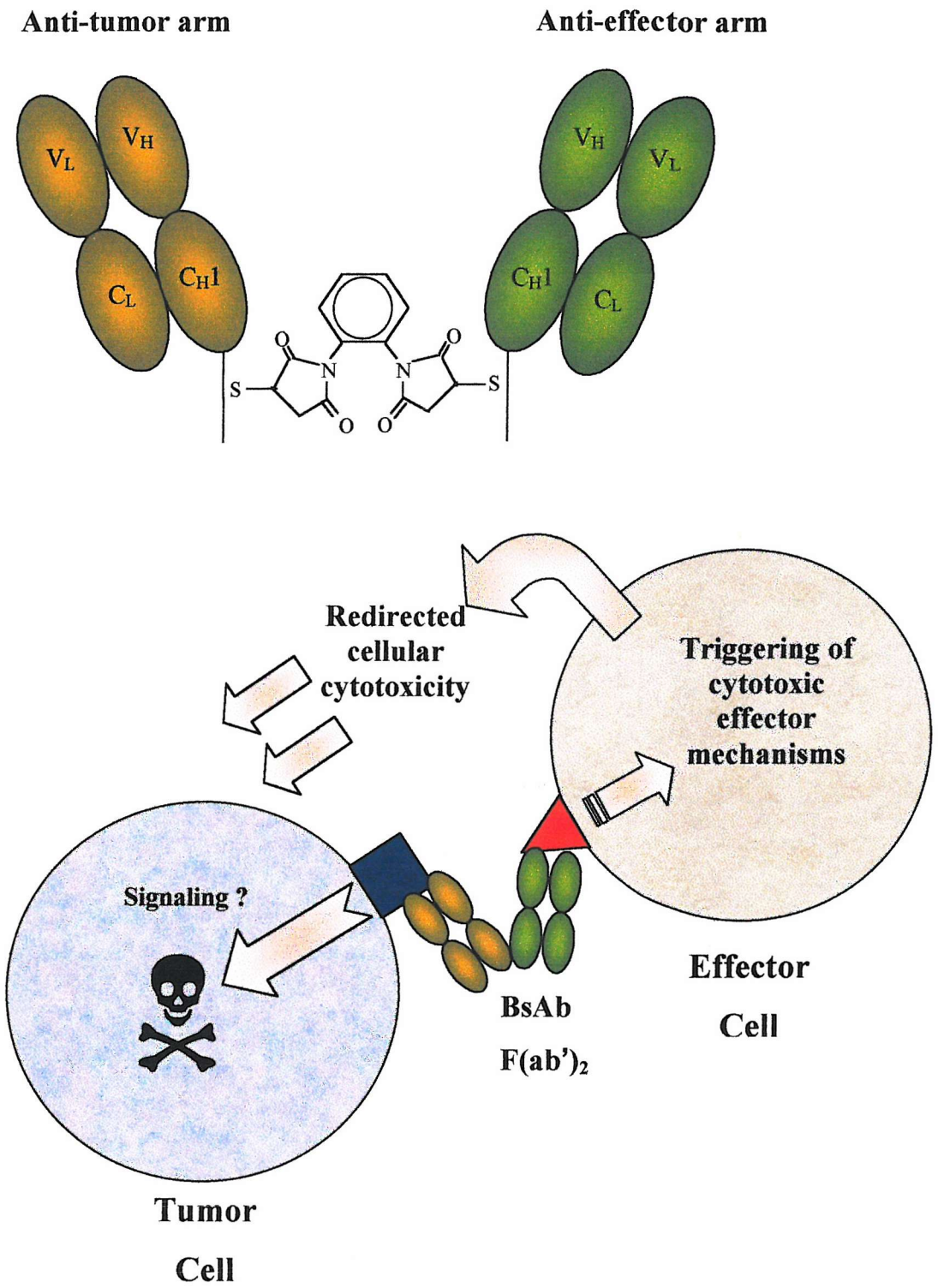

Fig.1.3 Bispecific antibody F(ab')$_2$. Schematic showing a BsAb F(ab')$_2$ derivative and proposed mechanisms of anti-tumor activity. Depending on the nature of the target antigen, bridging of the tumor and effector cell results in tumor destruction by redirected cellular cytotoxicity and signaling.

secretes a mAb of given specificity (one for tumor cell, one for effector cell), resulting in the generation of a bispecific IgG molecule. Whilst relatively simple to perform, the technique suffers from random association of parental heavy and light chain molecules (72). Consequently, in some cases only one in ten of the pairings formed constitutes the desired homologous coupling of H-L chains. Subsequent purification of this population is extensive and laborious, and the final yield is usually low.

An alternative method of manufacture is chemical conjugation. Development of prototype $F(ab')_2$ constructs from the direct joining of two rabbit (IgG) Fab' fragments via their hinge region SH groups, was first described by Mandy and Nisonoff in 1962 (73). However, this methodology was based on random association, so both homo-, as well as the desired hetero-conjugates were produced, necessitating a more directed process of linkage. Many, more precise, techniques are in application today.

Fab' fragments can be linked genetically as described by Kostelny et al. (74). This involves the use of leucine zipper regions of the Fos and Jun transcription factors. Peptides derived from these proteins can be genetically fused to parental Fab' arms, joining them together into $F(ab'\text{-zipper})_2$ heterodimers. Although yields are good, purity is still somewhat variable as it is difficult to get equal expression of both Fab'-zipper products, with the excess having a tendency to homodimerise.

An alternative approach is that adopted by Glennie et al (75). Here, individual Fab' fragments are linked by thioether bonds. Primary reduction to Fab'-SH and subsequent labelling of one derivative with o-phenylenedimaleimide procures a high percentage of $F(ab')_2$ heterodimer following the cross-linking reaction. Purification is relatively straightforward, with the only major contaminant being unreacted Fab', which is removed by size chromatography.

It is possible to directly conjugate two entire IgG molecules using chemical linkers such as SPDP, as reported by Kaprovsky et al. (76) These BsAb are functional, but are not appropriate for use *in vivo* due to their relatively large size and instability.

Advances in protein-engineering have led to even more radical bispecific single-chain (BsscFv) dimers. Constructs consist of the VH and VL regions of two different Ab, assembled so as the VH of one polypeptide joins with the VL of the second, and vice versa (77). Antigen binding sites orientate at opposite ends of the molecule and are thus able to bridge both the tumor and effector cell together. Using a [CD3 x Id] derivative, this approach has been shown to elicit 10 times as great a killing of BCL_1 lymphoma as a bispecific IgG (78). Alternatively, production of tetravalent BsAb containing four Ag binding domains can also be achieved, resulting in higher affinity and greater serum stability (79).

1.9.2. $F(ab')_2$ v IgG

There are advantages and disadvantages in using either a $F(ab')_2$ or an entire IgG construct for therapy. For the most part, these are a reflection of the presence or absence of the Fc region, which has implications on the activity and serum half-life of the derivative. A comparison of the two is given below in Table 1.4.

In vitro, intact IgG BsAb retaining an albeit hybrid Fc portion are able to induce T cell proliferation in the absence of tumor, whereas $F(ab')_2$ cannot (80). This is believed to be a result of additional binding to FcγR displaying cells such as monocytes, causing cross-linking of CD3 by the anti-CD3 arm of the derivative and induction of non-specific T cell activation. BsAb retaining their Fc are also able to recruit these FcR expressing cells for ADCC, as well as bind complement, offering additional mechanisms of killing over those of their specifically re-targeted effector species. Of course, such activity is dependent on Ab isotype and class.

In vivo a single dose of BsAb IgG ([CD3 x Id]) is capable of effecting almost complete cure, whilst protection with the equivalent $F(ab')_2$ derivative is minimal (81). This could in part be due to less efficient T cell activation by the $F(ab')_2$, although *in vitro* assays indicate that in the presence of tumor, both IgG and $F(ab')_2$ BsAb show similar levels of lymphocyte activation and retargeting. Differences in performance are most likely a reflection of serum half-life. The bispecific IgG has an advantage in that it is able to bind FcRn as well as its specific target, thus gaining

Table 1.4 Comparison of $F(ab')_2$ versus IgG BsAb derivatives

Property	$F(ab')_2$ Bispecific	IgG Bispecific
Size	100 kDa	150 kDa
Fc	Absent	Present
Half-life	Relatively short	Relatively long
Induces T cell activation in absence of tumor	No	Yes
Induces T cell activation in presence of tumor	Yes	Yes
Induces reverse T cell lysis	No	Yes
Induces ADCC	No	Yes
Induces complement activation	No	Yes
Redirects T cell lysis	Yes	Yes

Based on information given in: Weiner G.J. (1995) (Ref. 83)

some protection from catabolism (82). $F(ab')_2$ derivatives, lacking Fc, are unable to do this, but administration of multiple doses can provide some compensation.

The presence of Fc is not entirely beneficial. The larger size of intact BsAb may mean that they have difficulty in penetrating certain tumor sites. Further, the recruitment of phagocytic or NK cells via their FcγR may have an adverse effect, in that the effector targets of the BsAb themselves come under attack (83). It has also been documented that anti-CD3 mAb administration induces substantial levels of lymphokine production, presenting quite severe toxic side effects (84, 85). This can be reduced by limiting reactions to those between targeted effector and tumor cells, such as is achieved with $F(ab')_2$. Additionally, such constructs are much easier to manufacture and purify, a critical factor when considering the potentially large doses required for clinical treatment.

1.9.3. Potential Therapeutic Effector Cells

A number of immune cells have been selected as targets for BsAb, due to their cytolytic activity (86). These include T, NK and phagocytic cells. To gain therapeutic benefit from mobilising immune effector cells it is important that BsAb not only redirect effector species to the tumor, but also activate the cytotoxic mechanisms of that cell. Potential targets on effector cells are those molecules that give potent stimulatory signals such as CD3, (part of the T cell receptor complex; TCR), or certain FcγR on myeloid cells (Table 1.5).

Table 1.5 Major effector populations and trigger molecules for BsAb

Effector Cell	Target Molecule
T cell	CD2 CD3 CD28
Natural Killer Cell	CD16
Monocyte/Macrophage	CD32 CD64 CD89
Dendritic Cell (DC)	CD64
Granulocyte	CD64 CD89

Adapted from: de Gast G. C. et al. (1997) (Ref. 86).

1.9.4. T cell recruitment

T cells function as immune killer cells, directed against targets in an antigen specific fashion. They have a natural role in destruction of infected cells, and activation of other immune defence systems. Although T cells have also been indicated in having a natural role in controlling abnormal B cell proliferation, generally, tumors are poor activators of T cells (87). However, the potent cytotoxic capability of T cells makes them tempting targets for therapeutic protocols. Recruitment of T cells by BsAb has been reported since the mid-1980s (88, 89), and has since been employed against a range of tumor types, although we are particularly interested in their application against lymphoma.

Normally, T cell activation is achieved by recognition of a specific peptide displayed in the context of MHC I (endogenously derived peptide, presented to CD8 positive T cells), or MHC II (exogenously derived peptide, presented to CD4 positive T_H cells). One major advantage of BsAb is that they can circumvent the requirement for MHC restriction and provide their own specificity (ie. that of the anti-tumor arm of the BsAb). In this way T cells can be recruited independently of their TCR identity. This "bispecific over-ride" does not interfere with the natural specificity of the cell, and it remains able to kill targets for which its TCR is programmed - cells expressing the natural target are in fact preferentially eliminated even in the presence of BsAb and corresponding tumor (90).

In order to trigger the effector mechanisms of the cell, the anti-T cell arm of the bispecific must target a signaling molecule on the cell. The prime candidate for targeting is CD3. CD3 is a complex of up to five membrane molecules which form part of the TCR complex and is appealing as it is expressed on all T cells, and has a natural role in the signal transduction events that lead to T cell activation.

1.9.5. The T cell receptor

The TCR is a multi-subunit complex composed of two heterologous disulphide bonded α and β polypeptide chains (although γ/δ sub-sets also exist), non-covalently associated with CD3 γ, δ and ε chains, and a cytoplasmic ζ chain (91). Antigen recognition occurs via the α/β heterodimer, with diversity achieved through variable region domains in a similar fashion to Ig chains. Each α and β chain has a hydrophobic transmembrane region which displays positively charged amino acids critical for association with the CD3 proteins, which carry negatively charged residues. The CD3 proteins are functionally equivalent to the CD79 molecules of the BCR, bearing cytoplasmic extensions with ITAM motifs, and thus providing the signaling capability of the TCR complex (91). They also play a critical role in receptor transport, as sequences containing the basic and acidic residues appear vital for expression on the cell surface. The final component of the complex is the ζ protein, present mostly as a homodimer, which contains three ITAM groups, and provides additional signal transduction machinery. Antigen binding results in

activation of a number of ITAM associated PTKs including Src and Zap70/ Syk, which in turn phosphorylate downstream target molecules resulting in the activation of genes and cytoskeletal reorganisation events involved in T cell proliferation and differentiation (reviewed in 92)

An alternative route for mobilising T cell resources is to target adhesion molecules participating in T cell/APC association, or co-stimulatory molecules involved in instigation of IL-2 production, the cytokine primarily responsible for T cell proliferation and expansion.

1.9.6. Co-stimulation

As well as the antigen induced TCR signal, the lymphocyte also requires a second co-stimulatory signal in order to undergo antigen specific differentiation and expansion. MHC-antigen recognition occurring in the absence of co-stimulation leads to the T cell entering a state of unresponsiveness, or anergy. In recent years a great number of co-stimulatory molecules on the T cell have come to light including CD28 (93), CTLA-4, 4-1BB, ICOS and OX40 (reviewed in 94). Many of these molecules are currently being investigated as targets for mAb to modulate T cell responses to tumor. However, BsAb therapy has traditionally focused on CD28 as a target molecule. CD28 interacts with B7.1 (CD80), and B7.2 (CD86) on the APC. Cross-linking of these molecules is crucial to the synthesis of IL-2, which drives T cell differentiation. B7/ CD28 interaction facilitates this process by stabilising IL-2 mRNA and activating nuclear transcription factors such as NF-κB which increase rates of transcription of IL-2 mRNA (95). Lymphocyte proliferation is negatively regulated through a second co-stimulatory molecule, CTLA-4. This has a great deal of homology to CD28, but binds B7 with a higher avidity thus out-competing CD28 for B7 ligation (96).

1.9.7. Anti-CD28 BsAb

The necessity for two signals in the activation of T cells is crucial - thus tumor cells with little or no expression of co-stimulatory molecules do not trigger effective cytotoxic T cell (CTL) responses. Some evidence suggests that transfection of co-

stimulatory molecules into such tumor cells can counteract this CTL evasion. Chen et al. have demonstrated that murine melanoma cells expressing the E7 human papillomavirus gene product as a target antigen do not naturally generate an immune response in mice, but are rejected if transfected with B7 (97). This appears to be due to direct stimulation of a CTL response in the transfectants. A similar effect has been reported by Gerstmayer et al. who constructed a chimeric fusion protein comprising B7.2 and ErbB2 which localised to ErbB2 presenting target cells (98). B7 expressed in this manner was also able to stimulate proliferation of syngeneic T cells. However, expression of B7 does not in itself guarantee an anti-tumor T cell response, as many lymphomas present B7 on their surface, but are not rejected by the host (99). Anti-CD28 mAb offer a further possibility for augmenting an IL-2 driven immune attack, but such mAb would elicit activation of a wide spectrum of T cells of varying specificity, not just those specific for tumor. One way to overcome this is to cross-link CD28 with a BsAb that is directed specifically against a tumor antigen. [CD28 x tumor] lysis of cells has been demonstrated *in vitro* by Pohl et al. (100), and *in vivo* by Mezzanzanica, using a xenografted mouse model with pre-activated (anti-CD3/IL-2) T cells as effectors (101). That BsAb are capable of initiating a T cell response without pre-stimulation has been demonstrated by Jung et al.(102). They observed significant proliferation and lysis by T cells in response to [CD28 x CD30] BsAb, but only in conjunction with a second [CD3 x CD30] Ab. The effects were greater in combination than with either derivative alone. This combinatorial approach has been mirrored in treatment of human tumors such as the LS40CY Hodgkin's tumor, where dual application of [CD3 x CD30] and [CD28 x CD30] BsAb completely cured SCID mice carrying human PBL and tumor xenografts (103).

1.9.8. Anti-CD3 BsAb

[CD3 x tumor] BsAb have proved most successful either when used as a single derivative, or in combination therapy. Many groups report *in vitro* lysis of tumor cells when targeted by bispecific derivatives engaging peripheral blood lymphocytes (PBL) via CD3 (81, 104). For *in vivo* studies it is necessary to have a well characterised animal model, and much of the work as been conducted using the BCL_1 lymphoma of BALB/c mice. Brissinck et al. have consistently shown that hybrid-hybridoma generated [CD3 x Id] provides excellent therapy when treating intravenously, nine

days post-tumor inoculation (81). Investigation into the T cell sub-set responsible for conferring long-term survival (LTS) of immunised mice revealed that both CD8 positive and CD4 positive cells were important to the therapeutic outcome (105). CD8 cells aid in therapy by direct cytolytic activity, whereas CD4 cells, particularly of T_H1 phenotype, release cytokines such as Interferon gamma (IFN-γ), IL-2 and TNF-α into the environment, critical to cytolysis and activation of additional effector species such as NK cells (106).

A two stage therapeutic strategy has been adopted by Tutt et al. first priming T cells with one derivative, and then redirecting them to the tumor with a second (107). [TCR α/β x CD2] proves highly mitogenic both *in vitro* and *in vivo*, causing preferential expansion of $CD8^+$ cells. An additional [TCR x tumor] BsAb is then employed to focus the attack of these pre-primed CTLs against the malignancy. The [TCR α/β x CD2] derivative is probably an extremely effective stimulator because it mimics both the activation and co-stimulation signals required for T cell proliferation. Other groups have utilised alternative protocols to induce a co-stimulatory signal in an attempt to enhance BsAb mediated immunotherapy. Wooldridge et al. have used soluble CD40 ligand, known to up regulate co-stimulatory molecule expression, to try and enhance the amount of proliferation observed with their [CD3 x tumor] reagent (108). Application of soluble CD40 ligand induced B7 expression on the V 38C13 murine lymphoma, and demonstrated an increase in T cell activation over non-ligand treated cells during culture.

Bispecific trimers involving three Fab' fragments have been shown to exhibit even greater levels of RCC. A bispecific trimer with twio anti-CD3 arms, has been reported to be 40 times more potent than the $F(ab')_2$ [CD3 x CRBC] derivative (109), in recruiting and activating unprimed T cells against chick RBC. The same group also reported in excess of a 100 fold increase in cytotoxicity for a trispecific derivative containing two anti-target arms. This is probably due to an increase in avidity.

Heteroconjugates targeting CD3 to CD4 and CD8 have also been shown to be an effective way of activating T cells *in vitro* (110).

1.9.9. Bispecific toxin/radio-conjugates

As well as redirecting cellular effector mechanisms, BsAb also provide convenient vehicles to transport radioisotopes and immunotoxins specifically to tumor (111). This approach has an advantage over mAb in that there is an absence of chemical damage to the toxin normally arising from the process of conjugation to a mAb (112), and also, in principle, the BsAb can block the natural ligand-binding site of the toxin, thus reducing non-specific toxicity (113).

BsAb transporting a tumorcidal tag have been used successfully against the guinea pig leukaemia L_2C (114, 115). Bispecific $F(ab')_2$ constructed against L_2C Id, and carrying the ribosome inactivating protein (RIP), saporin, were able to destroy tumor both *in vitro* and *in vivo*. Similar results have been obtained targeting gelonin to human B cell tumors via CD22 and CD38 antigens (116).

1.10. Fc Receptors

The interaction of Ab-Ag complexes with cellular effectors is dependent on the Fc region of the Ig molecule, which binds to specialised FcR present on hematopoietic cells. Fc ligation to an appropriate receptor induces a number of cellular activities including phagocytosis, cytolysis, ADCC, inflammation and allergic responses. The FcR can be divided into two groups based broadly on their function. The neonatal receptor (FcRn) and the polyclonal Ig receptor (pIgR) form the first group, specialising in transport of Ig across epithelial tissue. The second group are present largely on effector cell populations, where they are involved in triggering biological responses following ligation, and include receptors for IgA, IgE, and IgG.

1.10.1. FcRn

In 1964, Brambell postulated the existence of two receptors for IgG, one involved in protection from catabolism and a second responsible for transport of IgG across the gut epithelium of neonatal rodents (117). More recently, Junghans and Anderson (118) have demonstrated these receptors to be one and the same. The receptor, designated FcRn, exists as a heterodimer, comprising a class I like α chain, and a $\beta 2$

microglobulin sub-unit. It functions to transport IgG from the mother to young thus conferring some degree of humoural immunity. In man, transport occurs prior to birth across placental syncytiotrophoblasts at the maternofetal interface (119). Trafficking is pH dependent with IgG endocytosed across the plasma membrane becoming bound to FcRn in the slightly acidic endosomal environment. Vesicles then transport the bound IgG to the stromal surface of the cell, where it is released due to the more neutral pH (82). In rodents, postnatal transport of IgG from maternal milk is believed to occur in a similar fashion.

Studies from β2m deficient mice have also confirmed a requirement for FcRn in regulating IgG catabolism, as homozygous knockouts show abnormally low levels of serum IgG (120). FcRn on endothelial cells is capable of binding IgG taken up by fluid-phase endocytosis. If serum levels are high, competition for receptor binding and subsequent saturation of the receptor means more IgG enters a degredation pathway. If levels are low, competition is less, and more IgG is salvaged for recycling back into serum.

1.10.2. pIgR

The pIgR is a membrane bound receptor, primarily involved in the trans-cellular transport of polymeric IgA (and IgM). The ligand-binding portion of the receptor consists of five highly conserved extracellular domains, showing a great deal of homology to Ig V region domains (121). It is present on the basolateral face of epithelial cells lining mucosal surfaces, where it engages IgA produced by mucosal lymphocytes (122). Following ligation, endocytosis, and vesicular transport, IgA-R complexes are exocytosed at the apical cell surface. Here, IgA release is mediated by proteolytic cleavage of the receptor, so as disengaged IgA remains attached to a fragment of the receptor, known as the secretory component (123).

FcR specific for all classes of Ig have been identified. We shall briefly mention the role some of these receptors play before focusing our attention on the receptors for IgG, the FcγR. Although it is necessary to mention details of signaling pathways activated by receptor cross-linking in these earlier discussions, more in-depth

descriptions of these events will be reserved for the FcγR section of this chapter and so details, for example concerning ITAM motifs, will be left until then.

1.10.3. IgA Fc Receptor

Human FcαR (CD89) is encoded by a single gene, and expressed as a transmembrane glycoprotein of a single isoform, bearing two extracellular Ig like domains, a transmembrane region and a short cytoplasmic domain, and binds IgA1, IgA2, and secreted IgA, all with medium affinity (124). It is expressed on a number of immune effector cells including monocytes, macrophages, PMN (125), and eosinophils (126), where its expression can be regulated either positively by LPS, GM-CSF, TNFα, IL-1β and IL-8, or negatively by TGFβ. Despite being expressed as a single isoform, the receptor does show great molecular heterogeneity between cell type, with a core protein of 32 kDa becoming heavily glycosylated to give a final surface molecule of variable size (125).

Functionally, FcαR exists as a hetero-oligomeric complex with the ligand-binding α chain of the receptor associating with a γ-chain homodimer, which functions as the signal transduction unit. Association between the two occurs at a positively charged amino acid residue in the membrane spanning domain of the α receptor (127). Receptor aggregation following engagement of immune complexes has been shown to triggers ADCC, phagocytosis, antigen presentation, cytokine release and inflammatory responses.

1.10.4. IgD Fc Receptor

Receptors for IgD (FcδR) have been reported on human CD4 and CD8 T cell subsets. Receptor expression is linked to exposure to oligomeric (but not monomeric) IgD, and can also be induced by IFN-γ, IL-2 and IL-4 (128). A function for FcδR remains to be established, though may involve regulation of T-helper responses.

1.10.5. IgE Fc Receptor

There are two receptors for IgE, one having high affinity (FcεRI) and one of low affinity (FcεRII, CD23).

1.10.5.1. FcεRI

FcεRI is a high affinity receptor, expressed as a 45 - 65 kDa molecule, bearing two extracellular Ig like domains, a transmembrane region, and a cytoplasmic tail. It is present on monocytes, DC, Langerhans cells, basophils, eosinophils and platelets (129). The ligand-binding α chain of the receptor lacks any signaling capacity, so the receptor associates with FcR γ chains (for signal transduction) and β chains (for signal amplification). Receptor aggregation leads to tyrosine phosphorylation of the γ and β chains by src-family members, a process regulated by CD45 (130). Depending on the cell type, receptor activation can lead to degranulation and release of inflammatory mediators (basophils and mast cells), or play a role in regulation of APC immune responses.

1.10.5.2. FcεRII

The low affinity IgE receptor (FcεRII, CD23) exists as a 45 kDa type II integral membrane glycoprotein. Unlike other FcR, it lacks Ig like domains, instead being a member of the lectin family. There are two isoforms, differing by 6 amino acids in the cytoplasmic tail (as well as in untranslated regions), which show differing expression patterns. FcεRIIa is present on B cells and follicular DC, where expression can be upregulated by the cytokines IL-3 and IL-4, and down modulated by IFN. The second isoform, FcεRIIb, shows a broader pattern of expression, on monocytes, eosinophils, mast cells, platelets, Langerhans cells, T cells, and CD5 positive B cells. It can also be enzymatically cleaved from the cell surface to produce a soluble receptor form. However, expression of FcεRIIb on these cells is not constitutive, but instead dependent on IL-4 . In addition, IFN can upregulate receptor expression, and TNFα can decrease the membrane bound form, but increase levels of soluble receptor (131).

Functionally, FcεRII has a role in B cell proliferation and differentiation, regulation of IgE production, antigen presentation, and cell adhesion. On monocytes/ macrophages it can induce phagocytosis and IgE dependent cytotoxicity.

1.10.6. IgM Fc Receptor

IgM binding FcμR have been described on human B, and T (132), as well as NK cell populations, although the precise function of the receptor on these cells remains elusive. Recently, a murine FcR designated Fcμ/αR has been described, that together with its human homolog, binds IgM and IgA with medium to high affinity (133). The receptor is expressed on B cells and macrophages and is believed to play a role in the initial immune response to microbial infection.

1.10.7. IgG Fc Receptors

The existence of a receptor specific for IgG was initially speculated by Berken and Benacerraf in 1965 (134). Several years later the first example of an IgG FcR was characterised (135) and isolated (136) from a human macrophage cell line, U937. This was the high affinity gamma receptor, FcγRI (CD64). Now, three main classes of human FcR have been identified for IgG, designated FcγRI (CD64); FcγRII (CD32); and FcγRIII (CD16), as well as the aforementioned FcRn. The three main leukocyte FcγR classes are represented in the schematic, (Figure 1.4), along with the major receptor isoforms and polymorphisms that exist for each class. All are members of the Ig supergene family and map to the long arm of chromosome one (137). They exist as hetero-oligomeric complexes, comprising two distinct sub-units. Specificity is displayed by an α chain, which determines not only the sub-class of IgG that the receptor will bind, but also the affinity with which it will do so. A second γ, or β chain serves as the signaling component of the complex, and in some instances is important in mediating cell surface expression of the receptor (138).

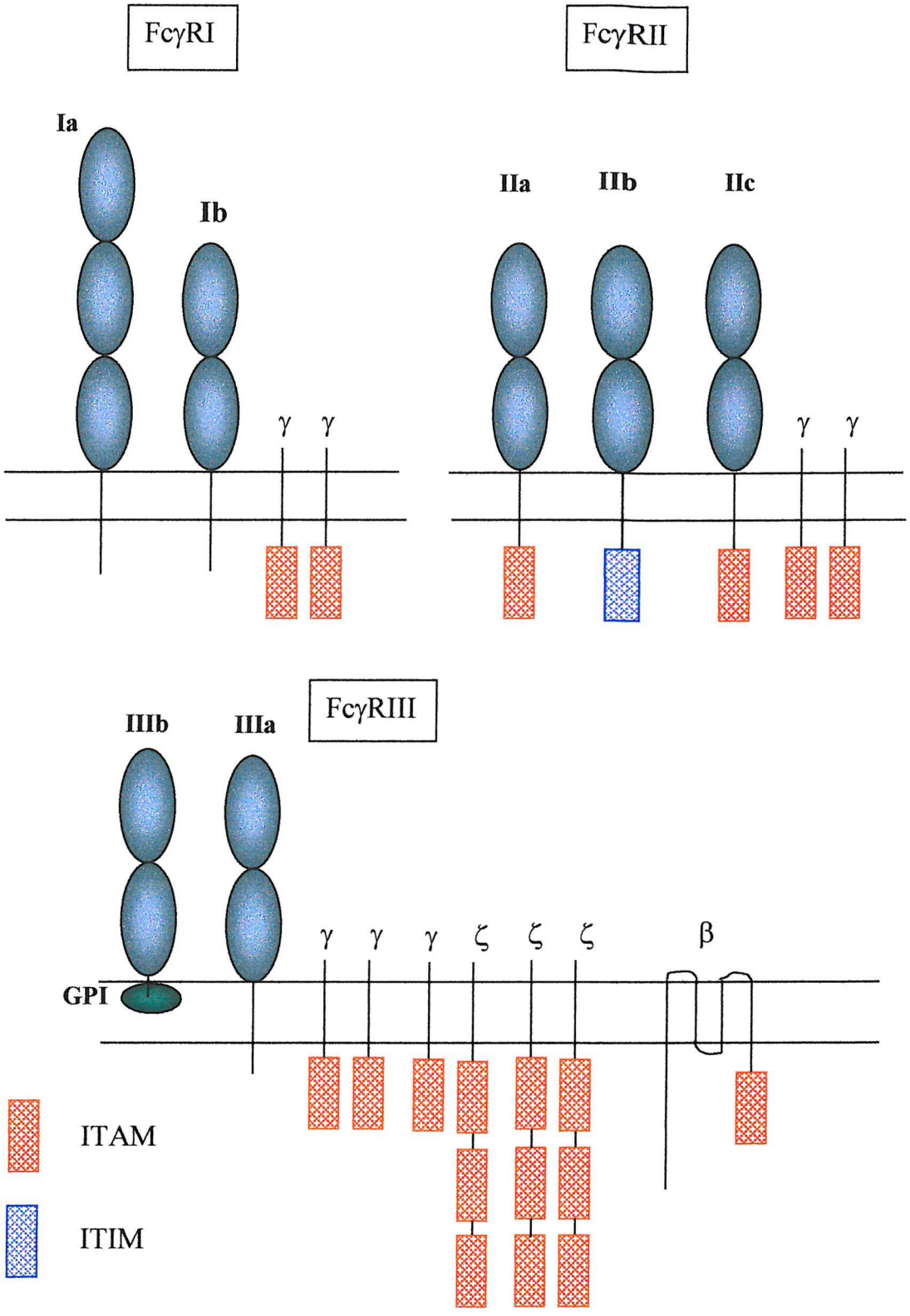

Fig.1.4 The human leukocyte FcγR family. Schematic illustrating the 3 main classes of the IgG receptor family (FcγRI, FcγRII, FcγRIII). Receptor polymorphisms and soluble receptors are not shown. Based on a figure from: van de Winkel J.G.J. and Capel P.J.A. (1993) (Ref. 152).

FcγR are expressed on a wide range of cells, many of which, such as NK, monocytes, macrophages, PMN, B cells, and eosinophils, function as immune effector populations. This makes FcγR attractive targets for BsAb based immunotherapeutic strategies. Coupling to Ab can install specificity to these otherwise reasonably indiscriminate effector species, providing a means of bridging the cellular and humoural branches of the immune system. Biologically, they serve many functions. They can act as trigger molecules for phagocytosis, ADCC, and secretion of inflammatory mediators (139), as well as being involved in clearance of immune complexes, and enhancement of antigen presentation (140). Although mAb can trigger effector mechanisms through FcR ligation, the effectiveness of this process *in vivo* is somewhat questionable. Ab of an inappropriate isotype will not engage specific receptors, and Ab may bind to receptors on cells such as platelets, that lack appropriate effector mechanisms. BsAb are advantageous in that they can specifically target cytotoxic effector cells through the appropriate FcR class, irrespective of isotype, and redirect these effector cells to their neoplastic target.
The general characteristics and properties of all three classes of FcγR are summarised in Table 1.6. Throughout the text, the FcR referred to will be of human origin unless otherwise stated.

1.10.7.1. FcγRI (CD64)

FcγRI is unique amongst this family of receptors in that it is capable of binding both monomeric and immune complexed IgG. Moreover, it is the only receptor capable of binding IgG with high affinity (see Table 1.6). First isolated by Anderson et al (136) the ligand-binding α-chain is expressed as a 72 kDa glycoprotein, having three extracellular Ig like domains. The other FcγR family members all bear only two extracellular domains, and it is the presence of this third domain (EC3) that is believed to confer the high binding affinity (141). FcγRI is encoded by three highly homologous genes – IA, IB and IC (142). The IA gene encodes the full sized receptor, whereas the other two genes contain stop codons in their EC3 exons.

Table 1.6 Comparison of Fcγ receptors on human leukocytes.

	FcγRI	FcγRII	FcγRIII
CD Number	64	32	16
Molecular Mass	72 kDa	40 kDa	50-80 kDa
Binding Affinity (Ka)	High (10^8-10^9 M^{-1})	Low (<10^7 M^{-1})	IIIa:medium (~3x10^7 M^{-1}) IIIb:low (<10^7 M^{-1})
Affinity			
Murine IgG	2a=3>>>1,2b	1,2b>>2a	2a>2b>>1
Human IgG	3>1>4>>>2	3>1*	1=3>>>2,4
Receptor subunit	γ chain	IIa:γ chain	IIIa:γ, ζ, β chain
Distribution	CD34+ myeloid progenitors, monocytes, macrophages, dendritic cells PMN (inducible)	Monocytes, macrophages, B cells, platelets, basophils, PMN, Langerhans cells, eosinophils, endothelial cells[a], T cells[a], dendritic cells[a].	IIIa:macrophages, NK cells, monocytes[a], T cells[a] IIIb: PMN
Modulation: Up	GCSF, IFN-γ, IL10		TGF-β
Down	IL4, IL13	IL4	IL4

* FcγRII has three subclasses each with different affinity for human IgG:
IIa-R131, 3>1>>>2,4; IIa-H131, 3>1=2>>>4; IIb1, 3>1>4>>2

[a] denotes sub-population only

Table adapted from: Deo Y. et al. (1997) (Ref. 138)

Alternative splicing of the IB genes can generate two further transcripts, FcγRIb1 and FcγRIb2 (141, 142), the second being a transmembrane receptor lacking the entire third domain. Whilst this receptor isoform can still bind immune complexes, its ability to bind monomeric IgG is lost.

As a consequence of high affinity binding, circulating monocytes are typically saturated with serum Ig. MAb targeted against the receptor must therefore bind outside of the natural ligand-binding domain of the molecule if they are to bind in the presence of this barrier. With the exception of 10.1 that does partly block ligand-binding, the majority, including mAb-22, have been shown to bind outside of the natural Fc binding site (143). MAb-22 is generally considered one of the best mAb available, and is the Ab used in the bispecific derivatives described in this thesis.

Various cytokines have been shown to upregulate and even induce FcγRI expression on certain cells. Monocytes and macrophages show constitutive expression of the receptor, with basal levels being at around 15-40 x 10^3 and 50 x 10^3 molecules / cell respectively. Receptor levels are increased 10 fold on exposure to IFN-γ or G-CSF (144). FcγRI expression can be induced on PMN following G-CSF treatment (145, and chapter 4) as well as with IFN-γ.

1.10.7.2. FcγRII (CD32)

FcγRII is a 40 kDa glycoprotein low affinity receptor, displaying an impressively broad pattern of distribution on a variety of cells including monocytes, macrophages, PMN, large granular lymphocytes, and B cells (146), as well as platelets, langerhans, and endothelial cells (147). There are six isoforms (IIa1-2, IIb1-3, IIc) encoded by three distinct genes, IIA, IIB, and IIC. Structurally, all have two Ig like extracellular domains, sharing a high degree of homology, the main differences between each isoform lying in the transmembrane/cytoplasmic domains. The IIB gene undergoes alternative splicing events to generate the FcγRIIb1-3 products (148). The FcγRIIb1 receptor has a 19 amino acid insertion, and the FcγRIIb3 isoform a 21 amino acid deletion as compared to FcγRIIb2. The IIA gene is closely related to IIB, except for an internal deletion, and it appears that IIC may well have arisen from an unequal

cross over event between the two (148).

1.10.7.2.1. Polymorphisms

Two allotypic forms of FcγRIIa are known (149). These have been designated HR (high responder) and LR (low responder) according to whether their expression on monocytes will stimulate high or low levels of T cell proliferation in response to anti-CD3 murine IgG1. Studies with mAb 41H16 show the polymorphism to be expressed on mononcytes, macrophages, PMN, and platelets (146). Molecular discrepancies between the polymorphisms have been charted to amino acid substitutions at two distinct sites. The first is at position 27 in the first Ig like domain, where a tryptophan residue is present in the LR, replaced by a glutamine in the HR (149). The second lies at position 131 located in the second Ig like domain of the receptor, which has an arginine (HR) versus a histidine (LR) (150). It is the variation at this position that is critical for the functional polymorphism (151). Whereas the HR polymorphism is associated with IgG1 binding, the LR receptor is the only FcγR capable of binding human IgG2. This Ig class has particular relevance to the clearance of encapsulated bacteria and studies have revealed a correlation between FcγRIIa allotype expression and susceptibility to infection by bacteria such as Streptococcus pneumoniae. Children frequently suffering from recurrent bacterial infections show a tendency to present the HR polymorhism (152). Individuals with monocytes/PMN expressing the HR form also show less efficient phagocytosis of IgG2 opsonised bacteria than those carrying the LR form. This points to a crucial role of the LR receptor in resistance to certain bacterial infections.

A further polymorphism in FcγRIIb1 has been noted, with a single amino acid change in the cytoplasmic tail from a tyrosine to an aspartic acid (152). The functional consequence of this is unknown.

1.10.7.3. FcγRIII (CD16)

FcγRIII is a 50-80 kDa glycoprotein bearing two Ig like extracellular domains. Two distinct genes – IIIA and IIIB – encode two isoforms of the receptor, which are

presented in a cell type specific manner. The first molecule, FcγRIIIa, is a medium affinity, transmembrane receptor found predominantly on macrophages and NK cells as well as a small sub-population of peripheral blood monocytes (139). The membrane bound α-chain associates with various signaling sub-units. On macrophages it forms a heterodimer with the γ chain of the high affinity FcεR, on NK cells it is coupled to the ζ chain signal transduction molecule of the TCR, and on mast cells it associates with the β-chain of FcεRI (153, 154).

The IIIb isoform is a low affinity, glycosylphosphatidylinositol (GPI) linked receptor, expressed at high levels on the plasma membrane of PMN populations. However, on exposure to the cytokine TNF, levels of FcγRIIIb on the surface of PMN have been shown to drop. This is believed to be due to the activation of an endogenous phospholipase by the TNF, which cleaves the GPI bond, releasing the receptor from the cell (155). Functionally, FcγRIIIb would appear to have no obvious access to signaling pathways itself. On PMN it has been shown capable of initiating exocytosis (156) but not phagocytosis or respiratory burst systems. It has been postulated that it is employed as a mobile binding molecule, capable of presenting ligand to FcγRII, which then activates cellular responses. However, some conflictory evidence suggests that FcγRIIIb can mediate signaling events independently of any association with FcγRII. In PMN, increases in intracellular calcium levels following engagement have been reported (157), as well as phagocytosis of concanavalin A treated erythrocytes (158), and induction of actin polymerisation (159), a precursor of various effector functions. Whether these events are an indication of independent FcγRIIIb signaling remains controversial, but they could be explained by interactions with receptors other than FcγRII. An association with complement receptor 3 (CR3, MAC-1) has been implied as FcγRIII and CR3 co-cap on the surface of PMN, and co-operation between the two is necessary for certain phagocytic and respiratory burst activities (160).

The genes encoding the IIIa and IIIb receptor isoforms are extremely homologous. On translation, the critical difference between the two in determining whether the encoded receptor will be transmembrane or GPI-linked has been charted to a single amino acid at position 203. The IIIa gene encodes a phenylalanine at this position, which confers membrane integration, whereas the IIIb has a serine residue, specifying

GPI-linkage (161).

1.10.7.3.1. Polymorphisms

There are two major polymorphisms of FcγRIII. The first is in the IIIa receptor, which has two allotypes defined by a single amino acid change at position 158 (substituting a valine for a phenylalanine) (152). The functional consequence of this variation is the differential capacity of the two allotypes to bind IgG1, IgG3 and IgG4.

A second polymorphism is exhibited by the IIIb receptor expressed on PMN. Denoted NA, shorthand for the biallelic neutrophil antigen system, there are two forms NA1 and NA2 (162). These were first identified by their involvement in blood transfusion reactions and autoimmune neutropenias. They are characterised by differences in molecular weights following N-glycanase digestion: NA1 runs on SDS-PAGE as a 29 kDa band, and the NA2 as a 33 kDa band. They are further distinguishable by their reactivity with mAb specific for either form. At the molecular level individuals homozygous for either polymorphism revealed cDNA sequence discrepancies, corresponding to variations at specific amino acid positions (163). Amino acids at two positions – 63 and 82 – are accountable for the structural differences between the two, manifested as an extra pair of glycosylation sites in the NA2 form, giving it six rather than the four observed in the NA1 allotype (164). Functionally, the NA2 form has been shown to trigger much lower levels of phagocytosis than the NA1.

1.10.7.4. Soluble Fcγ Receptors

As well as the nine membrane bound FcR mentioned above, there are also soluble variants for all three classes. These can be generated either at a genetic level by mutations in coding regions, or by proteolytic cleavage of transmembrane receptors from the cell surface. FcγRII has two soluble receptors. Langerhans cells encode an isoform of FcγRIIa (IIa2) which lacks a transmembrane coding exon, and is therefore released in a soluble form; and a secreted FcγRIIb1 molecule, released by proteolytic cleavage from B cells has been reported (165). Similarly, FcγRIIIa can be solublised - NK cells release the receptor on activation. Likewise, the GPI-linked IIIb receptor can

be proteolytically cleaved from the surface of PMN by serine proteases following their activation (155). The FcγRI transcripts that encode a stop codon in their EC3 domain (FcγRIb1 and FcγRIc) may well, if translated in their entirety, also encode soluble products (152).

The soluble receptors appear to have a role in immune regulation, especially with regards to IgG, where several reports indicate inhibition of complement binding/activation, as well as interference with ADCC and regulation of Ig production (Reviewed in 165).

1.10.7.5. FcγR Signaling

The initial step in triggering activation is cross-linking of the receptor by multivalent antigens, a process simulated by anti-FcγR mAb. Cross-linking the receptor causes aggregation, a pre-requisite of signal induction. A complex cascade involving numerous protein tyrosine kinases (ptk's) and other molecules is then activated, leading to instigation of effector functions such as ADCC, phagocytosis and mediator release.

The primary event following receptor aggregation is phosphorylation which occurs at defined motifs (ITAM) within the cytoplasmic tail of the γ ,ζ,and β sub-units as well as in the α chain of FcγRIIa (see Figure 1.4). The ITAM serves as a molecular scaffold for recruitment of various signaling molecules in a defined cascade. Src-family PTK associated with the receptors become activated, resulting in ITAM phosphorylation and recruitment of Syk/ Zap-70 PTK. These are in turn responsible for the observed tyrosine phosphorylation of phospholipase C (PLC) and protein kinase C (PKC) which act on a variety of downstream molecules, ultimately resulting in cellular activation. A full review of the signaling pathways involved can be found in (166 and 167).

The ITAM motifs present in the FcγRIIa α and γ chain display functional differences in their ability to trigger IL-2 release and antigen presentation (168). Moreover, the FcγRIIb isoform contains an inhibitory ITIM motif (rather than an ITAM) functioning

as a negative regulator of B and mast cell activation.

1.10.7.6. Biological Function

The type of biological response initiated by receptor ligation can be categorised as either an internalisation process, such as phagocytosis, or a specific cellular activation event, such as ADCC or the release of inflammatory mediators. By and large, effector functions are determined by the cell type and the activation or differentiation state of that cell, rather than by the class of receptor expressed on its surface.

1.10.7.6.1. ADCC

In vitro mAb studies have demonstrated a variety of cells competent for ADCC when signalled through FcγR. Indeed, on myeloid cells such as monocytes, macrophages and PMN, FcγR are the only molecules capable of initiating ADCC of tumor cells (169). Monocytes are capable of erythrocyte lysis triggered exclusively through FcγR, regardless of the receptor class (170). ADCC by PMN is primarily triggered through FcγRIIa (171), but reports show cytoxicity can be achieved via FcγIIIb (170). On administration of cytokines, such as IFN-γ, induction of FcγRI mediated ADCC becomes evident, a process at which FcγRI is particularly efficient (172). NK cell mediated ADCC occurs via FcγRIIIa (168)

1.10.7.6.2 Phagocytosis

Cellular transfection studies have been invaluable in determining the molecular mechanisms underlying phagocytosis. Prime candidates for transfection are COS cells which lack endogenous gamma receptors, but retain functional phagocytic capability when transfected with FcγR of any class (166). Transfection studies have shown that all three classes of receptor are able to mediate phagocytic signals. However, there is a critical requirement for ITAM. FcγRIIa which is unique in having endogenous α-chain ITAM is able to induce phagocytosis, providing the motif is intact (173). However, wild type IIb isoforms do not induce phagocytosis (174) and FcγRI/ FcγRIII transfectants are only able to do so in the presence of a common γ sub-unit

(175). The precise signaling pathways involved in phagocytosis are reviewed in (176).

FcγR of all classes can trigger phagocytosis/ endocytosis by macrophages (177), whereas on PMN FcγRIIa is the most active constitutively expressed receptor, and on DC both FcγRII and FcγRI can induce such processes (178). Internalisation mediated by FcγR appears to play an important role in enhancing antigen presentation by APC and subsequent activation of immune responses (179, 180).

1.10.7.6.3. Mediator Release

Cross-linking of FcγRs may also result in the release of a variety of soluble mediators including leukotriene C, prostaglandins, and lysosymal enzymes (181, 182, 183). These have roles in effector activation and ADCC.

Cytokine release has also been demonstrated following stimulation of all three receptor classes. Cross-linking of FcγRI induces secretion of IL-1 (184), IL-6 (185) and TNF-α (186) by monocytes. IL-6 production by PMN is also mediated through FcγRI (and FcγRII) (187). On monocytes, FcγRIIa induces cytokine synthesis in an isoform dependent fashion. Cross-linking of the HR isoform results in production of TNF-α, IFN-γ, and IL-6, whereas LR cross-linking fails to stimulate production of any of these cytokines (188). Finally, FcγRIII expressed by NK cells has been shown to mediate IFN-γ and TNF-α production following interaction with B cell bound Ig (189).

1.10.7.6.4. FcγRIIb1: Negative Regulation

FcγRIIb1 is present on B cells where co-ligation with the BCR, brought about by cross-linking with immune complexed IgG, leads to production of a dominant, negative signal (190). This results in inhibition of proliferation and cessation of Ab production by the lymphocyte. Signaling through the FcγR is mediated by a 13 amino acid ITIM motif in its cytoplasmic domain, which binds SH2 containing proteins on phosphorylation. Two proteins in particular have been shown to associate with

activated ITIM: the phosphotyrosine phosphatase SHP-1 (191), and the SH2-domain containing inositol polyphosphate 5-phosphatase, SHIP (192). Whilst precise signaling pathways remain to be resolved, an absolute requirement for SHIP has been shown, with the molecule believed to function by competitive binding of Shc, thus preventing induction of Ras activation and other downstream kinases (193). Hippen et al. have also demonstrated that cross-linking of BCR with FcγRIIb can promote negative signaling through dephosphorylation of the co-receptor CD19 (194). A similar role has been reported for FcγRIIb on mast cells, where co-ligation with FcεRI can modulate IgE-mediated activation (195).

More recently, Clynes et al. (196) have demonstrated a role for FcγRIIB in regulating ADCC. The inhibitory receptor is capable of modulating the activity of FcγRIII, and mice deficient for FcγRIIB show increased ADCC activity.

1.10.7.6.5. Autoimmunity and Inflammation

FcγR have been implicated in a variety of autoimmune/inflammatory disorders such as systemic lupus erythematosus (SLE) (197), rheumatoid arthritus (RA) (198), and autoimmune hemolytic anaemia (199). The involvement of FcγR in these disorders has been clearly demonstrated through the use of γ chain knockout mice (200). Immune complexes formed with autoantibodies can bind FcγR on leukocytes, and also activate complement, initiating an inflammatory response. The local increase in vascular permeability promotes PMN infiltration and development of a type III hypersensitivity (Arthus) reaction, in particular linked to FcγRIII (201). Self reactive Ab binding to FcγR on mononuclear phagocytes has also been demonstrated to be responsible for the erythrophagocytosis observed in hemolytic anaemia, and the clearance of platelets in thrombocytopenia, linking FcγR to type II hypersensitivity reactions (199). Similarly, anti-FcγRIII Ab have been detected in RA patients (198). These could be responsible for activation of macrophages in synovium, which in turn potentiate the connective tissue destruction observed in RA sufferers (202).
Failure to clear immune complexes in an efficient manner contributes to the pathogenesis of a variety of immune conditions. Down regulation of FcγR or disruption of their signaling pathways may well be responsible for the build up of

autoantibody complexes observed in disorders such as SLE (197). Receptor polymorphisms may also contribute to certain conditions. For example, the R/R-131 FcγRII allotype has been associated with increased levels of autoantibody in SLE patients, and a higher susceptibility to autoimmune haemolytic anaemia (203).

1.10.7.7 Fcγ BsAb

The capacity to trigger a variety of biological functions, and their presence on a range of readily mobilised effector cells, makes FcR an ideal target for BsAb. To date FcγRI, FcγRIII and FcαRI have proven the most suitable target molecules. BsAb directed against CD16 on NK cells have demonstrated high levels of ADCC *in vitro* (204) and a number of clinical trials have been performed showing their potential in treatment of Hodgkin's lymphoma, breast, ovarian, and colorectal cancers (205, 206). Much attention has been focused on FcγRI, particularly in the recruitment of PMN. Several clinical trials are in progress, with particular attention aimed at the HER-2/neu proto-oncogene product, c-erbB-2. This protein is overexpressed by a variety of malignancies, including many breast cancer cells (207). PMN show efficient killing of HER-2/neu positive breast cancer lines, when stimulated with IFN-γ/G-CSF and retargeted by BsAb directed to FcγRI (208). Furthermore, Heijnen et al (209) have demonstrated that PMN can be effectively recruited *in vivo* with such derivatives, and it is becoming increasingly clear that PMN are a highly effective cellular population for tumor depletion. Other groups have employed BsAb targeting FcγRI expressing effectors towards CD15 on acute myelogenous leukaemia (AML) cells (210), and epidermal growth factor (EGF) receptor on myeloma cell lines (211). Recently, the FcαR (CD89) has become a favoured target on PMN, not least because it is constitutively expressed, unlike FcγRI. BsAb to FcαRI display activity against a range of tumor antigens (212), and have proved particularly effective at clearing bacterial infections (213).

1.11. Neutrophils

PMN constitute 45-70% of the total circulating human leukocyte population, at between 2.5 – 7.5 x 10^9/ml. During an infection these numbers increase further (a

process known as leukocytosis). PMN are attracted to sites of infection and inflammation, and are able to destroy infectious agents opsonised by Ab or complement. Processes of engulfment and degranulation then release a cocktail of cytotoxic substances from PMN granules which are capable of destroying the opsonised target (214). There are four classes of PMN granule: azurophil, specific, gelatinase and storage, which are developed at different stages of PMN differentiation, and contain a range of neutral proteinases, acid hydrolases, antimicrobial peptides and other defence molecules (as detailed in Figure 1.5).

The most effective antimicrobial defence mechanism in the PMN arsenal is the myeloperoxidase (MPO) system. MPO is stored in azurophil granules, and is an enzyme that catalyses the conversion of hydrogen peroxide (H_2O_2) to hypochlorous acid (HOCL) (215). H_2O_2 is formed during the respiratory burst, a process involving rapid oxygen consumption by activated PMN, simultaneous to phagocytosis. HOCL is the most powerful antimicrobial substance generated by PMN, being up to 1000 times more toxic than H_2O_2 and inducing rapid cell death. In addition to HOCL, a number of other reactive oxygen and nitrogen intermediates are formed including superoxide, hydroxyl radical, singlet oxygen, nitric oxide and peroxynitrite (reviewed in 215), as well as a variety of proteinases (reviewed in 216).

PMN activity can be regulated both positively and negatively by a variety of biological mediators. Leukotrienes, platelet activating factor (PAF), insulin-like growth factor 1, and prolactin all enhance PMN activity by priming the oxidative burst; whilst prostaglandins, lipoxins, glucocorticoids, opioids, and histamine all serve to suppress PMN anti-microbial responses (217). A number of cytokines also potentiate or dampen PMN functions - some produced by surrounding cells, some by the PMN themselves. Of particular interest are cytokines such as IFN-γ and G-CSF, which amplify levels of FcγRI on PMN, as well as increasing actual numbers of circulating PMN (145 and chapter 4).

Fig.1.5. PMN granules: their contents and activity. Shown is a cartoon depicting the four classes of PMN granule (azurophil, specific, gelatinase, and secretory), together with the developmental stage at which they are produced. Listed are the main granule contents, and their specific activity. Adapted from: Gullberg U et al. (1997) (Ref. 214)

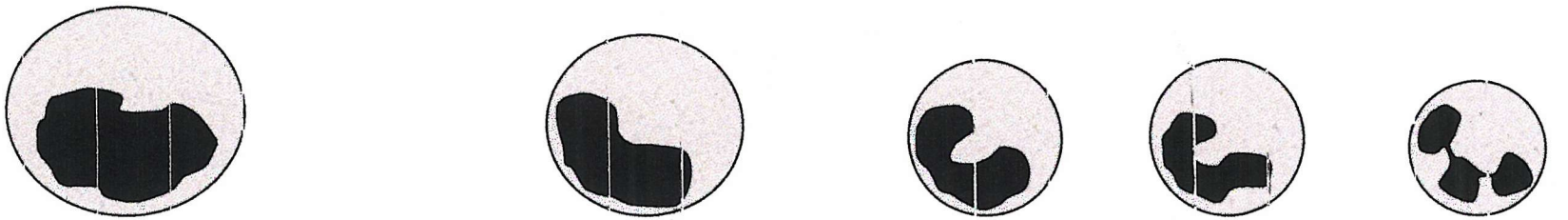

AZUROPHIL (PRIMARY)

CONSTITUENT	ACTIVITY
BPI	Perforin type protein, highly toxic to gram-negative bacteria, also able to neutralise endotoxin.
Defensin	Small, membrane permeabilising peptides cytotoxic to a range of fungi, bacteria and viruses. Constitute 30-50 % granule contents.
Lysosyme	Degrades cell walls of gram-positive bacteria.
Myeloperoxidase	Converts H_2O_2 to HOCL.
Cathepsin B	Digests internalised proteins, activates proenzymes.
Cathepsin D	Degrades intracellular proteins, and proteoglycans.
Phospholipase A2	Cleaves phospholipids.
Cathepsin G	Hydrolyses proteins in bacterial cell envelopes.
Elastase	Hydrolyses proteins in bacterial cell envelopes.
Proteinase 3	Degrades extracellular matrix proteins.

SPECIFIC (SECONDARY)

CONSTITUENT	ACTIVITY
Cathelicidins	Anti-microbial proteins eg.hCAP-18
Collagenase	Cleaves helical collagens, serpins and other matrix macromolecules.
Gelatinase	Degradation of gelatins, some collagens and components of the basement membrane.
Lactoferrin	Sequesters free iron preventing microbial growth, and increases permeability to lysosyme.
Lysosyme	Degrades cell walls of gram-positive bacteria.
Histaminase	Degradation of histamine

GELATINASE (TERTIARY)

CONSTITUENT	ACTIVITY
Gelatinase	Degradation of gelatins, some collagens and components of the basement membrane.

SECRETORY VESICLE

CONSTITUENT
Mainly plasma proteins

Membrane-bound cytochrome b_{558}, FMLP-R, CR3/CR4, Laminin-R

To date, the majority of mAb examined both in the clinic and in murine models have proved to offer little benefit in terms of therapy. Whilst there are exceptions (such as anti-CD20, and anti-CD40), most are relatively ineffective. One of the reasons for this failure has been attributed to inefficient effector cell recruitment by mAb. In an effort to overcome this, BsAb can be produced to redirect host immune cells to tumor, directly the bridging the two together, and focusing an attack against the malignancy. The aim of this project was to determine which antigens on the tumor, and which cytotoxic trigger molecules on the effector cell, made the most successful targets for therapy. To address this question, two murine models of B cell lymphoma – A31 and BCL_1 - have been employed. A panel of $F(ab')_2$ BsAb were produced against a range of B cell antigens, including tumor Id, MHC II, CD19, CD22, and CD40 to determine which made the most suitable tumor molecule to target. The second arm of the derivative was aimed at two different effector species, T cells via CD3 and CD2, and PMN via human FcγRI. In the second instance, a transgenic model, produced by Ingmar Heijnen and Jan van de Winkel, University of Utrecht, was employed, with BsAb given in combination with G-CSF.

We aimed to examine the activity of the panel of BsAb derivatives in both models and assess the relative therapeutic merits of targeting the different effector species (T cell or PMN), to the different tumor antigens. A major part of the work was to investigate their activity *in vivo*, a feat that is not often possible, due to lack of suitable animal models. We also aimed to identify the mechanism of activity for any of the BsAb that did prove to be therapeutic, as understanding how these derivatives function *in vivo*, is critical to the future design of BsAb for clinical application.

We also wished to investigate the potential for improving the activity of traditionally non-functional mAb, through a process of homodimerisation. Again, a panel of Ab dimers was produced against human B cell lymphoma antigens, and the activity of the dimers compared to monomeric IgG, using extensive *in vitro* and *in vivo* analysis.

Chapter 2
Materials and methods

2.1 Cell lines and animals

Daudi, Raji, and EHRB cell lines (European Collection of Animal Cell Cultures [ECACC], Porton Down), were cultured in RPMI 1640 medium (Life Technologies, Paisley, Scotland), supplemented with 100 Units (U) /ml penicillin (Glaxo), 100 μg/ml streptomycin (Evans), 50 U/ml amphotericin B (Fungizone; Squibb and Sons), 2 mM L-glutamine (Life Technologies), 1 mM pyruvate (Life Technologies) and 10 % Foetal Calf Serum (FCS) (Myoclone Plus; Life Technologies).

The π BCL_1 cell line (218) is a variant of the BCL_1 tumor that can be maintained both in culture and *in vivo*. Cells in culture are grown in supplemented RPMI 1640 medium (as above) with 20 % FCS and 50 μM 2-Me (BDH, Poole, U.K).

All *in vitro* cell lines were maintained at 37^0C in a 5 % CO_2 humidified incubator. Media was replenished every 2-3 days. Cells used for growth inhibition or apoptosis studies were maintained in log phase of growth for 24 hours prior to experiment.

BCL_1 (219) and A31 (220) mouse B-cell lymphoma lines were maintained by *in vivo*, intra-peritoneal (i.p) passage in BALB/c and CBA mice respectively. Enlarged spleens were taken at the terminal stage of disease, homogenised and lymphocytes isolated by centrifugation on lymphoprep at 2500 rpm for 20 mins. Single cell suspensions were passaged at 10^6 - 10^7/mouse. BALB/c and CBA/H mice were all supplied by Harlan UK (Blackthorn, U.K.). FcγRI transgenic FVB/n male mice were a kind gift from I. A. F. M. Heijnen and Prof. J. G. J. van de Winkel, University of Utrecht, Netherlands (221).

2.2 Cell quantitation

Cell concentrations were determined using a Coulter Industrial D Cell counter (Coulter Electronics, Bedfordshire)

2.3 Monoclonal antibody production

MAb was prepared from ascites, essentially by the method of Elliot et al. (222), prior to further purification.

2.3.1 IgG preparation from ascites

Ascitic fluid was pre-cleared by centrifugation at 1000 g for 20 mins, prior to passage through a 0.2 μm filter. The ascites was then passed through a G25 fine (Pharmacia Biotech) column in 0.03 M Tris buffer containing 0.01 M EDTA, pH 6.5 and directly onto an S-Sepharose (Pharmacia Biotech) column equilibrated in the same buffer. Unbound protein was then washed by the addition of two column volumes of buffer, and the bound protein eluted with buffer containing 0.5 M NaCl/ 0.5 M Tris and 0.01 M EDTA, pH 8.7. Eluted protein was then blended with an equal volume of this buffer and passed onto a protein A (Pharmacia Biotech) column, equilibrated in 0.5 M Tris buffer containign 0.01 M EDTA, pH 8.7. Unbound protein was then washed off, using this buffer. Bound Ig was subsequently eluted by the addition of 0.1 M glycine containing 0.001 M EDTA, pH 3. The pH of the collected protein was then adjusted with the addition of 0.2 M Tris to pH 4.8.

2.4 Enzyme-linked immunsorbant assay (ELISA)

ELISA were routinely performed to detect for the presence of various proteins. Primary antibody or coating molecule was diluted in coating buffer (15 mM Na_2C0_3, 28.5 mM $NaHC0_3$, pH 9.6) and added 100 µl/well to treated 96 well plates (Maxisorb, Nunc) either for 1 hour at 37°C or overnight at 4°C. Unbound antibody was removed by flicking the solution from the plate and the plates non-specific binding sites blocked by the addition of blocking solution (1% (w/v) BSA in PBS) for 1 hour at 37°C. The plate was then washed twice with wash solution (PBS-T) and the next reagent added, in a final volume of 100 µl/well, with all dilutions being made in blocking solution. Following incubation for 90 mins at 37°C, the plate was washed again (x 5 in wash solution).

An HRP-conjugated antibody, specific for the previous reagent, was then diluted to its working concentration in blocking buffer and added (100 µl/well) for a final 90 mins. Following washing (x 5), HRP substrate (20 mg o-phenyldiamine free base (o-PD), 100 ml phospo-buffered citrate pH 5.0 + 20 µl (60% w/v) H_20_2) was added and incubated in the dark at 37°C. The reaction was terminated by the addition of 50 µl/well 5 M H_2S0_4 and the subsequent colour change quantified by measurement of absorbance at 495 nm on an automatic fluorometer (Dynatec 400, Dynatec). Colour change was proportional to protein concentration and unknowns were determined using standard calibration curves of known concentration, on the day of each ELISA.

2.5 Dialysis

Dialysis of samples was performed using Visking tubing (Medicell, London). Samples were dialysed 1:1000 in at least 3 changes for a time of at least 2 hours per change.

2.6 F(ab')$_2$ production

F(ab')$_2$ fragments were commonly prepared by pepsin digestion using the methods detailed by Glennie et al. (223). For digestion of polyclonal IgG, the sample was first concentrated to approximately 10 mg/ml and dialysed with 0.07 M sodium acetate /0.05 M NaCl, pH 4.0. The sample was then digested with 0.1 mg/ml pepsin (Sigma chemicals, Poole, Dorset) for 18 hours at 37°C. Monoclonal IgG was concentrated to 10-20 mg/ml, dialysed with 0.2 M TE8.0 and the pH of the sample decreased to 4.1 by addition of 2 M sodium acetate. Digestion was performed by addition of pepsin to a final concentration of 0.3 mg/ml and incubation at 37°C. Samples were removed at intervals and analysed on HPLC (Zorbax GF250 column; Dupont) to monitor the generation of F(ab')$_2$. The digestion was halted when either less than 10% of the sample remained as IgG or when the proportion of F(ab')$_2$ was no longer increasing. This was done by increasing the pH of the solution to pH 8.0, by addition of 1 M Tris.

Digestions usually required 4 - 8 hours to achieve completion. Digestion products were then separated on 0.2 M TE8.0 equilibrated Ultrogel ACA44 (Pharmacia). All products were dialysed with PBS prior to use.

2.7 BsAb F(ab')$_2$ production

The production of bispecific derivatives was performed essentially as described by Glennie et al. (223). Firstly, F(ab')$_2$ fragments of the 2 mAb partners were produced and concentrated to 5 mg/ml. One of the antibodies was then reduced with 5 mM 2-mercaptoethanol (2-ME, BDH) for 30 mins at room temperature to generate Fab'γ-SH fragments which were then stored on ice. Pure Fab'γ-SH fragments were then obtained by

passage through Sephadex G-25 medium (Pharmacia) at 4°C, which had previously been equilibrated with 0.05 M acetate buffer containing 0.0005 M EDTA, pH 5.3 and nitrogen purged.

The above process was then repeated for the second mAb. From this point onwards in the preparation the temperature was kept at 4°C. One of the antibodies was selected for alkylation.

Alkylation was achieved by addition of a half volume of 12 mM o-phenylenedimaleimide (o-PDM; Sigma) in dimethylformamide (DMF, BDH) for 30 mins (at 4°C) and Fab'γ-mal fragments subsequently separated on the Sephadex G25 column used above.

The Fab'γ-mal was then added to the Fab'γ-SH fragments of the first mAb at a ratio of 1:1 and immediately concentrated to 5 mg/ml by ultrafiltration under nitrogen gas at 4°C. After 18 hours the pH of the reaction mixture was adjusted to pH 8.0 using 1 M Tris-HCl (pH 8.0) before reduction with 2-ME (20 mM) for 30 mins and subsequent alkylation with IAA (25 mM). Bispecific $F(ab')_2$ antibody fragments were then separated on 0.2 M TE8.0 equilibrated ACA44 and dialysed with PBS prior to use.

2.8 Immunosorption

Immunosorption, using antigen-linked Sepharose-4B was used to remove irrelevant antibodies from immune sera or remove residual Fc contaminants from $F(ab')_2$ or Fab'γ preparations. Cyanogen bromide activated Sepharose-4B (Pharmacia), was washed in 0.1 M HCl and suspended in 0.2 M citrate, pH 6.5 before addition to the antigen. The mixture was then incubated at 4°C overnight. The linked Sepharose was then washed in citrate buffer before incubation with 1 M ethanolamine-HCl, pH 9.5 for 1 hour at room temperature and further washing with 0.5 M NaCl / 0.1 M Tris-HCl / 0.005 M EDTA (HM Tris). Using this protocol, antigen was linked to Sepharose-4B at a concentration of 10 mg protein/ml gel.

Polyclonal anti-mouse Fab'γ fragments were purified using an anti-mouse $F(ab')_2$-linked Sepharose-4B column. Bound material was eluted by addition of 2 column lengths of 0.5 M ammonium / 1 M potassium thiocyanate, and dialysed immediately with cold HM Tris. Aggregates were removed by passage through Ultrogel ACA34 (Pharmacia) and the purified fragments collected, pooled and dialysed with PBS prior to use. For monoclonal $F(ab')_2$ or Fab'γ preparations, a sheep anti-mouse Fcγ linked sepharose column was utilised. To purify sheep polyclonal preparations a rabbit anti-sheep Fcγ Sepharose-4B column was used. In both instances, the unbound fraction was collected, concentrated, and dialysed with PBS prior to use.

2.9 Fluorescein conjugation of Ab

Antibody was fluorescein labelled by the method of Holborrow and Johnson (224). 4.5 ml of normal saline (0.15 M NaCl, pH7.4) was added to 50 mg of Ab in the presence of 1 mg of the FITC isomer I (BDH) dissolved in 0.5 M carbonate buffer pH 9.5 and incubated for 45 mins at 25°C. Unconjugated FITC was then removed by passage of the reaction mixture through a G-25 Fine (Pharmacia) column, equilibrated with 0.0175 M phosphate buffer, pH 6.3, followed by passage through a DEAE-cellulose column.

The majority of the FITC-conjugated mAb was eluted with 0.5 M NaCl in 0.0175 M phosphate as determined by measuring conjugate:protein ratios during elution (calculated as absorbance at 495 nm and 278 nm respectively). Material with a ratio of 0.4-1.0 was pooled for use with final mAb concentration calculated as:

Antibody concentration (mg/ml) = Absorbance (278 nm) - (0.26 x Absorbance (495 nm)) / 1.35

2.10 FACS analysis

In general, cells at $1x10^6$/ml were incubated at 4°C for 30 mins with the fluorescein conjugated (direct) or unlabelled (indirect) antibody of choice (20 –50 μg/ml). Cells were

then washed once (direct) or twice (indirect) in PBS-BSA-Azide (PBS, 1 % Bovine Serum Albumin fraction V (BSA; Wilfred Smith Ltd, Middlesex), 20 mM NaN_3) and resuspended at approximately $1x10^6$/ml. For indirect immunofluorescence, cells were further incubated for 30 mins at 4°C with an FITC-conjugated secondary antibody directed to the first antibody and washed once in PBS-BSA-Azide before resuspension to $1x10^6$/ml and subsequent analysis

Analysis was performed on a FACScan flow cytometer or FACS Calibur (Becton Dickinson, Mountain View, CA, USA). Routinely, 5 - 10,000 events were collected per sample for analysis. Cell debris was excluded by adjustment of the forward scatter (FSC) threshold parameter. FITC was excited at 488 nm with emission intensity being recorded in the 515-545 nm wavelength region. Samples were analysed using LYSIS II software (Becton Dickinson). Fluorescence intensities were assessed in comparison to negative control samples and expressed as histograms of fluorescence intensity versus cell number.

2.11 Measurement of Cell Cycle and Apoptosis

2.11.1 Propidium Iodide (PI) assay

Samples were analysed essentially as per the method of Nicoletti et al., (225). Briefly, samples of 0.5 x 10^6 cells were taken and centrifuged for 5 mins at 500 g. Samples were then washed x1 in PBS, resuspended in hypotonic fluorochrome solution (50 μg/ml Propidium Iodide, 0.1 % (w/v) Sodium citrate, 0.1 % (v/v) Triton X-100) (hypo-PI), and stored in the dark at 4°C overnight or 1 hour at room temperature.

Analysis of samples was performed on a FACScan flow cytometer (Becton Dickinson). Due to the small size of these particles all analysis was performed at low speed. PI bound nuclei fluoresce in the red wavelength. This was analysed using a 488 nm argon laser for excitation and a 560 nm dichroic mirror and 600 nm band pass filter (bandwidth 35 nm) for detection. All fluorescence data was expressed on a logarithmic scale, as this gave

tighter DNA peaks and lower coefficients of variation. The red fluorescence peak was adjusted to around channel 250 on the logarithmic scale, using the G1 peak of a sample as standard. Simultaneous Forward light scatter (Fsc) and Side light scatter (Ssc) data were also collected. Fsc threshold was adjusted experimentally to exclude debris.

2.11.2 FSC vs SSC Analysis

Another method of measuring apoptosis utilised in this study was based upon the physical characteristics of apoptotic versus viable cells and was adapted from the method of Dive et al. (226). Apoptotic cells undergo cytoplasmic shrinkage and condensation as well as nuclear condensation, such that cells which display both reduced Fsc (smaller) and increased Ssc (more granular) characteristics can be distinguished as apoptotic.

In practice, cells were seeded at 0.5 x 10^6/ml in small flasks and incubated in a humidified CO_2 incubator at 37°C for the required time in the desired treatment. Cell samples (400 µl) were then harvested and washed once in PBS, before re-suspension into 1 % (w/v) paraformaldehyde and incubation at 4°C for 16 - 24 hours. Samples were subsequently agitated just prior to analysis, which was performed via flow cytometry using a FACScan. Fsc and Ssc parameters were adjusted to maximise separation of viable and apoptotic populations. LYSIS II software was used for data analysis. Fsc versus Ssc dot plots were generated for analysis. Gating of viable and apoptotic regions, based upon positive and negative controls, was used to quantify apoptosis.

2.12 ADCC/ RCC

Cells were labelled at 1x10^7/ml in supplement free media with 100 µl $Na_2{}^{51}CrO_4$ (Amersham, UK) per ml for 30 mins at 37°C. Excess ^{51}Cr was then removed by washing 4 times with media (supplement free) and the cells resuspended in complete media at 2x10^5/ml. 50 µl of labelled cells was then added to 50 µl of treatment Ab and incubated at 4°C for 15 mins before addition of correctly diluted effector cells and incubation for 30 mins at 37°C. Following incubation, cells were sedimented at 520 g for 5 mins and 200 µl

aliquots of supernatant removed for counting on a γ-scintillation counter (Rackgamma II, LKB) to determine levels of ^{51}Cr release. A sample of cells was treated with 1 % Nonidet P40 (NP40) to determine maximal release under detergent lysis.

Samples were prepared in duplicate, the mean values determined and expressed in terms of % specific lysis, (taking NP-40 lysis as 100%), using the equation below. Background was determined as the amount of spontaneous ^{51}Cr release.

$$\%\ ^{51}Cr\ release = \frac{Sample\ release - background\ release}{maximum\ release - background\ release} \times 100$$

2.13 Preparation of effector cells

For studies using T-cells as effector cells, lymphocytes isolated from homogenised spleens of BALB/c mice were cultured at 10^6/ml in 10 % supplemented RPMI plus anti-CD3 (1452C11; 1 μg/ml), for 72 hours at 37^0C in a CO_2 incubator. Cells were washed once in medium before use in the assay.

For studies using PMN as effector cells, PMN were isolated from murine blood obtained from cardiac puncture into a heparin coated syringe. Where appropriate mice were primed with 2 μg muG-CSF, sub-cutaneously (s.c), 4 days prior to bleeding. Whole blood was mixed in a ratio of 4:1 v/v with a 5 % solution of Dextran T500, at 37^0C for 30 mins. Supernatant was then layered onto a discontinuous Percoll gradient of 63 % and 68.5 % Percoll according to the method of Repp et al. (242). Samples were spun at 2300 rpm for 20 mins, and PMN collected at the interface between the two Percoll layers. PMN were washed once in 10% RPMI and resuspended in the same media at an appropriate working concentration.

2.14 Complement assay

^{51}Cr labelled target cells (prepared as for ADCC assay) were incubated with various concentrations of each antibody or control reagent on ice for 30 mins. Fresh rat serum (final dilution, 1/5 in supplemented DMEM0 was added as a source of complement, and the samples incubated at 37^0C for 45 min. Samples were then centrifuged at 2000 rpm for 5 min to sediment cells, and specific ^{51}Cr release assessed by counting 150 µl of supernatant. All samples were performed in triplicate, and maximum release determined by addition of 1 % Nonidet P-40 to cells. Specific release was calculated as before.

2.15 Serum preparation

Serum from all species was prepared as follows. Whole blood was allowed to clot at room temperature for 30-60 mins. Subsequently, clotted material was collected and centrifuged at 900 g for 20 mins to remove any precipitate. Serum was then stored at -80^oC until use.

2.16 Proliferation assay

Proliferation status of cells was determined by measuring radio-labelled thymidine ($[^3H]$ thymidine) incorporation. Only replicating S phase cells will incorporate ($[^3H]$) thymidine. Therefore, if cells have growth arrested or died, this will be evidenced by a decrease in $[^3H]$ thymidine incorporation compared to controls. Cells were cultured with various reagents at a concentration of $1x10^6$/ml in a final volume of 0.2 ml in flat-bottomed 96 well plates (Nunc). $[^3H]$thymidine was then added (0.5 µCi/well; Amersham, Buckingham) after various times and the cells harvested 16 hours later onto glass fibres (Whatman) with an automated harvester.

Long-term growth inhibition analysis typically involved addition of $[^3H]$ thymidine 24, 48 or 72 hours after cells had been incubated with the given reagent, with a 16 hour incubation being used prior to harvesting.

[^{3}H]thymidine incorporation was subsequently determined via liquid scintillation counting. In all experiments a minimum of triplicates was determined for each sample, with the arithmetic means being calculated and compared.

2.17 Determination of mAb serum half-life

MAb at 1 mg/ml were trace radio-labelled using carrier-free ^{125}I (Amersham International, Aylesbury, U.K) and Iodo-beads (Pierce, Rockford, IL) as the oxidising reagent and were extensively dialysed to remove excess unbound ^{125} I.

200 µl of protein was then injected intra-veinously (i.v) into the tail vein of mice at time zero. Counts were obtained from 10 µl blood samples taken by tail bleeding mice at various sequential time points following injection. Samples were analysed on a β-counter and radioactive decay calculated from 1 min counts. All determinants were performed in duplicate.

2.18 Immunotherapy

For all therapies, groups of age matched CBA or BALB/c mice were injected i.p with 2 x 10^5 A31 or 10^5 BCL_1 tumor cells respectively day 0. For most experiments mice were treated with Ab (i. p) twice daily on days 1 - 5 after the tumor. Both tumors develop primarily in the spleen, with a leukaemic overspill toward the end of the disease.

For FcγRI therapies, groups of age matched F1 mice (BALB/c x FVB/n) or (CBA x FVB/n) mice were utilised. Where appropriate, mice received 2 µg/ day muG-CSF, s.c, administered daily over a 10 day period extending 4 days before and 5 days after the tumor inoculum to mobilise PMN.

CB.17 severe combined immunodeficient (SCID) mice (Harlan, UK) were maintained in isolation in a ventilated cage system (Thoren Caging Systems, Hazleton, PA). Mice

received 5 x 10^6 tumor cells, i.v, day 0 and were treated with antibody on day 7, also i.v, at doses indicated in the text.

Animal immunotherapy was cleared through our local ethical committee and is performed under Home Office licence.

2.19 Tumor cell tracking *in vivo*

To investigate the activity of our BsAb early in the course of tumor development, groups of mice were inoculated with 10^7 BCL_1 tumor cells i.p. on day 0, and then treated with 50 μg BsAb (i. p.), twice daily, on days 1 to 5 (500 μg/mouse in total). Where necessary mice also received muG-CSF (2 μg/day) administered s. c., on days -4 to +5 (10 days in total). Mice were sacrificed on consecutive days throughout the course of therapy, and peritoneal cells removed by lavage with PBS. Cells were washed once by centrifugation, and resuspended in supplemented RPMI at 10^6/ ml.

To detect tumor cells in the exudate, dual-fluorescence staining was performed using FITC-NIMR6 (rat anti-mouse CD22) and PE-Mc10-6A5 (rat anti-BCL_1 Id). Cells were stained with mAb (50 μg/ml) on ice for 15 min. In the case of mice treated with anti-Id mAb, which caused blocking or modulation of the surface Id, cells were stained with FITC-NIMR6 (rat anti-mouse CD22) and PE-ID3 (rat anti-mouse CD19) instead. Following staining, cells were treated with FACS lysis solution to lyse RBC and then washed with PBS containing 1 % BSA, before being analysed.

To detect the presence of tumor cells in the spleen, splenic homogenates were first washed by centrifugation and the cells resuspended in supplemented RPMI at a concentration of 10^6/ml. Dual-fluorescence was then performed (as above) using FITC-NIMR6 versus PE-Mc10-6A5 to detect BCL_1 cells; or FITC-M22 (anti-human CD64) and PE-7/4 (rat anti-mouse PMN; VH Bio, U.K.) to detect PMN.

2.20 Calcium signaling

Intracellular free calcium concentration was measured using the cell permeable fluorescent probe Indo-1-AM (Sigma). Indo-1-AM gives a large shift in fluorescence emission from 482nm to 398nm upon calcium binding, and an increase in the ratio of the 398nm/482nm signal is indicative of increased intracellular free calcium. Cultured πBCL_1 cells (10^7/ml) were washed twice in serum-free media and loaded with Indo-1-AM at 5μM for 30 min at 37^0C. Cells were then washed twice by centrifugation in serum-free RPMI to remove excess dye and resuspended in supplemented RPMI at 2 x 10^6 cell/ml. Labelled cells were stored in the dark at room temperature until used. For the assay, 250 μl of this cell suspension was warmed to 37^0C for 5 min, an equal volume of Ab solution added at a final concentration of 2 μg/ml (or as indicated in the text), and immediately analysed using flow cytometry on a FACS Vantage (Becton Dickinson). Where appropriate, hyper-crosslinking sheep anti-rat IgG, or rabbit anti-hamster IgG was added at a final concentration of 20 μg/ ml immediately prior to analysis. Intracellular calcium mobilisation was estimated by determining the mean fluorescence ratio of Indo-1 bound (398nm, FL5) to free-calcium (482nm, FL4) against time. The response was measured over 300 seconds, and recorded using the Cell Quest program (Becton Dickinson).

2.21 Homodimer production

Homodimer constructs were prepared according to the method described by Ghetie et al (227). 50mg of mAb was divided into two portions for labelling with linker. 25 mg of mAb at approximately 10mg/ml in 0.05M phosphate buffer containing 3 mM Na2-EDTA (PBE) pH 7.5 was mixed with 25 μl of SMCC [succinimidyl 4 – (maleimidomethyl)cyclohexane - 1 – carboxylate] (Pierce) (at 10mg/ml in DMF) for 1 hour at RT. Excess linker was removed by chromatography on a Sephadex G25 column and protein concentrated down to 10mg/ml by Vivaspin 15ml concentrators (Vivascience, Binbrook, UK). 25 mg of mAb at approximately 10 mg/ml was mixed with SATA (N-succinimidyl S-acethylthio-acetate) (Pierce) (at 6.3 mg/ml in DMF) for 1 hour

at RT. Protein was purified on a Sephadex G25 column and concentrated as before. SATA labelled protein was deacetylated with 0.15 M hydroxylamine-HCL for 5 min at RT, before both protein fractions were mixed for 1 hour at room temperature. Mixtures were analysed by HPLC and SDS-PAGE, and dialysed with 0.05M PBE pH7.5 O/N at 4 ^{0}C. Dimers were crudely purified on an AcA44 column, checked by HPLC, concentrated to 5 mg/ml, and filter sterilised with a 0.22 um filter unit (Schleichler and Schuell).

2.22 SDS PAGE analysis

SDS PAGE was performed using a mini-gel system (Hoeffer SE-250) and essentially as described by Lammeli (228). In all cases both the resolving and stacking gels were constructed from a 30 % (w/v) Acrylamide: 0.8 % (w/v) Bisacrylamide stock solution (National Diagnostics; Atlanta, Georgia) which contained 0.1 % (w/v) SDS. Resolving gels were made using a 1.5 M Tris pH 8.7 stock solution and were, unless otherwise stated, 10 % acrylamide. Stacking gels were created using a 0.5 M Tris pH 6.8 stock solution yielding a final acrylamide concentration of 3.0 %. The reaction was catalyzed with N N N' N'-Tetramethylethylene (TEMED) at a final concentration of 0.05 % and 0.1 % for the resolving and stacking gels respectively.

The reaction was initiated with a fresh 10 % (w/v in H_20) solution of Ammonium Persulfate (APS), added at a final concentration of 0.4 % in resolving gels and 1.0 % in stacking gels.

Non-reduced samples were diluted 1:3 in 3X sample buffer (30 % Glycerol (w/v), 9 % SDS (v/v), 0.1875 M Tris-Cl, 0.03 % (w/v) Bromophenol Blue, pH 6.8). Reduced samples were diluted in 3X sample buffer + 10 % (v/v) 2-ME.

Diluted samples were then heated at 100°C for 5 mins and either loaded immediately or stored at -20°C until required.

Gels were run at a constant current of 20 mA per gel, until markers (Rainbow markers; Amersham) had reached their desired position, and were water cooled throughout.

Protein was detected using the coomassie brilliant blue stain (0.025 % (w/v) in 40 % (v/v) Methanol, 7 % (v/v) Acetic acid), either for 1 hour at 37°C or overnight at room temeprature. Gels were destained with destain solution to the extent desired (30 % (v/v) Methanol, 10 % (v/v) Acetic acid).

Chapter 3
T cell directed BsAb

3.1 Introduction

BsAb, constructed to display dual specificity for both a tumor target and immune effector cell, are able to combine the specificity of mAb with the ability to activate potent cytotoxic mechanisms. In this way, they are able to provide an effective means of redirecting the host immune system in a direct attack against tumor. Optimisation of the most potent trigger molecule to engage, and the most effective cytotoxic effector cell to employ, are a continual source of investigation. One of the most studied trigger molecules to date, is the TCR. T cells are especially attractive as effectors for B cell lymphoma therapy, as they are known to engage in mutual signaling interactions, and have been demonstrated to naturally control abnormal B cell proliferation (83). BsAb directed against components of the TCR, most commonly CD3, thus offer an opportunity to activate and recruit these potentially highly cytotoxic cells, independently of MHC restriction. However, whilst both CD4 and CD8 positive T cells can be recruited in this fashion, the nature of the response depends on the cytokine milieu and differentiation/ maturation state of the T cell engaged.

Some success has already been met adopting this approach with [CD3 x Id] BsAb. Brissinck et al. (81) have achieved much success when treating the murine lymphoma, BCL_1, using hybrid-hybridoma derived IgG BsAb. Such derivatives not only activate T cells as measured by IL-2 production and proliferation, but also trigger redirected cellular cytotoxicity (RCC). Moreover, mice treated *in vivo* with the BsAb, showed long-term protection against BCL_1 challenge. The same group have recently engineered a bispecific single-chain Fv molecule of identical specificity to produce a more clinically applicable model. This derivative too has proven highly efficacious in pre-clinical studies, and confers a high degree of protection to mice when used in combination with exogenous cytokine or staphylococcal enterotoxin B (SEB) (229).

Whilst anti-Id derivatives are clearly successful, their clinical application is limited by a number of factors, and so emphasis has been placed on finding other suitable target antigens. We have constructed a panel of anti-T cell BsAb targeting a range of tumor antigens, including tumor-Id, MHC II, CD19 and CD22, and assessed their performance both *in vitro* and *in vivo*. Given the difficulty in preparing BsAb IgG, we opted to create chemically linked bifunctional $F(ab')_2$ derivatives. In this respect, we may also overcome problems of non-specific T cell activation and tumor penetration, as discussed in chapter 1.

3.2 Materials and Methods

All BsAb were chemically conjugated $F(ab')_2$ derivatives produced according to the protocol in chapter two. Essentially, limited digestion of parental IgG was performed to yield monoclonal $F(ab')_2$ precursor species, which were further reduced to Fab'_{SH} molecules. The two heterologous Fab'_{SH} fragments were then joined by a bismaleimide crosslinker to produce BsAb, which was subsequently purified by gel filtration. The parental mAb used in the production of BsAb are listed below, in Table 3.2.1.

Antibody	Specificity	Class	Reference
Mc106A5	Anti-BCL_1 Id	Rat; γ2a	George et al. (230)
Mc39-16	Anti-A31 Id	Rat; γ2a	Tutt et. al. (231)
N22	Anti-MHC II	Hamster IgG	ATCC
ID3	Anti-CD19	Rat; γ2a	Krop et al. (232)
NIMR6	Anti-CD22	Rat; γ1	Torres et al. (233)
KT3	Anti CD3	Rat; γ2a	Tomonari (234)
7D6	Anti-CD3	Mouse; γ2a	Coulie et al. (235)
1452C11	Anti-CD3	Hamster IgG	ATCC
AT37	Anti-CD2	Rat; γ2a	Tenovus (unpublished)

Table 3.2.1 Origin and specificity of mAb used in the production of BsAb.

Serum half-life of IgG versus $F(ab')_2$ was determined by ^{125}I radio-labelling studies. Mc39-16, anti-A31 Id IgG and $F(ab')_2$ at 1 mg/ml, was labelled with 250 µl ^{125}I according to the method described. CBA mice (two animals/ group), were inoculated with 200 µl radio-labelled IgG or $F(ab')_2$, i.v, at time 0, and the serum half-life of Ab calculated from measurements of radioactive activity present in 10 µl samples of blood, obtained by tail bleeding of mice at regular intervals. Serum half-life was calculated from the β-phase of decay. A similar protocol was employed to determine the serum half-life of [CD3 x MHCII] BsAb derivatives.

In vitro assessments of proliferation were based on a standard [^{3}H]thymidine incorporation assay. Tumor ($1x10^6$ cells/ml in a final volume of 0.2 ml) was co-cultured with murine splenocytes at a ratio of 1:5 in a flat-bottomed 96 well plate, together with BsAb at concentrations as indicated in the text. [^{3}H]thymidine was then added (0.5 µCi/well) after 48 hours and the cells harvested 16 hours later with an automated harvester. [^{3}H]thymidine incorporation was then assessed using 1 min counts on a β-counter.

RCC activity was measured using a standard chromium release assay. Briefly, ^{51}Cr labelled A31 or BCL_1 tumor cells prepared from homogenised spleens of terminal animals, were coated with BsAb on ice for 15 min. Murine splenocytes activated *in vitro* with anti-CD3 (1452C11; 1µg/ml) for 72 hours prior to use were then added at an E:T ratio of 50:1. Cells were incubated for 4 hours at 37^0C, centrifuged at 1500 rpm for 5 mins, and 100 µl supernatant harvested from each well to estimate ^{51}Cr release. Maximal release of ^{51}Cr was determined from target cells to which 150 µl of Nonidet P-40 had been added. The percentage specific release was determined using the formula:

$$\%\ ^{51}Cr\ release = \frac{Sample\ release - background\ release}{maximum\ release - background\ release} \times 100$$

In vivo efficacy of the derivatives was estimated by injection of CBA or BALB/c mice, with 2×10^5 or 10^5 A31 or BCL_1 tumour cells respectively, i.p, day 0, followed by twice

daily inoculations of BsAb derivative, to a total dose as indicated in the text. In all cases, control cohorts received 200 µl PBS i.p. The general therapeutic protocol is illustrated below:

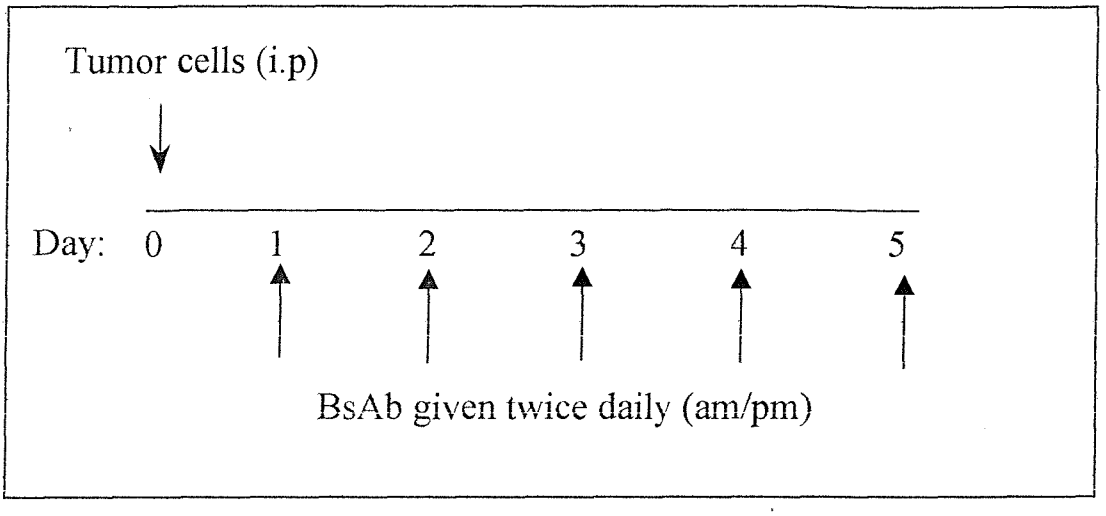

Fig. 3.2.1 Standard therapy protocol.

3.3 Results

3.3.1 Production of BsAb

A panel of BsAb $F(ab')_2$ was produced to evaluate the efficacy of targeting T cells to a range of murine B cell associated tumor antigens. Targets chosen included tumor specific Id, MHC II, CD19 and CD22. T cell engagement was achieved via the CD3 or CD2 molecules. In addition, a panel of anti-MHC II BsAb were constructed using different anti-CD3 mAb arms. A full list of reagents is given overleaf in Table 3.3.1. Previous experiments conducted in this laboratory have shown $F(ab')_2$ derivatives to bind B and T cells at comparable levels to parental mAb and that these levels of binding are also similar to those observed with bispecific IgG (Cruise A. unpublished).

BsAb $F(ab')_2$		
[CD3 x A31-Id]	[CD2 x A31-Id]	[KT3 x MHC II]
[CD3 x BCL_1-Id]	[CD2 x BCL_1-Id]	[1452C11 x MHC II]
[CD3 x MHC II]		[7D6 x MHC II]
[CD3 x CD19]		
[CD3 x CD22]		

Table 3.3.1 List of BsAb $F(ab')_2$ derivatives produced and tested. CD3 BsAb all contain the rat-anti-mouse CD3 mAb, KT3, as the anti-Tcell arm. The anti-CD3 arm of the MHC II BsAb have been listed according to the clone name.

3.3.2 *In vitro* proliferation

We first wished to determine that the $F(ab')_2$ derivatives could successfully link T cells to tumor, thus inducing T cell proliferation *in vitro*. Shown are levels of T cell proliferation for BsAb in the presence of BCL_1 tumor (Fig.3.3.1). All derivatives contained identical anti-CD3 arms so any differences in proliferation are a reflection of the nature of the tumor antigen targeted. The [CD3 x MHC II] derivative proved most potent at stimulating T cell proliferation, with BsAb to CD19, Id and CD22 showing decreasing activity. [CD2 x Id] also gave a small degree of proliferative response over control non-binding BsAb (anti-A31 Id), reaching levels similar to those achieved with the [CD3 x CD22] derivative. The response was proportional to the concentration of BsAb added, such that at the lowest concentration (0.01μg/ml) virtually no proliferation was detectable. Similar responses with BsAb in the presence of A31 tumor were also recorded (not shown).

3.3.3 *In vitro* redirected cellular cytotoxicity (RCC)

We next wished to determine the ability of BsAb to trigger the lytic activity of T cells using a standard ^{51}Cr release RCC assay. Findings indicate that at an E:T ratio of 50:1,

syngeneic T cells pre-stimulated with anti-CD3 mAb, are able to lyse tumor in the presence of BsAb (Fig.3.3.2). Again, there is a clear grading of response according to the tumor antigen targeted that is reflected in both tumor models. MHC II proved the most effective antigen against which to target T cells, with 35 – 40 % specific ^{51}Cr release achieved in the presence of 1μg/ml BsAb. [CD3 x CD19] produced approximately 25 % specific ^{51}Cr release, [CD3 x Id] around 20 %, and [CD3 x CD22] proved the least efficacious target with only 5 % specific ^{51}Cr release. The [CD2 x Id] BsAb produced around 10 % specific ^{51}Cr release against either tumor model. With the exception of BsAb to CD22, RCC was still achieved by all derivatives at concentrations as low as 0.01μg/ml, particularly when targeted to the A31 tumor. No killing was observed in the absence of BsAb by T cells alone, or by non-binding control BsAb (not shown).

3.3.4 *In vivo* efficacy of BsAb derivatives

It is clear that F(ab')$_2$ BsAb are able to trigger T–cell responses *in vitro*, and that derivatives binding to MHC II are the most effective in terms of stimulating T cell proliferation and tumor lysis. We next wished to evaluate the therapeutic efficacy of the BsAb *in vivo*.

Initial experiments were conducted comparing treatment with the [CD3 x Id] BsAb on a single or multiple days. Fig.3.3.3 shows that mice receiving two 25 μg inoculations of [CD3 x Id] day 1 only, i.p (a total of 50 μg/mouse) failed to show more than a few days protection over PBS treated controls. However, mice receiving a total of 50 μg given as twice daily inoculations of 5 μg for 5 days were protected. 80 % of treated animals, challenged with either tumor line, entered long-term survival (LTS) over 100 days.

Serum half-life analysis of IgG and F(ab')$_2$ was conducted in CBA mice using radio-labelled Ab to quantify differences between derivatives which did or did not carry Fc (Fig.3.3.4). Approximately 200 μg ^{125}I labelled anti-Id IgG or F(ab')$_2$ (prepared by pepsin digestion of IgG) were injected into animals i.v at time zero and serum decay determined by measuring radioactivity present in 10 μl blood samples obtained from tail-bleeds at

various intervals following injection. Any differences would not be due to differences in antigen binding (as anti-Id mAb were used in non-tumor bearing animals), but rather, would be a direct reflection of the presence or absence of Fc. IgG was determined to have a half-life of around 30 hours, compared to that of approximately 9 hours for $F(ab')_2$. Given that the IgG serum retention time is 3 times that of the $F(ab')_2$ we proceeded to treat animals with multiple inoculations of BsAb derivative to compensate for lack of Fc.

The full panel of $F(ab')_2$ derivatives was tested for *in vivo* activity against both the A31 and BCL_1 lymphoma lines (Fig 3.3.5). A standard protocol of twice daily infusions of 5 μg BsAb was employed throughout this, and subsequent therapies. BsAb [CD3 x MHC II], [CD3 x CD19], and [CD3 x CD22] were able to provide a small survival advantage over controls, that was statistically significant ($p < 0.01$). Interestingly, derivatives containing an anti-Id arm were able to provide complete protection to the majority of animals. Against A31, the [CD3 x Id] and the [CD2 x Id] both gave 60 % LTS (over 100 days protection). For the BCL_1 model the [CD3 x Id] proved slightly more efficacious providing 60 % LTS compared to the [CD2 x Id] which provided 40% of treated animals with LTS (over 100 days).

To further test the activity of our [CD3 x Id] constructs we innoculated animals with the same tumour load as before (10^5 BCL_1 cells, 2 x 10^5 A31) but treated at later time points to allow the tumor to become more established. Treating an initial inoculum of 2 x 10^5 A31 cells given day 0, through days 1 - 5 gave 60 % LTS (Fig.3.3.6). Delaying therapy to days 4 - 8, enhanced protection so as all animals entered LTS. A further delay to days 9 - 13 showed a dramatic decrease in therapeutic efficacy, with no long-term protection, and benefit to survival over controls cut to around only 8 days. For the BCL_1 model a similar profile was obtained, with later treatment (day 7-11) decreasing therapeutic activity from 60 % of animals entering LTS, to a benefit in survival of around 10 days.

To verify that therapeutic activity of the anti-Id BsAb was indeed due to direct contact between the tumor cell and the T cell, therapy was conducted with unconjugated parental $F(ab')_2$, either as single species, or as a cocktail (Fig.3.3.7). No advantage in survival over

control cohorts was observed when treating with either anti-CD3 $F(ab')_2$, anti-Id $F(ab')_2$, or a mixture of the both, against either A31 or BCL_1 lymphoma. The [CD3 x Id] derivatives were used as a positive control, again giving long-term protection to treated cohorts.

3.3.5 *In vitro* evaluation of a panel of [CD3 x MHC II] BsAb

We also wished to investigate the possibility of increasing BsAb activity by altering the CD3 binding arm of the derivative. MHC II was selected as the tumor antigen for targeting, given the previous derivatives promising *in vitro* but poor *in vivo* performance when targeted to MHC II. By altering the anti-CD3 arm it was hoped we might increase T cell activation or proliferation *in vitro* and/or *in vivo*, and hence increase therapeutic efficacy. Previous BsAb all contained a rat anti-mouse CD3 arm, mAb KT3. BsAb were now produced with hamster anti-mouse CD3 (1452C11) and mouse anti-mouse CD3 (7D6) arms.

Firstly, *in vitro* proliferation and RCC capability were compared. BsAb (20 μg/ml to 2 μg/ml) incubated with BCL_1 tumor and murine splenocytes again showed substantial T cell proliferation (Fig.3.3.8). Interestingly, both the 1452C11 and 7D6 containing derivatives out-performed the KT3 BsAb. The 7D6 containing BsAb proved most potent with levels of proliferation around 4 times that of the KT3 BsAb, whilst the 1452C11 was able to stimulate a moderate level of proliferation.

RCC activity mediated by each derivative when engaging pre-activated T cells (cultured as before) was also assessed. All three derivatives generated similar levels of tumor lysis Fig.3.3.9 shows that against both the A31 and BCL_1 lymphoma, T cells were able to produce around 35 – 45 % specific ^{51}Cr release in the presence of 1 μg/ml of BsAb, regardless of the nature of the anti-CD3 arm. Activity decreased as BsAb was titrated out, but all derivatives still provided around 15 % specific lysis even at 0.01 μg/ml. Again, no activity was observed when incubating any of the derivatives with tumor in the absence of T cells or with T cells in the presence of a non-tumor binding BsAb (not shown).

3.3.6 *In vivo* evaluation of a panel of [CD3 x MHC II] BsAb

Finally, the activity of these derivatives was compared *in vivo*. Shown are the results of a therapeutic trial against A31 tumor, giving 2 x 10^5 cells i.p day 0, and treating, as before, with twice daily inoculations of 5 μg BsAb for 5 days (Fig.3.3.10.A). Control animals received 200 μl PBS on each day. All derivatives performed to a similar level, providing only a few days protection over control animals. Thus, there was no increased benefit to survival by changing the anti-CD3 arm from KT3 to 1452C11 or 7D6. Serum half-life was also compared. 200 μg of ^{125}I labelled F(ab')$_2$ was injected i.v into mice at time zero, and serum decay calculated from 10 μl tail bleed samples taken at various successive time points. All determinants were taken in duplicate. All three derivatives presented a similar serum half-life of around 3 – 4 hours (Fig.3.3.10.B).

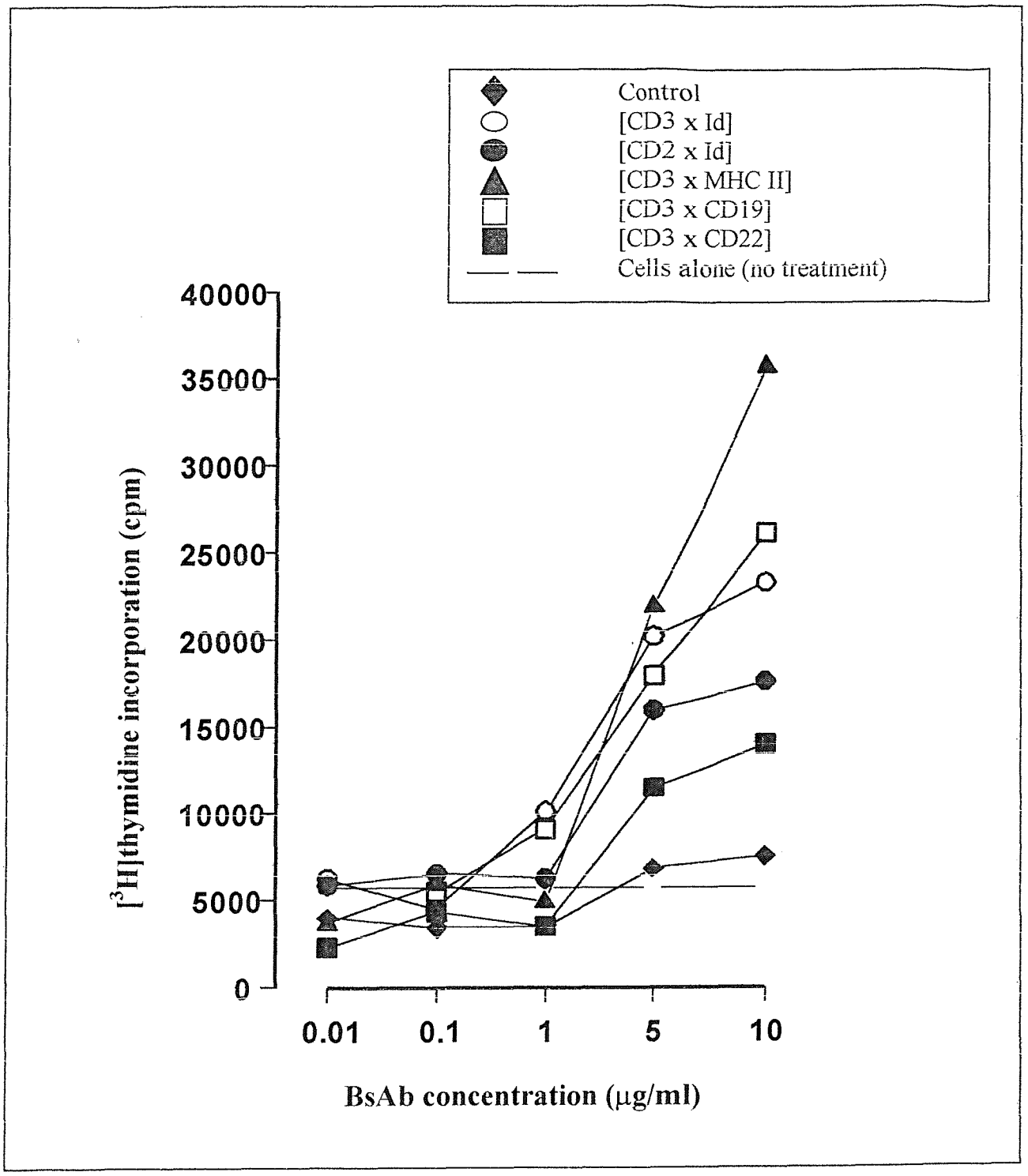

Fig.3.3.1 BsAb mediated T cell proliferation. BCL_1 tumor cells and BALB/c T cells were co-incubated at a ratio of 1:5 with BsAb of various specificities, at a range of concentrations (as indicated), for 48 hours at 37^0C. Cells were the pulsed with [^{3}H]thymidine (0.5 μCi/well) for a further 16 hours. Cells were harvested and T cell proliferation measured as the degree of [^{3}H]thymidine incorporation obtained. Results show the mean of triplicate readings. Control was the [CD3 x A31-Id]

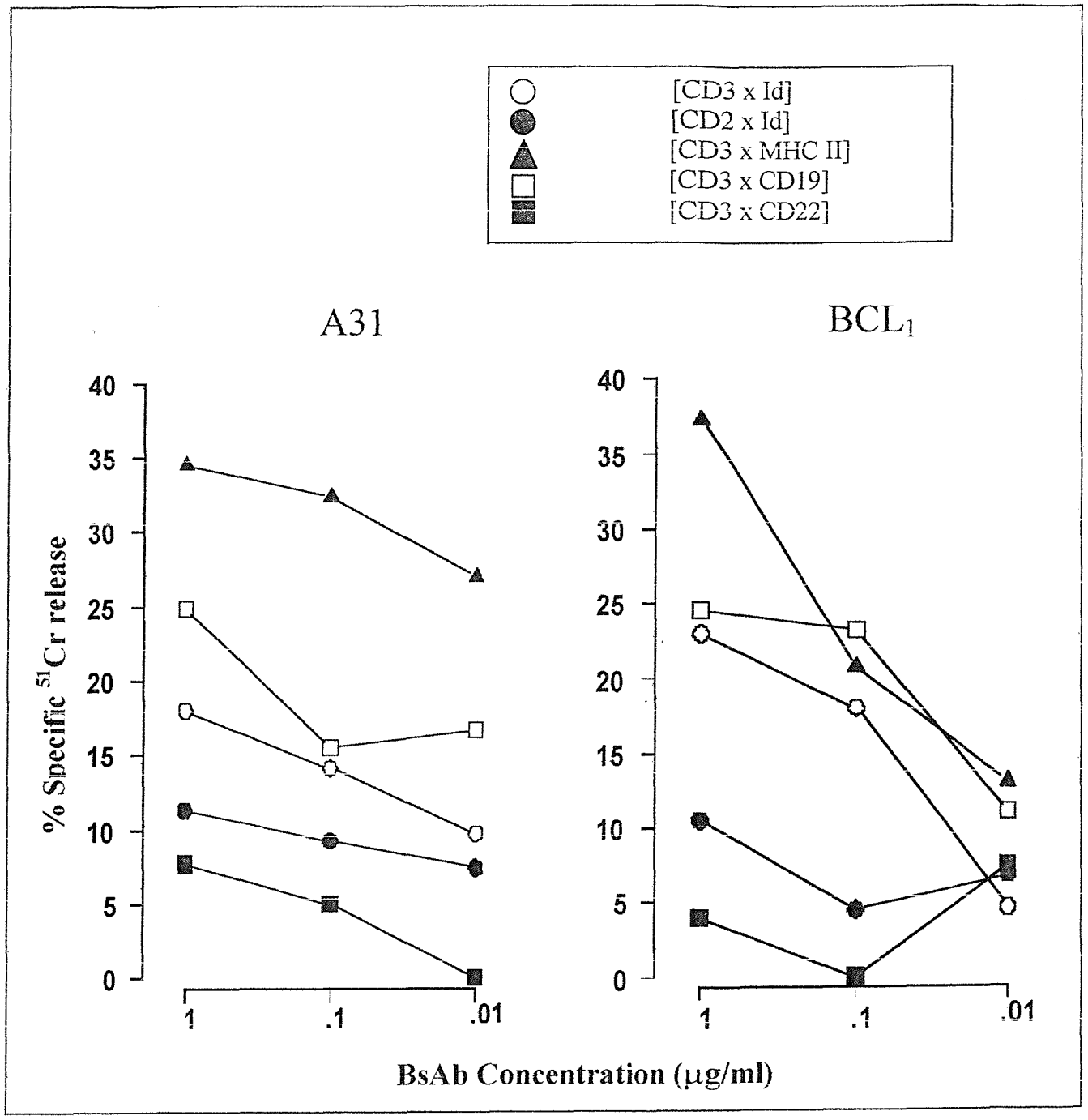

Fig.3.3.2 RCC of A31 and BCL_1. RCC activity was determined using a standard ^{51}Cr release assay. T cells from CBA or BALB/c mice were stimulated *in vitro* for 72 hours with anti-CD3 mAb (1452C11; 1 μg/ml) and then incubated with ^{51}Cr labelled A31 or BCL_1 tumor cells respectively, at an effector to target ratio of 50:1, in the presence of BsAb as indicated above. All determinants were performed in triplicate.

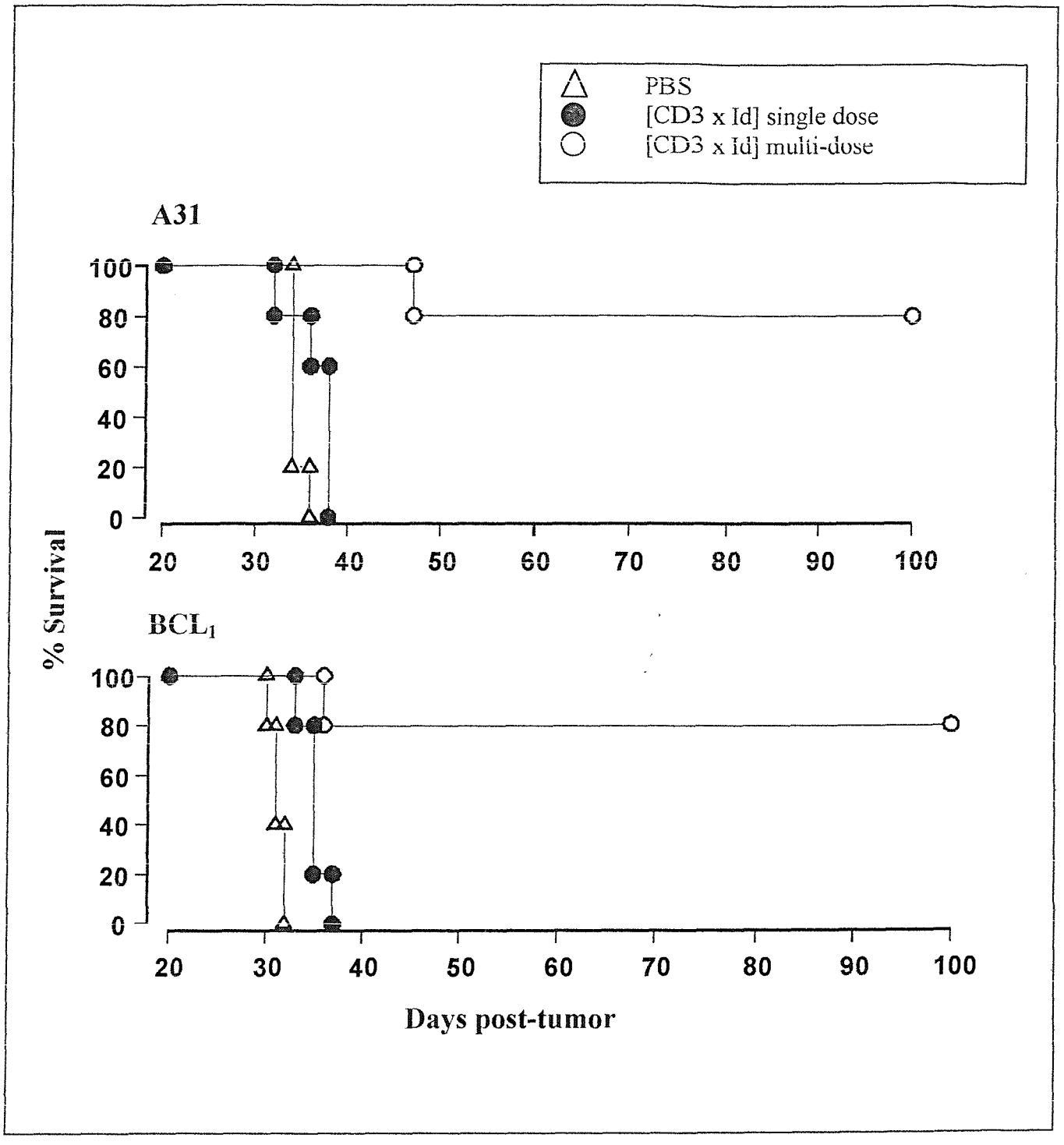

Fig.3.3.3 Single dose versus multi-dose therapy. Groups of 5 age matched CBA or BALB/c mice received 2 x10^5 A31 or 10^5 BCL_1 tumor cells respectively, i.p, day 0. Mice were then treated with either a single days therapy of 2 x 25 μg BsAb (●), or multiple days therapy of 2 x 5 μg BsAb per day for 5 days (○) (a total of 50μg/mouse). Control animals received 200 μl PBS (△). Survival was recorded daily.

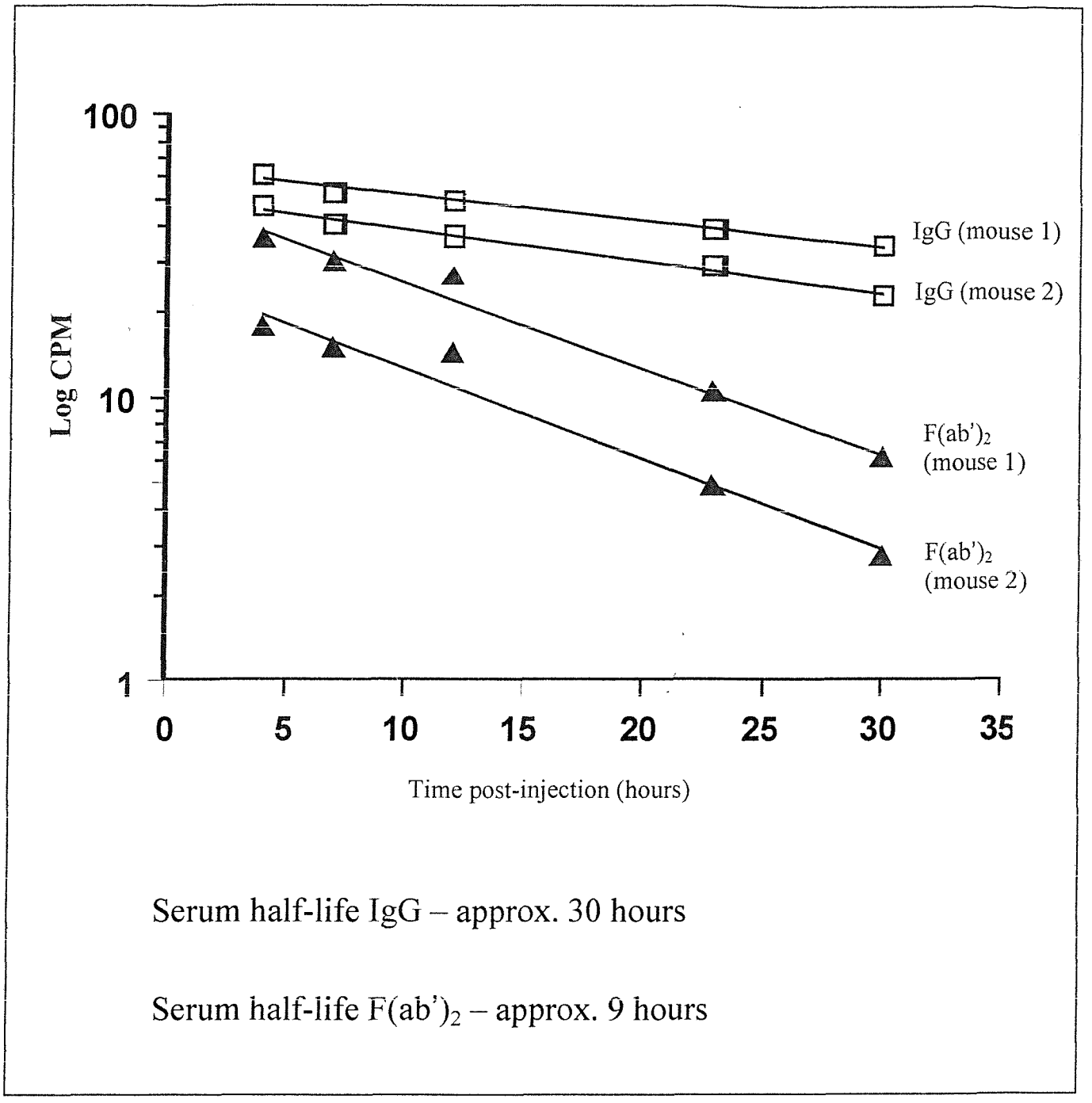

Fig. 3.3.4 Serum half-life of IgG versus F(ab')$_2$. Anti-Id IgG or F(ab')$_2$ at 1 mg/ml was labelled with ^{125}I as described in chapter 2, and injected i.v into groups of two animals, time zero. 10 µl samples obtained from tail bleeds were measured on a γ-counter at regular intervals to determine the rate of serum decay. Shown are log radioactive counts versus time in hours for the β stage of decay. IgG was determined to have a serum half-life of around 30 hours, F(ab')$_2$ of around 9 hours.

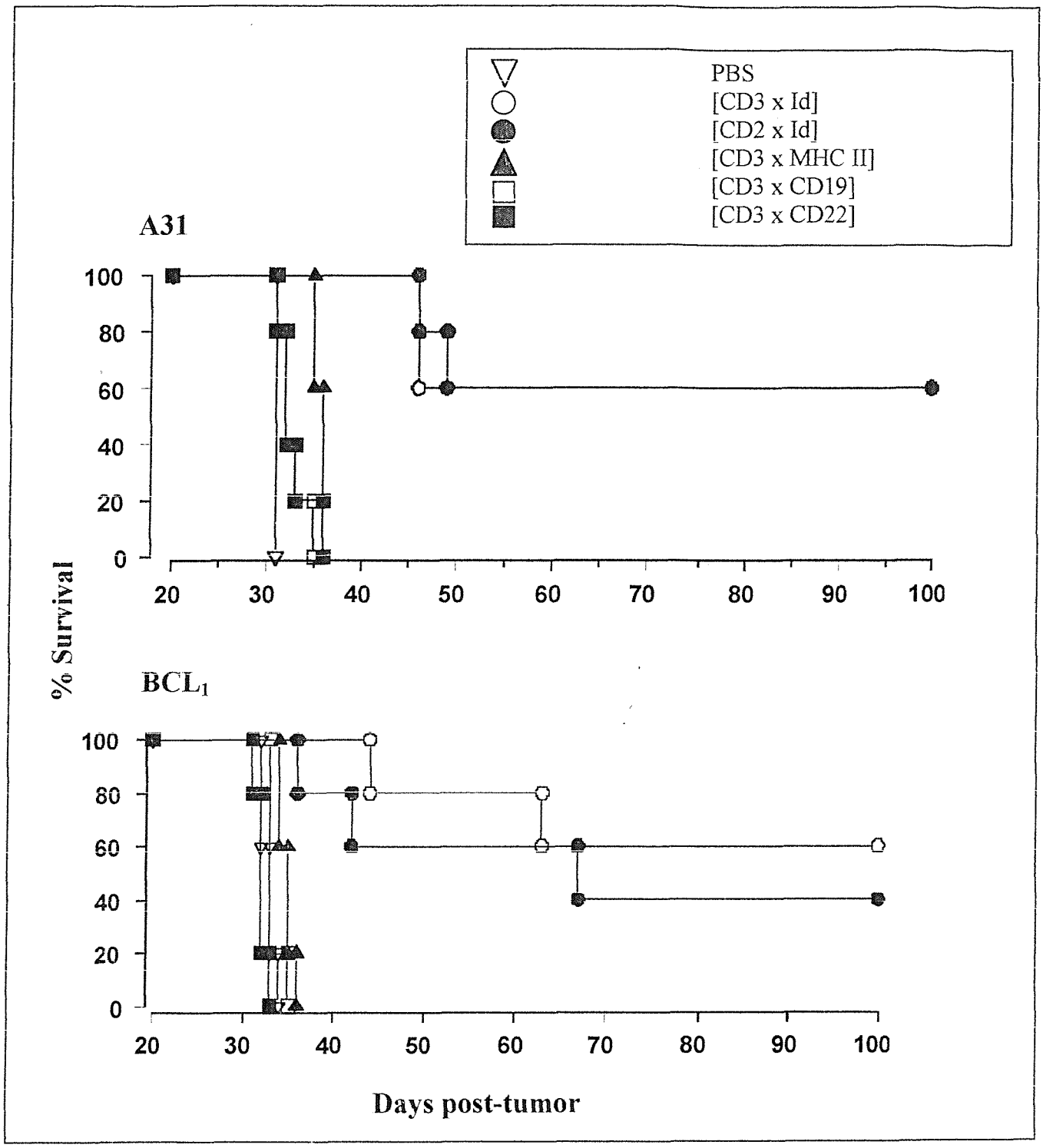

Fig.3.3.5 BsAb therapy of A31 and BCL_1. Groups of 5 age matched CBA or BALB/c were inoculated with 2 x 10^5 A31 or 10^5 BCL_1 tumor cells respectively, i.p, day 0. Mice were then treated with twice daily doses of 5 μg BsAb, i.p, days 1 to 5 (50 μg/mouse total). Treatment was as indicated: PBS (▽); [CD3 x Id] (○); [CD2 x Id] (●); [CD3 x MHC II] (▲); [CD3 x CD19] (□); [CD3 x CD22] (■). Survival was recorded daily.

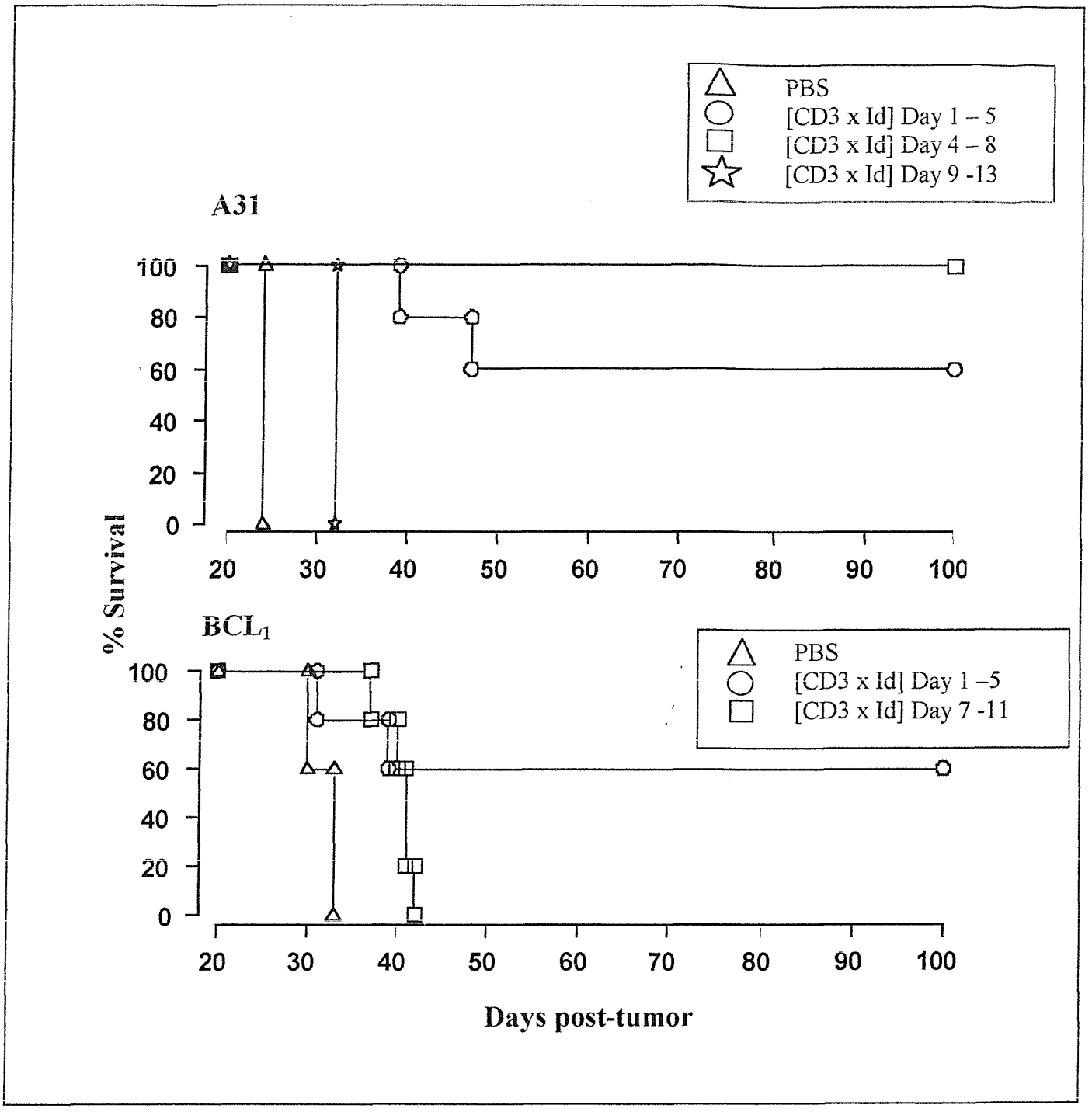

Fig.3.3.6 Delayed BsAb therapy of A31 and BCL_1 tumor. Groups of 5 age matched CBA or BALB/c mice were inoculated with 2 x 10^5 A31 or 10^5 BCL_1 tumor cells respectively, i.p day 0. Mice were then treated with twice daily doses of 5 μg [CD3 x Id] BsAb at various time intervals following inoculation (as indicated above). Control animals received 200 μl PBS ip. Survival was recorded daily.

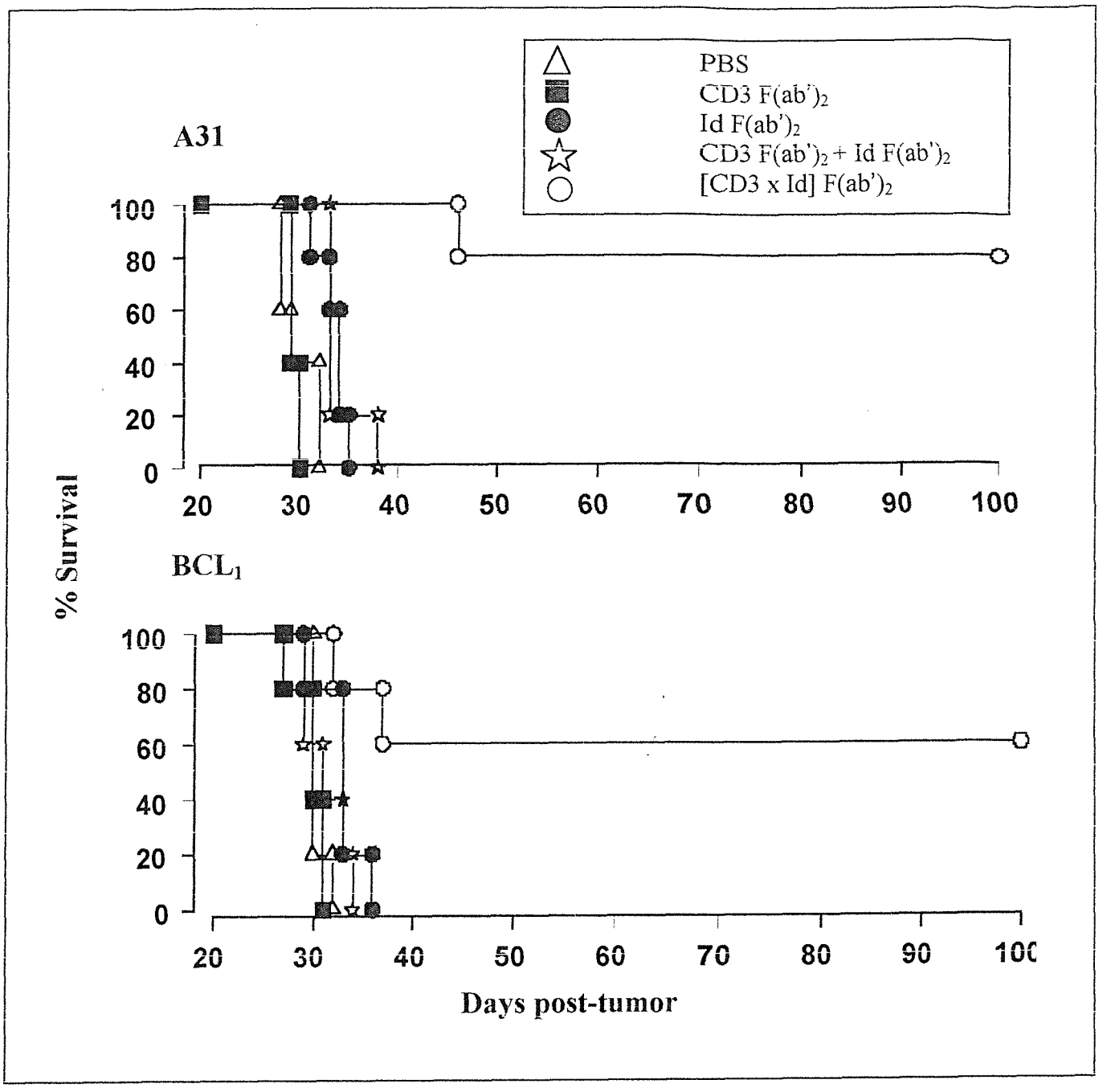

Fig.3.3.7 Unconjugated F(ab')$_2$ therapy. Groups of 5 age matched CBA or BALB/c mice received 2 x 10^5 or 10^5 A31 or BCL_1 tumor cells respectively, i.p day 0. Mice were treated with twice daily doses of 5 μg of either anti-CD3 (■) or anti-Id F(ab')$_2$ (●) alone, a mixture of the two (☆), or conjugated as a BsAb (○), i.p days 1- 5 (a total of 50 μg/mouse). Control animals received 200 μl PBS (△). Survival was recorded daily.

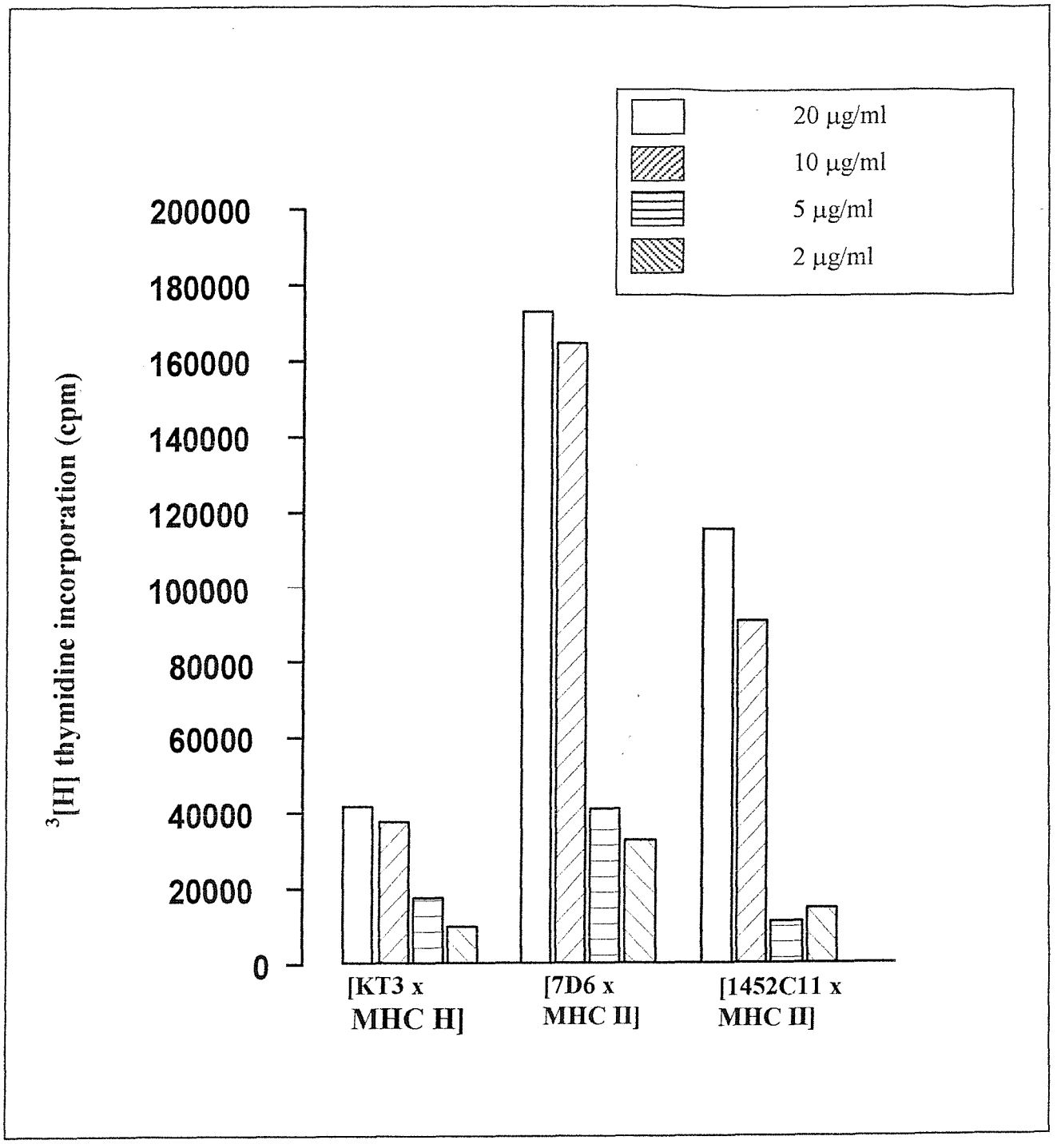

Fig.3.3.8 BsAb mediated T-cell proliferation with [CD3 x MHC II]. BCL_1 tumor cells and BALB/c T cells were co-incubated at a ratio of 1:5 with [CD3 x MHC II] BsAb (as indicated), at a range of concentrations (2 – 20 µg/ml), for 48 hours at 37^0C. Cells were the pulsed with [^{3}H]thymidine (0.5 µCi/well) for a further 16 hours. Cells were harvested and T-cell proliferation measured as the degree of [^{3}H]thymidine incorporation obtained. Results show the mean of triplicate readings.

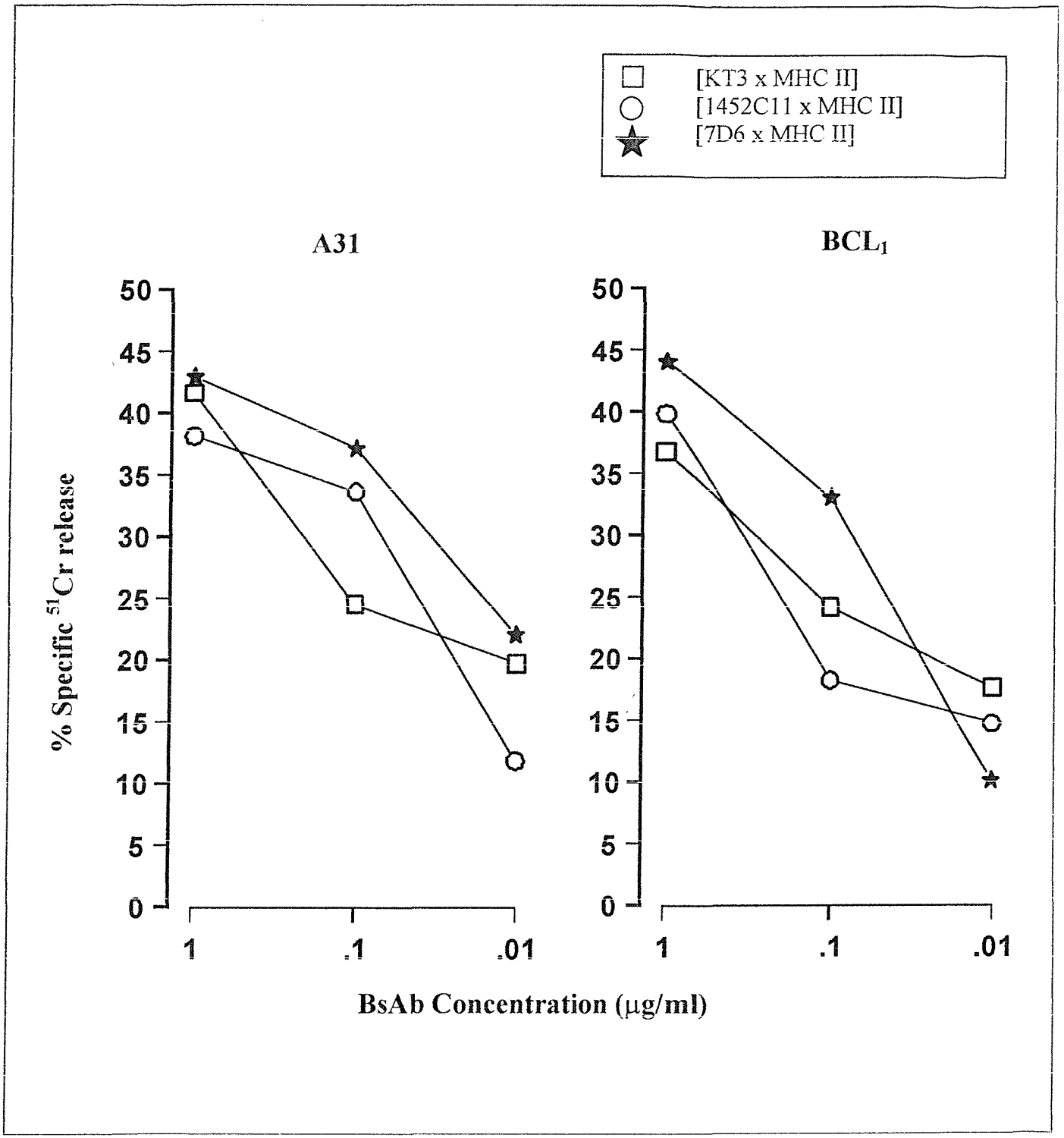

Fig.3.3.9 BsAb mediated RCC with [CD3 x MHC II]. RCC activity was determined using a standard ^{51}Cr release assay. T cells from CBA or BALB/c mice were stimulated *in vitro* for 72 hours with anti-CD3 mAb (1452C11) and then incubated with ^{51}Cr labelled A31 or BCL_1 tumor cells respectively, at an effector to target ratio of 50:1, in the presence of BsAb as indicated above. All determinants were performed in triplicate.

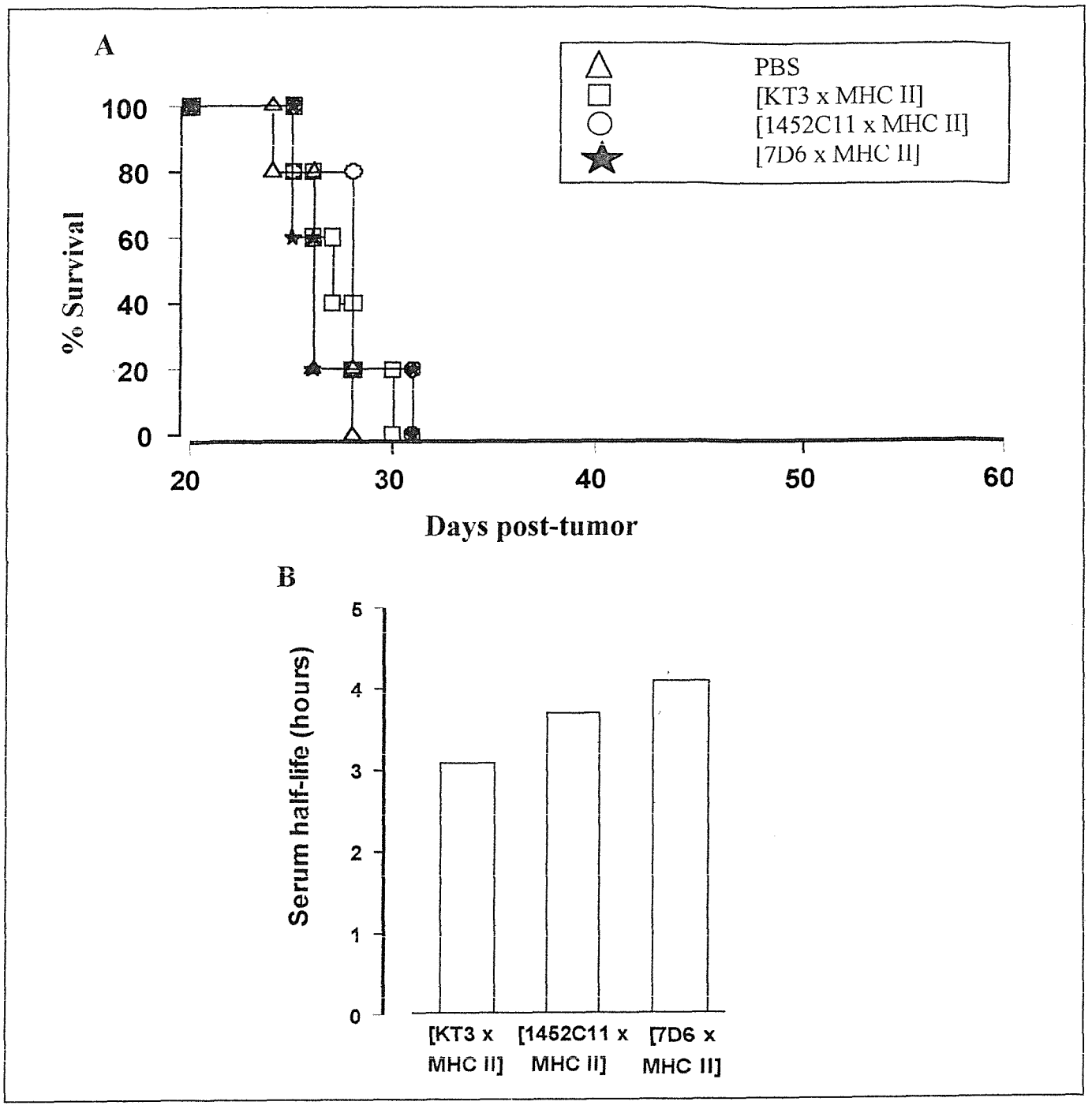

Fig.3.3.10 Activity of [CD3 x MHC II] *in vivo*. (A) Groups of 5 CBA mice received 2 x 10^5 A31 tumor cells i.p day 0, and were treated with twice daily inoculations of 5 μg BsAb for 5 days (a total of 50 μg/mouse). Groups were as follows: PBS (△), [KT3 x MHC II] (□), [1452C11 x MHC II] (○), [7D6 x MHC II] (★). Survival was recorded daily. **(B)** The serum half-life of the BsAb was also compared, according to the method previously described. Shown is the serum half-life, in hours, for each derivative. All three had a half-life of around 3 – 4 hours.

3.4 Discussion

Previous studies have shown that intact IgG BsAb targeting T cells to tumor Id are able to clear tumor *in vivo* (81, 105). However, IgG BsAb are difficult to prepare and purify, and are not the most suitable composition for clinical application. Clinically, hybrid-hybridoma derived BsAb have been shown to induce a dose dependent immunosuppression, limiting the number of administrations, a phenomenon most likely related to Fc (236). Likewise, Id, although tumor specific, and to date one of the most effective targets for immunotherapy, requires tailor-made design on a patient-to-patient basis, making it expensive and time consuming to produce (237). Hence, alternative target antigens are sought. To address the question of which antigens are most effective for BsAb therapy of B cell lymphoma, a panel of $F(ab')_2$ BsAb to a wide range of tumor associated molecules (Id, MHC II, CD19, CD22) were produced, and their therapeutic efficacy *in vitro* and *in vivo* compared.

The critical difference between these derivatives and IgG BsAb is the absence of an Fc fragment. Many of the properties of T cell activation *in vitro* by BsAb have been attributed to this Fc region (105). In the absence of tumour cells, ligation of FcR on antigen presenting cells can increase the degree of cross-linking of the CD3 molecule, hence enhancing the resulting proliferative signal. Even in the presence of tumour cells, allowing BsAb to cross-link the T cells to their targets, $F(ab')_2$ bispecifics have been shown to be less efficient at delivering an activatory signal than their IgG counterparts (105). Previous studies in this laboratory have confirmed the superiority of anti-Id hybrid-hybridoma derivatives over equivalent $F(ab')_2$ constructs in this respect (unpublished). However, as demonstrated here, $F(ab')_2$ derivatives are capable of binding T cells and inducing a proliferative response (Fig.3.3.1). A clear order of activity was established with BsAb to MHC II proving most efficacious, followed, in decreasing order, by those to CD19, Id and CD22. The [CD2 x Id] $F(ab')_2$ was also able to generate some small degree of T cell stimulation, although at far lower levels than the [CD3 x Id], in-keeping with the notion that CD2 is not able to trigger T cell responses when engaged alone.

Interestingly, the $F(ab')_2$ BsAb, whilst less effective than IgG BsAb in terms of triggering T cell proliferation, have been shown to be as effective at triggering cytotoxicity. Previous studies in this laboratory have shown that both bispecific IgG and $F(ab')_2$ were equally efficient in RCC assays (Cruise,A Thesis 1996). Here, all derivatives were able to mediate tumour cell lysis to some extent when incubated with pre-stimulated T cells *in vitro* (Fig.3.3.2). Again there was a clear ranking of Ab effectiveness in the order anti-MHC II > anti-CD19> anti-Id > anti-CD22. These observations indicate that *in vitro* stimulation of T cells by BsAb is to some degree a reflection of the surface mobility and density of the target tumor antigen. Previous flow cytometric analysis of the murine tumors used here have revealed MHC II to be highly expressed, Id to have slightly lower levels of expression, and CD19 and CD22 to be present at equal but relatively low levels (data not shown). This has been confirmed by binding affinity studies (231). In particular, MHC II is very highly expressed on the BCL_1 lymphoma.

However, antigen density is not an entirely adequate explanation for the *in vitro* activity of the BsAb derivatives. Indeed, the pattern of activity displayed by the BsAb fits more closely with the tendency of the target antigen to undergo modulation. Removal of BsAb from the cell surface due to modulation will obviously have a negative effect on its ability to retarget cellular effectors to the tumour. The known order of antigenic modulation (CD22> Id> CD19> MHC II), inversely correlates with the observed proliferative and cytotoxic responses mediated by the derivatives. This pattern is duplicated by mAb targeting these tumor antigens. When tested against a variety of tumour cell lines, we consistently observed the highest degree of ADCC or complement killing to be mediated by anti-MHC II antibodies, then those against CD19, Id and CD22 (own data; 231).

Thus, based on *in vitro* observations $F(ab')_2$ BsAb would appear to be an effective tool for stimulating T cell mediated elimination of tumor. It would also appear likely that MHC II was a most suitable candidate antigen for BsAb mediated immunotherapy. The activity of the derivatives was thus tested *in vivo*. Here once again, the presence of Fc has previously

been though of as beneficial. Additional effector recruitment through Fc, or the activation of complement has been attributed to the therapy given by IgG BsAb. Fc binding to FcRn also extends the serum half-life of such derivatives (5).

The rapid clearance of $F(ab')_2$ compared to IgG (Fig.3.3.4) could prove a major obstacle to immunotherapy. Indeed, this most likely explains the lack of activity of the anti-Id BsAb when administered as a single days treatment (Fig.3.3.3). Compensation for the reduced half-life by giving multiple inoculations over a number of days (but delivering the same total treatment dose), significantly increases the therapeutic activity of anti-Id $F(ab')_2$ derivatives. Under such a regime [CD3 x Id] is able to provide long-term protection against both A31 and BCL_1 tumor. This protection is clearly due to *in vivo* cross-linking of T cells to tumor (Fig.3.3.7) as cohorts treated with either parental $F(ab')_2$ alone, or a mixture of anti-Id and CD3 $F(ab')_2$ demonstrated no enhanced survival over controls. Only treatment with bispecific $F(ab')_2$ was sufficient to eradicate tumor. However, timing is critical to therapeutic efficacy, as leaving treatment too late results in a loss of protection (Fig.3.3.6) presumably because the tumor burden is too great at this time, and overwhelms the effector mechanisms in operation.

BsAb to antigens other than Id were less effective in therapy, able to provide only a small survival advantage over controls (Fig.3.3.5). In this respect there is a distinct lack of correlation between *in vitro* and *in vivo* activity. This is especially striking for derivatives to MHC II, which proved most effective in proliferation and cytotoxicity assays, but performed poorly in therapy. This failure may in part be due to binding of non-tumour cells, as antigens other than Id are not restricted to the malignant clone. In the case of the anti-CD19 and anti-CD22 BsAb it may also be a reflection of rapid target internalisation. However, recent observations with the highly therapeutic anti-CD40 mAb (despite targeting an antigen showing a broad pattern of distribution, and a tendency to modulate) indicate that such factors may not greatly influence therapeutic outcome (36). Even when the origin of the anti-CD3 arm of the BsAb was altered to try and increase T cell responses, therapy could not be enhanced. Anti-MHC II BsAb were constructed with 7D6 (mouse), 1452C11 (hamster) or KT3 (rat) Fab' to CD3. MHC II was chosen as the target

antigen on the basis of the *in vitro* performance of the original [CD3 x MHC II] BsAb. *In vitro* there was a clear difference in terms of T cell proliferation with the 7D6 containing derivative generating the highest level of response (Fig.3.3.8). However, in terms of RCC and therapy there were no significant differences between any of the BsAb. Thus, therapy was not enhanced by altering the species of anti-CD3 to hopefully increase T cell binding and activation *in vivo*.

It appears that requirements other than the ability of a BsAb to trigger T cell responses as defined by *in vitro* assays, or target a highly expressed tumor antigen, are important for therapeutic outcome. Instead, this data indicates that factors relating directly to the tumor antigen itself, for example signaling activity, may be of more importance. Anti-Id mAb are known to induce anti-proliferative signals (238), and effector cells coupled to BsAb may serve to cross-link BCR, generating such signals. Both [CD3 x Id] and [CD2 x Id] gave long-term protection despite CD2 being less proficient at triggering T cell activity than CD3. Moreover, an [Id x MHC II] derivative, tested only in therapy against A31, also mediated substantial protection of around 30 days over controls (data not shown).

Whilst anti-Id BsAb lead to remission from primary challenge, tumor dormancy has been reported in long-term surviving mice "cured" from BCL_1 tumor. A residual population of around 0.5×10^6 tumor cells remains in a quiescent state for several months before dormancy is broken and tumor regrows (239). PCR techniques have been used to determine the presence of such populations by others, but often give false positives. An alternative approach, and one that is more reliable, is to passage spleens of "cured" animals into naïve mice and watch for tumor development. Spleens of LTS from [CD3 x Id] treated mice were transferred to naïve mice at a dose of 10^7 cells per animal i.p but no subsequent tumor development was observed (data not shown). This would indicate that BsAb are extremely effective at eliminating tumor. Moreover, as anti-Id mAb in these models have never given long-term protection (231), BsAb to Id appear to be more potent at delivering anti-tumor effects.

As a whole, these observations indicate that target antigen selection is critical to therapeutic outcome and that *in vitro* assays are not predictive of therapeutic efficacy. Most likely a combination of effector cell cytotoxicity and signaling are required for long-term protection. However, to further investigate the roles for target antigen and ADCC/ RCC in BsAb therapy further investigations have been conducted in a second system. Here, BsAb in combination with G-CSF were used to target transgenic PMN through human FcγRI as the effector species.. Cytokine stimulated PMN are highly aggressive effectors when triggered through FcγRI (a potent stimulator of ADCC) so it was hoped that this model could be used to further define the role of ADCC in therapy.

Chapter 4

FcγRI BsAb *in vitro*

4.1 Introduction

Ab mediated cancer therapy can be achieved through a number of routes, including induction of tumor dormancy, apoptosis, complement recruitment, and ADCC. In the latter, mAb mediate contact between tumor cells and effectors by engaging specific FcγR on the surface of immune cells. These receptors are highly effective stimulatory molecules, initiating cellular activation and mediating a variety of immune responses, including target cell phagocytosis and lysis. Of the three classes of FcR capable of triggering effector mechanisms, FcγRI (CD64) represents a particularly attractive target. FcγRI is uniquely a high affinity receptor for monomeric as well as immune complexed IgG, and acts as an extremely potent trigger molecule for ADCC capable of initiating destruction of a variety of tumor cell lines *in vitro* (145). Receptor expression is restricted to potential effector cell populations such as monocytes and macrophages. However, it is also inducible on PMN following administration of IFN-γ and G-CSF (144). Moreover, pre-clinical studies have shown G-CSF also induces an increase in PMN numbers and activation (208). As PMN have been demonstrated to have a natural role in immuno-surveillance of tumor (240) this makes them appealing candidates as effector cells in FcγRI directed immunotherapy. Furthermore, G-CSF primed human PMN have shown the ability to lyse tumor cell lines sensitised with anti-HLA class II mAb *in vitro* (145). Hence, a strategy combining G-CSF administration and targeting to class II molecules seems an ideal method of recruiting PMN in a clinical setting.

Being a high affinity receptor for monomeric IgG, FcγRI is typically saturated *in vivo* with serum Ig, which can pose problems for engagement by tumor targeting mAb. However, the anti-FcγRI Fab' arm of the bispecific can recognise epitopes outside of the Fc binding domain (143). Thus, BsAb have an advantage over mAb in that they can avoid competition from serum IgG that typically saturates the receptor under physiological conditions. Also, such derivatives would not bind FcγRIIb, thus preventing

triggering of negative signals that can reduce ADCC (196). To evaluate the potential of such an approach we have utilised a transgenic murine model, with mice bearing human FcγRI. We aim to retarget FcγRI positive, G-CSF primed PMN to tumor using a panel of BsAb $F(ab')_2$, against a range of tumor markers. These include Id, MHC II, CD19, and CD40. In this way we hope to determine which antigen is the most appropriate target for PMN recruited by BsAb, not only *in vitro* but also *in vivo*.

It is important to stress that from now on throughout the text FcγRI is intended to mean human FcγRI.

4.2 Materials and methods

The animal test models used in these studies are based on the FVB/n FcγRI transgenic mouse model generated by Heijnen and van de Winkel (221). Transgenic founders carry not only the FcγRIA gene, but also additional elements including the IFN-γ response region and the myeloid activating transcription element (MATE). FcγRI positive FVB/n male mice, kindly donated by I. A. F. M. Heijnen and J.G.J. van de Winkel (University Medical Centre, Utrecht), were crossed on to a CBA or BALB/c background. Approximately fifty percent of the F1 progeny were thus positive for the transgene and able to take our tumor lines, A31 and BCL_1 respectively.

Mice were screened for the presence of the transgene using FITC-anti-FcγRI mAb on whole blood, obtained from tail bleeds of F1 mice. Receptor expression on PMN was determined by dual fluorescence staining using PE-labelled 7/4 mAb (anti-PMN) versus FITC-anti-FcγRI. Levels of receptor on macrophages were similarly identified using PE-labelled F4/80 as a phage specific marker. Levels of MHC II expression were determined using FITC-labelled mAb N22 (hamster anti-mouse MHC II).

BsAb were produced as before (chapter 2, chapter 3) using the parental mAb to tumor Id, CD19 and MHC II as described in chapter 3, as well as CD40 (mAb 3/23; Rat γ2a; ref. 241). The anti-FcγRI arm of the derivative was derived from mAb-M22 (143).

Binding levels of BsAb to both receptor and tumor were estimated using FITC-labelled BsAb and compared to the equivalent FITC-labelled parental mAb. Fluorescination of Ab derivatives was achieved by the technique described in chapter 2. FcγRI binding was assessed on muG-CSF primed PMN. Tumor binding was determined using A31 or BCL_1 as appropriate. 10^5 target cells were labelled with mAb or BsAb (20 μg/ml) for 15 min on ice, washed, and analysed on a FACS Calibur.

PMN were isolated from whole blood obtained by cardiac bleeding of mice, and red blood cells removed by incubating with 5 % Dextran T500 solution at a ratio of 4:1 v/v, at 37^0C for 30 mins. The resulting supernatant was then layered onto a discontinuous Percoll gradient of 63 % and 68.5 %, spun at 2300 rpm for 20 mins, and PMN removed from the interface between the two Percoll layers (242).

In vitro ADCC activity was calculated using a standard chromium-release assay. Briefly, ^{51}Cr labelled A31 or BCL_1target cells, prepared from homogenised spleens of terminal animals, were coated with BsAb on ice, for 15 min, at concentrations as described, and incubated with isolated murine PMN at E:T ratios as indicated. Where appropriate, mice received muG-CSF (2 μg/day, for 4 days) prior to PMN extraction. Cells were incubated for 4 hours at 37^0C, centrifuged at 1500 rpm, for 5 mins, and 100 μl supernatant harvested from each well to estimate ^{51}Cr release. Maximal release of ^{51}Cr was calculated using target cells to which 150 μl Nonidet P-40 had been added. The percentage specific release was calculated as before (chapter 3). Control experiments were also conducted using unprimed transgenic effector cells, or primed/ unprimed non-transgenic PMN. A similar protocol was employed for measuring PMN mediated ADCC with mAb. Antibody blocking of ADCC was achieved by the addition of polyclonal mouse serum IgG, or M22 $F(ab')_2$ (50 μg/ml) to PMN for 15 mins on ice prior to addition to targets.

4.3 Results

4.3.1 Determination of FcγRI expression levels

A breeding program between FVB/n FcγRI transgenic males and BALB/c or CBA female mice was conducted to establish a colony of receptor positive animals. All experiments were conducted in first generation (F1) mice screened for the presence of the receptor by flow cytometry. As expected, approximately 50 percent of the mice proved to carry the transgene.

The receptor expression profile on leukocytes from the F1 colony was determined by flow cytometry. Figure 4.3.1 shows that FcγRI was detectable at low levels on peripheral blood PMN (Fig.4.3.1A), absent from lymphocytes (Fig.4.3.1.B), and present on peritoneal macrophages (Fig.4.3.1.C). To determine the *in vivo* effect of cytokines on our models, levels of FcγRI expression following muG-CSF administration were analysed. Mice received either 0.5, 1 or 2 μg of muG-CSF per day, s.c, for four days. Levels of FcγRI expression prior to cytokine application, and after 4 days of treatment were then compared using FITC-anti-FcγRI. As a control, non-transgenic siblings and normal BALB/c or CBA mice were also tested under similar conditions. Receptor expression was elevated in both BALB/c x FVB/n (Fig.4.3.2) and CBA x FVB/n (data not shown) animals at all dose ranges. Similarly, receptor expression increased following recombinant human G-CSF (rhG-CSF) therapy (data not shown). No FcγRI expression was induced on PMN of receptor negative F1 mice, or non-transgenic founders, following cytokine treatment (data not shown).

G-CSF is also known to enhance peripheral PMN numbers (144) by driving a premature exodus of these cells from the bone marrow compartment during early stages of development. We compared PMN numbers prior to, and following, cytokine therapy with 0.5, 1 or 2 μg muG-CSF. PMN populations (estimated as a percentage of circulating white blood cell numbers), clearly increased in transgenic mice receiving cytokine, as determined by FACS analysis (Fig.4.3.3). However, this rise in PMN numbers was

observed only at the higher (2 μg/day) dose of muG-CSF (Table 4.3.1). Based on these observations, priming of PMN and FcγRI in subsequent experiments was conducted using the regime of 2 μg/day for four days. Both the increase in FcγRI expression and PMN numbers was transient in that following cessation of cytokine administration, levels returned to those observed prior to treatment within 2-3 days (data not shown).

Although human PMN do not generally express HLA class II, reports have shown that the molecule can be induced on PMN following IFN-γ, IL-3 or GM-CSF stimulation (243). In this capacity PMN can function as APC to CD4+ T cells. Moreover, it appears that this phenomenon is donor dependent, with some individuals expressing high levels of HLA class II and some only low levels. Obviously, expression of the MHC II molecule in the transgenic system would have considerable bearing on the effect of the [FcγRI x MHC II] BsAb. We wished to verify that MHC II expression was not induced on transgenic PMN following muG-CSF administration. Five BALB/c mice, receiving 2 μg muG-CSF/day for 4 days, were tested following that period, for both FcγRI and MHC expression, using FITC labelled mAbs. Profiles for one representative out of the five mice screened are given in Fig.4.3.4. Similar results were obtained for all animals, demonstrating that MHC II expression does not appear to be induced by muG-CSF.
For all the data above, findings were analogous in both our CBA and BALB/c transgenic lines, although only the data for BALB/c x FVB F1 mice has been presented.

4.3.2 Binding of BsAb to target cells

To determine the most effective tumor antigen against which to target PMN, a number of BsAb with a range of specificity (Id, MHC II, CD19, CD40) were produced. All derivatives were $F(ab')_2$ conjugates, derived from chemically linked parental Fab' fragments as described. BsAb were passed through an anti-Fc column to remove contaminating residual IgG, resulting in a pure $F(ab')_2$ population as determined by HPLC analysis (data not shown). The specific binding of these BsAb to tumor cells and FcγRI-expressing PMN was determined by flow cytometry. Direct immunofluorescence using FITC-labelled BsAb, demonstrated that the derivatives were able to bind FcγRI on

peripheral blood PMN from transgenic mice treated with muG-CSF (2 μg/day, 4 days, s.c) (Fig.4.3.5). No binding of either BsAb or FcγRI $F(ab')_2$ was observed on PMN from non-transgenic mice, and only very low levels of binding were observed on PMN from transgenic mice without muG-CSF priming (not shown). Fig.4.3.6 shows that BsAb were also able to bind their respective tumor antigens at levels comparable to those observed with FITC-labelled parental mAb. Shown, are levels of binding to BCL_1 only, although A31 binding profiles were similar.

4.3.3 *In vitro* activity of PMN

We now wished to determine if FcγRI positive PMN could be effectively engaged to kill tumor cells *in vitro*, which tumor antigen made the most effective target, and whether BsAb were better at triggering tumor lysis than mAb. ADCC activity was calculated by a standard chromium-release assay using isolated PMN as effectors. A pure population of PMN was obtained for the assay by whole blood separation on a discontinuous percoll gradient (Fig.4.3.7). To confirm the cells isolated were indeed PMN, the resultant pool was examined by flow cytometry and found to be approximately 90 % pure, with elevated levels of FcγRI, as detected by FITC-anti-FcγRI (data not shown). BCL_1 and A31 lymphoma targets were exposed to PMN isolated from mice at an E:T ratio of 50:1, over a range of antibody concentrations (1, 0.1, 0.01 μg/ml). Firstly, the ability of a range of mAb to induce PMN mediated tumor lysis was determined. mAb to Id, MHC II, CD19 and CD40 were incubated with A31 tumor cells, together with PMN from unprimed, non-transgenic mice (Fig.4.3.8.A); G-CSF primed, non-transgenic mice (Fig.4.3.8.B); unprimed transgenic mice (Fig.4.3.9.A); or G-CSF primed transgenic mice (Fig.4.3.9.B). An isotype matched mAb of non-tumor binding specificity (anti-BCL_1 Id) and the [FcγRI x MHC II] BsAb were included as negative and positive controls respectively. In the absence of cytokine priming, PMN from both non-transgenic and transgenic animals, were unable to kill tumor when directed against antigen of any specificity. PMN from primed animals were able to kill tumor when triggered by anti-MHC II mAb exclusively, independent of the presence of (human) FcγRI. The BsAb was only able to mediate substantial tumor destruction by cytokine primed, transgenic PMN. Interestingly, PMN

triggered by BsAb appeared to be more potent than when triggered by the mAb of identical specificity. Similar findings were observed against the second tumor model, BCL_1. Again, PMN from mice not receiving G-CSF were unable to kill tumor, irrespective of whether they did, or did not carry the transgenic receptor (Fig.4.3.10.A, and 4.3.11.A). However, primed PMN were able to destroy tumor when directed against MHC II (Fig.4.3.10.B, and 4.3.11.B). The BsAb was again only able to trigger killing by G-CSF primed, FcγRI positive PMN (Fig.4.3.11.B), and at levels similar, but not substantially greater than, that observed for the anti-MHC II mAb. The activity of the anti-MHC II mAb could be blocked in the presence of competing polyclonal murine IgG. This had no effect on the activity of the BsAb (Fig.4.3.12.A). Instead, addition of excess M22 $F(ab')_2$ to PMN prior to the assay was able to inhibit BsAb mediated killing (Fig.4.3.12.B).

We also wished to determine if PMN displayed similar antigen restriction when targeted to tumor by BsAb. A31 and BCL_1 targets were incubated with BsAb (1, 0.1, and 0.01 μg/ml), and isolated PMN as before, at an E:T ratio of 50:1 and 10:1. Again, the [FcγRI x MHC II] derivative proved superior to any other in terms of killing, with over 90% specific ^{51}Cr release in the A31 model (Fig.4.3.13). Cytotoxicity was titratable, decreasing with both antibody concentration, and E:T ratio. However, unlike PMN targeted by mAb, which show antigen restricted killing, all BsAb derivatives mediated some degree of lysis, irrespective of antigen specificity. For A31 (Fig.4.3.13) killing can be ranked in the order of MHC II>CD19>CD40>Id; and for BCL_1 (Fig.4.3.14) the order of activity was MHC II>Id>CD40>CD19. PMN from non-cytokine treated, transgenic animals, failed to produce any significant degree of killing, indicating the requirement for G-CSF mediated, FcγRI upregulation and priming of PMN in RCC (Fig.4.3.15 solid histograms). Similarly, PMN from non-transgenic mice, either treated (striped histograms), or left untreated with muG-CSF (open histograms), failed to lyse tumor in the presence of BsAb, confirming that killing was specifically induced through binding to the human FcγRI molecule. In addition, lysis required specific PMN recruitment and retargeting, as neither PMN or BsAb alone, or BsAb of non-tumor binding specificity, produced any killing (data not shown).

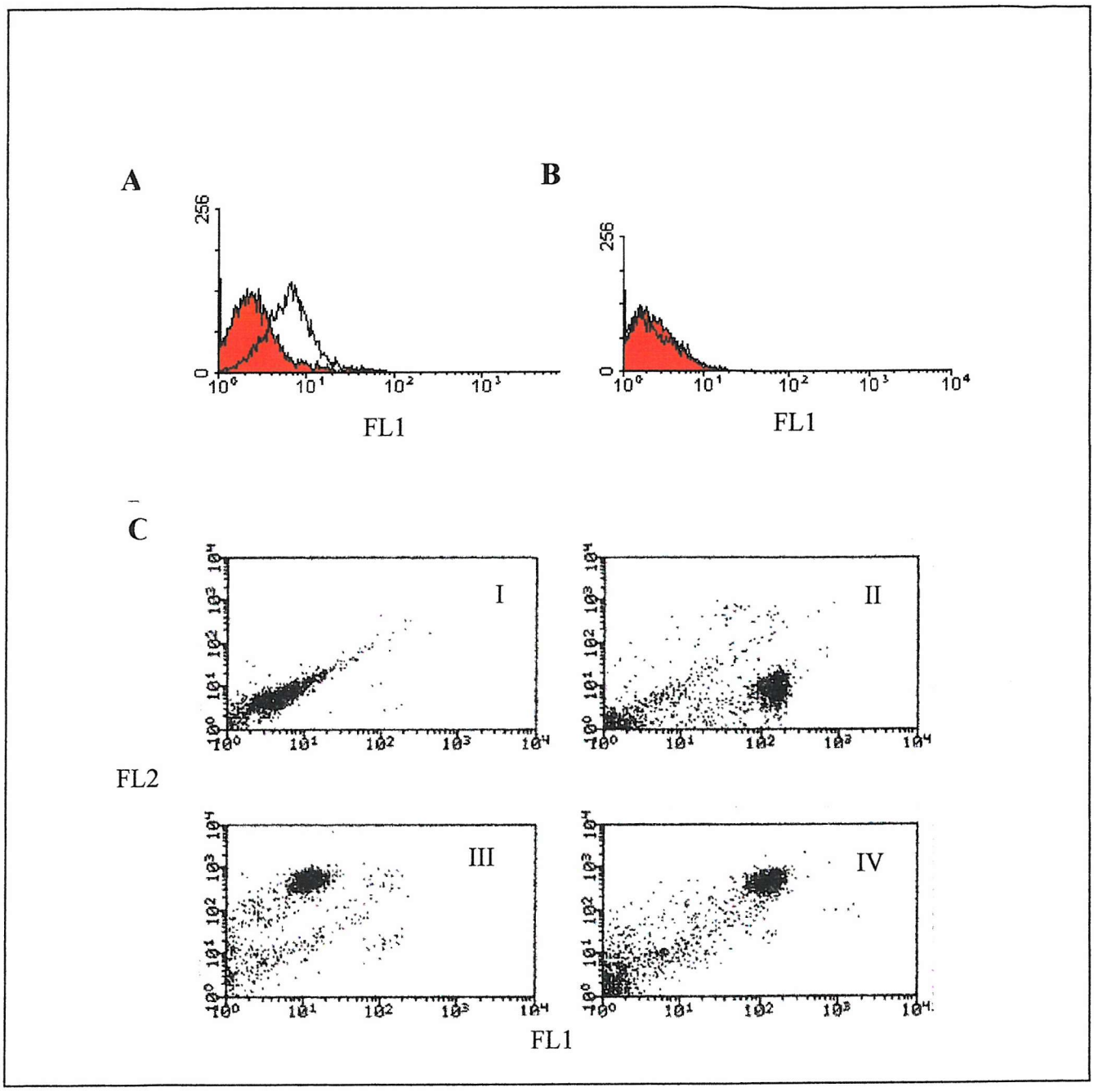

Fig.4.3.1 Expression profile of FcγRI in transgenic mice. Peripheral blood leukocytes from F1 transgenic animals were screened for the presence of FcγRI by flow cytometry. **(A)** shows the level of expression of FcγRI on PMN from a transgenic animal (open histogram) compared to a non-transgenic littermate (solid histogram) as determined with a FITC- anti-FcγRI mAb. **(B)** shows receptor expression on lymphocytes, again taken from a transgenic mouse (open histogram) and a non-transgenic mouse (solid histogram), as before. **(C)** shows levels of receptor expression on peritoneal macrophages from a transgenic animal. Cells were labelled with FITC-anti-FcγRI versus Pe-anti-F/480, (which recognises a macrophage surface glycoprotein, absent from PMN and monocytes). (I) represents unlabelled cells; (II) anti-FcγRI alone; (III) anti-F/480 alone; and (IV) dual staining to identify receptor positive macrophages.

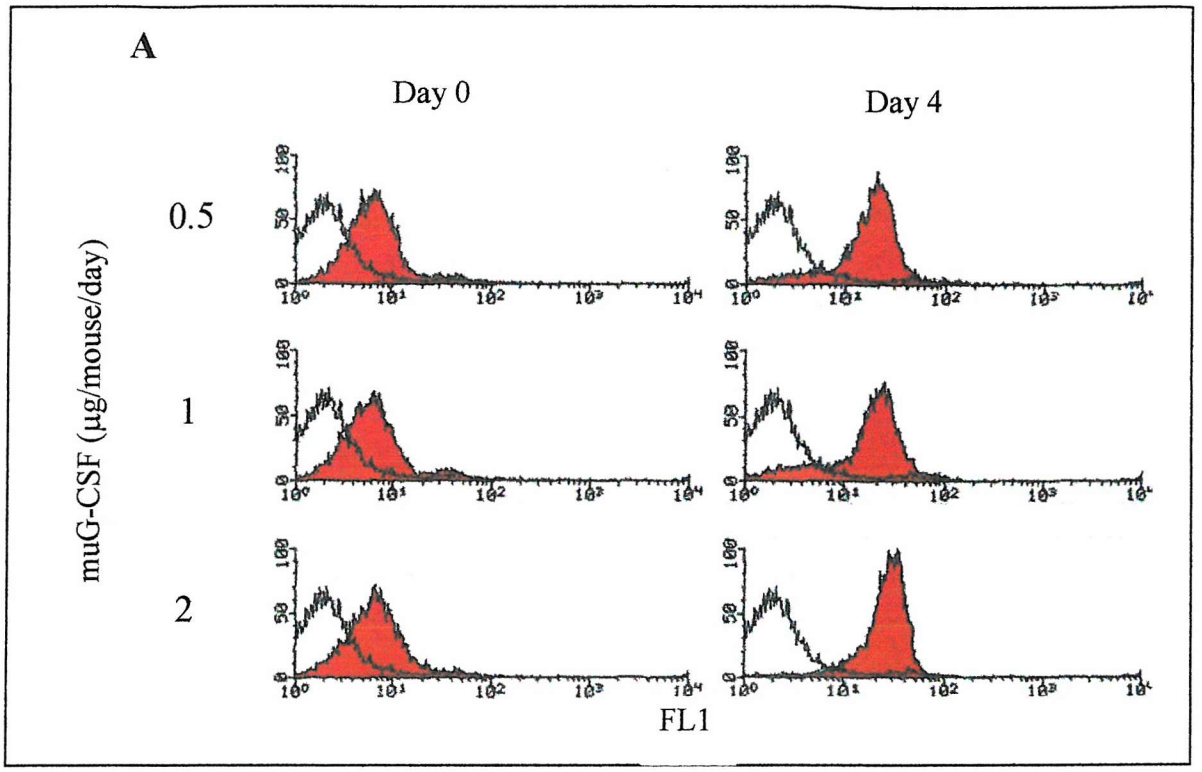

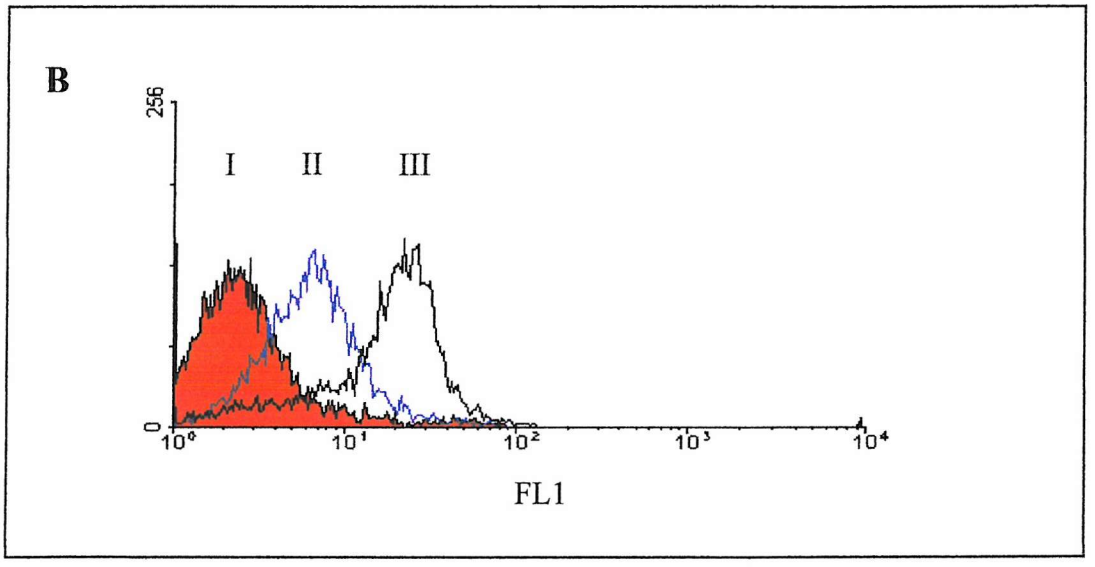

Fig.4.3.2 FcγRI expression on PMN from transgenic BALB/c x FVB/n F1 mice.

(A) Receptor expression on PMN following treatment with either 0.5, 1, or 2 µg muG-CSF/day, for 4 days, s.c. Levels of FcγRI on a gated PMN population were determined by FITC-anti-FcγRI labelling of whole blood (20 µg/ml), analysed by flow cytometry on a FACScan. Solid histograms represent receptor levels pre-muG-CSF (Day 0), compared to levels post- muG-CSF treatment (Day 4). Open histograms represent expression on PMN from control, non-transgenic mice under identical conditions. **(B)** is a composite, showing expression of FcγRI on a non-transgenic mouse (I), and transgenic mouse pre- (II) and post- (III) muG-CSF treatment.

Fig. 4.3.3

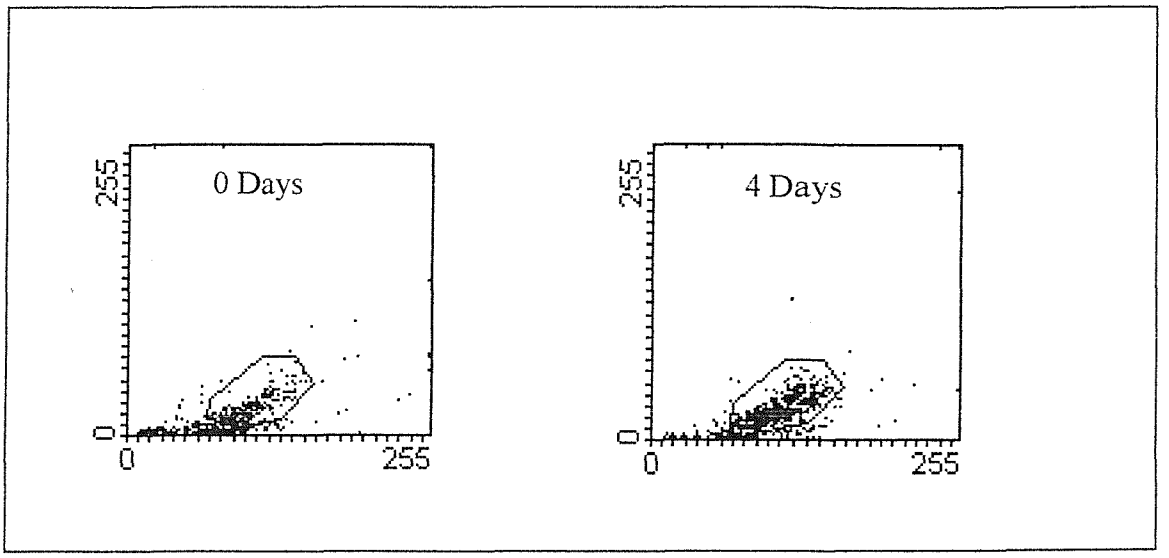

Table 4.3.1

Dose muG-CSF (μg)	% Circulating PMN (day 4)
0	12.03
0.5	12.94
1	12.26
2	45.44

Fig. 4.3.3 PMN numbers can be upregulated in mice by muG-CSF. Transgenic BALB/c x FVB F1 mice were treated with muG-CSF (0.5, 1, or 2 μg/day) for 4 days and the percentage of PMN in the circulation, analysed using Fsc v Ssc flow cytometry. FITC-anti-FcγRI was used as a positive marker for PMN. Shown are PMN from mice at 0 days treatment, and 4 days treatment, with 2 μg muG-CSF/day. **Table 4.3.1** lists the percentage of circulating PMN from transgenic animals treated with a range of cytokine doses. Only a dose of 2 μg/ day was able to increase the percentage of PMN

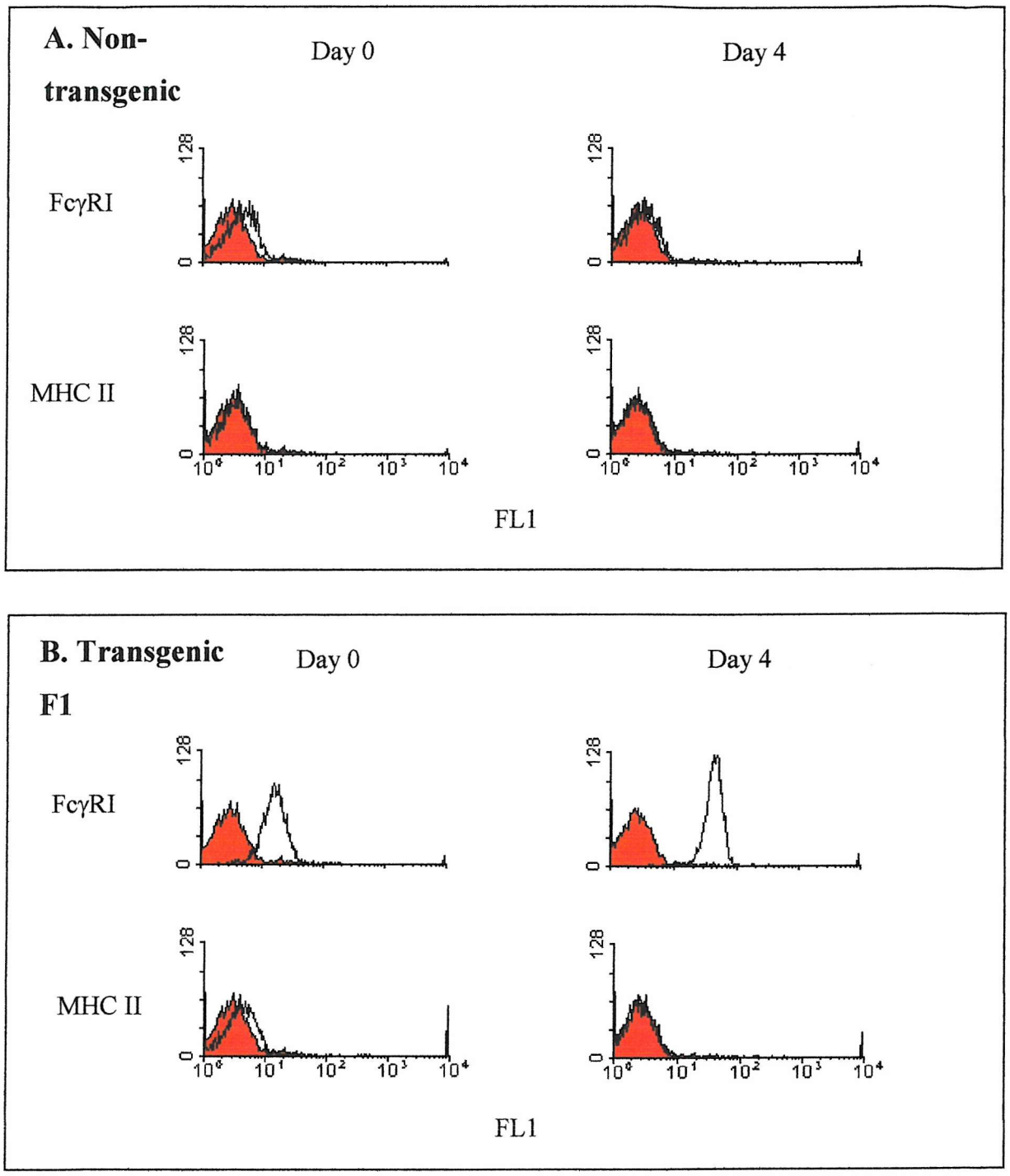

Fig.4.3.4 MHC II expression by muG-CSF primed PMN. PMN from non-transgenic mice **(A)** and transgenic F1 mice **(B)** treated with muG-CSF (2 μg/day, for 4 days, s.c), were analysed for expression of MHC II. Levels of expression, as determined by flow cytometry using a FITC-anti-MHC II mAb, were compared prior to treatment (Day 0) and post muG-CSF (Day 4) on a gated population of PMN obtained from analysis of whole blood. As a control, levels of FcγRI were also analysed. Solid histograms represent binding of control FITC-anti-

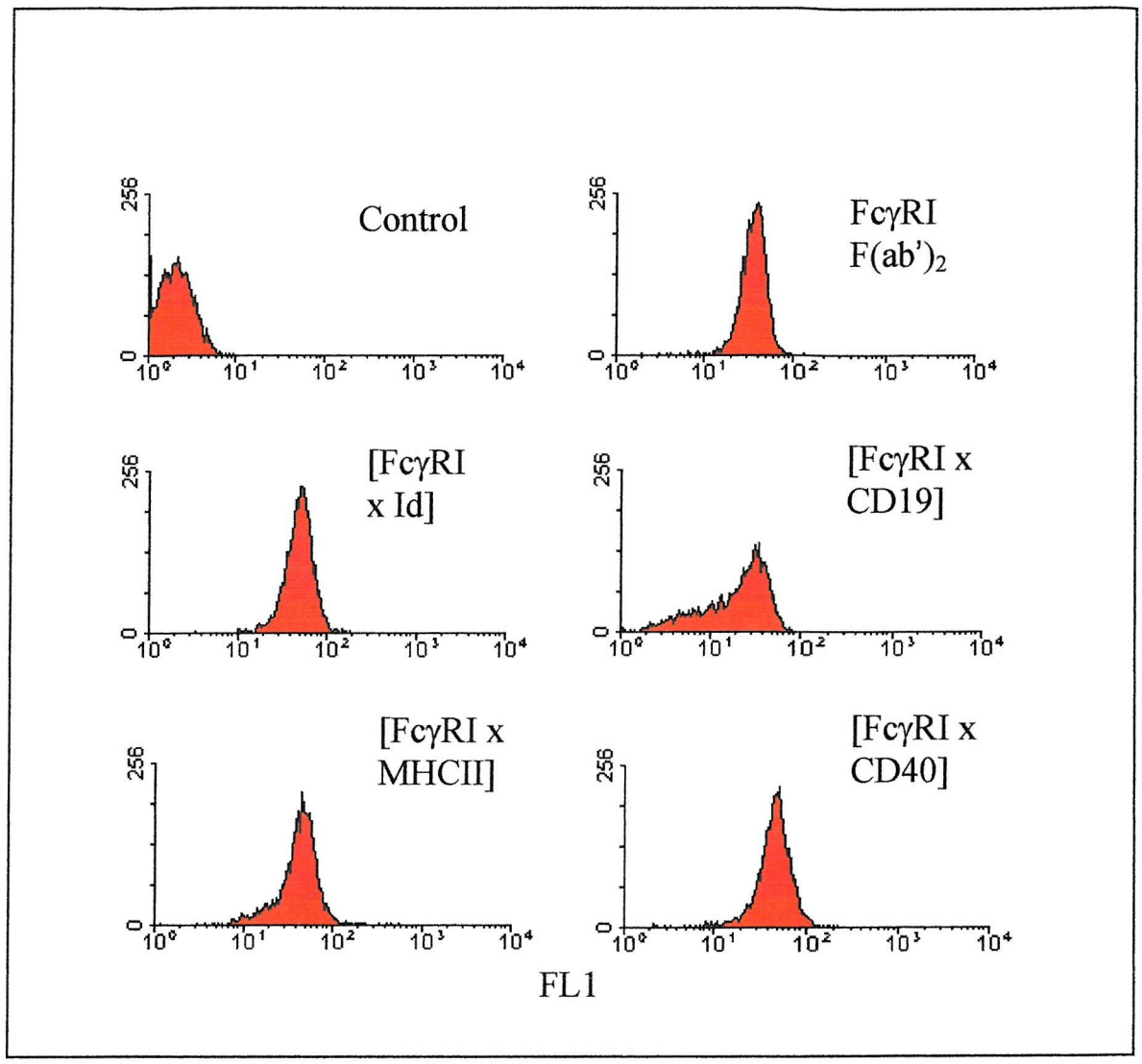

Fig.4.3.5 Binding of BsAb to BALB/c x FVB/n F1 FcγRI$^+$ PMN. Levels of binding of FITC-BsAb, to muG-CSF primed (2 μg/day, s.c, 4 days), FcγRI positive, transgenic PMN, was compared to that of FITC-anti-FcγRI F(ab')$_2$. Isolated PMN (10^5/sample) were incubated with 20 μg/ml FITC-labelled Ab, for 15 min on ice, washed and cells analysed on a FACS Calibur. Control was the non-binding [CD3 x BCL_1 Id] F(ab')$_2$ BsAb. All derivatives bound to PMN at levels similar to the anti-FcγRI F(ab')$_2$ Ab.

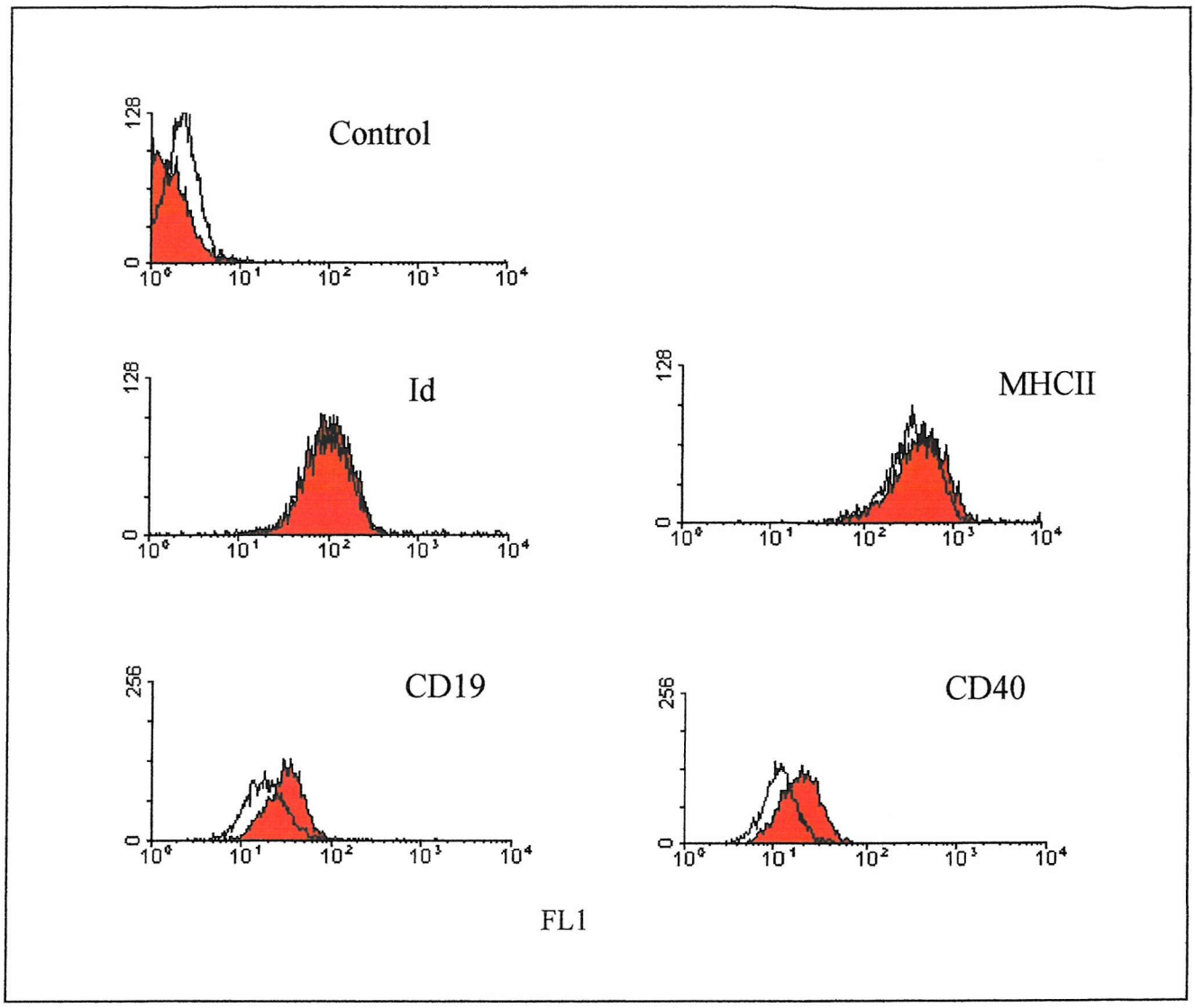

Fig.4.3.6 Binding of BsAb to BCL_1. Shown are the binding profiles of FITC-labelled BsAb (open histograms) compared to FITC-labelled, parental mAb (solid histograms). 100 µl BCL_1tumor cells (10^6/ml) were incubated with Ab at a final concentration of 20 µg/ml, for 15 min on ice, washed, and analysed on a FACS Calibur. Ab specificity is as indicated above, the control being the non-binding, anti-A31 Id mAb or BsAb. All derivatives were able to bind their respective tumor antigens at levels comparable to parental mAb.

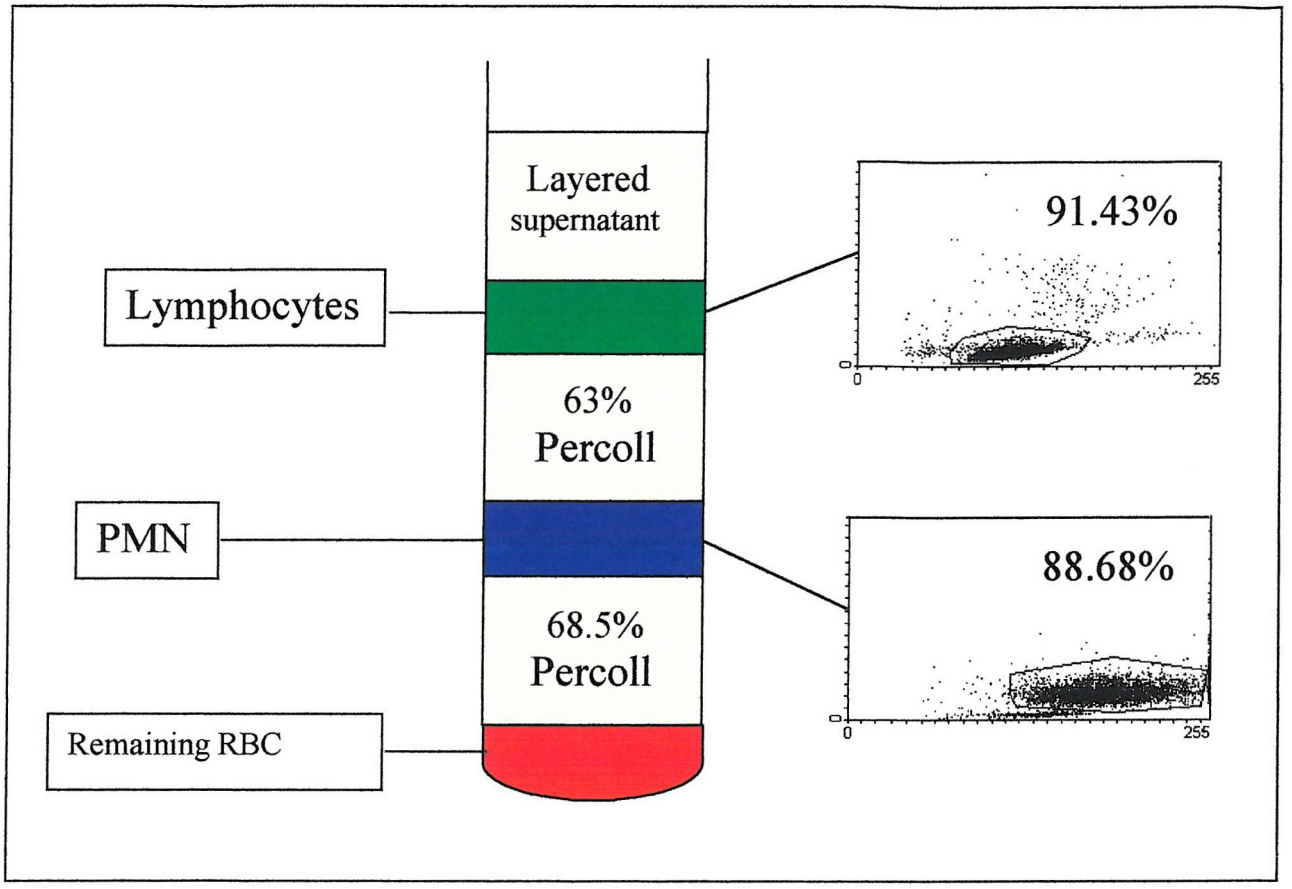

Fig.4.3.7 Percoll purification of PMN. Whole blood from G-CSF primed animals was obtained by cardiac puncture into heparin coated syringes. Blood was incubated with a 5 % Dextran T500 solution, at a ratio of 4:1, at 37^{0}C, for 30 mins, to remove the majority of RBC. Resulting supernatant was layered on to a discontinuous gradient of 68.5 % and 63 % Percoll, and centrifuged at 2300 rpm, for 20 mins. The resulting interface between the two layers of Percoll was found to contain a purified population of PMN (approx. 90 %), whilst lymphocytes remained at the interface between the lower density Percoll and the supernatant. Any remaining RBC pelleted at the bottom of the tube.

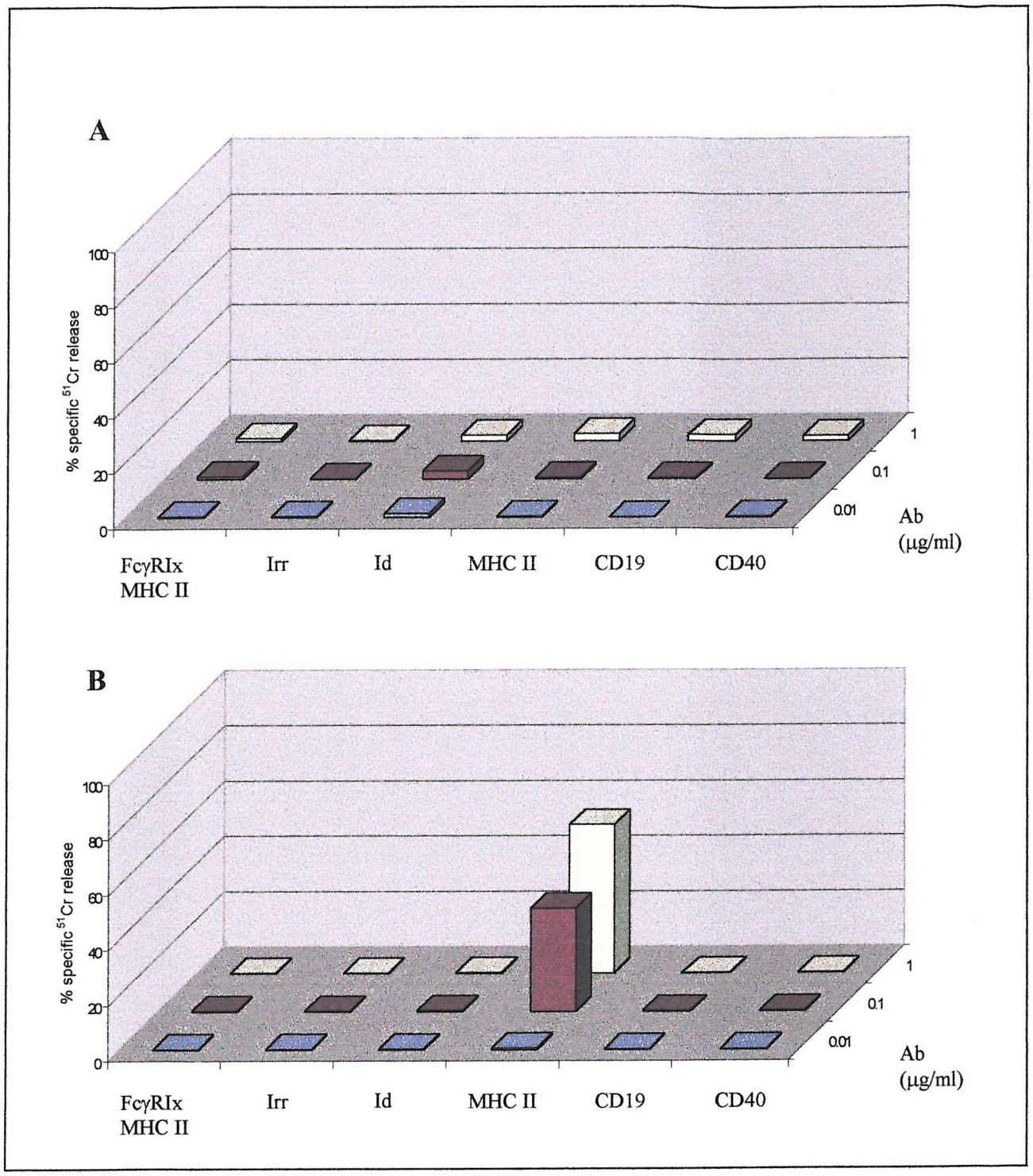

Fig.4.3.8 ADCC of A31 using murine PMN. ADCC was determined using a standard chromium-release assay as described. ^{51}Cr labelled target cells were mixed with mAb of varying specificity (as indicated) at either 1, 0.1, or 0.01 μg/ml. Murine PMN isolated from whole blood of non-transgenic mice, either unprimed **(A)**, or given 2 μg muG-CSF/day, for 4 days, s.c **(B)**, were added at an E:T ratio of 50:1. The control irrelevant mAb was the alternative non-binding anti-BCL_1 Id. [FcγRI x MHC II] was also included as a positive control. All determinations were performed in triplicate.

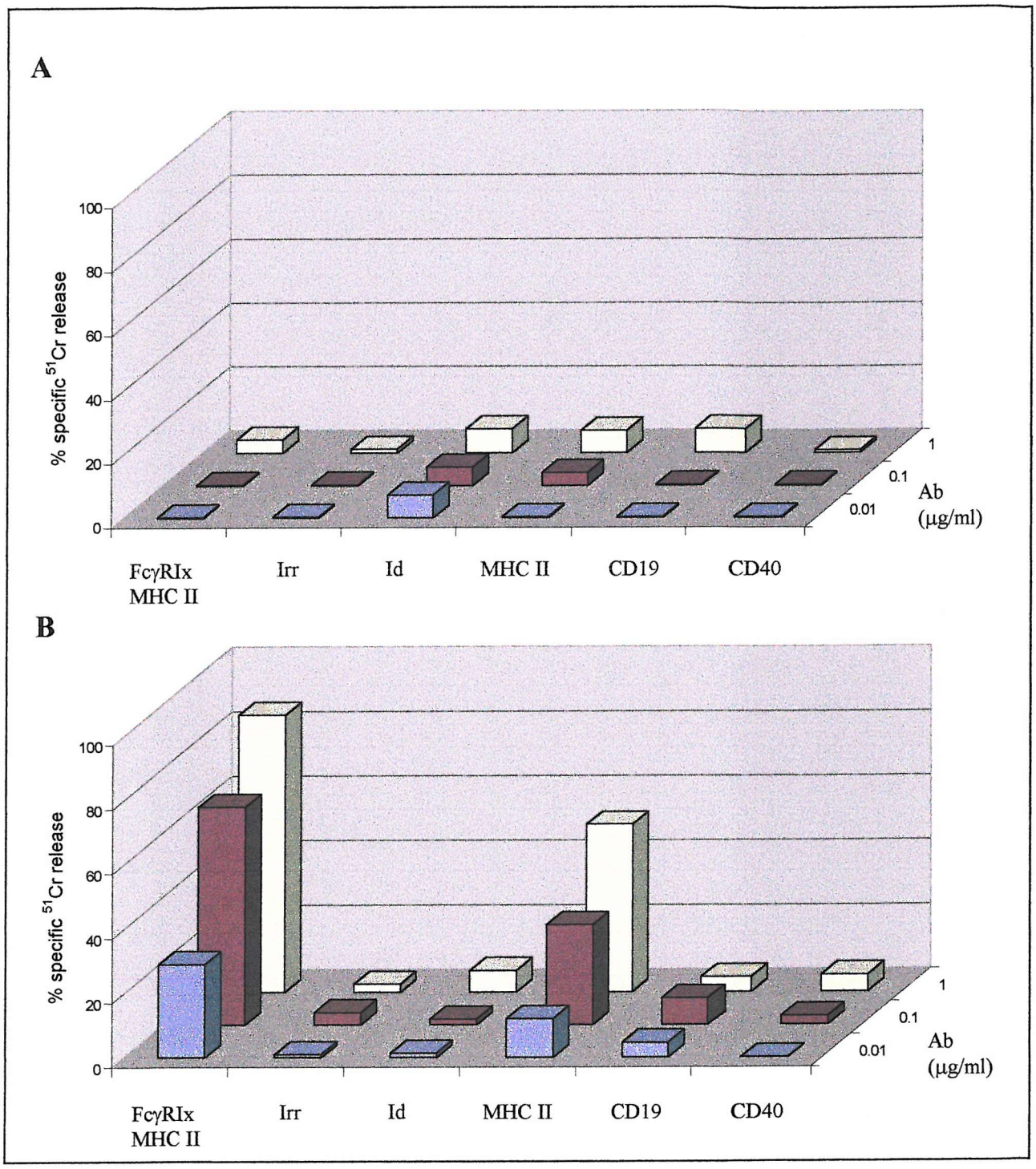

Fig.4.3.9 ADCC of A31 using transgenic murine PMN. ADCC was determined using a standard chromium-release assay as described. ^{51}Cr labelled target cells were mixed with mAb of varying specificity (as indicated) at either 1, 0.1, or 0.01 µg/ml. Murine PMN isolated from whole blood of transgenic mice, either unprimed **(A)**, or given 2 µg muG-CSF/day, for 4 days, s.c **(B)**, were added at an E:T ratio of 50:1. The control irrelevant mAb was the alternative non-binding anti-BCL_1 Id. FcγRI x MHC II was also included as a positive control. All determinations were performed in triplicate.

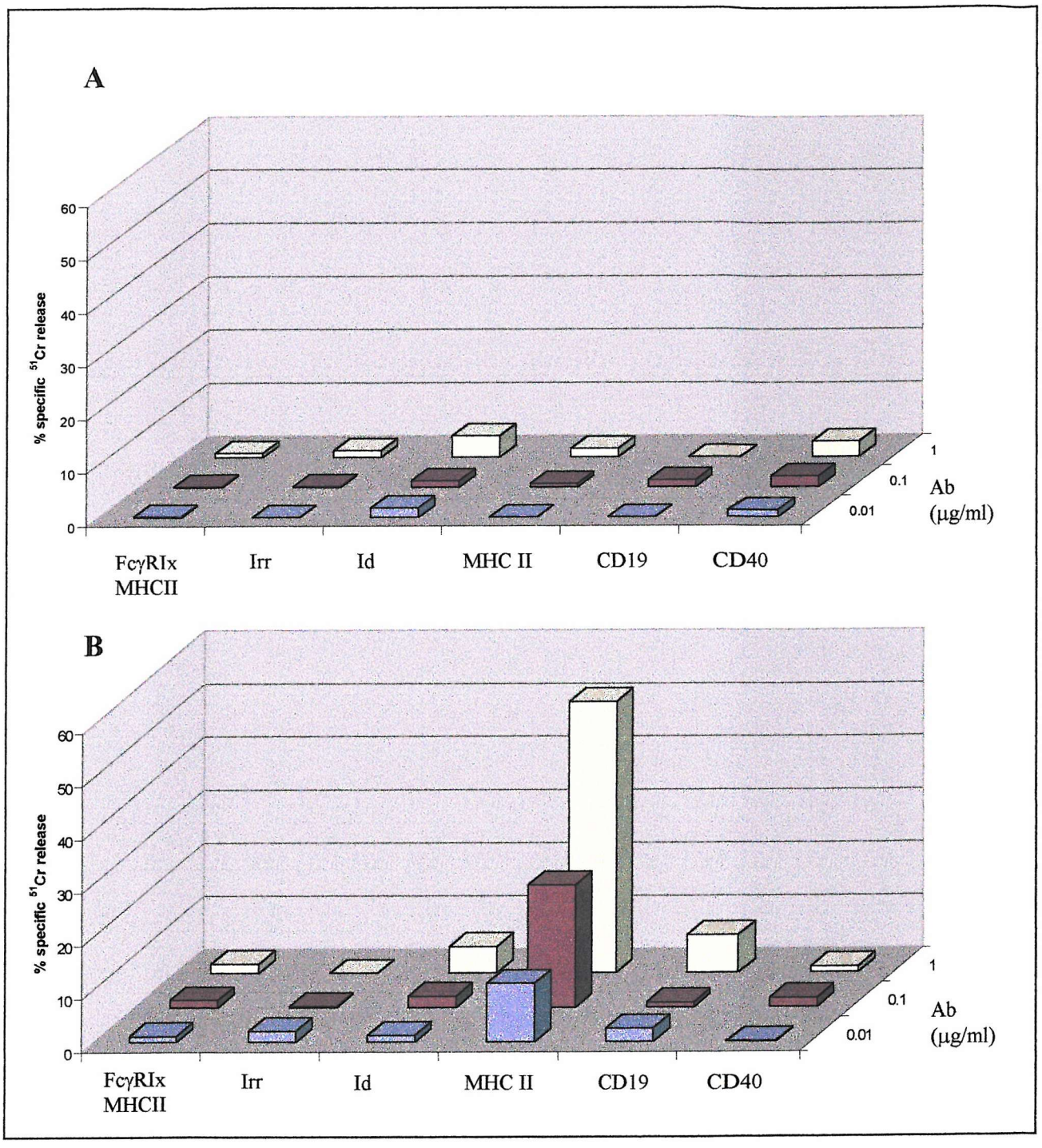

Fig.4.3.10 ADCC of BCL_1 using murine PMN. ADCC was determined using a standard chromium-release assay as described. ^{51}Cr labelled target cells were mixed with mAb of varying specificity (as indicated) at either 1, 0.1, or 0.01 µg/ml. Murine PMN isolated from whole blood of non-transgenic mice, either unprimed **(A)**, or given 2 µg muG-CSF/day, for 4 days, s.c **(B)**, were added at an E:T ratio of 50:1. The control irrelevant mAb was the alternative non-binding anti-A31 Id. [FcγRI x MHC II] was also included as a positive control. All determinations were performed in triplicate

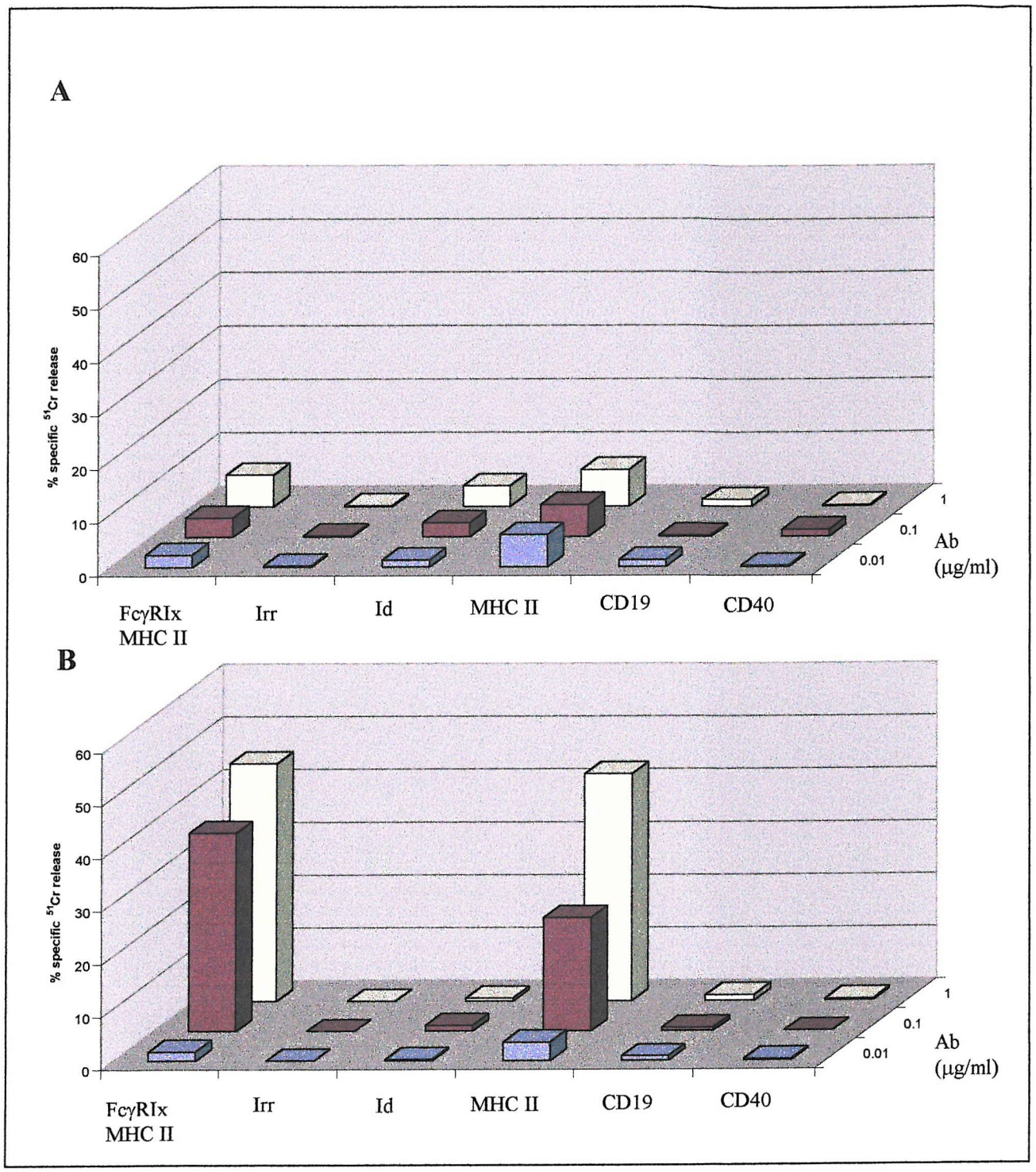

Fig.4.3.11 ADCC of BCL_1 using transgenic murine PMN. ADCC was determined using a standard chromium-release assay as described. ^{51}Cr labelled target cells were mixed with mAb of varying specificity (as indicated) at either 1, 0.1, or 0.01 μg/ml. Murine PMN isolated from whole blood of transgenic mice, either unprimed **(A)**, or given 2 μg muG-CSF/day, for 4 days, s.c **(B)**, were added at an E:T ratio of 50:1. The control irrelevant mAb was the alternative non-binding anti-A31 Id. [FcγRI x MHC II] was also included as a positive control. All determinations were performed in triplicate.

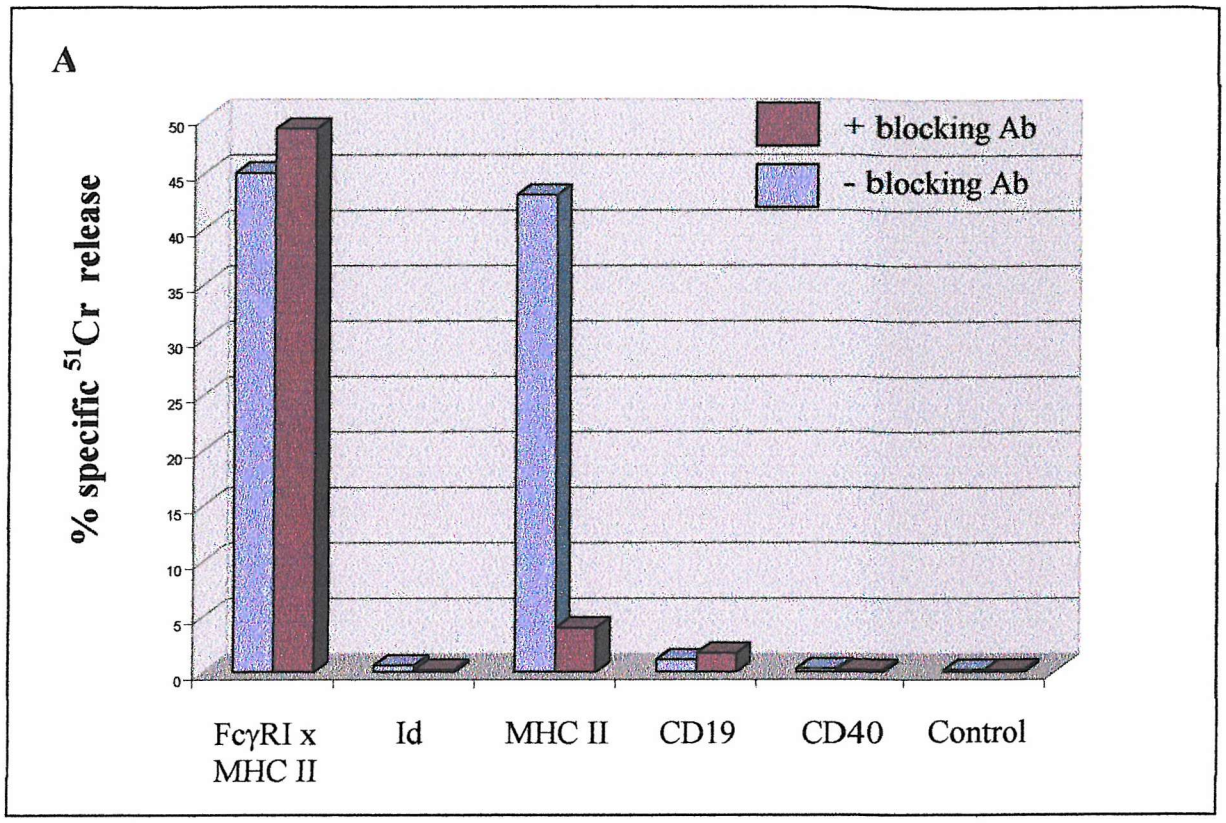

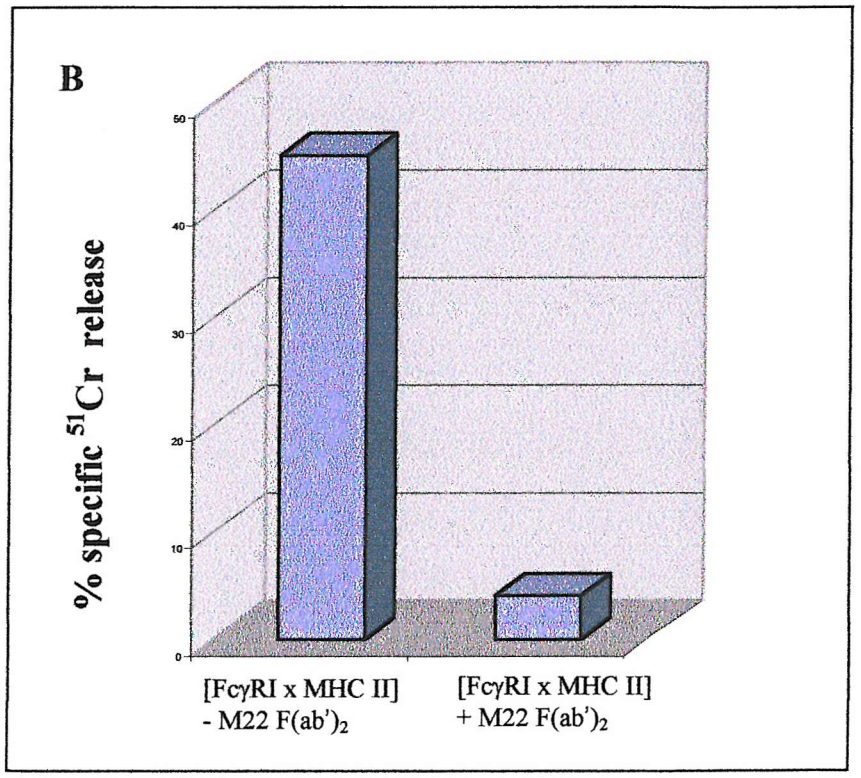

Fig.4.3.12 Blocking of ADCC activity. ADCC was determined as before using a standard chromium-release assay. BCL_1 target cells were mixed with antibody (1μg/ml) of specificity as indicated, and cytokine primed, FcγRI positive murine PMN at an E:T ratio of 50:1, **(A)** in the presence of polyclonal murine serum IgG (50 μg/ml), or **(B)** M22 F(ab')$_2$ (50 μg/ml). The control was the non-binding A31-Id.

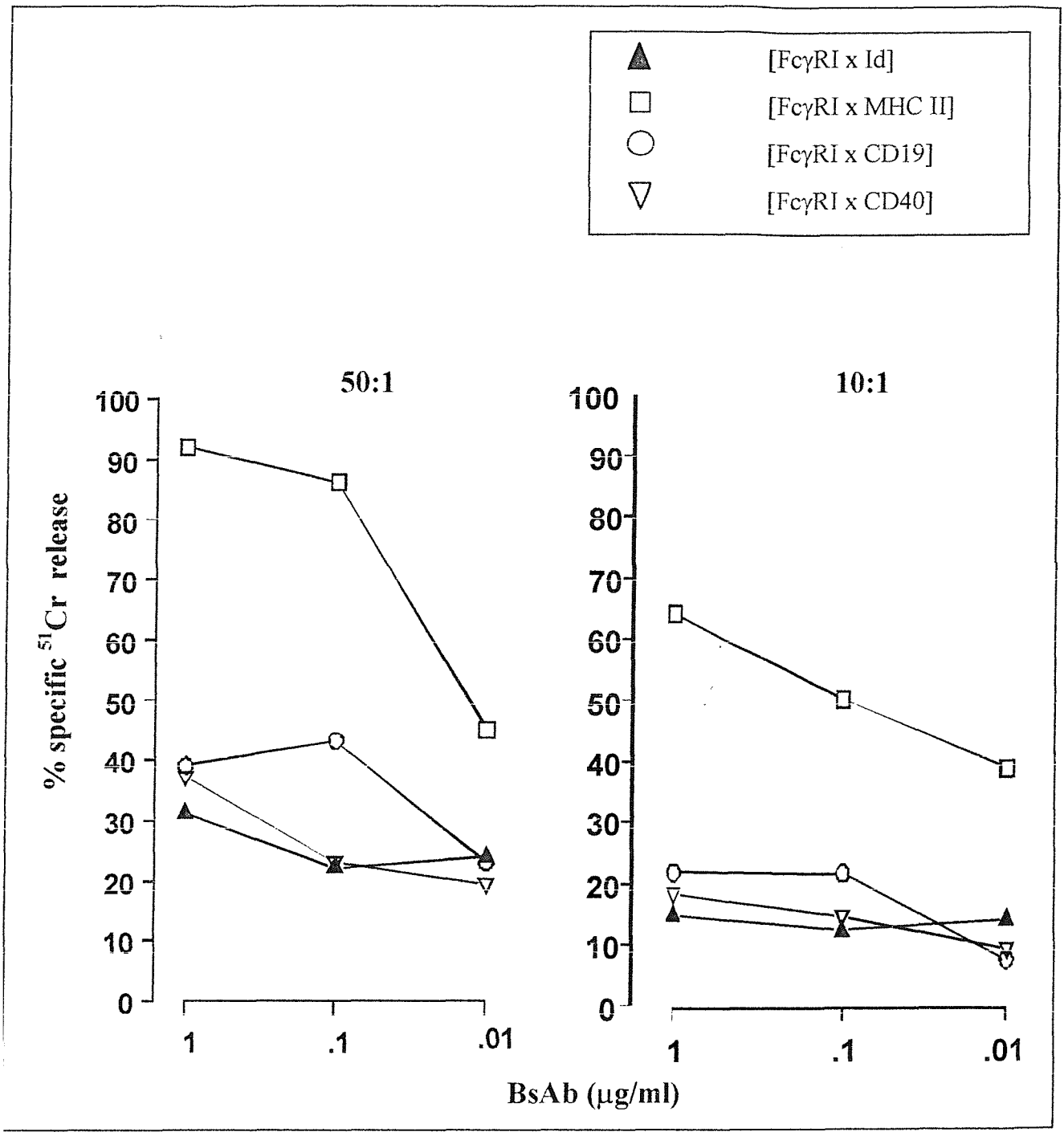

Fig.4.3.13 RCC of A31 by transgenic murine PMN. RCC activity was determined using a standard chromium-release assay as described. Chromium labelled target cells were mixed with BsAb of varying specificity (as indicated) at a final concentration of either 1, 0.1, or 0.01 μg/ml. PMN isolated from whole blood of FcγRI positive animals, stimulated with 2 μg muG-CSF/day, for 4 days, s.c, were added at a ratio of 50:1or 10:1 (as indicated). All determinations were performed in triplicate.

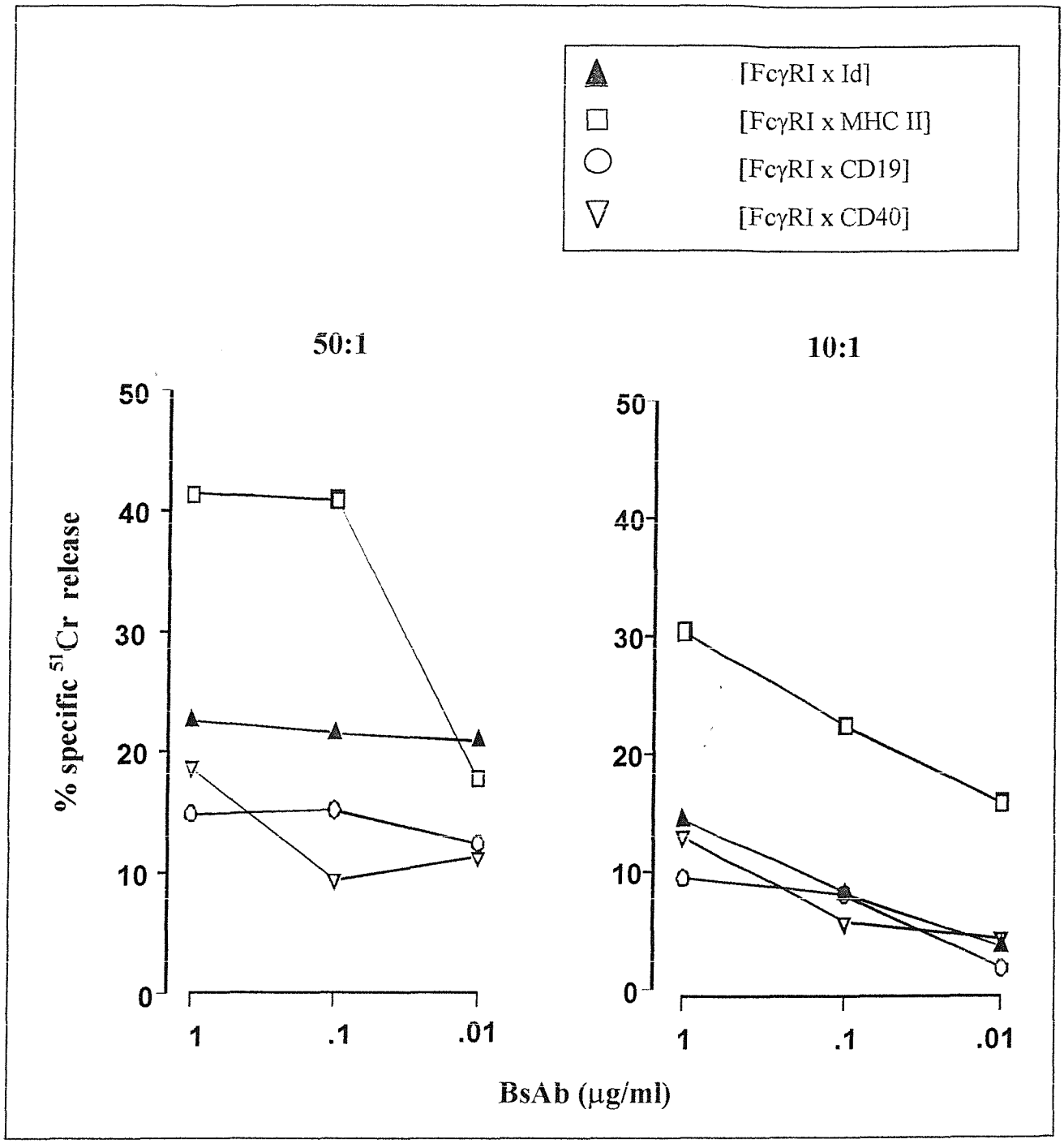

Fig.4.3.14 RCC of BCL_1 by transgenic murine PMN. RCC activity was determined using a standard chromium-release assay as described. Chromium labelled target cells were mixed with BsAb of varying specificity (as indicated) at a final concentration of either 1, 0.1, or 0.01 μg/ml. PMN isolated from whole blood of FcγRI positive animals, stimulated with 2 μg muG-CSF/day, for 4 days, s.c, were added at a ratio of 50:1 or 10:1 (as indicated). All determinations were performed in triplicate.

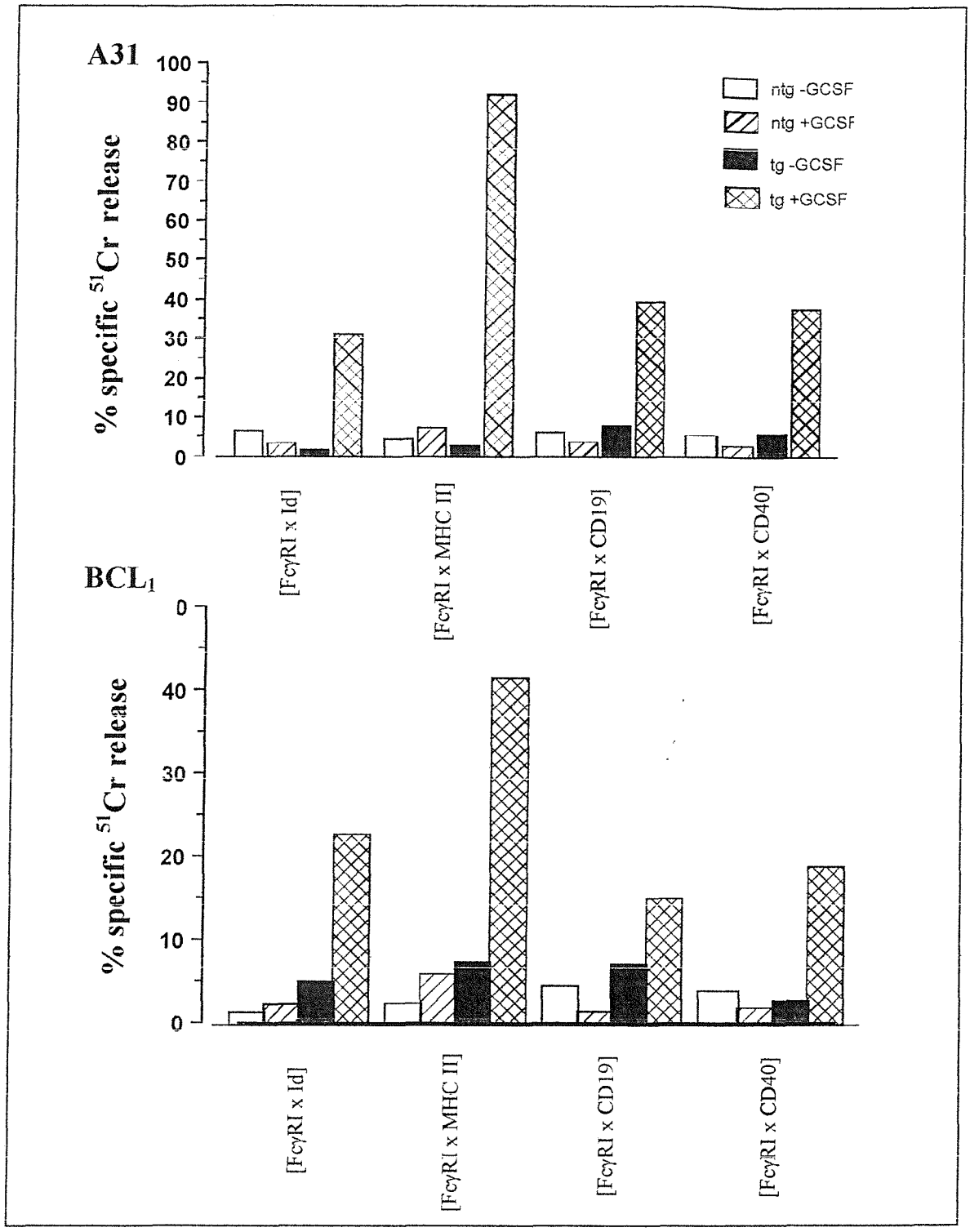

Fig.4.3.15 RCC of A31 and BCL_1 with murine PMN. ^{51}Cr labelled A31 or BCL_1 target cells were mixed with BsAb of varying specificity (as indicated) at 1 μg/ml, and then murine PMN were added at a ratio of 50:1. PMN isolated from FcγRI positive animals either without (■) or with muG-CSF priming (▤) were compared to non-transgenic littermates, again either unprimed (□) or muG-CSF treated (▨). Where appropriate mice received 2 μg muG-CSF/day, for 4 days, s.c. PMN were isolated from whole blood as described. All determinations were performed in triplicate.

4.4 Discussion

In this chapter, we describe the ability of a panel of $F(ab')_2$ BsAb to trigger the cytotoxic activity of FcγRI expressing PMN, against two lymphoma lines, A31 and BCL_1. FcγRI is a highly potent trigger molecule for ADCC, capable of instigating tumor cell lysis by PMN (145). Although its expression is normally confined to monocytes and macrophages, it can be induced on PMN following application of IFN-γ or G-CSF (144). Moreover, development of a transgenic murine model expressing the human receptor allows us to more clearly differentiate between the function of FcγRI as opposed to other Fc receptors, which generally show some overlap in binding characteristics. As no anti-murine FcγRI mAb exists, and ethical considerations preclude testing in humans, this model provides an excellent opportunity to study the functional activity of FcγRI in tumor lysis.

In man, FcγRI is constitutively expressed on macrophages, monocytes, some DC, and at low levels on PMN (138). This expression profile was reflected in the F1 progeny of our transgenic model (Fig.4.3.1). FcγRI was expressed on macrophages, and at low levels on PMN, but increased following cytokine administration, and was absent from lymphocytes. These observations indicate that receptor expression in the F1 mice matches that in humans. It is known that FcγRI levels are naturally increased on PMN during inflammation or bacterial infections due to cytokines such as IL-10, or IFN-γ. *In vitro* studies of IFN-γ application reveal that cytokines not only stimulate increased surface expression of membrane receptor complexes on PMN, but also prime PMN for destruction of pathogens by enhancing expression of components crucial to signaling and the oxidative burst (244). Systemic application of IFN-γ also upregulates FcγRI in human patients, as does G-CSF. Increasing receptor expression on effector cells is obviously of importance in immunotherapeutic strategies targeting FcγRI, either in man, or in pre-clinical models. Application of muG-CSF to transgenic animals was demonstrated to increase receptor levels on PMN (Fig.4.3.2). At sufficient dose, this also led to a simultaneous increase in numbers of PMN circulating in the periphery from

approximately 14 % to 45 % (Fig.4.3.3). With continued cytokine administration this rose to nearly 70 % in some mice (data not shown). Once cytokine supplementation is halted, levels of PMN return to normal within 2 to 3 days (not shown). G-CSF induced *in vivo* expansion of the PMN population has been noted in human patients, when treated systemically, and can be used to combat conditions of neutropenia (244). This enhancement of PMN numbers is of great significance to immunotherapy, effectively increasing the available effector pool *in vivo*.

Cytokine treatment, for example with IFN-γ, has been reported to induce expression of MHC II on PMN (243). This was a concern for application of the [FcγRI x MHC II] derivative. Whilst MHC II expression has been noted to be donor dependent, we observed no expression on any of the mice tested, indicating that this is not a problem in this system.

To determine the cytotoxic activity of these PMN against murine lymphoma, a panel of BsAb were produced bearing dual specificity for FcγRI and a range of B-antigens (tumor Id, MHC II, CD19, CD40). These derivatives were all chemically linked $F(ab')_2$ molecules. Before *in vitro* activity was assessed, we wished to determine that all derivatives could bind both FcγRI and the target antigen of choice. This was confirmed using flow cytometry. All BsAb were able to bind to their target antigens, and we observed no decrease in the binding levels with the univalent bispecific derivatives compared to the parental mAb (Fig.4.3.5 and 4.3.6). Others have reported decreased binding activity of BsAb compared to mAb (245). However, here a secondary polyclonal reagent was used to detect bound antibody, which recognises more determinants on IgG than Fab', thus being less sensitive for the BsAb. We overcame this problem by direct fluorescence labelling of derivatives.

ADCC assays were performed with isolated, muG-CSF primed PMN, to deduce which antigen made the most effective target, and whether BsAb were better able to trigger anti-tumor activity than mAb. A number of reports indicate that human PMN are able to kill a variety of B-lymphoma lines *in vitro*, but do so in an antigen restricted fashion with only

mAb of specificity to HLA epitopes being able to mediate tumor lysis (246). Other surface antigens such as CD19, CD37, and CD38 consistently prove to be poor targets for this effector pool. Furthermore, this killing is only observed with G-CSF primed PMN. Studies with [FcγRI x CD37] and [FcγRI x HLA II] BsAb also showed that the anti-CD37 BsAb was a poor mediator of RCC, whereas the anti-HLA II derivative was effective. *In vitro* cytotoxicity has also been reported for transgenic murine effectors, targeted against the murine lymphoma line IIA1.6 with an [FcγRI x MHC II] BsAb (245). Such antigen restricted cytotoxicity is not observed for other cells, such as macrophages, targeted via FcγRI (247).

We too observed MHC II antigen restricted killing of lymphoma targets sensitised with mAb. Anti-MHC II mAb produced tumor lysis of up to 50 % whereas mAb of other specificity (Id, CD19, CD40) failed to mediate PMN induced tumor lysis (Fig.4.3.6 – 9). Lysis was dependent on muG-CSF priming, indicating that ADCC was dependent on PMN activation. This activity could be blocked in the presence of excess normal, polyclonal, mouse IgG. This is presumably due to receptor saturation by the IgG, thus blocking interaction of the mAb Fc.

Interestingly, BsAb of all specificity were able to trigger some degree of target cell destruction, indicating that BsAb were able to effectively bridge activated PMN to tumor. Once again, the anti-MHC II BsAb proved most potent, particularly against the A31 lymphoma, where up to 90% specific activity was achieved (Fig.4.3.13). Activity against BCL_1 lymphoma was less impressive, (around 40 %), but the anti-MHC II was clearly the most potent. Other derivatives all directed considerably lower levels of lysis, at around 30 - 40 % (A31) and 20 % (BCL_1). These levels, while lower than those observed with MHC II BsAb, were clearly specific. The ability of PMN triggered via FcγRI to kill when targeted against antigens other than MHC II is in contrast to the current literature. However, the apparent lack of antigen restriction here, could in part be due to differing sensitivities of the murine tumors, compared to the human cell lines used by others. In addition, whilst enriched PMN populations were used as effectors, they were not 100 %

pure, and it is possible that some contaminating cells may be contributing to killing at a small level, explaining the activity of non-MHC II targeting derivatives.

RCC triggered by BsAb was consistently higher than that observed with mAb. This activity was due to the specific triggering of FcγRI on PMN as (1) no killing was observed with PMN from non-transgenic mice, or transgenic mice that had not received muG-CSF; (2) no antibody independent killing was observed with PMN alone (not shown); (3) target cells were not lysed by antibody in the absence of effector cells; (4) control, non-tumor binding BsAb were not able to trigger PMN mediated target destruction and (5) addition of excess M22 $F(ab')_2$ (anti-FcγRI), but not polyclonal serum IgG, could block BsAb RCC. This last issue reflects the ability of the BsAb to bind FcγRI outside of its natural ligand binding domain, and indicates that BsAb will be able to overcome receptor saturation *in vivo*.

Target antigen restriction to class II has been postulated to be due to upregulation of adhesion molecules such as LFA-1 following ligation of the class II molecule, which may mediate a closer interaction between the lymphocyte and PMN (248). In addition, malignant B cells have been demonstrated to produce TNF-α, an activator of PMN, following cross-linking of HLA II (249). A role for antigenic modulation is also plausible, as MHC II internalises slowly as compared to other antigens. Thus, BsAb bound to this target will remain at the cell surface longer, and therefore, be better able to recruit effector cells. However, a definitive mechanism behind this restriction remains to be found.

It is a well documented concept that FcγR bearing effector cells play an important role in mAb mediated tumor therapy. Isotype switching studies have demonstrated a clear correlation between enhanced FcγR engagement by mAb and tumor destruction in mice and man (9). Given that BsAb appear more capable of triggering PMN cytotoxicity through FcγRI than mAb, and that on targeting this receptor *in vivo* would not suffer competition from serum IgG, it seems this data would suggest that BsAb would perform well in therapy. Furthermore, as PMN are known to be especially active when targeted

against class II molecules, and given the exceptional potency of the [FcγRI x MHC II] *in vitro* against the murine lymphoma lines studied, it seems logical that this derivative should have highest levels of therapeutic activity. To examine the efficacy *in vivo*, a series of therapeutic trials were conducted, and these form the basis of the next chapter.

Chapter 5

FcγRI BsAb activity *in vivo*

5.1 Introduction

In the previous chapter, we examined the ability of PMN to kill tumor *in vitro* when engaged via FcγRI. Findings indicate that BsAb mediated PMN lysis is extremely potent when targeted to MHC II. These findings are in accordance with the general literature. However, there remains little evidence of the efficacy of Ab triggering of these cytotoxic processes *in vivo*. This has been due largely to the lack of an appropriate animal model. Indeed, investigations into the performance of Ab targeting of human effector cell molecules *in vivo*, particularly with BsAb, have in general been fairly limited. Those that have been conducted have taken place in severe-combined immunodeficient (SCID) or nude mice repopulated with human PBMC or PBL. Whilst BsAb targeting CD3, FcγRIII, and FcγRI prove capable of localising to, and inducing regression of xenografted tumor in these models, the severely immunocompromised status of these animals makes them a less than ideal model (101). Ideally, pre-clinical studies would be performed in an immunocompetent system. Recently, development of the human FcγRI transgenic mouse has provided an opportunity to do this.

FcγRI expression in these mice closely resembles that in man, and the receptor obeys similar regulatory processes (221). We have further demonstrated that PMN in our transgenic F1 hybrids express FcγRI following muG-CSF treatment and that the receptor is functionally active when targeted with BsAb *in vitro*. Our findings, in accordance with others (246), reveal that MHC II is the most appropriate antigenic target for muG-CSF primed PMN *in vitro*. However, we do observe some killing with PMN targeted by BsAb against other lymphoma antigens: tumor Id, CD19 and CD40. Early reports also indicate that that an [FcγRI x MHC II] BsAb can also provide some protection *in vivo*. Animals inoculated with a syngeneic B-lymphoma line (IIA1.6, a variant of A20), and treated with BsAb in combination with G-CSF showed marginal protection over control cohorts (Ingmar Heijnen; unpublished). Taken together, this data would indicate that a BsAb with specificity for both FcγRI and MHC II, in

combination with G-CSF therapy, offers great potential for the treatment of lymphoma.

To assess the functional activity of such a BsAb in triggering PMN cytotoxic machinery *in vivo*, we have conducted a series of therapeutic strategies against two lymphoma models: A31 and BCL_1. We also compared the efficacy of this derivative to the therapeutic activity of the remaining panel of FcγRI BsAb (bearing specificity to Id, CD19 and CD40), to determine which antigen represents the most appropriate *in vivo* target. Moreover, as our PMN are transgenic for human FcγRI, the model has direct relevance to possible clinical trials.

5.2 Materials and methods

All therapies were conducted using BALB/c x FVB/n or CBA x FVB/n F1 progeny, bred in facilities at Tenovus. Mice were screened as before by FACS analysis of whole blood obtained from tail bleeds from 6 week old mice, using FITC-M22 mAb to detect the presence of FcγRI on a gated PMN population. Negative littermates were used as control animals where appropriate.

The standard protocol adopted for each therapeutic trial is as illustrated (Fig.4.2.1). Essentially, groups of 5 animals received 2 μg muG-CSF, s.c, for four days prior to tumor inoculation, and then continuously throughout the course of therapy. For standard therapies, tumor was given day 0, i.p, at a dose of 10^5 (BCL_1) or $2x10^5$ (A31) cells per animal. Mice were then treated with twice daily inoculations of BsAb (or mAb), on days 1 – 5 (once am and once pm), to a total dose as described throughout the text. Where PBS was used as a control, mice received 200 μl PBS twice daily.

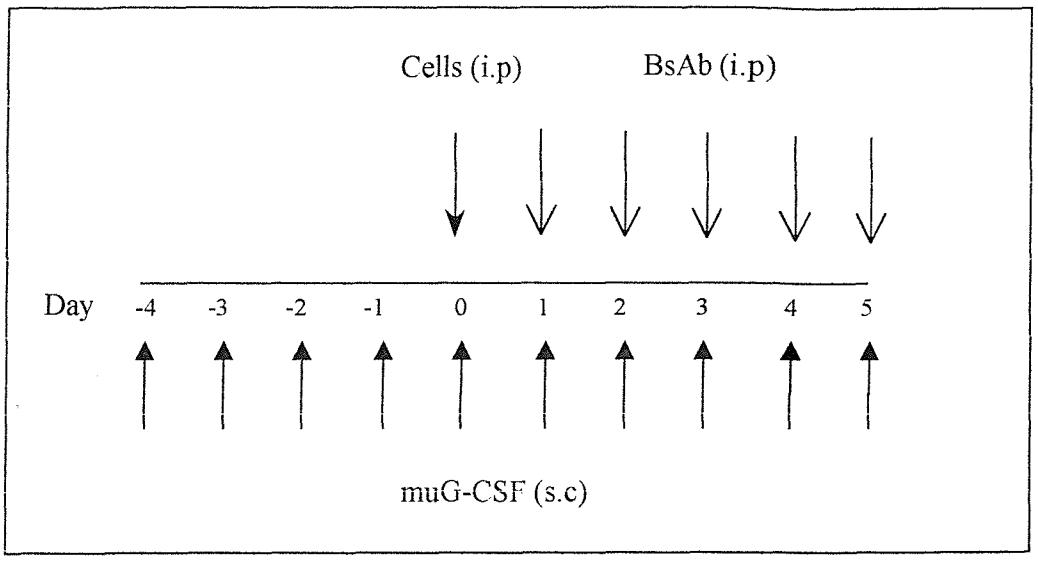

Fig.5.2.1 Standard therapy protocol

5.3 Results

5.3.1 Single dose versus multi-dose therapy

Preliminary trials were conducted against both lymphoma models to establish the most effective therapeutic regime. muG-CSF (2 μg/mouse) was administered s.c, 4 days post-tumor inoculation, and continued throughout the course of Ab treatment. Mice received A31 ($2x10^5$) or BCL_1 (10^5) cells i.p day 0, and were treated with either a single days treatment (2 x 25 μg), or multiple doses (5 μg twice a day, days 1-5) of [FcγRI x Id] BsAb, also ip. Although single dose therapies have previously proven insufficient due to the shortened half life of $F(ab')_2$, it was possible that the highly aggressive PMN population may prove sufficiently active to mediate protection with a single treatment. All groups contained 5 animals, with one group receiving saline buffer solution as a control. In both models control animals died around day 30, analogous to untreated animals in the non-transgenic parent models. Mice receiving a single dose of anti-Id BsAb gained no benefit in terms of survival over the control cohort, whereas multiple inoculations provided a high level of protection, with upwards of 60 % animals entering LTS (over 100 days) (Fig.5.3.1).

5.3.2. Low dose therapy (50 μg)

The efficacy of the full panel of BsAb in triggering PMN cytotoxicity *in vivo* was now assessed. Therapeutic trials were conducted as before with a multi-dose regime for delivery of anti-Id, anti-MHC II and anti-CD19 BsAb (anti-CD40 BsAb was produced several months after the other derivatives following observations with mAb anti-CD40, and so separate trials were conducted with this derivative). Cytokine primed mice received either A31 ($2x10^5$) or BCL_1 (10^5) cells i.p, and were treated with a total of 50 μg of derivative given as 5 μg, twice daily, over 5 days. Animals inoculated with A31 and treated with either [FcγRI x MHC II] or [FcγRI x CD19] showed only a modest advantage over controls, with at best 12 days protection (Fig.5.3.2). Likewise, these derivatives conferred only slight, although, statistically significant ($P < .02$) protection, of around 10 days against the BCL_1 lymphoma. Animals from both models treated with anti-Id BsAb showed almost complete protection, with 80 % entering LTS (over 100 days).

Given the activity of these derivatives *in vitro*, particularly the anti-MHC II BsAb, it was somewhat surprising that their activity *in vivo* was relatively less potent. As Id is the only tumor specific marker, it is possible that derivatives of other specificity are absorbed away from the primary tumor target, to other cells expressing CD19 and MHC II antigens. To investigate this issue, further trials were conducted with an altered protocol designed to compensate for this possible adverse sequestering of BsAb and favour PMN:tumor interactions.

5.3.3. LPS stimulated therapy

Bacterial lipopolysacchoride (LPS) has been demonstrated to actively stimulate PMN *in vivo*. We hoped to provide a closer interaction between the tumor cells, BsAb and activated PMN, by administering LPS (1 μg), i.p, prior to both tumor and BsAb inoculation, with the intention of drawing a large reservoir of activated PMN into the peritoneal cavity. Prior to therapeutic trials, mice given muG-CSF and LPS were sacrificed, and the peritoneal cavities flushed out. Resident cells were analysed using flow cytometry and a massive influx of PMN into the peritoneal cavity was observed

(around 60 % of cells being FcγRI positive/ F4/80 negative, and showing Fsc/Ssc profiles typical of PMN) (data not shown). Animals received the standard course of muG-CSF treatment and inoculating dose of tumor, together with a total of 50 μg BsAb, as before. LTS in 80 % of animals was again seen for both the A31 and BCL_1 tumor lines with the [FcγRI x Id] BsAb (Fig.5.3.3). However, treatment with either the anti-MHC II or anti-CD19 BsAb, failed to significantly reduce the rate of tumor progression compared to that observed in control mice, even in the presence of this enhanced effector pool.

5.3.4 High dose BsAb therapy

An alternative explanation for the lack of activity of BsAb other than anti-Id, could be due to treatment with a sub-optimal dose. To address this issue, therapeutic trials were repeated, with mice receiving an increased dose of 1 mg of BsAb over the period of 5 days (given as twice daily doses of 100 μg i.p). Again, animals were primed with muG-CSF and inoculated with either A31 ($2x10^5$) or BCL_1 (10^5) tumor cells i.p. Despite this dramatic increase in therapeutic dose, a corresponding increase in protection was not observed. Whilst the anti-Id derivatives now provided complete protection, with 100 % of animals in either lymphoma model being LTS (Fig.5.3.4), BsAb of other specificities still failed to enhance survival over control cohorts by more than a few days.

5.3.5 Combination BsAb therapy

Although CD19 is not a tumor specific marker, it is at least restricted to cells of the B-lineage. MHC II on the other hand presents a much wider range of distribution, including expression on other possible effector cells such as macrophages and monocytes. A role for these cells in protection from tumor challenge has not been ruled out, despite PMN being the major effector population in this system. It is possible that the [FcγRI x MHC II] BsAb is re-directing cytotoxic PMN against other effector cells, eliminating them from their role in tumor destruction. To verify that this was not the case, we simultaneously inoculated animals with both the [FcγRI x MHC II] and [FcγRI x Id] BsAb, to examine whether the protective effects of the anti-

Id derivative were lost. muG-CSF primed animals inoculated with the standard dose of A31 or BCL_1 tumor were treated with a total of 50 μg BsAb as previously. Control subjects were culled around day 30, with [FcγRI x MHC II] alone treated animals dying around the same time (Fig.5.3.5). Groups treated with the cocktail of BsAb showed similar survival curves to those obtained with [FcγRI x Id] treatment alone. For the A31 lymphoma model, 80 % of animals in either group entered LTS (Fig.5.3.5), and for the BCL_1 model, animals receiving the mixture of BsAb showed a complete remission rate of 60 %, as opposed to 80 % with the anti-Id BsAb alone.

5.3.6 Requirement for cytokine (muG-CSF) priming in BsAb therapy

Next, we more closely examined the activity of the anti-Id BsAb. We wished to verify the specific requirement for cytokine priming and PMN enhancement *in vivo* for successful therapy by conducting therapeutic trials in non-transgenic mice (receptor negative littermates) and transgenic mice, with or without G-CSF priming. We also compared the effects of the anti-Id BsAb to anti-Id IgG in this system. In all cases mice were inoculated with the standard dose of tumor cells as before, and where relevant, G-CSF treatment, also as before. BsAb and mAb were given i.p, twice daily, days 1 –5, to a total of 50 μg/animal. Similar observations were noted for both A31 (Fig.5.3.6) and BCL_1 (Fig.5.3.7) tumor models. No therapeutic benefit over control animals was observed with the BsAb in non-transgenic animals (plus or minus G-CSF treatment) or in unprimed transgenic animals. The anti-Id BsAb were, however, extremely active in transgenic mice that had received G-CSF. Anti-Id IgG was equally effective regardless of the genetic background or cytokine status of the animal. Anti-A31 Id provided around 85 days protection in this model, whereas anti-BCL_1 Id conferred negligible benefit over controls.

Moreover, these animals were only protected by bispecific $F(ab')_2$ and not by a mixture of anti-Id and anti-FcγRI unconjugated $F(ab')_2$, indicating a requirement for the precise coupling of effector cells to tumor (Fig.5.3.8).

5.3.7 BsAb versus mAb therapy

To directly contrast the activity of anti-Id BsAb to mAb, cytokine primed, receptor positive animals, were inoculated with the standard dose of tumor, and treated with a range of Ab doses (1, 10, 100, and 10000 μg total). For A31 (Fig.5.3.9), the BsAb only slightly enhanced protection at the lower doses, whereas mAb was able to provide around 30 – 50 days advantage over controls. However, at higher doses the BsAb was able to completely protect 100 % of treated animals, with mAb still only providing around 50 days benefit over controls. In the BCL_1 model (Fig.5.3.10), the distinction between the two was much clearer. MAb conferred no enhancement over controls at lower doses, and modest protection of around 30 days at the highest dose. At all concentrations, BsAb anti-Id conferred a greater level of protection than the mAb, although differences were less pronounced at lower doses.
At higher doses (100 – 1000 μg) BsAb conferred LTS in over 80 % of treated animals. These data clearly demonstrate that the BsAb is more effective at inducing an anti-tumor response than mAb.

5.3.8 CD40 BsAb therapy

During the course of this work, both the A31 and BCL_1 lymphoma models were also demonstrated to be susceptible to monoclonal anti-CD40 treatment (36). We developed a small quantity of [FcγRI x CD40] to conduct preliminary trials in our transgenic mice. Due to the limited stocks of BsAb, experiments were conducted only in the BCL_1 model. Mice received a total dose of 50 μg of either anti-Id IgG, anti-CD40 IgG, [FcγRI x Id], or [FcγRI x CD40] according to the standard protocol. Control groups received PBS. Neither the anti-Id or anti-CD40 mAb were able to enhance survival over controls at this dose (Fig.5.3.11). This is in accordance with observations by French et al. (36), who also see no protection with low doses of anti-CD40. As expected, the bispecific anti-Id treated group gave long-term protection, but only in conjunction with cytokine (Fig.5.3.11.B). The CD40 BsAb also gave no benefit to unprimed animals, but a slight advantage of around 17 days in combination with muG-CSF.

Encouraged by these findings, experiments were repeated with an increased dose of 1 mg of Ab in total. It is also known that an increased tumor burden is a requirement for effective anti-CD40 therapy, so to simulate this, therapy here was delayed until days 9 – 13. To ensure that the PMN population was maximal at this time point, muG-CSF was also given later, to coincide with the BsAb therapy, starting 5 days prior to the first dose of BsAb (day 4), and continuing until the end of the treatment schedule.

At this dose of Ab, CD40 IgG is known to be therapeutic, and proved to be here, giving long-term protection to 60 % of treated animals (Fig.5.3.12). However, the BsAb gave a fairly ambiguous result. Even at this increased dose of derivative, and in the presence of increased tumor burden, only one animal was long-term protected (>100 days). The remaining animals showed a benefit to survival over controls of around 5-10 days.

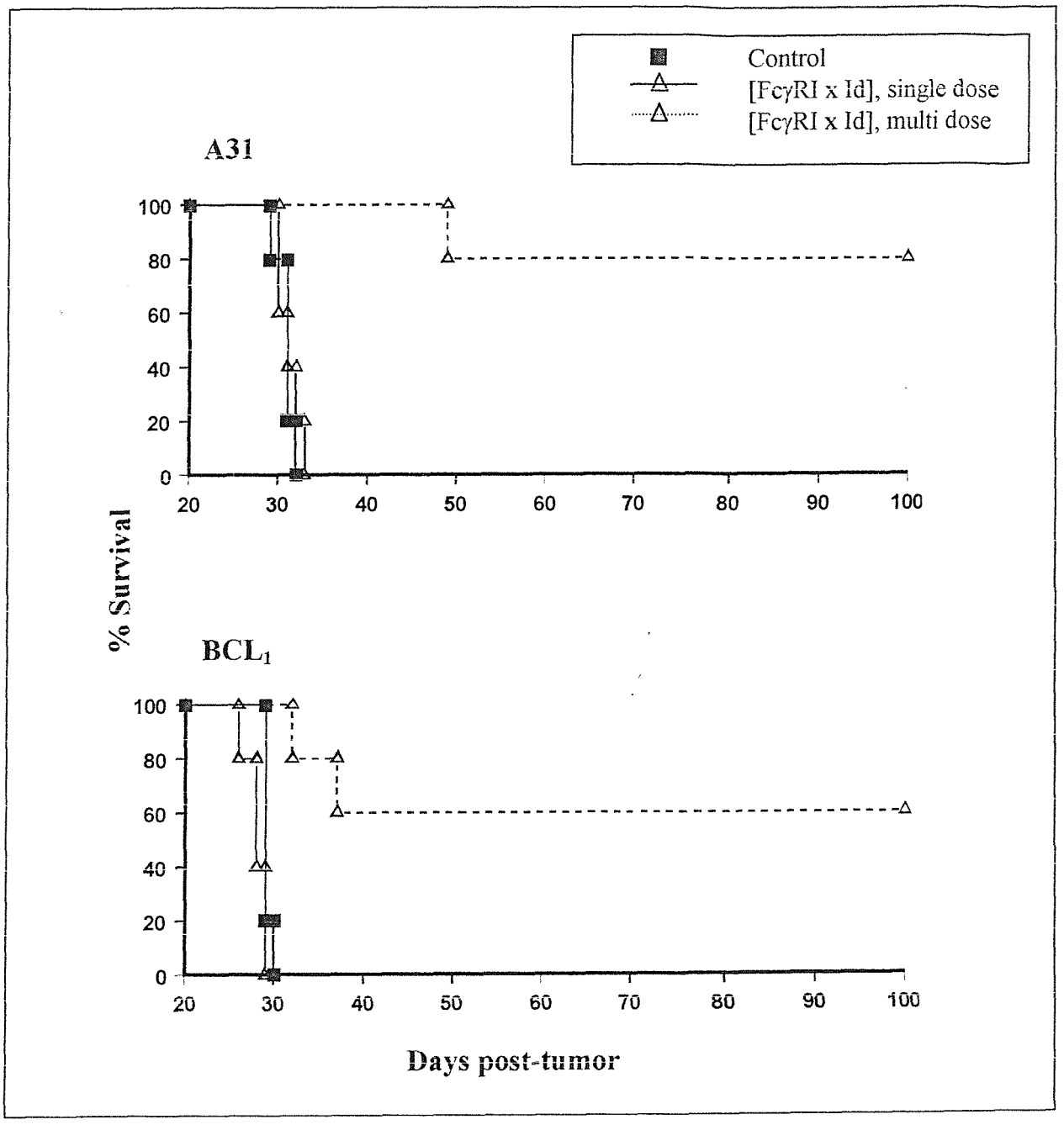

Fig. 5.3.1 Single versus multi-dose immunotherapy. Groups of 5 age matched CBA or BALB/c FcγRI positive F1 mice received 2 μg/day muG-CSF, days minus 4 to 5. Mice were inoculated with $2x10^5$ A31 or 10^5 BCL_1 tumor cells respectively, i.p, day 0 and treated with either a single days treatment of 2 x 25 μg [FcγRI x Id], i.p, day 1 (—△—); or multiple doses of 5 μg [FcγRI x Id], i.p, days 1 to 5 (50 μg/mouse total) (┈△┈). Control animals were given PBS (■). Survival was recorded daily.

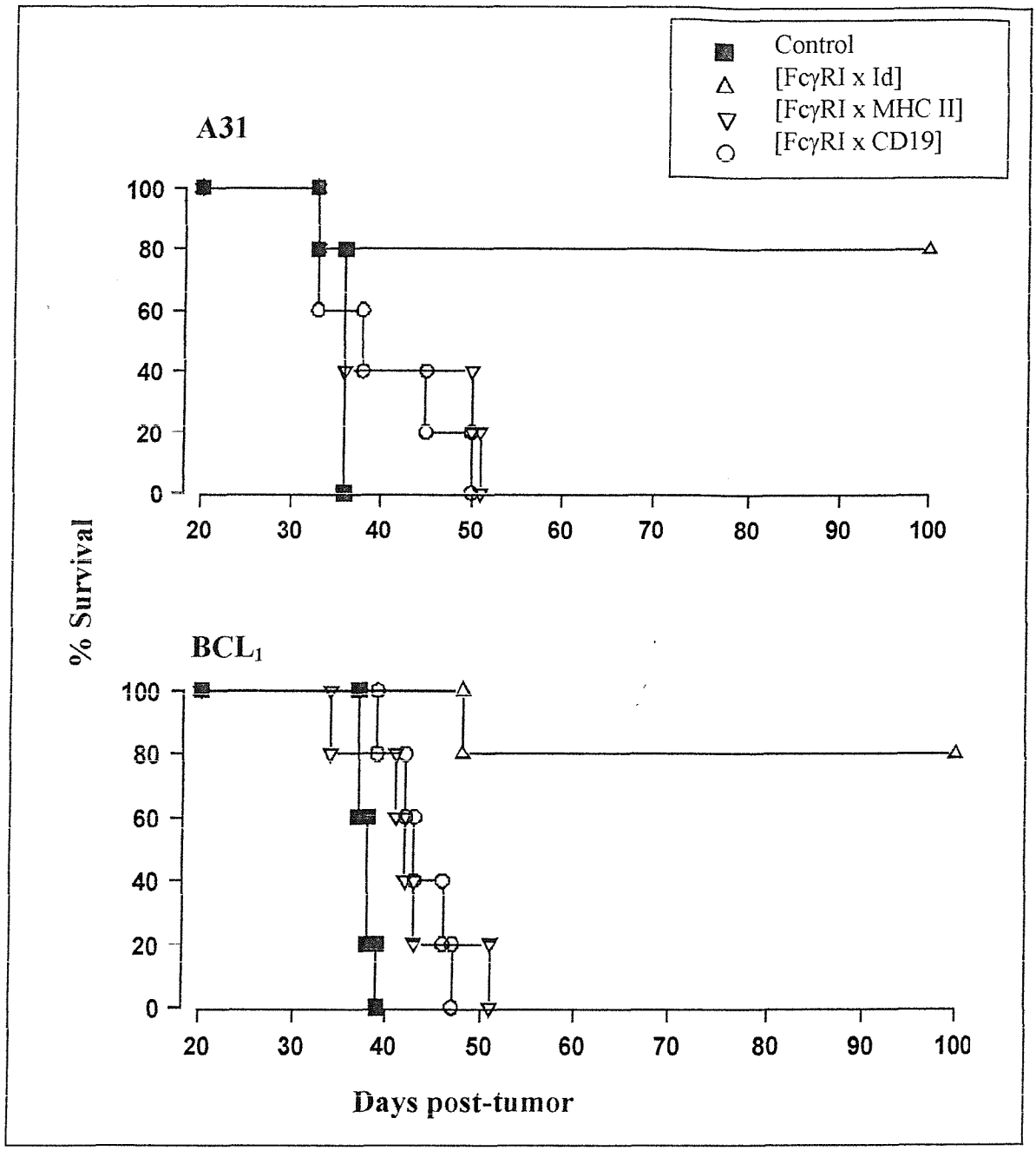

Fig. 5.3.2 FcγRI BsAb immunotherapy. Groups of 5 age matched CBA or BALB/c FcγRI positive F1 mice received 2 μg/day muG-CSF, days minus 4 to 5. Mice were inoculated with $2x10^5$ A31 or 10^5 BCL_1 tumor cells respectively, i.p, day 0 and treated with twice daily doses of 5 μg BsAb, i.p, days 1 to 5 (50 μg/mouse total). Treatment was as indicated: PBS (■); [FcγRI x CD19] (O); [FcγRI x MHC II] (▽); [FcγRI x Id] (△). Survival was recorded daily.

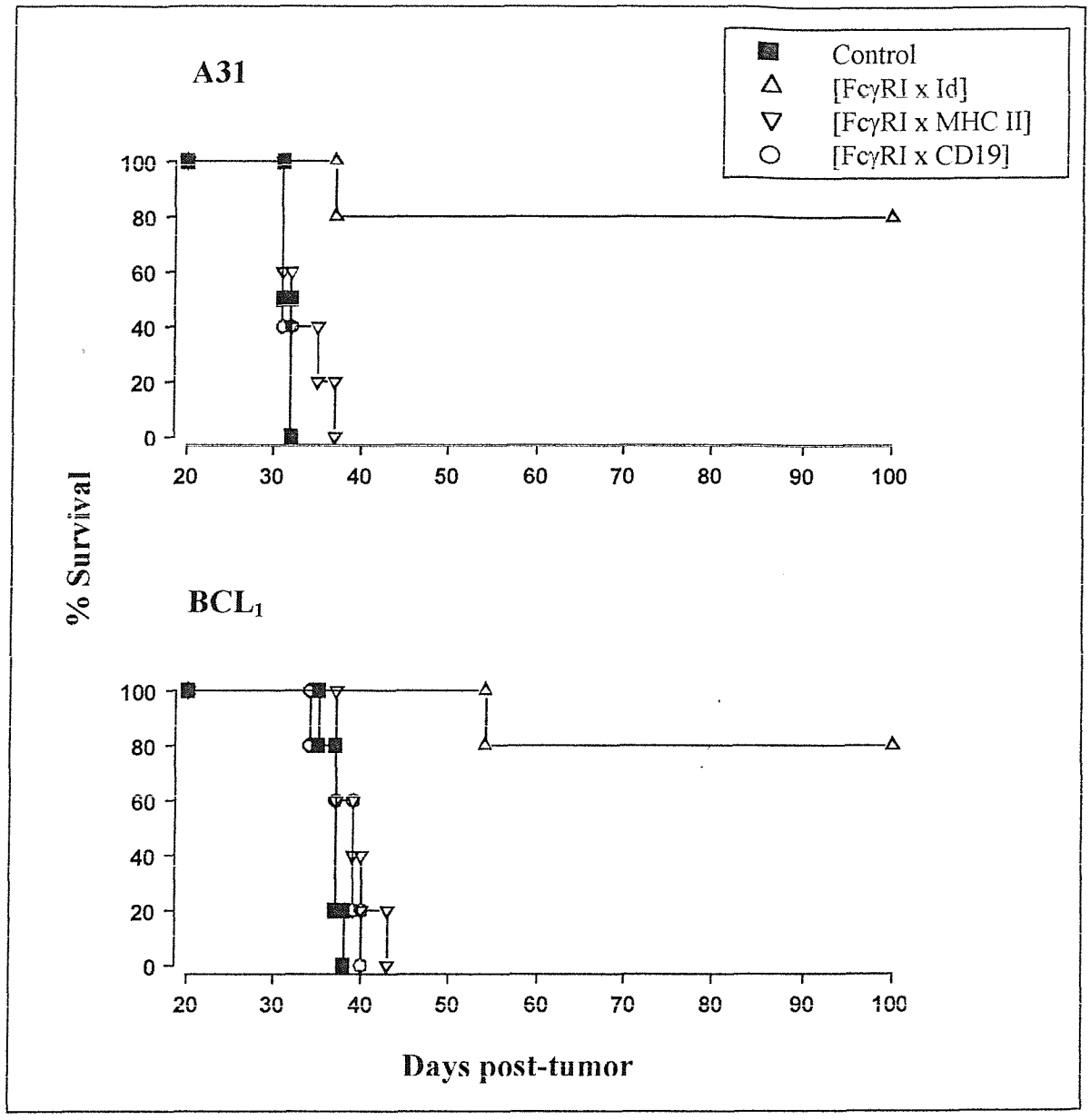

Fig. 5.3.3 BsAb plus LPS immunotherapy. Groups of 5 age matched CBA or BALB/c FcγRI positive F1 mice received 2 μg/day muG-CSF, days minus 4 to 5. Mice were inoculated with LPS (1 μg, i.p), day minus 1, $2x10^5$ A31 or 10^5 BCL_1 tumor cells respectively, i.p, day 0 and treated with twice daily doses of 5 μg BsAb, i.p, days 1 to 5 (50 μg/mouse total). Treatment was as indicated: PBS (■); [FcγRI x CD19] (○); [FcγRI x MHC II] (▽); [FcγRI x Id] (△). Survival was recorded daily.

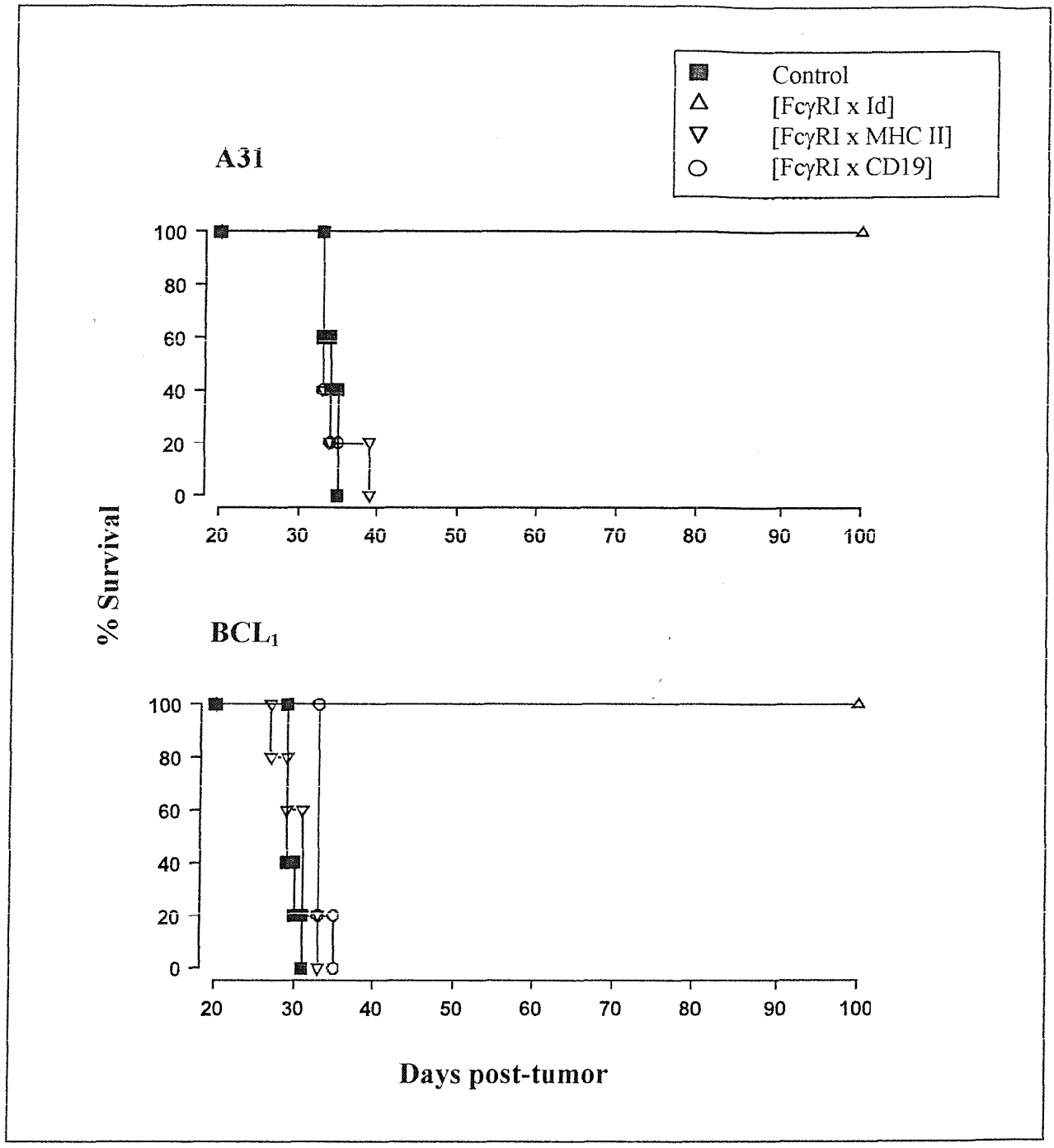

Fig. 5.3.4 High-dose FcγRI BsAb therapy. Groups of 5 age matched CBA or BALB/c FcγRI positive F1 mice received 2 μg/day muG-CSF, days minus 4 to 5. Mice were inoculated with $2x10^5$ A31 or 10^5 BCL_1 tumor cells respectively, i.p, day 0 and treated with twice daily doses of 100 μg BsAb, i.p, days 1 to 5 (1000 μg/mouse total). Treatment was as indicated: PBS (■); [FcγRI x CD19] (○); [FcγRI x MHC II] (▽); [FcγRI x Id] (△). Survival was recorded daily.

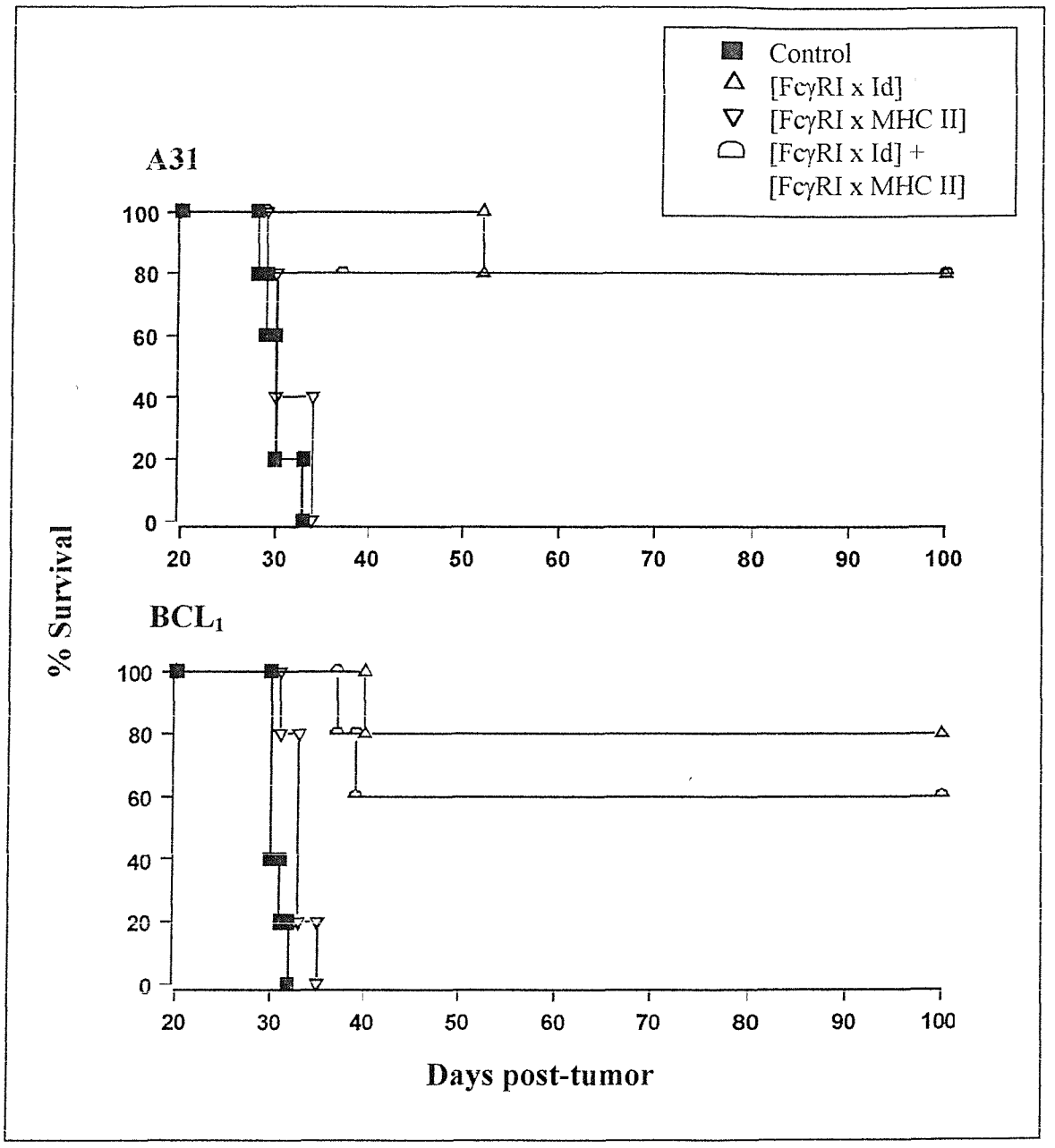

Fig. 5.3.5 Combination BsAb immunotherapy. Groups of 5 age matched CBA or BALB/c FcγRI positive F1 mice received 2 μg/day muG-CSF, days minus 4 to 5. Mice were inoculated with $2x10^5$ A31 or 10^5 BCL_1 tumor cells respectively, i.p, day 0 and treated with twice daily doses of 5 μg BsAb, i.p, days 1 to 5 (50 μg/mouse total). Treatment was as indicated: PBS (■); [FcγRI x MHC II] (▽); [FcγRI x Id] (△); [FcγRI x MHC II] + [FcγRI x Id] (⌓). Survival was recorded daily.

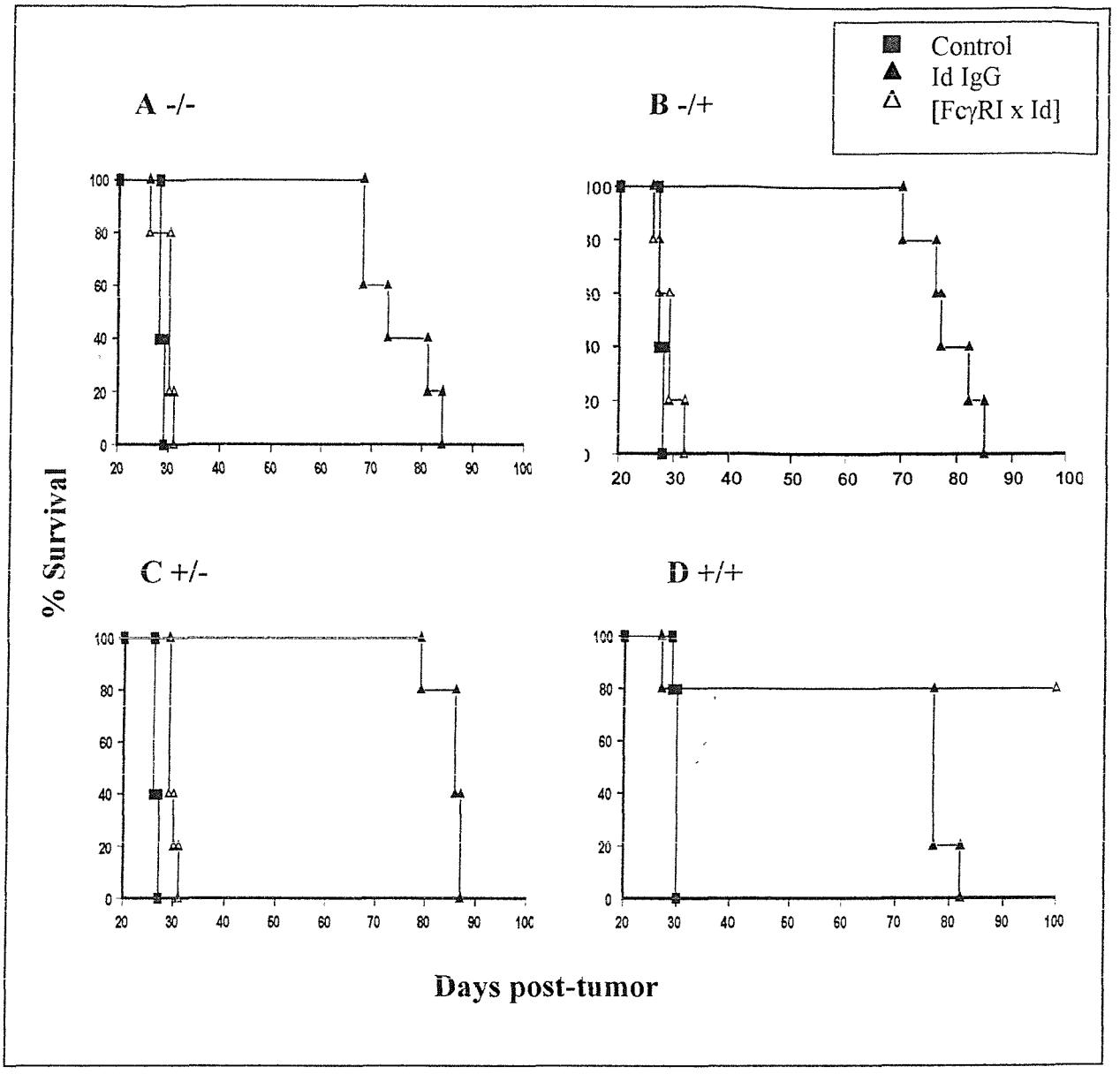

Fig. 5.3.6 Immunotherapy of A31 bearing mice. Groups of 5 age matched CBA x FVB F1 mice, were inoculated with $2x10^5$ A31 tumor cells, i.p, day 0, and were treated with twice daily inoculations of 5 μg anti-Id mAb (▲) or [FcγRI x Id] BsAb (Δ). i.p, days 1 to 5 (a total of 50 μg mAb/ BsAb per animal). Control groups were given PBS (■), i.p. Where appropriate mice also received 2 μg muG-CSF, days minus 4 to 5. Cohorts were as indicated: (**A**: -/-) non-transgenic, minus G-CSF; (**B**: -/+) non-transgenic plus G-CSF; (**C**: +/-) transgenic, minus G-CSF; (**D**: +/+) transgenic, plus G-CSF. Survival was recorded daily.

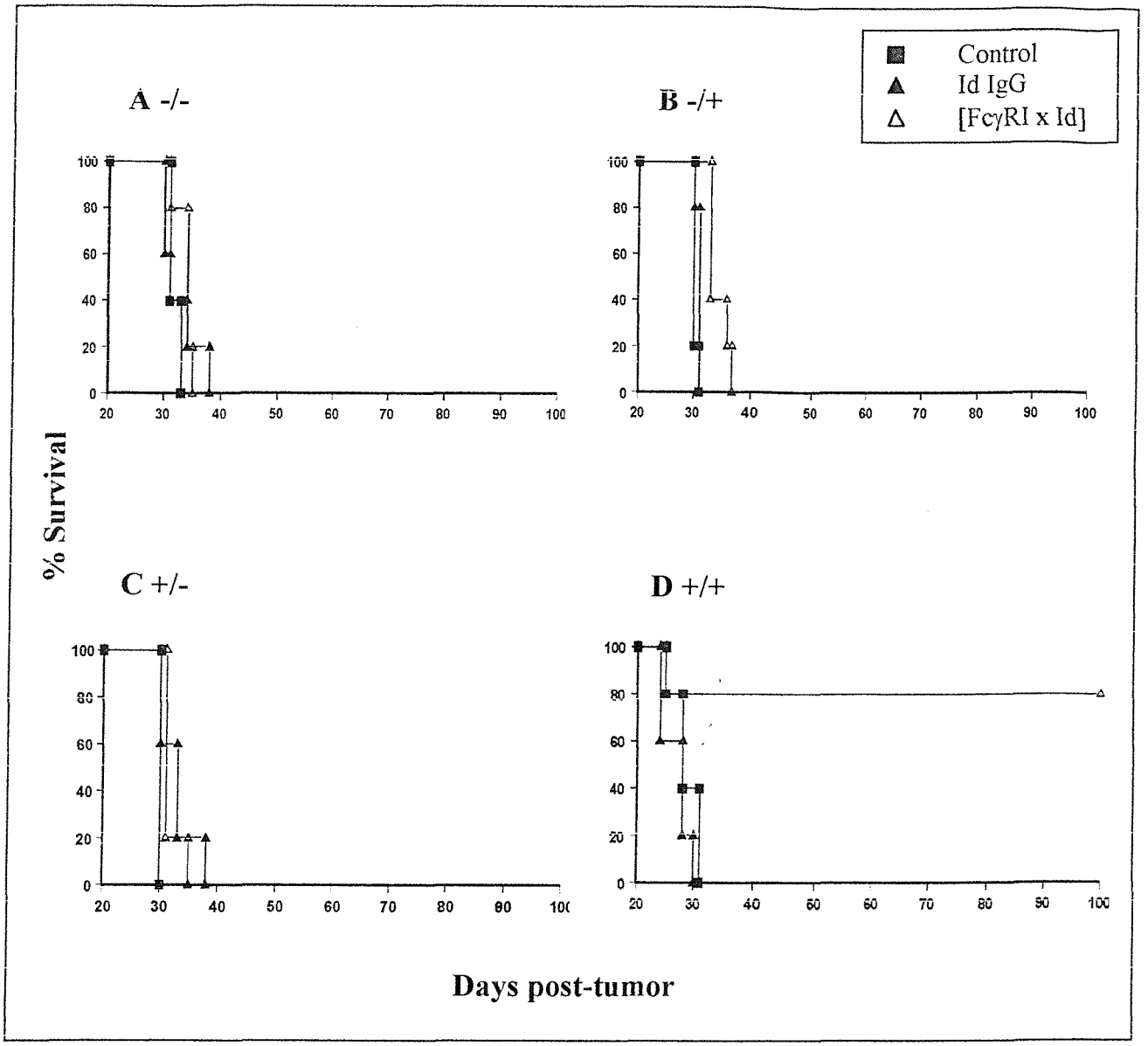

Fig. 5.3.7 Immunotherapy of BCL_1 bearing mice. Groups of 5 age matched BALB/c X FVB/n F1 mice, were inoculated with 10^5 BCL_1 tumor cells, i.p, day 0, and treated with twice daily inoculations of 5 μg anti-Id mAb (▲) or [FcγRI x Id] BsAb (Δ). i.p, days 1 to 5 (a total of 50 μg mAb/ BsAb per animal). Control groups were given PBS (■), i.p. Where appropriate mice also received 2 μg muG-CSF, days minus 4 to 5. Cohorts were as indicated: (**A**: -/-) non-transgenic, minus G-CSF; (**B**: -/+) non-transgenic plus G-CSF; (**C**: +/-) transgenic, minus G-CSF; (**D**: +/+) transgenic, plus G-CSF. Survival was recorded daily.

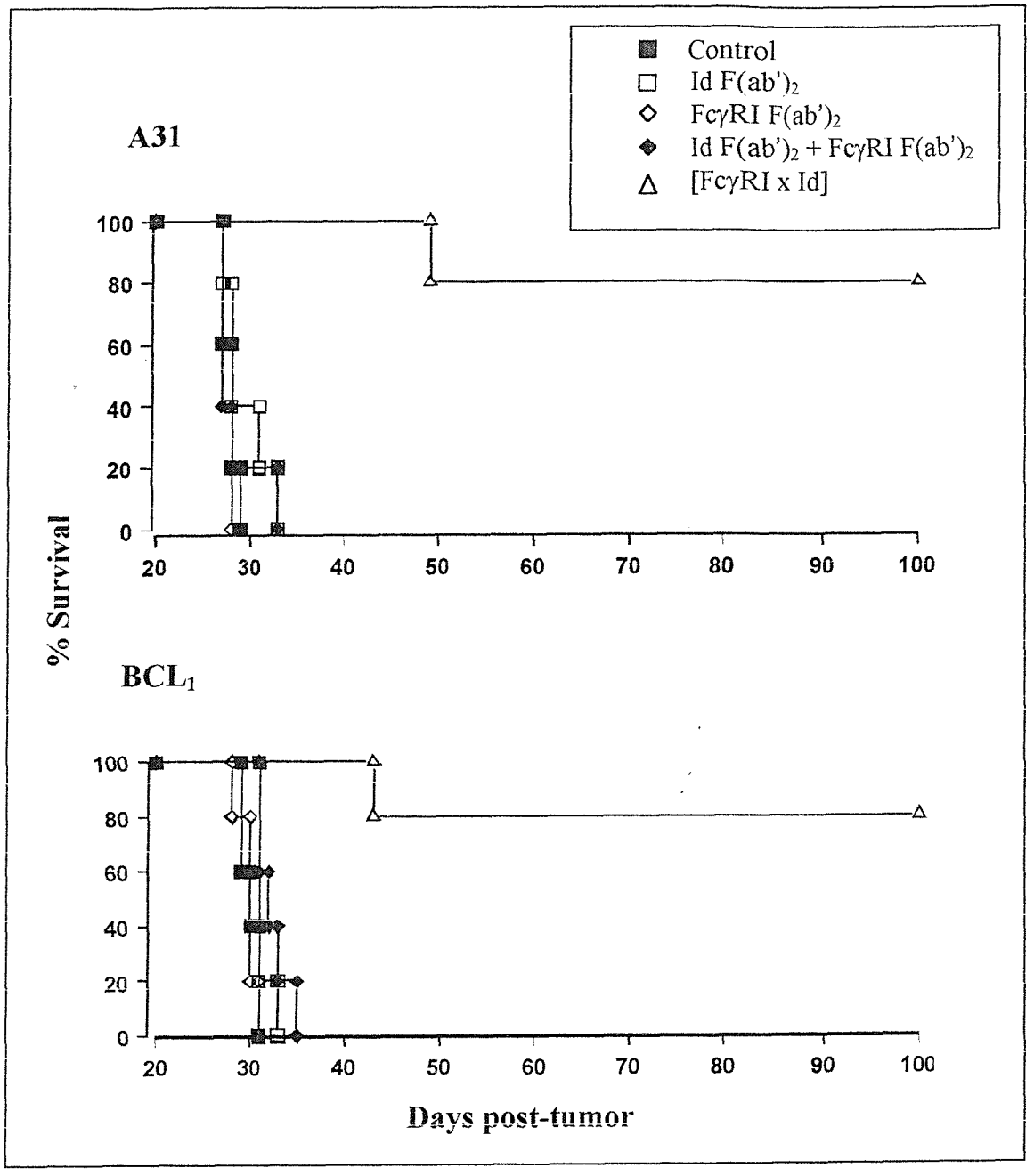

Fig. 5.3.8 Unconjugated F(ab)$_2$ immunotherapy. Groups of 5 age matched CBA or BALB/c FcγRI positive F1 mice received 2 μg/day muG-CSF, days minus 4 to 5. Mice were inoculated with 2x10^5 A31 or 10^5 BCL$_1$ tumor cells respectively, i.p, day 0 and treated with twice daily doses of 5 μg F(ab)$_2$, i.p, days 1 to 5 (50 μg/mouse total). Treatment was as indicated: PBS (■); Id F(ab)$_2$ (□); FcγRI F(ab)$_2$ (◇); Id F(ab)$_2$ + FcγRI F(ab)$_2$ (◆); [FcγRI x Id] (Δ). Survival was recorded daily.

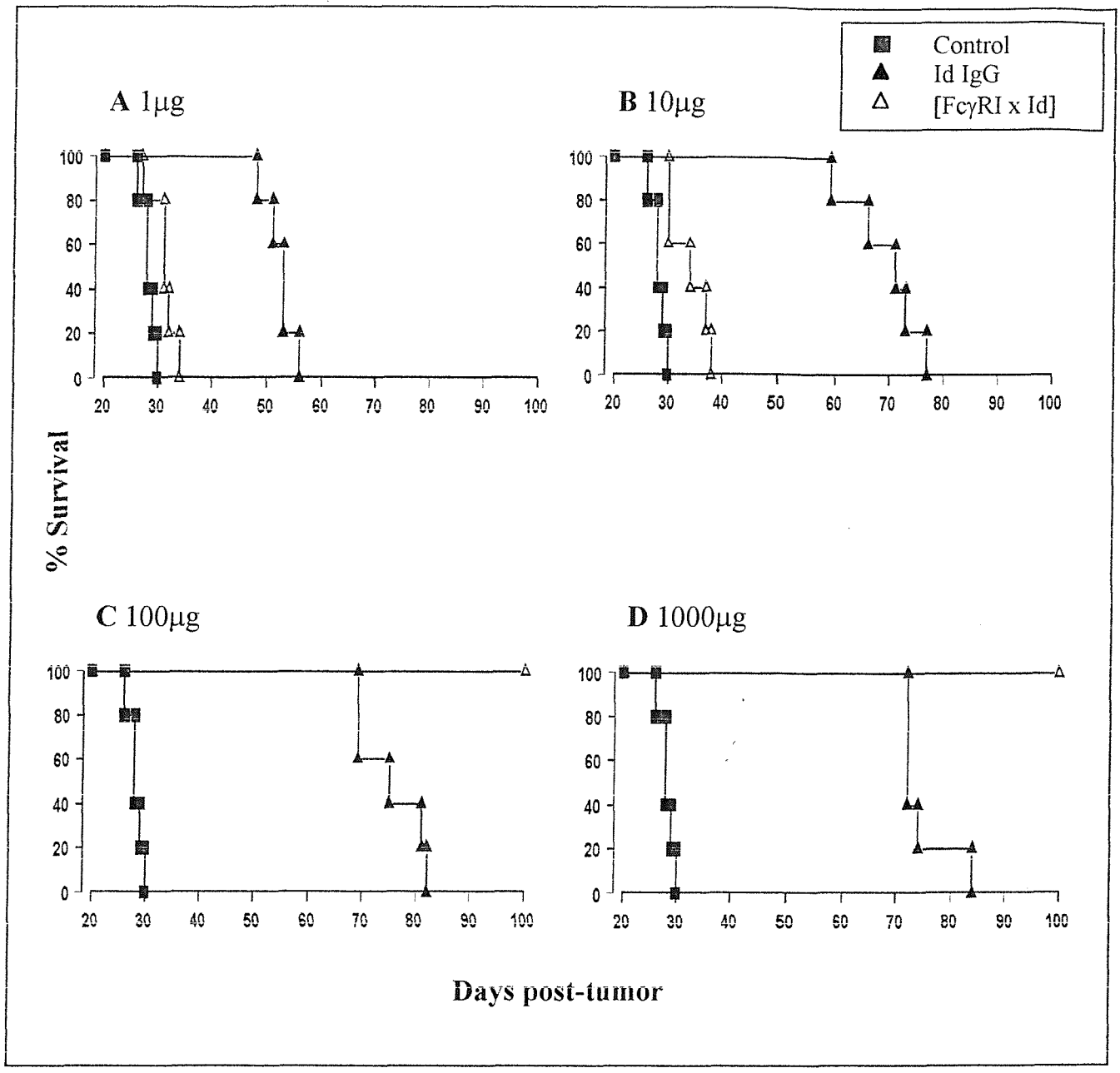

Fig. 5.3.9 BsAb versus mAb therapy of A31 bearing mice. Groups of 5 age matched CBA FcγRI positive F1 mice received 2 μg muG-CSF, days minus 4 to 5. Mice were inoculated with $2x10^5$ A31 tumor cells, i.p, day 0, and treated with twice daily doses of **(A)** 0.1; **(B)** 1; **(C)** 10; or **(D)** 100 μg mAb or BsAb, i.p, days 1 to 5 (giving a total dose of 1, 10, 100, or 1000 μg respectively). Treatment was as indicated: PBS (■); Id IgG (▲); [FcγRI x Id] (Δ). Survival was recorded daily.

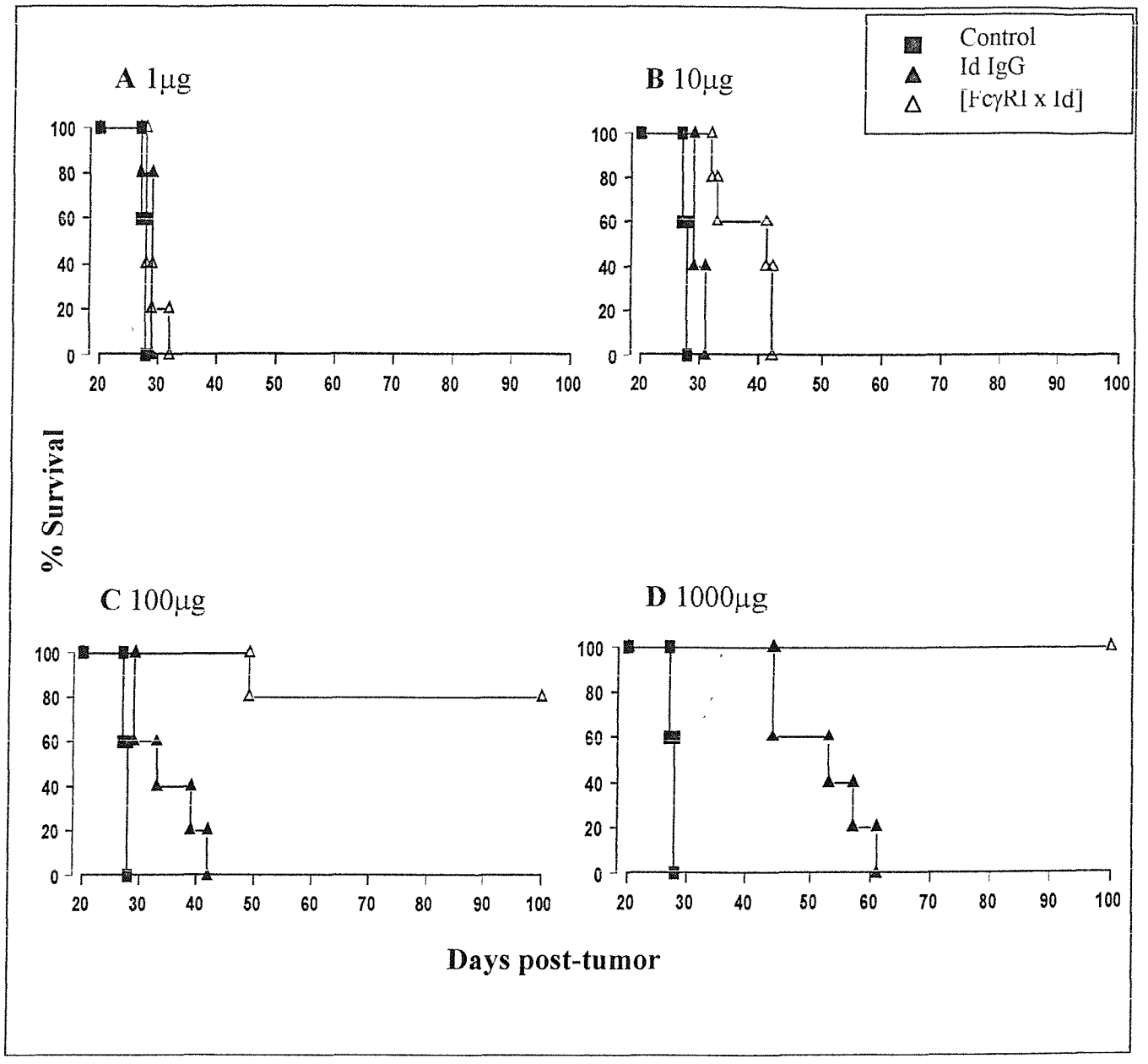

Fig. 5.3.10 BsAb versus mAb therapy of BCL_1 bearing mice. Groups of 5 age matched BALB/c FcγRI positive F1 mice received 2 μg muG-CSF, days minus 4 to 5. Mice were inoculated with 10^5 BCL_1 tumor cells, i.p, day 0, and treated with twice daily doses of **(A)** 0.1; **(B)** 1; **(C)** 10; or **(D)** 100 μg mAb or BsAb, i.p, days 1 to 5 (giving a total dose of 1, 10, 100, or 1000 μg respectively). Treatment was as indicated: PBS (■); Id IgG (▲); [FcγRI x Id] (Δ). Survival was recorded daily.

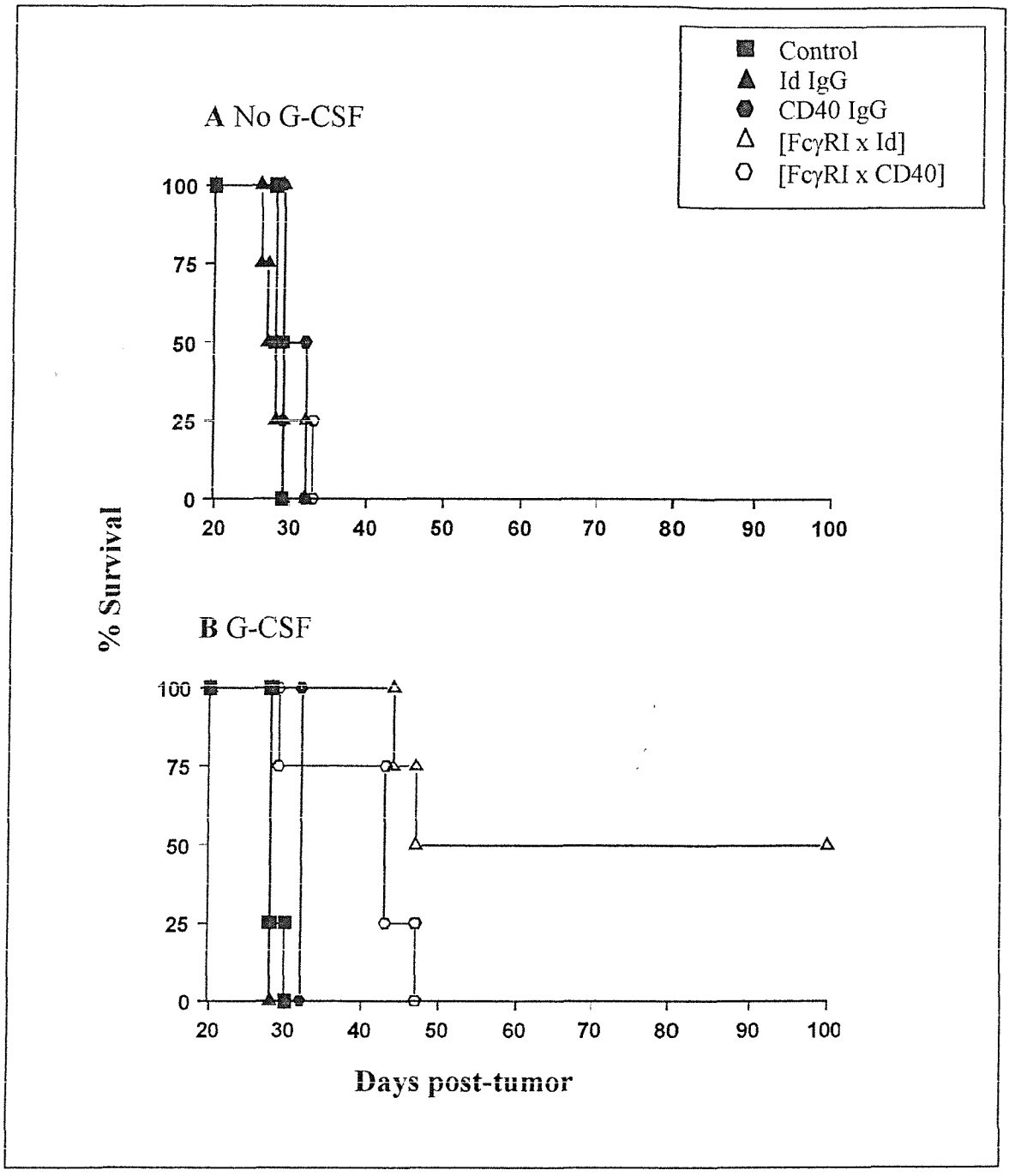

Fig. 5.3.11 [FcγRI x CD40] immunotherapy. Groups of 5 age matched BALB/c x FVB FcγRI positive F1 mice, were left unprimed **(A)** or given 2 μg/day muG-CSF **(B)**, days minus 4 to 5. Mice were inoculated with 10^5 BCL_1 tumor cells, i.p, day 0 and treated with twice daily doses of 5 μg mAb or BsAb, i.p, days 1 to 5 (50 μg/mouse total). Treatment was as indicated: PBS (■); Id IgG (▲); CD40 IgG (⬢); [FcγRI x Id] (△); [FcγRI x CD40] (○). Survival was recorded daily.

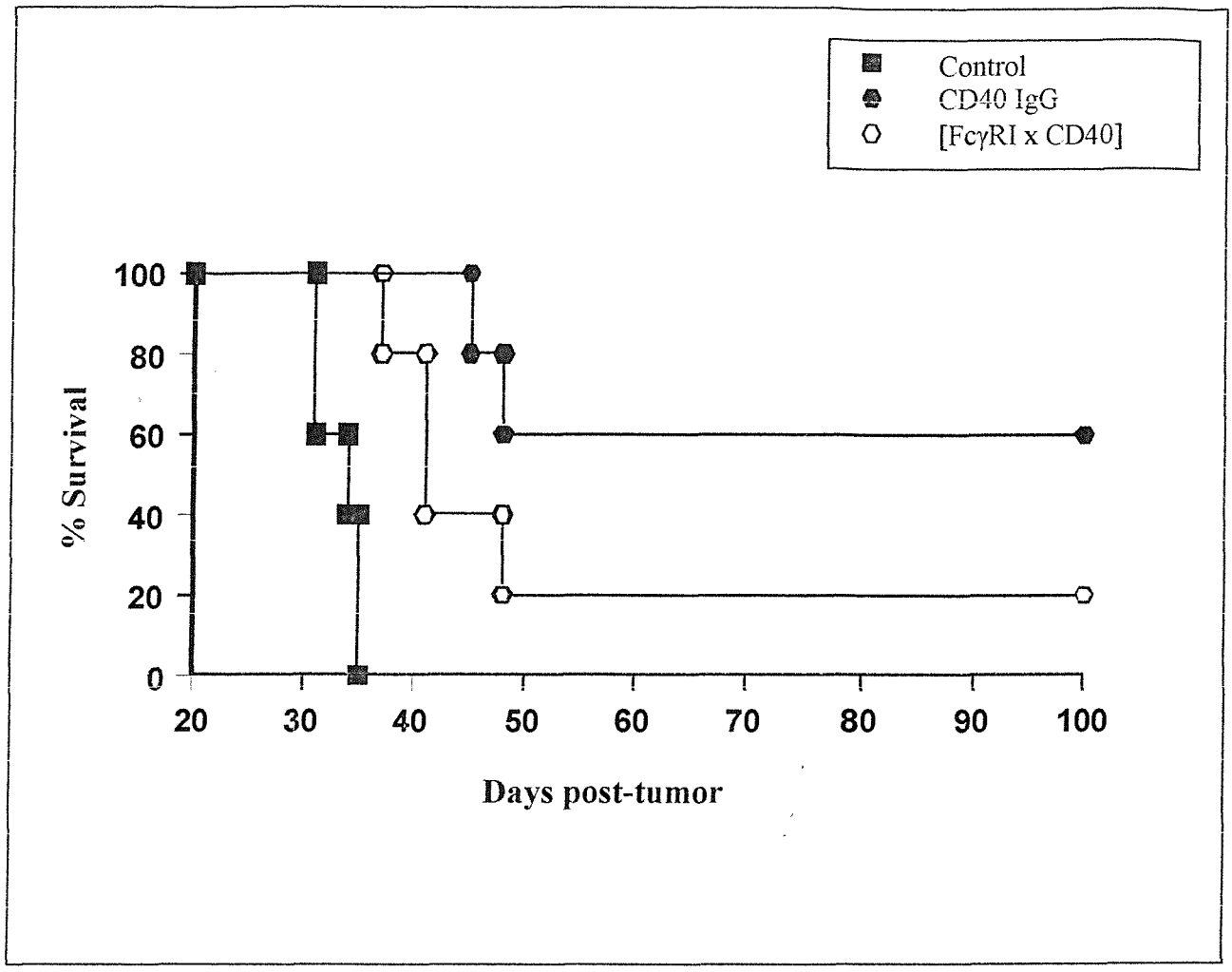

Fig. 5.3.12 [FcγRIxCD40] high dose immunotherapy. Groups of 5 age matched BALB/c x FVB/n FcγRI positive F1 mice were inoculated with 10^5 BCL_1 tumor cells, i.p, day 0. Mice received 2 μg/day muG-CSF, days 4 to 13, and were treated with twice daily doses of 100 μg anti-CD40 mAb or [FcγRI x CD40] BsAb, i.p, days 9 -13 (1000 μg/mouse total). Treatment was as indicated: PBS (■); anti-CD40 mAb (●); [FcγRI x CD40] (○). Survival was recorded daily.

5.4 Discussion

One of the most critical aspects of this work was to compare the activity of BsAb derivatives not only *in vitro*, but more importantly, *in vivo*. In this chapter we report on the efficacy of a panel of BsAb, used in combination with muG-CSF, to trigger PMN cytotoxic activity through FcγRI, against two murine lymphoma lines, *in vivo*.

Administration of G-CSF alone has been reported adequate to reduce development of melanoma and lymphoma in mice (250). Furthermore, transfection of the G-CSF gene into a murine colon adenocarcinoma line, C-26, has been demonstrated to induce PMN-T cell activation, sufficient to mediate tumor regression (251). However, we, and others (Ingmar Heijnen; unpublished), observed no benefit from cytokine dosing alone. Instead, G-CSF worked in combination with the appropriate BsAb. These discrepancies may well be related to differing dose and administration protocols, as well as differences in the immunogenicity of the tumors under study.

Therapeutic efficacy was, however, totally dependent on the presence of FcγRI and cytokine priming, as [FcγRI x Id] treated non-transgenic animals, with or without muG-CSF, failed to show enhanced survival over controls (Fig. 5.3.6 and 7). Lack of protection was also observed in unprimed transgenic animals, presumably because (1) FcγRI was not sufficiently upregulated and activated on PMN, and (2) the effector pool was greatly diminished. Moreover, therapy was dependent on direct contact between the tumor and effector cell, as no protection was observed with unconjugated $F(ab')_2$ fragments (5.3.8).

Perhaps the most surprising observation was that the exceptional potency displayed by the [FcγRI x MHC II] BsAb *in vitro* (chapter 4), did not translate into successful therapy (Fig.5.3.2). Consistently, cohorts treated with this (and the anti-CD19 derivative) showed only a small improvement in survival compared with control animals. The level of protection observed was around 10 days, and whilst only small, was still statistically significant in the BCL_1 model ($p < 0.2$). Conversely, those animals receiving [FcγRI x Id] consistently entered LTS (over 100 days).

The MHC II molecule itself is not an unattractive target for immunotherapy, in that it is expressed at high levels on target cells, and does not readily modulate or shed from the cell surface. *In vivo*, anti-MHC II mAb have previously demonstrated some success. Mice treated with the anti-I-A mAb showed increased survival over non-treated cohorts bearing L10A lymphoma (252). The anti-HLA II Ab Lym-1 has also shown activity against freshly isolated CLL, in the presence of IFN-γ activated effector cells (253) and was subsequently tested in clinical trials, where it showed minimal toxicity and gave modest responses. We too have observed some protection with anti-class II mAb against human tumor xenograft models in SCID mice (unpublished). However, we have never observed anti-tumor effects *in vivo* with anti-MHC II mAb against syngeneic murine lymphoma models, either as IgG alone, or in conjunction with muG-CSF (data not shown).

It was envisaged, given the antigen restriction displayed by FcγRI directed PMN, that MHC II would make an ideal therapeutic target for FcγRI targeting BsAb. However, despite multiple inoculations to extend serum half-life, and a range of doses from 10 μg to 1 mg, the [FcγRI x MHCII] derivative failed to dramatically enhance survival over PBS treated cohorts (Fig.5.3.2 and 5.3.4). Neither did enhancing the effector pool at the site of inoculation encourage MHC II directed tumor lysis (Fig.5.3.3). The explanation for the failure of this potentially highly potent derivative remains unresolved. Recent reports by Heijnen et al. have demonstrated that trials in a similar transgenic system have resulted in very limited therapy with an [FcγRI x MHC II] BsAb (unpublished). This could be due to the use of a different anti-MHC II targeting mAb (M5/114; rat anti-mouse IgG2a). The most likely explanation is that the modicum of success observed by Heijnen et al. could, at least in part, be due to the use of a much less aggressive tumor line.

Elimination of other MHC II bearing effector species by our highly aggressive PMN population when exposed to the anti-MHC II BsAb is also a possibility. For example, macrophages have been shown to mediate effective phagocytosis when triggered through FcγRI (221) As these cells also express MHC II, it is feasible that PMN could destroy macrophages (and other class II expressing cells), in the presence of an anti-MHC II BsAb. However, treatment with a combination of bispecific anti-Id and anti-

MHC II (Fig.5.3.5) resulted in levels of protection similar to those seen with anti-Id BsAb alone, indicating that even if this phenomenon does occur, it does not have a bearing on therapeutic outcome.

The anti-MHC II derivative was not the only bispecific that did little to enhance survival over controls. CD19 has long been considered a suitable target for immunotherapy. It is a B-lineage restricted marker, involved in regulating B-cell proliferation and differentiation. Clinical trials against NHL conducted with "naked" IgG, have demonstrated anti-CD19 mAb to provide limited remissions of short duration (2). Moreover, as CD19 shows a strong tendency to modulate on Ab binding (62), it also serves as a target for delivery of immunotoxin conjugates. Further, CD19 has also proved an effective target for BsAb mediated tumor lysis with other effector systems such as T-cells (254). In addition, we have found mAb to CD19 capable of mediating ADCC and complement activity against a range of murine lymphomas, as well as affording moderate protection against BCL_1 when used at relatively high doses (231). Low levels of protection by the [FcγRI x CD19] may therefore be a reflection of sub-optimal dosing, despite having given up to 1mg of derivative. It is also possible that modulation of the antigen upon cross-linking may be detrimental to therapeutic efficacy.

In some respects, most surprising was the activity of the [FcγRI x CD40] BsAb. In light of findings by French et al. (36), whereby mice treated with anti-CD40 mAb were not only cured of their first dose of tumor, but were immune to subsequent re-challenge, we had expected an anti-CD40 BsAb to perform efficiently. When treating with a relatively low dose of Ab (50 μg), at which the anti-Id BsAb is protective, the anti-CD40 derivative increased survival by around only 10 days (Fig.5.3.11). However, this level of protection was greater than that observed with the anti-CD40 IgG, which failed to enhance survival over control cohorts. At higher doses, (1 mg), where anti-CD40 IgG does mediate substantial tumor regression, the BsAb could not match the level of protection provided by the mAb, even in muG-CSF primed animals (Fig.5.3.12).

Several factors could be affecting the performance of the CD40 BsAb. Treatment conditions, both in terms of actual Ab dose, and dosing schedule, proved highly critical to the level of protection gained by CD40 mAb. Extensive therapeutic trials established two factors were critical for arresting tumor development: treating with a high dose of Ab, and having a large tumor load present at the time of treatment. Here, treating with 1 mg of BsAb at a late time point (day 9-13), to allow growth of tumor, conditions may not be optimal for BsAb therapy. From experience, we have found that treating late with BsAb decreases their efficacy (chapter 3). It may be that treating earlier with higher doses may prove more beneficial in this system.

It is known that CD40 mAb can function to replace T cell help, and directly activate antigen presenting cells conditioning them to present tumor antigens to $CD8^+$ T cells (255). Although it is believed that this phenomenon is responsible for generation of immunity in CD40 therapy, the nature of the APC remains unidentified. Moreover, as CD40 $F(ab')_2$ does not provide protection, there is a clear role for Fc in this process, probably by recruiting FcγR bearing accessory cells, which may release cytokines or other inflammatory factors. Again the exact nature of the specific FcγR, and the accessory cells required are unknown. It is possible that a bispecific IgG, or one against a different FcγR class, or effector population may therefore prove more therapeutic.

Finally, the finding that anti-Id BsAb are more therapeutically active than anti-Id mAb is important. In the A31 model, Id IgG is active at very low doses (1 μg can give around 40 days protection), but quickly reaches a threshold, with doses of 5 μg and over (up to 2 mg), increasing survival by no more than 60 days over controls. LTS has never been observed (231). BsAb are able to mediate LTS at relatively low doses (50 μg) and at 1 mg/ mouse give complete protection to all animals. In the BCL_1 model, these differences are more pronounced, as the anti-Id mAb is only therapeutic at higher doses (100 μg and over), mediating at best, approximately 30 days increased survival over controls. Even at low doses, the BsAb is superior, and again, at higher doses gives complete cure (Fig.5.3.10). There are a number of possible reasons for the greater potency of the anti-BsAb. Firstly, as the BsAb can bind outside of the natural ligand-binding domain of the receptor it is able to overcome problems of receptor

saturation by serum Ig. Secondly, both anti-Id mAb are of the rat IgG2a isotype which is not the optimal isotype for human receptor binding. In addition, the BsAb will only engage the specifically targeted receptor and not other inhibitory receptors such as FcγRIIb (196). Finally, the univalent BsAb may not induce BCR modulation as rapidly as the bivalent IgG (63).

Clearly, the anti-Id derivatives are therapeutically superior to the other reagents tested. It was important therefore, to investigate the functional activity of all the BsAb *in vivo* to try and establish the mechanism(s) by which protection is attained and explain the potency of the [FcγRI x Id]. These investigations are the subject of the next chapter.

Chapter 6

Functional activity of FcγRI BsAb *in vivo*

6.1 Introduction

The most striking observation when comparing *in vitro* activity of BsAb to therapeutic efficacy *in vivo*, is the distinct lack of correlation between the two in terms of performance. It appears that those BsAb which mediate high levels of *in vitro* RCC may not be most effective in the mouse, whilst other derivatives, which perform less well in cytotoxicity assays, are able to mediate substantial tumor regression. The most obvious examples are the activity of [FcγRI x MHC II] and [FcγRI x Id].

Given these differences, our primary interest in this chapter was to determine if the therapeutically active anti-Id BsAb were the only derivatives mediating tumor depletion *in vivo*, and to try and establish the mechanism(s) by which they may be operating. Although ADCC has long been proposed a major mechanism of activity for mAb in therapy, and we and others (145) have observed significant levels of ADCC and RCC with G-CSF primed PMN as effectors *in vitro*, it has never formally been proven that this activity is critical to successful therapy. It is known that removal of FcγR bearing effector cells has an adverse effect on therapy, and that isotype switching to increase effector binding can potentiate anti-tumor responses (38). However, evidence from Tutt et al. (231) indicates that ADCC may not be the key requisite for therapeutic efficacy by mAb. Instead, they propose that other properties more directly related to the nature of the target antigen on the tumor itself might play a more significant role in controlling tumor growth.

It has long been known that mAb capable of cross-linking the BCR are able to generate anti-proliferative signals that can negatively regulate tumor growth, driving lymphoma cells into CCA or apoptosis (238). Furthermore, the degree of cross-linking achieved is directly proportional to the strength of signal delivered. Grafton et al. using mAb directed at IgM on human B-lymphoma cells have revealed a direct correlation between rises in intracellular calcium levels and apoptosis, indicating that calcium mobilisation is involved in tumor depletion following cross-linking (256). It

is feasible that BsAb to the BCR may function in a similar manner, with effector cells recruited by the second arm of the derivative performing the cross-linking function, and that subsequent calcium flux may be involved in eliciting cell death.

In addition, we wished to examine more closely the mechanism of protection conferred by the [FcγRI x Id] BsAb, and to investigate whether LTS were protected from subsequent tumor re-challenge, and to investigate the role of $CD4^+$ and $CD8^+$ cells to the therapy.

6.2 Materials and methods

To investigate the early cytotoxic activity of the BsAb *in vivo*, groups of five age matched BALB/c x FVB/n FcγRI positive F1 mice were primed with 2 μg/ day muG-CSF, according to the standard protocol (chapter 4), inoculated with 10^7 BCL_1 tumor cells i.p, day 0, and treated twice daily with 50 μg BsAb, i.p (to a total of 500 μg). As a control, identical therapies were conducted in primed FcγRI negative mice.
One mouse per group was sacrificed on each consecutive day of treatment, and peritoneal cells removed by lavage with PBS. Cells were washed once, resuspended in RPMI, and screened for the presence of tumor using dual fluorescence staining with FITC-NIMR6 (anti-CD22 mAb) versus PE-Mc106a5 (anti-Id mAb). In the case of [FcγRI x Id] treated groups, PE-ID3 (anti-CD19 mAb) was used instead. In all cases, cells were stained with mAb (50 μg/ml) for 15 min on ice prior to analysis. Cells were analysed by flow cytometry on a FACS Calibur.

To assess the percentage of tumor cells present in the spleen taken towards the normal endpoint for this model, mice were sacrificed on days 5, 10 and 15 following the same course of therapy as above. Spleens were removed, homogenised, cells washed once and resuspended at 10^6/ml in RPMI. Tumor cells were detected using dual fluorescence staining as before. PMN were identified using FITC-M22 (anti-FcγRI) versus PE-anti-7/4 (which recognises a PMN associated glycoprotein). Cells were again analysed by flow cytometry on a FACS Calibur.

To assess the phenotype of tumor emerging in BsAb treated animals, spleens were prepared as above, resuspended at 10^6/ml in RPMI, and surface antigen expression determined using FITC-labelled N22 (anti-MHC II mAb); FITC-ID3 (as before); and FITC-3/23 (anti-CD40 mAb). Ab was added at a final concentration of 50 μg/ml, for 15 min, on ice. Cells were then washed, and analysed on a FACS Calibur.

Measurement of intracellular calcium flux was conducted using πBCL_1 cells (218), a variant of the BCL_1 tumor that can grow both *in vitro* and *in vivo*. Cells (10^7) were loaded with 5 μM indo-1-acetooxymethylester (Indo-1-AM) for 30 mins at 37^0C, washed to remove excess dye, and resuspended at 2 x 10^6/ ml. For the assay, cells were warmed to 37^0C, BsAb added to a final concentration of 2 μg/ml, and cells immediately analysed. Where appropriate, cross-linking polyclonal sheep anti-rat IgG, or rabbit anti-hamster IgG was added at a final concentration of 20 μg/ml immediately prior to analysis. The mean fluorescence ratio of Indo-1-AM bound to free calcium (FL5/FL4 ratio, a measure of the relative calcium concentration) was determined. Responses were measured over 300 seconds, and recorded using the Cell Quest program on a FACS Vantage.

Re-challenge experiments were conducted in mice previously cured of A31 or BCL_1 tumor (LTS over 100 days), by [FcγRI x Id] in combination with muG-CSF, as described in chapter 4. Cured animals were re-inoculated with the respective tumor (5 x 10^4 cells) i.p. Naïve (previously unchallenged) FcγRI positive mice were used as controls.

The role of T cells in [FcγRI x Id] therapy was investigated using T cell depletion therapies. Transgenic F1 BALB/c mice were treated with the standard regime of mu G-CSF, inoculated with 10^5 BCL_1 tumor cells day 0, and treated with 5 μg of [FcγRI x Id] given twice daily for 5 days as before. To deplete T cells, mice were inoculated with either 1 mg of GK1.5 (rat anti-mouse CD4) (257), 0.5 mg of YTS 169 (rat anti-mouse CD8) (257) or a combination of both, on days minus 1, 2 and 5.

6.3 Results

6.3.1 Tumor tracking *in vivo*

To more closely monitor the activity of the BsAb *in vivo*, tumor tracking experiments were conducted to follow the fate of BCL_1 cells treated with each specificity of derivative, and to establish the degree of tumor present in treated animals at early and late time-points during the course of the therapy. As a marker for early depletion we monitored tumor in the peritoneal cavity, and for late time-points, the spleen.
In order to track tumor by this technique, it was necessary to inoculate animals with a substantially higher dose of tumor cells than given in normal therapy – 10^7 rather than 10^5/ mouse. To compensate for the increased tumor burden, animals were treated with an increased dose of BsAb (500 μg as opposed to 50 μg total). The muG-CSF priming regime remained as before.

Firstly, the fate of tumor cells in the peritoneal cavity was monitored. Mice treated with BsAb were sacrificed on each successive day of therapy through days one to five. Fig.6.3.1 shows the scatter profiles obtained from analysis of the peritoneal exudate of non-transgenic, treated with PBS (control), or the [FcγRI x Id], or [FcγRI x MHC II] derivatives. As expected, neither derivative was able to clear tumor in no-transgenic mice, although the anti-Id BsAb did show a slightly reduced burden compared to controls.

However, in the transgenic mice, both BsAb were able to reduce the level of tumor dramatically. Less than 1 % of cells present in the peritoneum were Id positive by day 6, as compared to nearly 70 % for PBS treated controls. Interestingly, this early tumor depletion was observed for BsAb of all specificity. Moreover, the decrease in tumor bulk was extremely rapid with maximal depletion being reached after 24 hours for derivatives targeting Id, MHC II and CD40 (Fig.6.3.3). The anti-CD19 BsAb performed with slightly slower kinetics reaching maximal depletion by day 3.

Despite this dramatic early reduction in tumor volume, overall progress of disease did not appear to be delayed. All animals went on to develop splenic tumor at a rate comparable to control animals, except those given anti-Id. Progress of tumor in the

spleen was again monitored by flow cytometry using dual fluorescence staining to specifically identify lymphoma cells. Fig.6.3.4 shows the scatter profiles obtained from transgenic mice receiving the control, anti-Id or anti-MHC II BsAb at day 10 compared to day 15. Whilst at day 10 animals remain free of disease, just 5 days later those receiving control, or anti-MHC II BsAb had developed a significant tumor load (upwards of 60 % spleen cells being Id positive). Similar profiles were obtained for the anti-CD19 and CD40 BsAb (not shown). Animals given the anti-Id BsAb however, presented little sign of emerging tumor (less than 1 % of spleen cells staining for Id). In terms of absolute numbers, lymphoma bearing animals carried a tumor burden of around 2 x 10^8 cells, whereas the anti-Id treated group presented less than 10^6 tumor cells in the spleen at this time.

Over the period of treatment all animals showed an increase in PMN numbers within the spleen by day 5, which then dropped over the following days as muG-CSF treatment was halted. However, the kinetics of the disappearance of PMN from the spleen appeared faster in non-transgenic animals compared to transgenic mice. Concomitant with the decrease in PMN numbers was the observed appearance of tumor. Mice also presented a corresponding increase in spleen weight, approaching a 10 fold difference in some animals, as tumor developed (Fig.6.3.5 and Fig.6.3.6). However, whilst non-transgenic animals all developed enlarged spleens, and increased tumor burden, irrespective of treatment BsAb, transgenic mice treated with the anti-Id derivative did not develop tumor (Fig.6.3.6).

6.3.2 Emerging tumor phenotype

We also examined the phenotype of tumor from these animals, to verify that therapeutic inactivity was not due to emergence of antigen negative variants. Levels of expression of target molecules from treated animals were determined by flow cytometry, and compared to those levels observed on tumor taken from control animals. Expression levels of MHC II, CD19 and CD40 on tumor from control groups were found to be identical to those from the BsAb treated, transgenic mice (Fig.6.3.7). Levels of tumor Id are not shown, as there was insufficient tumor from the [FcγRI x

Id] treated group to determine expression. Levels of antigen expression, including Id, remained unchanged on tumor from non-transgenic animals (data not shown).

6.3.3 Calcium signaling

It is possible that anti-Id BsAb may be functioning by cross-linking the BCR and delivering a growth inhibitory, or apoptotic signal. In this scenario, effector cells engaged by the univalent BsAb would provide the cross-linking function. As a parameter for signaling, we looked for increases in intracellular calcium following antigen ligation by BsAb. πBCL_1 cells were labelled with Indo-1-AM, a dye that increases fluorescence on binding of intracellular calcium. Levels of calcium flux between cells incubated with BsAb alone, or in the presence of a secondary anti-Ig cross-linking Ab were compared.

Initially, experiments were conducted with BsAb in the presence of isolated PMN to provide effector cell mediated cross-linking of the BCR. However, these experiments proved extremely difficult to perform, and no signaling was observed. Instead, BsAb were incubated with cells in the presence of polyclonal anti-Ig serum to provide cross-linking. None of the BsAb were able to generate an intracellular signal as measured by calcium mobilisation in the absence of cross-linking. (Fig.6.3.8). However, in the presence of the secondary cross-linking agent, the anti-Id BsAb was able to induce a rapid, potent, but transient increase in intracellular calcium (Fig.6.3.8). Interestingly, signaling was also observed following cross-linking of the anti-CD40 derivative. BsAb of other specificity (anti-MHC II, anti-CD19) failed to generate any changes in calcium, as did the control, non-tumor binding BsAb (anti-A31 Id). Neither was signaling observed in the presence of cross-linking agent alone.

Furthermore, the strength and duration of calcium flux was directly proportional to the degree of cross-linking. Titration of the secondary reagent from 20 μg/ml down to1 μg/ml produced diminshed responses at lower levels of cross-linking of both the anti-Id (Fig.6.3.9) and the anti-CD40 (Fig.6.3.10) BsAb.

6.3.4 Tumor re-challenge

We also wished to determine if animals apparently "cured" with [FcγRI x Id] derivatives were subsequently immune to further tumor re-challenge. Long-term protected mice (surviving >100 days) received 5 x 10^4 A31 or BCL_1 cells i.p, and survival was compared to naïve (previously unchallenged) transgenic mice given a similar dose. No additional muG-CSF supplementation was provided. Interestingly, whereas control, naïve animals succumbed to tumor, cured animals remained free of disease (Fig.6.3.11). Although these experiments have only been conducted in a small number of animals (5 A31 cured mice, and 3 BCL_1 cured mice) the results are extremely exciting and indicate that [FcγRI x Id] BsAb are able to induce a vaccine effect in these transgenic animals.

6.3.5 T cell depletion therapy

Finally, we wished to determine the importance of T cells in the therapy obtained with the [FcγRI x Id]. Therapy was conducted in mice depleted of either CD4, CD8 or both sub-sets. Mice were inoculated with 10^5 BCL_1 tumor cells, and treated with the standard regime of muG-CSF and BsAb (to a total of 50 μg). Fig.6.3.12 clearly shows that depletion of either T cell population dramatically reduces the amount of protection observed in fully immunocompetent animals. 70 % of mice with intact T cells were long-term protected by the BsAb, whilst those depleted of T cells had a survival advantage over control cohorts of only a few days. Importantly, tumor develops with the same kinetics in T cell depleted mice as those with intact T cells (36), so it is possible to conclude that [FcγRI x Id] therapy is dependent on $CD4^+$ and $CD8^+$ cells.

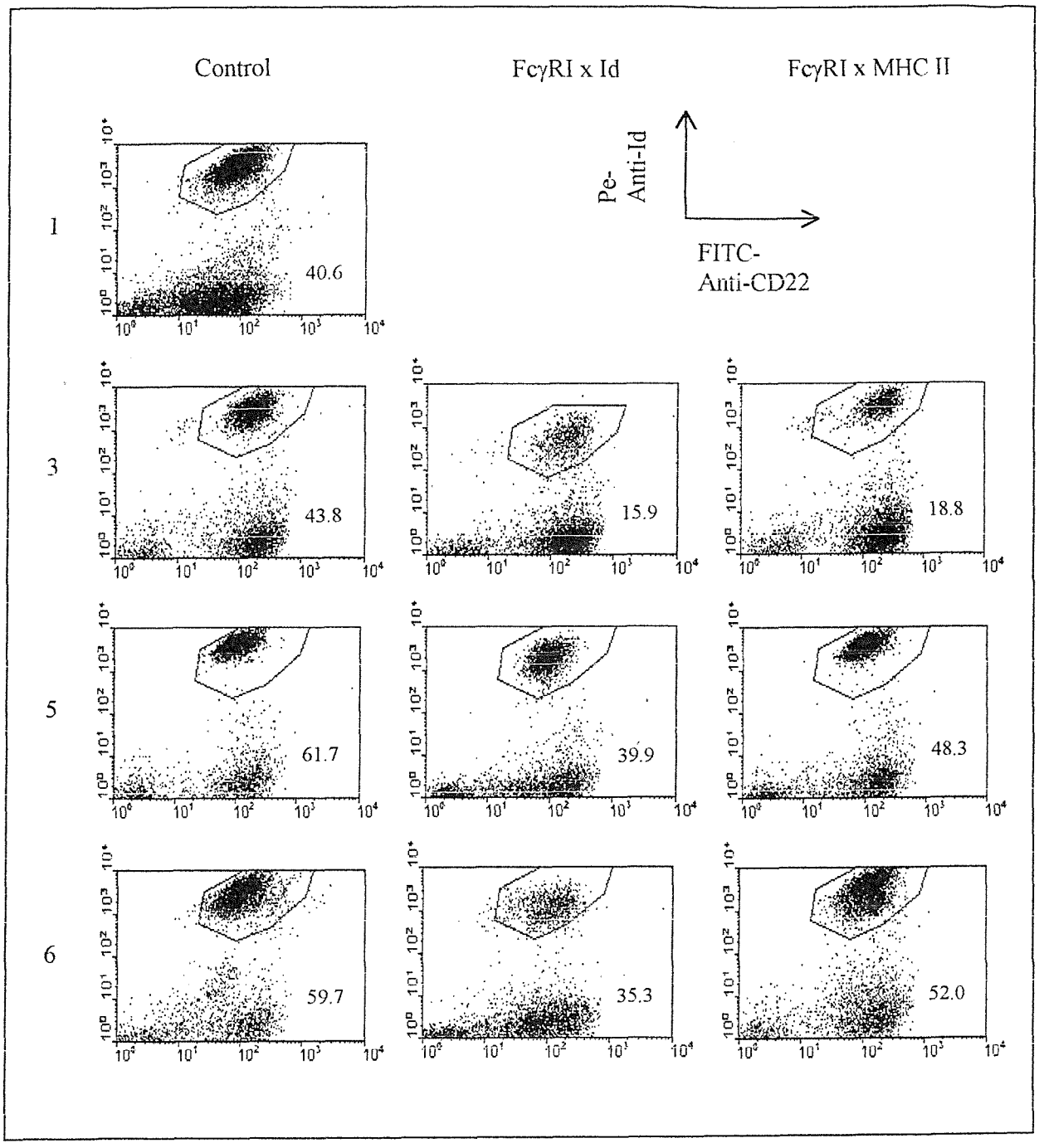

Fig.6.3.1 Peritoneal tumor tracking in non-transgenic mice. BALB/c x FVB/n F1 FcγRI non-transgenic mice received 2 μg muG-CSF/day, 4 days, s.c. Mice were inoculated with 10^7 BCL_1 tumor cells, i.p, day 0, and treated with 50 μg BsAb, i.p, twice a day, for 5 days (total of 500 μg). Shown are the scatter profiles obtained on day 1 post-tumor (no treatment) and days 3, 5 and 6 post-tumor (mice having received 200, 400, or 500μg BsAb respectively), for animals treated with control, anti-Id or anti-MHC II BsAb. Gated are Id positive cells as determined by flow cytometry. Control animals received PBS. Numbers shown indicate percent tumor cells.

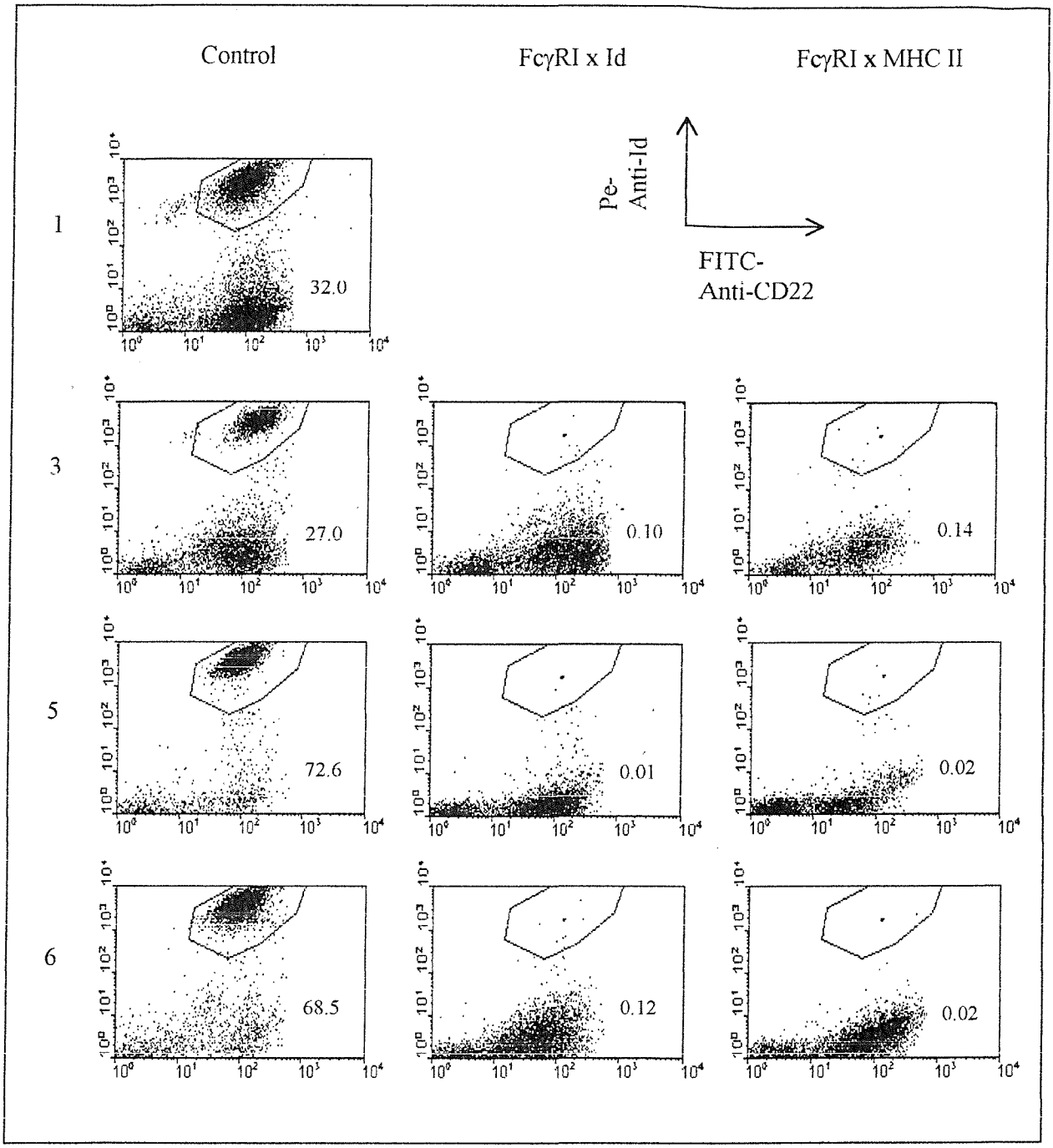

Fig.6.3.2 Peritoneal tumor tracking in transgenic mice. BALB/c x FVB/n F1 FcγRI transgenic mice received 2 μg muG-CSF/day, 4 days, s.c. Mice were inoculated with 10^7 BCL_1 tumor cells, i.p, day 0, and treated with 50 μg BsAb, i.p, twice a day, for 5 days (total of 500 μg). Shown are the scatter profiles obtained on day 1 post-tumor (no treatment) and days 3, 5 and 6 post-tumor (mice having received 200, 400, or 500μg BsAb respectively), for animals treated with control, anti-Id or anti-MHC II BsAb. Gated are Id positive cells as determined by flow cytometry. Control animals received PBS. Numbers shown indicate percent tumor cells.

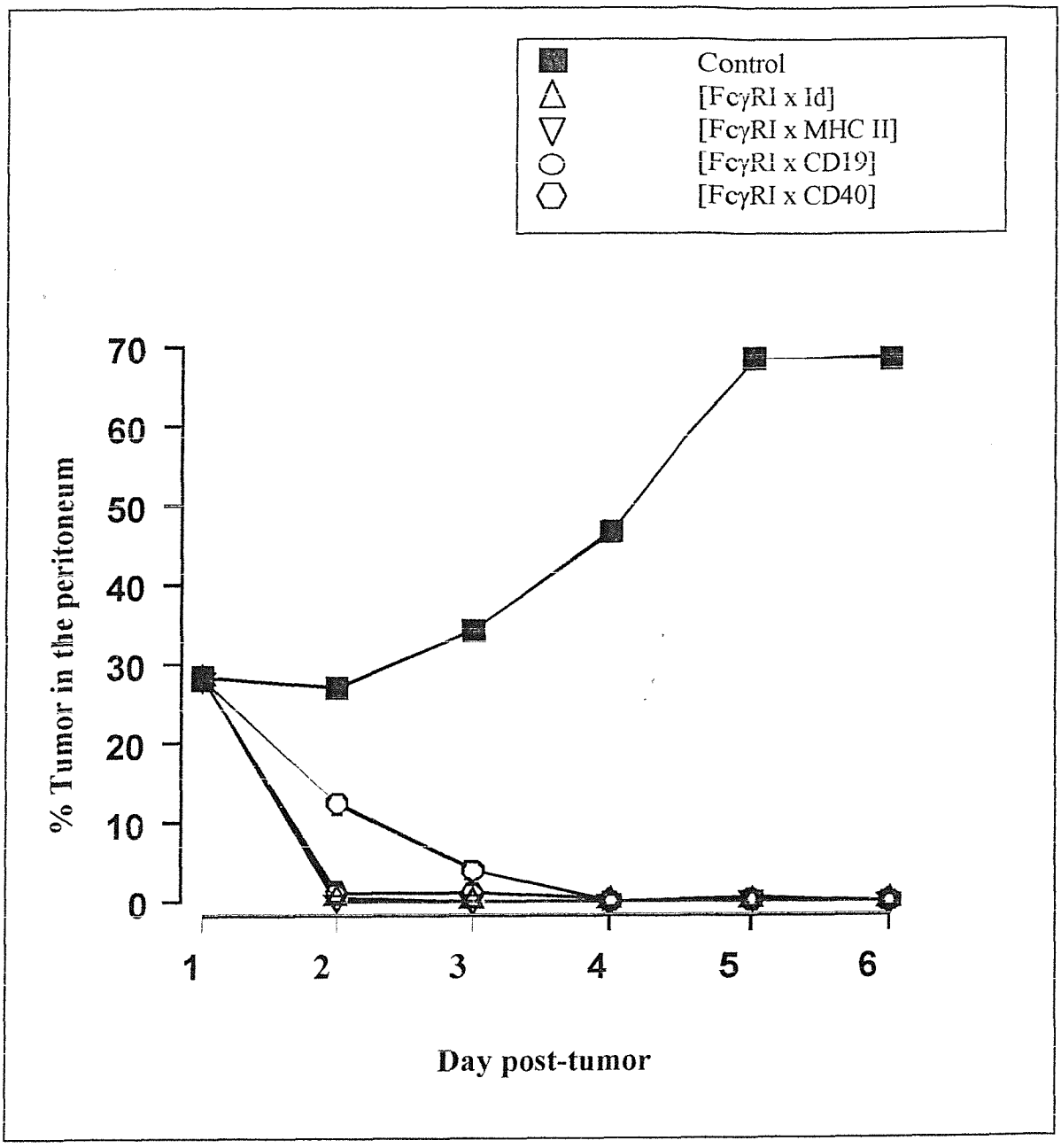

Fig.6.3.3 Tumor tracking in the peritoneal cavity. BALB/c x FVB/n F1 transgenic mice received 2 μg muG-CSF/day, day 0 – 4 , s.c. Mice were inoculated with 10^7 BCL_1 tumor cells, i.p, day 0, and treated with 50 μg BsAb, i.p, twice a day, for 5 days (total of 500 μg). One animal per group was sacrificed on each day of therapy, and the percentage of tumor cells in the peritoneum analysed using flow cytometry. Graphed are the percentage of tumor cells present on each day after inoculation, following treatment as indicated above. Control animals received PBS.

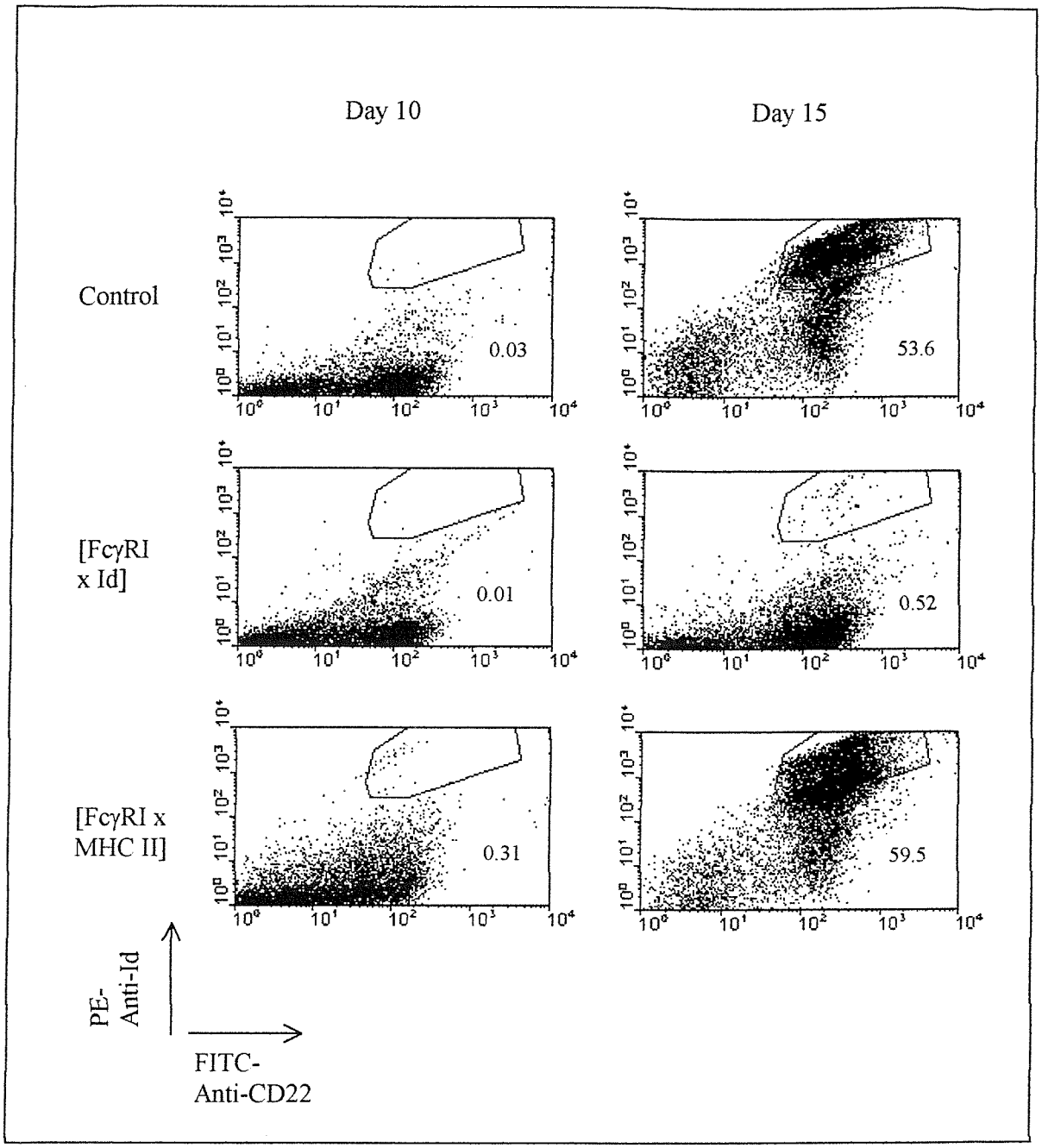

Fig.6.3.4 Splenic tumor tracking in transgenic mice. BALB/c x FVB/n F1 FcγRI positive mice received 2 μg muG-CSF/day, 4 days, s.c. Mice were inoculated with 10^7 BCL_1 tumor cells, i.p, day 0, and treated with 50 μg BsAb, i.p, twice a day, for 5 days (total of 500 μg). Shown are scatter profiles obtained from spleens taken from control, anti-Id or anti-MHC II BsAb treated animals on day 10 and day 15 post-tumor. Gated are Id positive cells as determined by flow cytometry. Control BsAb was the non-tumor binding [FcγRI x anti-A31-Id]. Numbers are percent tumor cells.

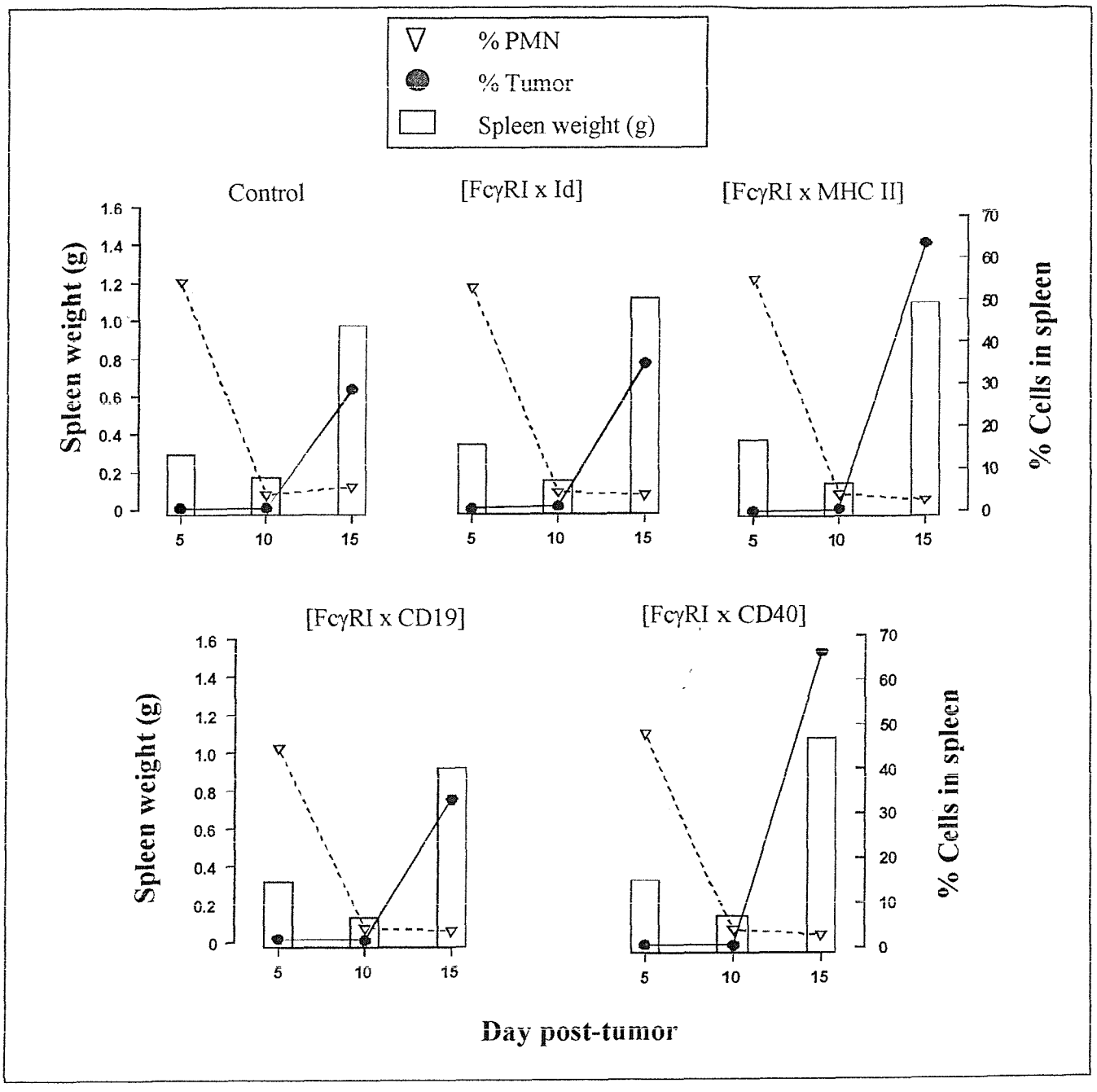

Fig.6.3.5 Analysis of tumor development in FcγRI negative mice. BALB/c x FVB/n F1 FcγRI non-transgenic mice received 2 μg muG-CSF/day, 4 days, s.c. Mice were inoculated with 10^7 BCL_1 tumor cells, i.p, day 0, and treated with 50 μg BsAb, i.p, twice a day, for 5 days (total of 500 μg). One mouse per group was then culled on day 5, 10 and 15 post-tumor inoculation, and splenic phenotype analysed. Shown are the changes in spleen weight (open bars) compared to the percentage PMN (∇) and tumor (●) over time, for animals treated as indicated. Control BsAb was the non-tumor binding [FcγRI x A31-Id].

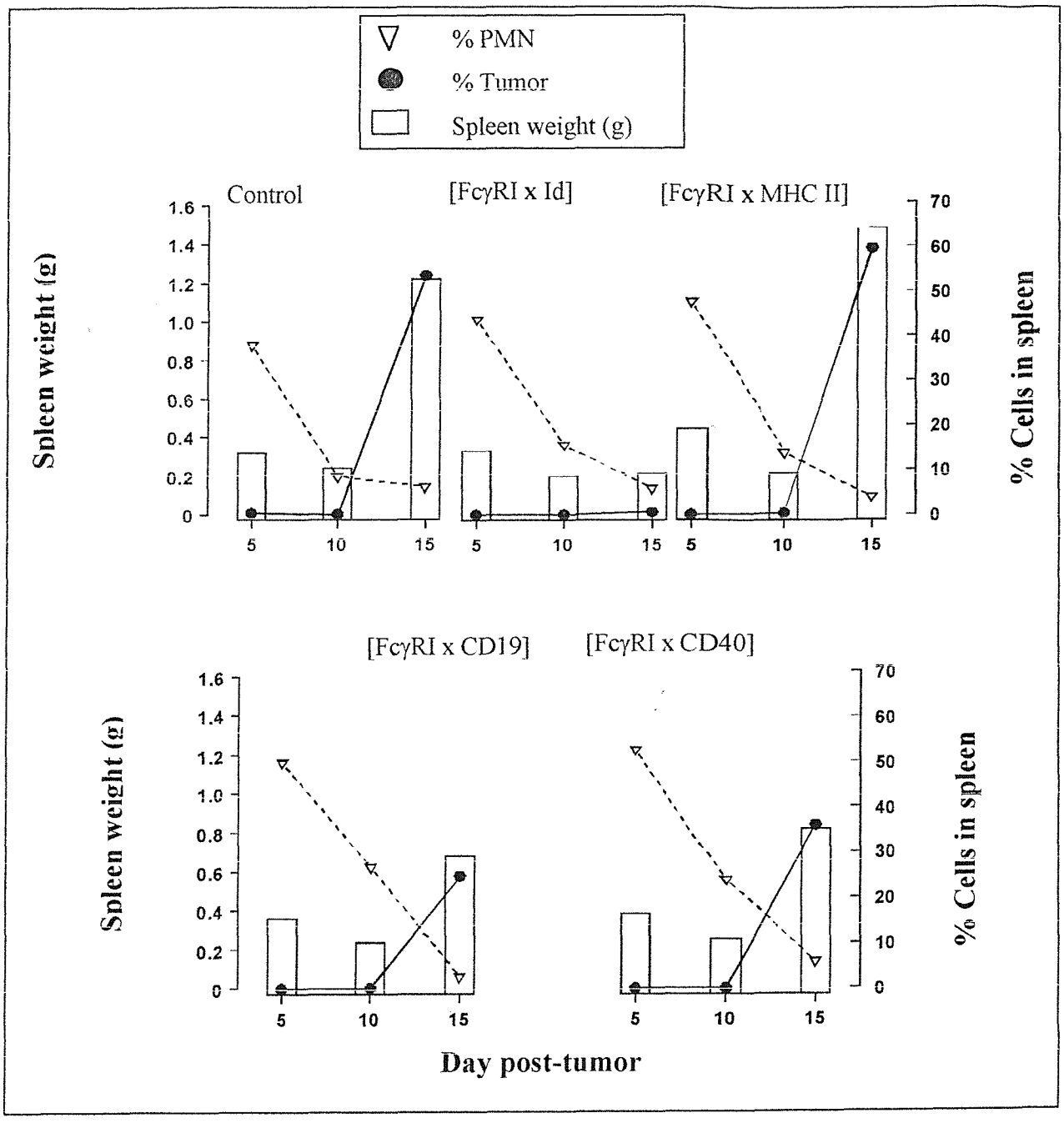

Fig.6.3.6 Analysis of tumor development in FcγRI positive mice. BALB/c x FVB/n F1 FcγRI transgenic mice received 2 μg muG-CSF/day, 4 days, s.c. Mice were inoculated with 10^7 BCL_1 tumor cells, i.p, day 0, and treated with 50 μg BsAb, i.p, twice a day, for 5 days (total of 500 μg). One mouse per group was then culled on day 5, 10 and 15 post-tumor inoculation, and splenic phenotype analysed. Shown are the changes in spleen weight (open bars) compared to the percentage PMN (▽) and tumor (●) over time, for animals treated as indicated. Control BsAb was the non-tumor binding [FcγRI x A31-Id].

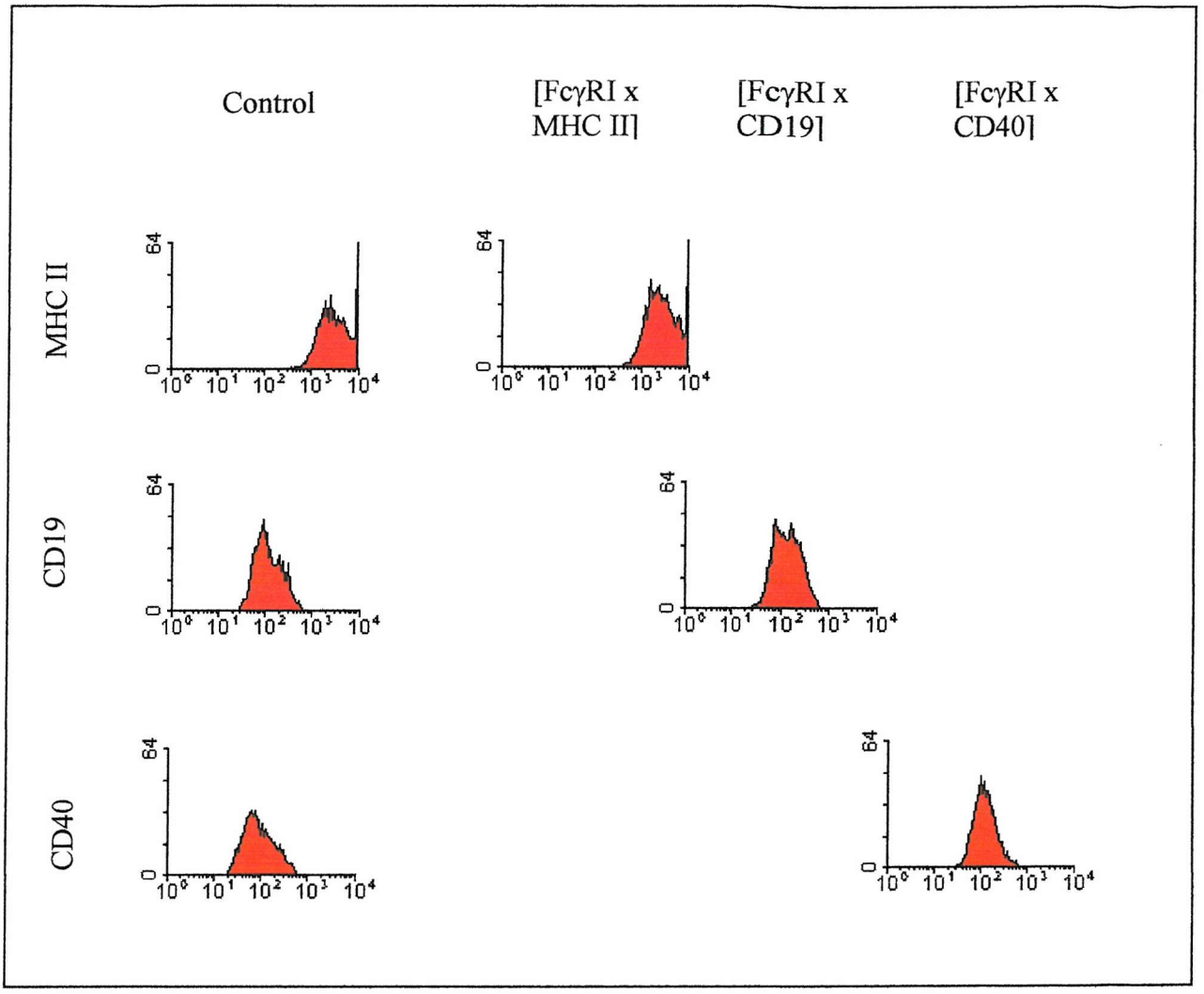

Fig.6.3.7 Emerging tumor phenotype. The phenotype of BCL_1 tumor developing on day 15 from FcγRI positive mice was assessed by flow cytometry. Cells staining positive with Pe-anti-Id were also analysed for expression of MHC II, CD19, and CD40 using appropriate FITC-labelled mAb. Shown are levels of expression on tumor from animals treated with control BsAb, the [FcγRI x A31-Id] (first column), as compared to tumor from animals treated with the respective BsAb. The second column shows expression levels of MHC II on tumor treated with anti-MHC II BsAb; the third column levels of CD19 on tumor treated with anti-CD19 BsAb; and the fourth column levels of CD40 on tumor treated with an anti-CD40 BsAb.

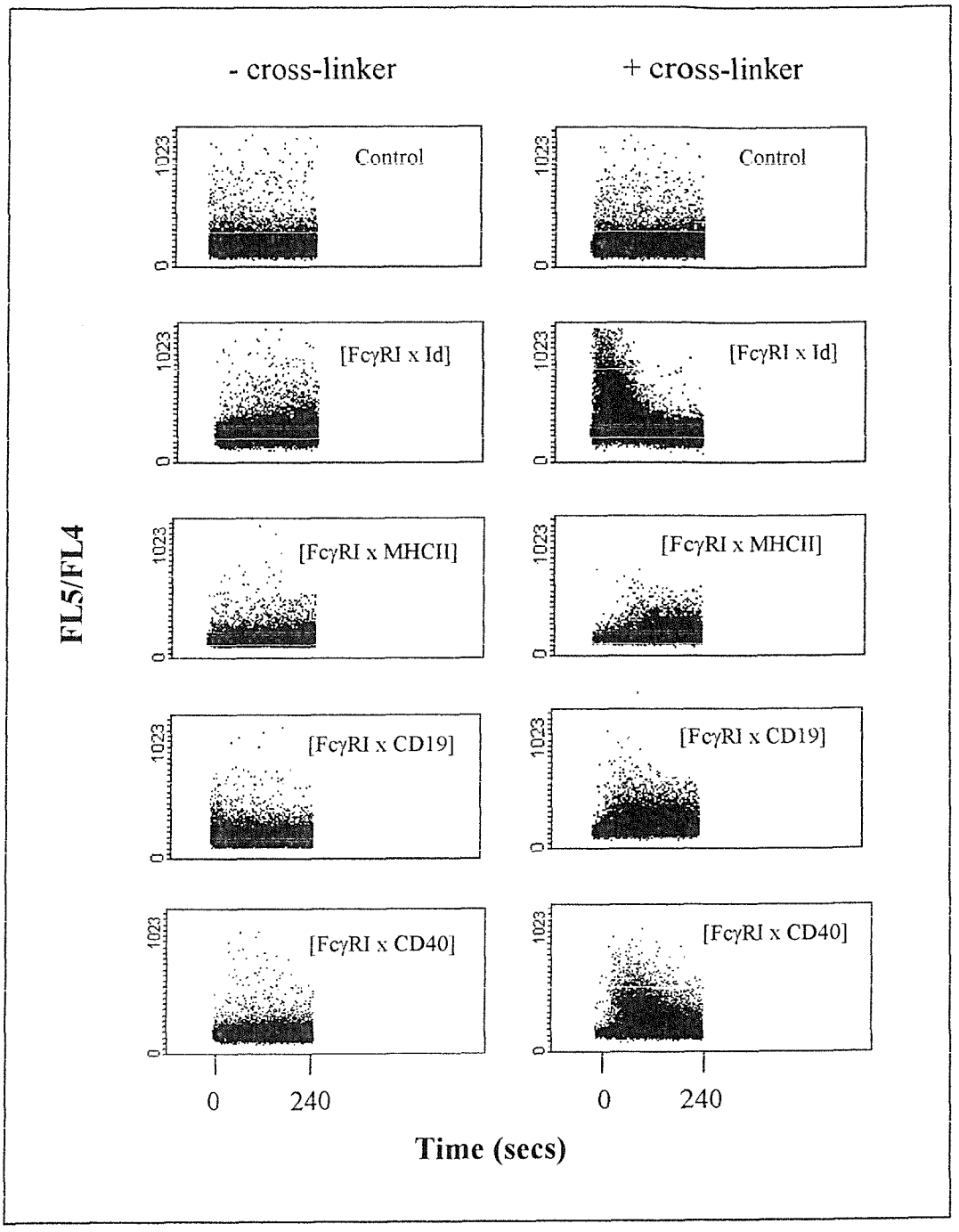

Fig.6.3.8 Intracellular calcium flux following cross-linking of BsAb. πBCL_1 cells loaded with the fluorescent dye Indo-1-AM were coated with BsAb (2 μg/ml) in the absence (first column) or presence (second column) of a secondary cross-linking reagent (20 μg/ml). Shown are traces depicting the ratio of intracellular calcium flux against time. BsAb are as indicated. Control BsAb is the non-tumor binding [FcγRI x A31 Id].

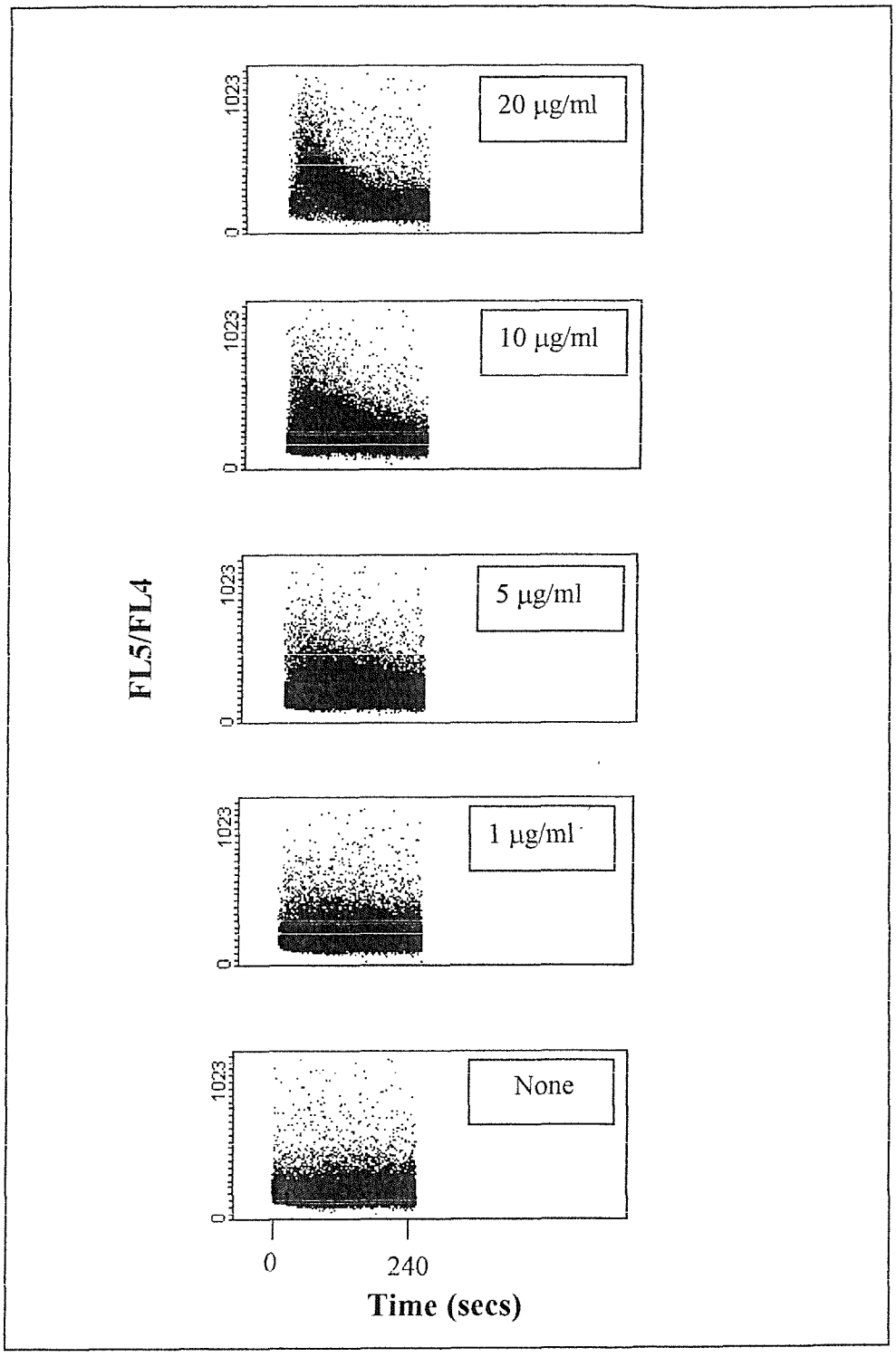

Fig.6.3.9 Intracellular calcium flux following titration of cross-linker with [FcγRI x Id]. πBCL$_1$ cells loaded with the fluorescent dye Indo-1-AM were coated with anti-Id BsAb (2 μg/ml) and exposed to a secondary cross-linking reagent at various concentrations (20, 10, 5, 1 or 0 μg/ml). Shown are traces depicting the ratio of intracellular calcium flux against time.

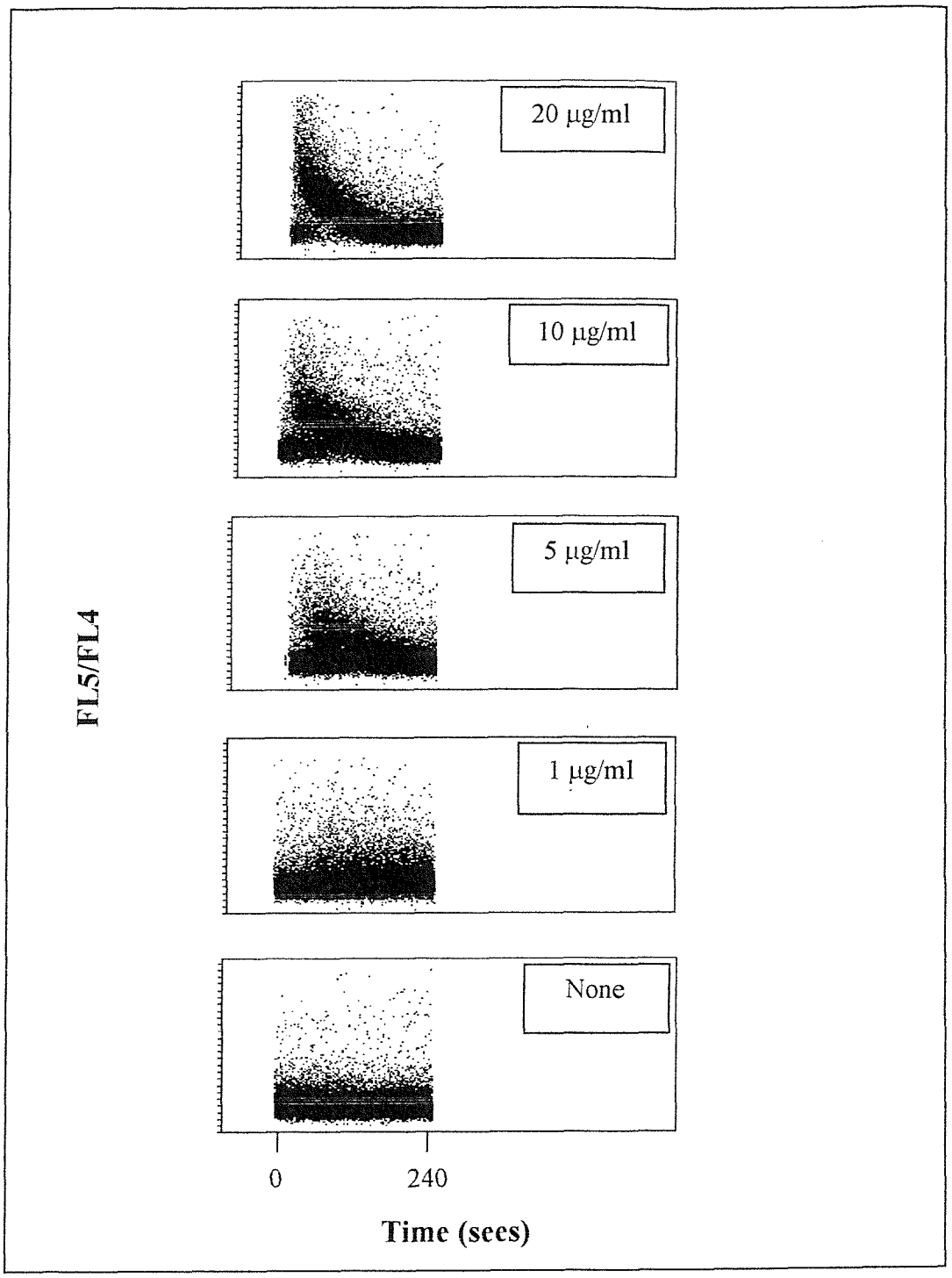

Fig.6.3.10 Intracellular calcium flux following titration of cross-linker with [FcγRI x CD40]. πBCL$_1$ cells loaded with the fluorescent dye Indo-1-AM were coated with anti-CD40 BsAb (2 μg/ml) and exposed to a secondary cross-linking reagent at various concentrations (20, 10, 5, 1 and 0 μg/ml). Shown are traces depicting the ratio of intracellular calcium flux against time.

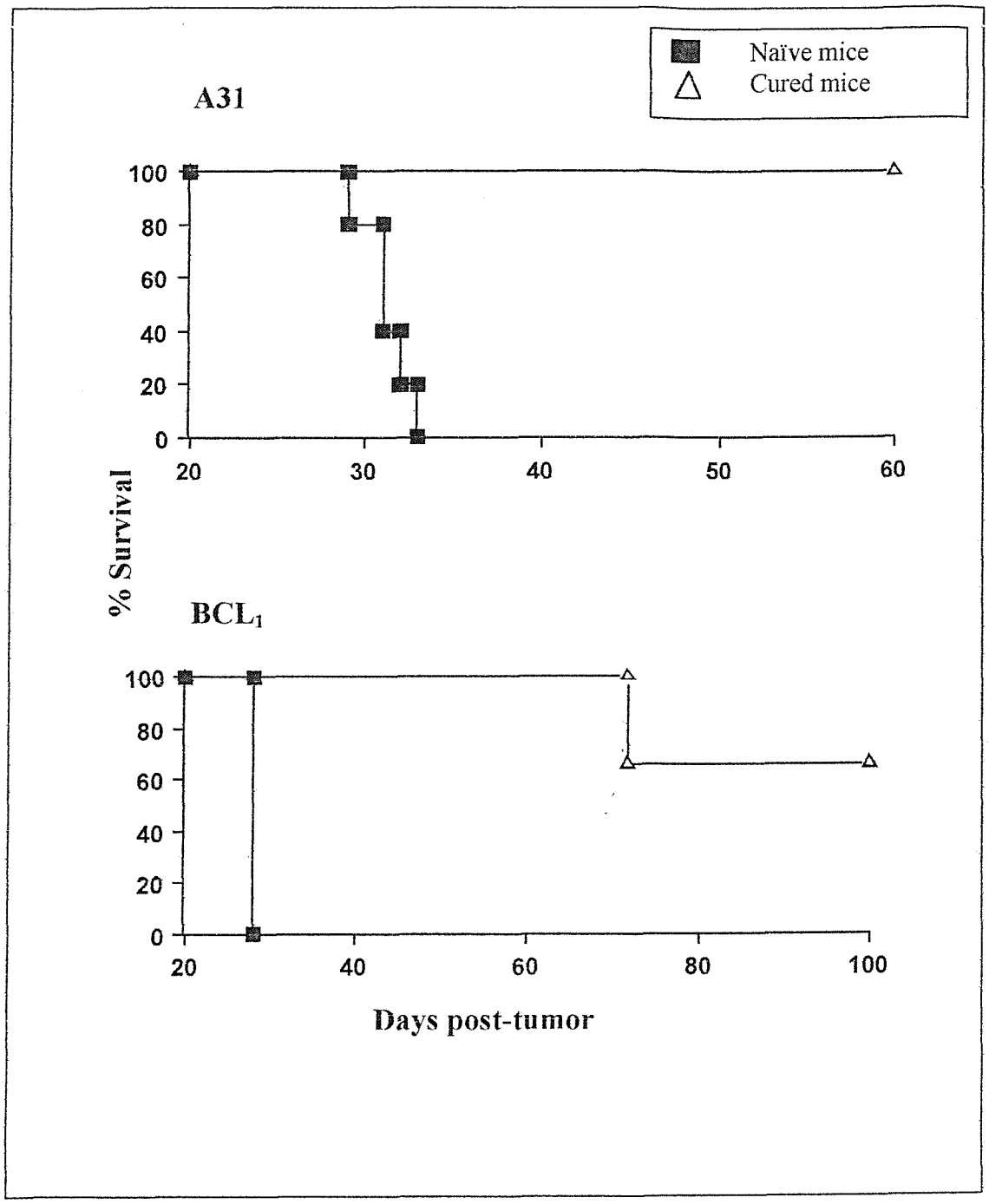

Fig. 6.3.11 Re-challenge therapy. Groups of 5 age matched CBA or BALB/c FcγRI positive F1 mice received 2 μg/day muG-CSF, days minus 4 to 5, s.c. Mice were inoculated with $2x10^5$ A31 or 10^5 BCL_1 tumor cells, i.p., day 0 and were treated with twice daily doses of 5 μg [FcγRIxId], i.p, days 1 to 5 (50 μg/mouse total). Animals surviving beyond day 100 were re-inoculated with $5x10^4$ A31 or BCL_1 tumor cells respectively, i.p. Naïve F1 transgenic animals were inoculated as controls. Survival was recorded daily.

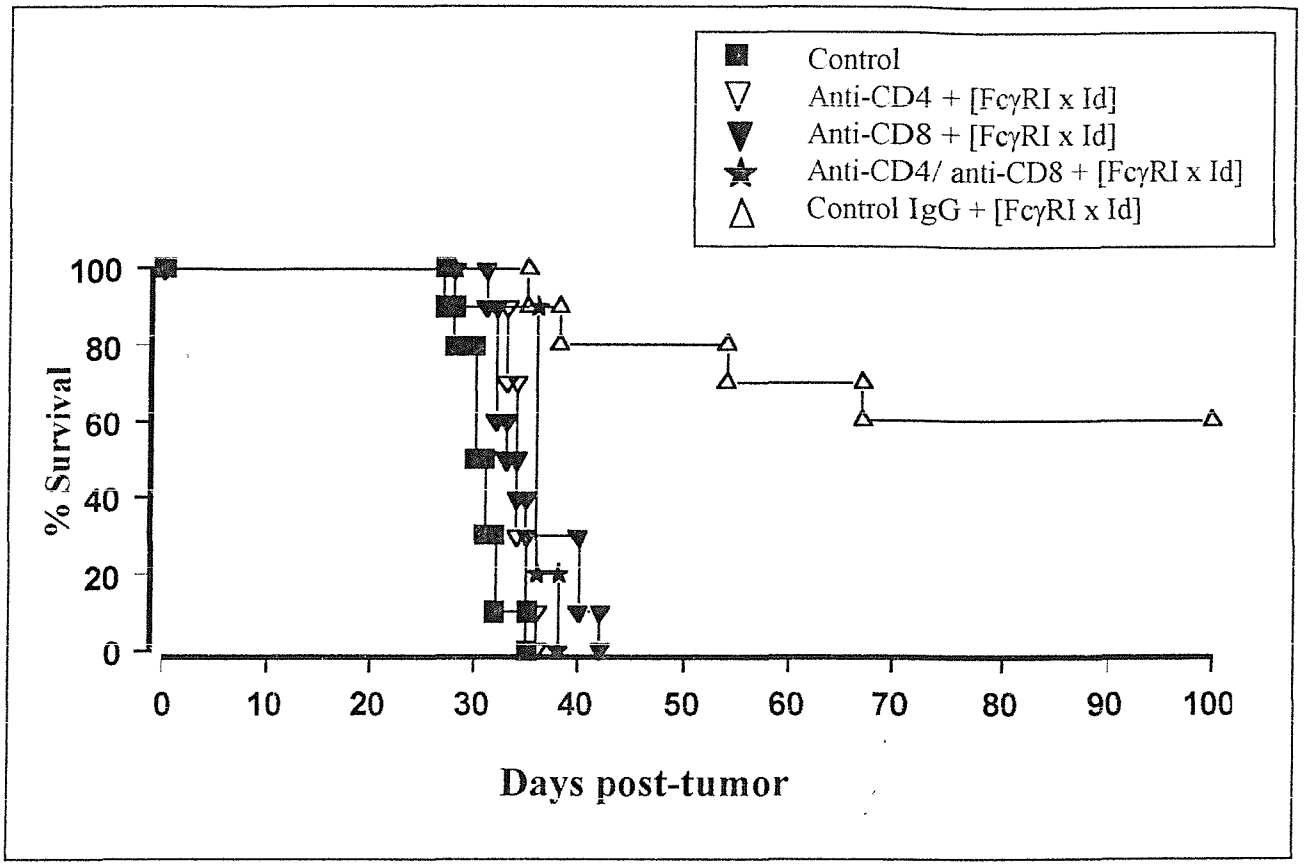

Fig.6.3.12 [FcγRI x Id] T cell depletion therapy. Groups of 5 FVB/n x BALB/c F1 mice were inoculated with BCL_1 (10^5, ip) day 0 together with the standard regime of muG-CSF and [FcγRI x Id] BsAb (as before). T cells were depleted with either anti-CD8 (YTS169; 0.5 mg), anti-CD4 (GK1.5; 1 mg), or a mixture of both, given ip, 1 day prior to tumor and again on days 2 and 5 after tumor inoculation. Treatment was as indicated: PBS (■), anti-CD4 + [FcγRI x Id] (▽), anti-CD8 + [FcγRI x Id] (▼), both anti-CD4 and anti-CD8 + [FcγRI x Id] (★), or control rat IgG + [FcγRI x Id] (△). Survival was recorded daily. Only cohorts treated without T cell depletion and [FcγRI x Id] showed a significantly extended survival over controls ($p < 0.01$)

6.4 Discussion

In this chapter, the functional activity of the FcγRI BsAb was more closely examined. Previous studies with mAb of similar tumor specificity to the BsAb have demonstrated that anti-Id and anti-CD40 antibodies are both able to control tumor growth *in vivo*, although probably via functionally distinct mechanisms (231). Recent evidence demonstrates that anti-CD40 is capable of inducing a cytotoxic CD8 positive T-cell response, possibly by cross-priming (36). Anti-Id mAb on the other hand most probably function by activating negative signaling pathways that lead to growth arrest and apoptosis (239). Although the [FcγRI x CD40] BsAb proved to be less efficacious than CD40 in terms of protection, the anti-Id BsAb were clearly better than the anti-Id mAb, generating LTS in the majority of animals, even at relatively low treatment doses.

Preliminary experiments were conducted using tumor cells labelled with CFSE, an intracellular green fluorescent dye. However, tumor cells tagged in this manner proved difficult to follow with any degree of certainty as cells and cell debris engulfed by PMN and macrophages, remained fluorescent and in turn caused the phagocytic cells to register on the green channel (data not shown). This made it difficult to clearly distinguish individual cell populations. Therefore, to monitor with confidence the progress of lymphoma cells present within the peritoneum and spleen, we decided to use flow cytometric analysis of cells labelled by dual fluorescent staining.

RCC does appear to be actively taking place *in vivo* as all derivatives were shown to reduce tumor bulk considerably during initial stages of therapy, as demonstrated by tracking experiments (Fig.6.3.3). This was not non-specific clearance of tumor cells, for example by resident phagocytes, as control animals did not present such a substantial decrease in tumor load, with a clearly identifiable population of tumor remaining established in the peritoneum over early time points. However, this primary clearance in BsAb treated groups was not, in itself, sufficient to mediate protection. All groups, except [FcγRI x Id] treated animals, went on to establish terminal disease (Fig.6.3.5 and 6). Depletion was not observed in non-transgenic animals given muG-CSF, indicating that tumor destruction was a direct consequence of retargeting

through FcγRI. As RCC is occurring at levels sufficient to rapidly clear 99 % of tumor, but still unable to confer long-term protection, these observations point to only a secondary roll for such effector mechanisms *in vivo*. Moreover, as tumor phenotype from treated groups remained similar to that for control groups, it seems likely that subsequent emergence of tumor in these animals was not due to escape by antigen low or negative variants.

Instead, it appears that anti-Id BsAb have additional anti-tumor effects over the activation of Fc mediated effector functions that account for the long-term protection observed following treatment with this derivative. It is possible that protection could be a consequence of the ability of anti-Id antibodies to propagate anti-proliferative signals to the tumor on cross-linking of BCR - a factor that has been clearly demonstrated for anti-Id mAb. A number of authors have shown that anti-Id, anti-IgM or antigen function by inducing signal transduction pathways that negatively regulate tumor growth (239, 258). These intracellular signals, generated by receptor cross-linking, drive B-lymphoma cells into CCA or apoptosis, with the majority of tumor being depleted, leaving only a small residual population of non-proliferating, dormant cells. We suggest that the anti-Id BsAb may well be functioning in a similar manner, by inducing anti-proliferative signals to the tumor. Evidence from studies using mAb directed at IgM on human B-lymphoma cells reveal a direct association between rises in intracellular calcium and apoptosis (256). We therefore looked at changes in calcium mobilisation following incubation with our BsAb, as a parameter for negative signaling in our murine tumor.

Although no signal was observed following exposure to BsAb alone, a strong signal was obtained after hyper-cross-linking of the anti-Id BsAb with polyclonal anti-IgG. This signal was not seen with either the anti-CD19 or anti-MHC II derivatives (Fig. 6.3.8). It is possibly more than coincidence that the only specificity of BsAb to give long-term protection, was also able to generate a direct signal to the tumor. Unfortunately, attempts to measure calcium flux using PMN, rather than secondary Ab, to hyper-crosslink BsAb coated BCR have so far met with failure. This is most probably due to differing dynamics of cell versus secondary Ab mediated hyper-cross-linking. Experiments by Brunswick et al. (259) using dextran bound Ig indicate

that multivalent ligands can stimulate very low level, repetitive signals over prolonged periods of time. An effector cell may well function in a similar manner, with our assay being too insensitive to detect any changes in calcium levels occurring.

There have been reports of successful therapy with Ab toCD19 against murine (231), and human tumor (254) and that this is related to anti-proliferative signaling. Likewise, anti-HLA II mAbs have been used with success in therapy, and indicated to have signaling potential (260). However, we saw no indication of calcium flux with BsAb targeting these antigens at doses studied. These discrepancies may be explained by recent observations by Ghetie et al. (227), showing that at high concentration mAbs spontaneously form homodimers, and that it is these aggregates which are responsible for generating intracellular signals, presumably by enhanced cross-linking. As our BsAb are highly purified, with all contaminating aggregates having been removed, this additional signaling potential may well have been removed. Significantly, *in vivo* protection by mAbs to antigens such as CD19 required a large inoculating dose (231), suggesting that therapeutic effect may be related to homodimerisation. The potential for enhancing antigen signaling by homodimerisation is investigated more closely in chapter 7.

The ability of CD40 to generate intracellular calcium signals remains somewhat contentious. Stimulation of murine CD40 is known to induce B-cell proliferation, possibly via a calcium dependent pathway. Klaus et al. (261) have demonstrated that ligation of CD40 by anti-CD40 mAb can indeed cause a modest increase in intracellular calcium. However, others have shown no calcium mobilisation following CD40 ligation on human B cells (262), and we too have not observed calcium flux with anti-murine CD40 mAb. BsAb to CD40 on the other hand, was capable of generating a rise in intracellular calcium following cross-linking. Why cross-linking of the BsAb, but not IgG, should generate calcium flux is intriguing, and cannot be explained at this time.

The most important observation gained from these studies, is that animals cured by anti-Id BsAb do not to succumb to disease on re-challenge with a second dose of tumor (Fig.6.3.11). In addition, LTS did not show tumor re-growth at a later date (indicating tumor dormancy had been induced and broken), and neither did animals

inoculated with splenocytes from LTS develop disease (data not shown). However, protection did appear to be directly related to the generation of a tumor specific CTL response, as depletion of either $CD4^+$ or $CD8^+$ cells completely abrogated [FcγRI x Id] mediated protection (Fig.6.3.12).. It has been shown that FcγRI is able to target antigens for immunisation (180). However, from the work described here, such presentation does not automatically lead to immunity as not all BsAb were able to generate a response. It seems likely therefore, that the response observed is intimately related to the anti-Id specificity. A possible scenario is that anti-Id is able to signal through the BCR leading to extensive tumor apoptosis, and that these apoptotic tumor cells are thus engulfed by APC, for example DC, thus leading to a T cell response through processes of cross-presentation (263). BsAb of other specificity may not be able to induce apoptotic signals, and may simply engulf targeted tumor. Moreover, cross-linking of the BCR may stimulate production of inflammatory cytokines by the B-lymphoma cell, thus creating an environment conducive to a T cell response.

In conclusion, it seems that whilst anti-FcγRI BsAb to a range of tumor associated antigens are able to induce a rapid clearance of tumor *in vivo*, this response is not sufficient to provide long-term protection. Instead, only anti-Id derivatives are capable of fulfilling this function. Given that [FcγRI x Id] has been shown to mobilise intracellular calcium, we propose this activity is related not only to processes of RCC, but also to direct growth control through signaling, and induction of T cell immunity.

As signaling would appear to be an important factor in the generation of an anti-tumor response, we wished to investigate the potential for converting traditionally non-signaling, or weakly signaling mAb into strongly signaling mAb through the process of homodimerisation. This work forms the basis of the next chapter.

Chapter 7

Production and activity of homodimer derivatives

7.1 Introduction

The studies with BsAb described in the previous chapters indicate that target antigen selection is of critical importance to therapeutic success. Further, it is clear that the performance of an Ab *in vitro* is not necessarily predictive of its activity *in vivo*. Whilst effector functions such as cellular cytotoxicity have been cited as important for mAb therapy, we have compiled data suggesting that these functions may only be of secondary importance. Instead, it appears that the capacity of an Ab to signal to tumor, or activate T cell immunity, is more important. With regards to the first point, a number of Ab are known to be able to trigger anti-proliferative or apoptotic signals, including Ab to the BCR and CD20 (265). However, a range of Ab to antigens such as CD19 and MHC II, have also been shown to signal under certain circumstances (23, 260).

Those mAb such as anti-CD19, which have been demonstrated to have a signaling capacity, only do so when delivered at comparatively high Ab concentrations, and in certain tumour models. Ghetie et al. (227) have investigated the physiochemical properties of such Ab and discovered an interesting phenomenon. Samples studied contained aggregates of around 300 kDa. When isolated, these aggregates represented spontaneously formed homodimers (HD). These dimers constitute approximately 20 % of the total IgG fraction, and were demonstrated to confer all the negative signaling capability within anti-CD19 mAb preparations. It was thus proposed that homodimerisation of mAb could confer signaling activity.

To further investigate the potential of such dimers we have constructed a panel of chemically synthesised HD against a number of human B cell tumor antigens. These have been tested against a variety of cell culture lines, to determine their ability to activate mechanisms of ADCC, complement recruitment, growth arrest and apoptosis. The *in vivo* efficacy of these Ab has also been investigated using a xenograft model, in SCID mice.

We have further tried to establish the nature of the signaling machinery activated by these derivatives, looking for evidence of intracellular calcium mobilisation following Ab binding.

7.2 Materials and Methods.

A list of the parental mAb from which HD were derived is given below in Table 7.2.1. The mAb selected were all done so on the basis that they had not previously shown any growth inhibitory or apoptotic effects against the Burkitt's lymphoma lines Daudi, Raji and EHRB tested in this chapter.

Clone	Antigen	Isotype
DB7/12	Anti-saporin	IgG1
HD37	Anti-CD19	IgG1
IF5	Anti-CD20	IgG2a
4KB	Anti-CD22	IgG1
AT13/5	Anti-CD38	IgG1
LOB 7/6	Anti-CD40	IgG2a

Table 7.2.1 Mab used in the production of HD derivatives. All were obtained from Tenovus or ATCC.

HD were constructed from parent mAb using a conventional chemical cross-linking protocol (227). One fraction of the Ab was labelled with Succinimidyl 4-(N-maleimidomethyl) cyclohexane-1-carboxylate (SMCC) and the second fraction with N-succinimidyl S-acetylthioacetate (SATA) (Pierce). Excess linker was removed on a Sepharose G25 column and dimerisation achieved by incubating the two samples together at room temperature for two hours. Homodimerisation was verified by SDS-PAGE and HPLC analysis respectively. Dimerised Ab was crudely purified by repeated fractionation on an AcA44 column.

Growth inhibition of human lymphoma lines was calculated using a [^{3}H]thymidine incorporation assay, as described in chapter 2. Cells were cultured at (1 x 10^6/ml) with monomeric or HD Ab at concentrations as indicated in the text. [^{3}H]thymidine (0.5 μCi/well) was added after culturing for 24 hours, and cells left to label for a further 16 hours before harvesting, and incorporation calculated using a liquid scintillation counter.

In vitro ADCC activity was calculated using a standard chromium-release assay as described previously. Human lymphoma target cells (5 x 10^3) labelled with ^{51}Cr were mixed with either monoclonal or HD Ab at concentrations shown, for 15 min on ice. Human effector cells were then added at an effector to target ratio of 50:1. Following incubation for 4 hours at 37^{0}C, samples were spun and 100 μl supernatant removed and counted to determine percentage lysis. Maximal lysis was calculated from target cells to which 150μl 1 % Nonidet P-40 had been added, using the equation given in chapter 2.

Complement lysis was determined as detailed in chapter 2. Human lymphoma target cells (1 x 10^5) were mixed with monomeric or HD Ab at concentrations shown in the text, for 15 min on ice. Cells were then incubated with 300 μl of 20 % human serum at 37^{0}C for 45 min. Samples were spun to pellet cells and 150 μl supernatant removed and counted to determine percentage complement lysis. Maximal lysis was determined as above.

Growth arrest and apoptosis was determined using Fsc v Ssc analysis or PI labelling. Cells (0.5 x 10^6/ml) were cultured in the presence of monomeric or HD Ab at concentrations indicated throughout the text for 24, 48 or 72 hours. Samples were then harvested, washed once in PBS and then labelled with 250 μl of hypo-PI solution (see chapter 2) at 4^{0}C overnight. Samples were analysed on a FACScan. For Fsc v Ssc analysis samples were incubated as above, harvested and analysed immediately comparing scatter profiles also on a FACScan.

Intracellular calcium signaling was determined as before. Briefly, Indo-1-AM labelled human lymphoma cells (1 x 10^7/ml) were warmed to 37^{0}C for 5 min, before being mixed

with either monomeric or HD Ab (150 μg/ml). Samples were immediately analysed on a FACS vantage, measuring the ratio of FL5/FL4 against time to calculate intracellular calcium mobilisation.

In vivo therapeutic efficacy was determined using tumor xenograft models in SCID mice. Animals were inoculated with tumor cells (5 x 10^6) iv, day 0, and treated with a single dose of either monomeric or HD Ab (100 μg) iv, day 7. Control groups received PBS. Survival was monitored daily.

7.3 Results

7.3.1 Homodimerisation of mAb

Due to the lack of murine lymphoma culture cell lines available (it should be pointed out that the πBCL_1 line used previously was a relatively late addition to the laboratory), we decided to switch models and utilise a number of human Burkitt's lymphoma lines. This enabled HD constructs to be tested on a variety of cell lines with well defined growth characteristics, using a number of in vitro assays, that would otherwise be extremely difficult to conduct on the murine models described previously. HD derivatives were prepared with heterobifunctional cross-linkers according to the protocol described. Equal quantities of mAb labelled either with SMCC (containing a reactive maleimide group) or SATA were reacted together to produce tetravelent HD Ab linked by thioether bonds. The precise orientation of binding is unknown, but samples were analysed by HPLC and SDS-PAGE to confirm dimerisation had occurred. Fig.7.3.1 shows that a proportion of mAb remained as unreacted monomeric IgG (M). HD derivatives appeared as a peak corresponding to approximately 300 kDa (HD). Other larger fractions were also observed at 450 kDa and greater (Trimers +) representing trimeric or aggregated IgG. Samples were crudely purified using gel filtration and the 300 kDa HD fraction selected for use in all subsequent experiments. SDS-PAGE analysis was performed to confirm we had purified the HD successfully (Fig.7.3.1.inset).

A panel of HD derivatives was constructed, targeting CD19, CD20, CD22, CD38 (a type II trans-membrane glycoprotein expressed at early stages of B-cell development), and CD40.

7.3.2 Growth inhibition by HD

The growth inhibitory activities of dimerised Ab as compared to monomeric IgG were compared using [^{3}H]thymidine incorporation as a measure of cell proliferation. Fig.7.3.2 shows the level of growth inhibition observed following 24 hours incubation of the anti-CD40 derivative with the Daudi, Raji and EHRB cell lines. In all cases the HD, but not the monomeric anti-CD40, was able to substantially inhibit growth. The derivative was extremely effective against the Daudi and Raji cell lines, but less effective against EHRB. HD of other specificity (anti-CD19, anti-CD20, anti-CD22, and anti-CD38) were then tested for inhibitory activity against the named cell lines. Fig. 7.3.3 shows the results obtained following culture of Daudi cells for 24 hours with the HD derivatives (150 μg/ml). All HD derivatives produced a marked decrease in cellular proliferation as compared to cells incubated with medium alone (untreated) (= 100 %). There seemed little difference in effect with relation to antigen specificity, with all HD providing similar levels of growth inhibition. Again, monomeric IgG was not effective at inhibiting growth. However, a control derivative, the non-binding anti-saporin HD was also able to induce some degree of growth inhibition.

Similar observations were recorded for Raji cells incubated with the same panel of monomeric and HD IgG (Fig.7.3.4). However, growth inhibitory properties were slightly less potent against this cell line than against the Daudi lymphoma line. All derivatives mediated similar levels of inhibition, with approximately 5 fold less growth observed for cells in the presence of HD, as compared to monomeric IgG, or medium alone (untreated). Some slight growth inhibition was again observed with the control anti-saporin HD.

Further analysis was conducted against the EHRB cell line (Fig.7.3.5). Again, the monomeric Ab did not have a growth inhibitory effect, whereas HD derivatives were able to induce some inhibition of growth (approximately 40 % [^{3}H] incorporation compared to untreated cells). Against EHRB the non-binding anti-saporin HD did not induce growth inhibition.

To determine the importance of Fc to the growth inhibitory effects of the HD derivatives an anti-CD40 F(ab')$_2$ HD was produced. Due to the limited stocks of the derivative, the F(ab')$_2$ HD could only be tested for growth inhibition against the Daudi and Raji cell lines. Fig.7.3.6 shows that even in the absence of Fc, HD anti- F(ab')$_2$ CD40 is able to substantially inhibit the growth of tumor cell lines *in vitro*. Moreover, the level of growth inhibition was approaching that observed with the HD intact IgG.

7.3.3 ADCC and complement activation by HD

Next we examined whether homodimerisation led to increased Ab activity, in terms of ADCC or complement mediated lysis of the lymphoma lines. Due to the difficulty in labelling certain of the human lymphoma lines with chromium, meaningful data was only obtainable for the Daudi and Raji cell lines. Firstly the ability of HD to enhance ADCC and complement lysis of Daudi cells was examined. For ADCC activity, cells were incubated with HD or monomer (10 – 0.1 μg/ml) in the presence of human effector cells, freshly isolated from blood, at an effector to target ratio of 50:1. Fig.7.3.7 shows that dimerisation does not enhance ADCC activity, with the level of tumor lysis achieved varying only on the basis of Ab specificity. Ab to CD38 and CD20 proved most potent at triggering cell lysis in this system, with approximately 30 % specific chromium-release at the highest Ab concentration (10 μg/ml). Ab to CD19 and CD40 gave around 20 % specific activity at this concentration, whilst Ab to CD22 were the least effective (10 % specific release). The control, anti-saporin HD was non-functional in this assay.

Complement lysis of target cells was estimated using fresh human serum diluted 1/5 with RPMI as a source of complement. ^{51}Cr labelled cells were incubated with Ab (20 μg/ml

to 0.01 μg/ml) and serum at 37^{0}C for 45 mins, and the degree of complement lysis calculated from specific chromium-release. Fig.7.3.8 shows that Ab to CD20 proved most potent at fixing complement, in-keeping with previous observations in the laboratory. Even as monomeric IgG, 90 % specific chromium-release was observed (20 μg/ml Ab). The HD derivative was as effective at the highest Ab concentration, and more active than the monomer at lower concentrations (1, 0.1 μg/ml). Whilst little or no lysis was observed with monomeric Ab to CD19, CD22, CD38 or CD40, HD to CD38 and CD40 were able to mediate some complement lysis. Ab to CD40 showed the greatest increase in activity following dimerisation, achieving nearly 20 % specific activity. Lysis mediated by HD was antigen specific, as the control HD failed to induce complement attack.

ADCC and complement activity was also investigated against the Raji cell line. Fig.7.3.9 shows that Raji cells are relatively insensitive to ADCC as determined by this assay. The anti-CD40 Ab was the most active derivative, but still only gave approximately 10 % specific chromium-release. Again, dimerisation did not lead to any enhancement in ADCC, and if anything, appeared to decrease the activity of the anti-CD40 Ab.

HD mediated complement lysis of Raji targets was also determined. Here, to further test the potency of HD derivatives at inducing complement mediated cell death, a variant of the Raji cell line lacking the complement protection molecules CD55 and CD59 was also used as a target (Gift from Paul Morgan, Cardiff). HD to the wild type Raji (Fig.7.3.10) were effective at inducing complement lysis, with CD20 proving the most suitable antigen, as before. Both HD and monomer performed to the same level, giving roughly 60 % specific activity at 20 μg/ml Ab. However, dimerisation was able to increase the activity of Ab to CD40. The level of specific chromium-release increased from below 10 % (monomer) to over 30 % (HD) at the highest Ab concentration. Again, lysis was antigen specific as the non-binding HD failed to induce complement lysis.

Against the mutant Raji cell line, lacking complement protection molecules, the HD proved extremely potent mediators of complement attack (Fig.7.3.10). HD to CD20 and

CD40 were again superior to Ab of other specificity. In particular, the efficacy of the anti-CD40 HD was increased dramatically, rising from around 40 % to nearly 100 % specific activity, at the highest Ab concentration. Indeed, HD anti-CD40 proved as effective at mediating complement lysis of the mutant Raji as the anti-CD20 Ab, typically the most active Ab in such assays. The anti-CD38 HD also showed a small increase in activity (around 15 % ^{51}Cr release), whilst the non-binding, control HD was ineffective.

7.3.4 The ability of HD to induce cell cycle arrest and apoptosis

Next, the ability of HD derivatives to induce cell cycle arrest and apoptosis was examined. Cell cycle analysis of lymphoma lines incubated with monomeric or HD Ab was performed using PI staining of cellular DNA. Fig.7.3.11 shows an example of the profiles obtained using Raji cells treated with anti-CD40 and anti-CD22 HD (which respectively, proved most potent at inducing CCA and apoptosis in this cell line). Raji show a distinct increase in cells in the G2/M phase of the CC by 48 hours, when cultured with HD, and undergo increased apoptosis by 72 hours. The degree of growth arrest and apoptosis observed for all three cell lines was analysed, and the results given in tabulated form, as follows.

Firstly, Daudi cells were co-cultured with monomeric or HD Ab at a final concentration of 150 μg/ml, and cell cycle analysis performed after 24 hours. Cells incubated with monomeric IgG showed no change in cell cycle status compared to untreated controls. However, a proportion of those cells incubated with HD derivatives became arrested in the G1 phase of the cell cycle (Table.7.3.1). The most effective HD was the anti-CD40 derivative, which increased the percentage of cells in G1 from approximately 40 % (untreated cells, or those incubated with monomeric anti-CD40) to 56.9 %. The control HD derivative did not increase the percentage of cells in G1, indicating that the observed arrest was related to specific antigen binding. There was no increase in the percentage of arrested cells at later time points (48 and 72 hours) (data not shown).

Similar studies were performed on the second Burkitt's lymphoma cell line, Raji. Again differences in the cell cycle were observed following incubation with HD as opposed to monomeric IgG. However, whereas Daudi cells showed an increase in the G1 phase of the cycle, Raji cells seemed to arrest in the G2/M phase (Table.7.3.2). Moreover, onset of arrest was not evident until cells had been cultured with the HD derivatives for 48 hours. Approximately 43 % of the population of untreated cells, or those cultured with monomeric mAb, were observed to be cycling through the G2/M phase after 48 hours. Raji cells cultured with HD showed around 50 – 60 % of the population in the G2/M phase, again with anti-CD40 proving most potent. The control derivative did not induce such changes, and no further increase in the percentage of cells in G2/M was observed by 72 hours (not shown).

The activity of the HD derivatives was also examined against EHRB. However, PI analysis of these cells after 24, and 48 hours culture with either monomeric or HD Ab, revealed no obvious changes in cell cycle status (Table.7.3.3). Shown are the percentage of cells in G1 and G2/M after 24 hours and 48 hours culture to allow direct comparison to the changes observed in the Daudi and Raji cell lines at these time intervals.

Next, we examined whether HD were able to induce apoptosis in the three cell lines tested. Daudi, Raji and EHRB cells were co-cultured with either monomeric or HD Ab at a final concentration of 150 μg/ml for 72 hours and then the percentage of apoptosis determined by Fsc v Ssc analysis. The Daudi cell line appeared extremely sensitive, in particular to both anti-CD40 and anti-CD20 HD (Table.7.3.4). After 72 hours, around 10 % of untreated cells, and only 17 % of those incubated with the control HD were judged to be apoptotic. However, around 42 % and 52 % of cells incubated with anti-CD20 and anti-CD40 HD respectively, were judged to be dead. Incubation with monomeric anti-CD20, anti-CD40 or other Ab specificities resulted in no increase in apoptosis over untreated cells. All HD were able to increase apoptosis to some extent.

Raji cells proved less sensitive to the induction of apoptosis by HD derivatives, although there was a clear increase in cell death at 72 hours as compared to controls, or culturing

with monomeric IgG (Table.7.3.5). Whilst the basal level of apoptosis was lower than for Daudi (around 3 %), culturing with HD increased the percentage of apoptotic cells only to around 10 – 15 %, with the exception of the anti-CD22 HD which was able to induce nearly 25 % apoptosis. Again, monomeric IgG did not induce apoptosis, and neither did the control HD.

Finally, the degree of apoptosis induced in EHRB cells following 72 hours culture with HD was assessed. As shown in Table.7.3.6, there was very little induction of apoptosis by any of the derivatives. Basal levels of cell death were around 7 %, and incubation with either monomeric or HD Ab failed to increase this level of apoptosis in the time frame studied.

7.3.5 Signaling studies

Given that HD derivatives appear potent stimulators of growth arrest and apoptosis against the Daudi cell line, evidence for intracellular signaling was sought. As anti-BCR signaling pathways which produce a similar response (ie. growth arrest/apoptosis) in the cell lines studied involve changes in calcium levels, we looked for evidence of such changes in cells treated with HD.

Cells (1 x 10^7/ml) were loaded with Indo-1-AM, warmed to 37^0C, and monomeric or HD IgG added at a final concentration of 150 μg/ml. Samples were immediately analysed on a FACS Vantage for changes in intracellular calcium flux as determined by the ratio of FL5/FL4 against time (chapter 2). Maximal levels of calcium flux were determined from incubation with ionomycin, a potent calcium ionophore. Incubation with monomeric IgG to CD19, CD20, CD38 or CD40 failed to produce changes in calcium levels (Fig.7.3.12). Similarly, incubation with HD of the same specificity, also failed to induce any changes in intracellular calcium flux.

7.3.6 The *in vivo* activity of HD

Finally, the *in vivo* activity of the HD derivatives was analysed using a human tumor xenograft model in SCID mice. Derivatives were tested in therapeutic trials against the Daudi cell line, which represented the most consistent xenograft model at that time. Groups of four age and sex matched SCID mice were inoculated i.v with $5x10^6$ freshly harvested Daudi cells during log phase of growth. Animals were then treated with control (200 µl PBS), monomeric or HD Ab (100 µg/mouse), i.v, day 7. Survival was monitored daily thereafter, with the terminal endpoint being paralysis of the hind-quarters. Fig.7.3.13 shows the level of protection obtained with the anti-CD19 and anti-CD38 monomers and HD. Ab to CD19, either as a monomer or as a HD, was unable to extend survival over PBS controls by more than a couple of days. However, the anti-CD38 Ab functioned considerably better. The monomer gave a median survival time of 40 days, and the HD 51 days, with one LTS. The level of protection was greater still with Ab to CD40. Fig.7.3.14 shows that monomeric anti-CD40 Ab gave long-term protection to over 75 % of treated animals, and the HD derivative conferred slightly better protection, with 100 % LTS.

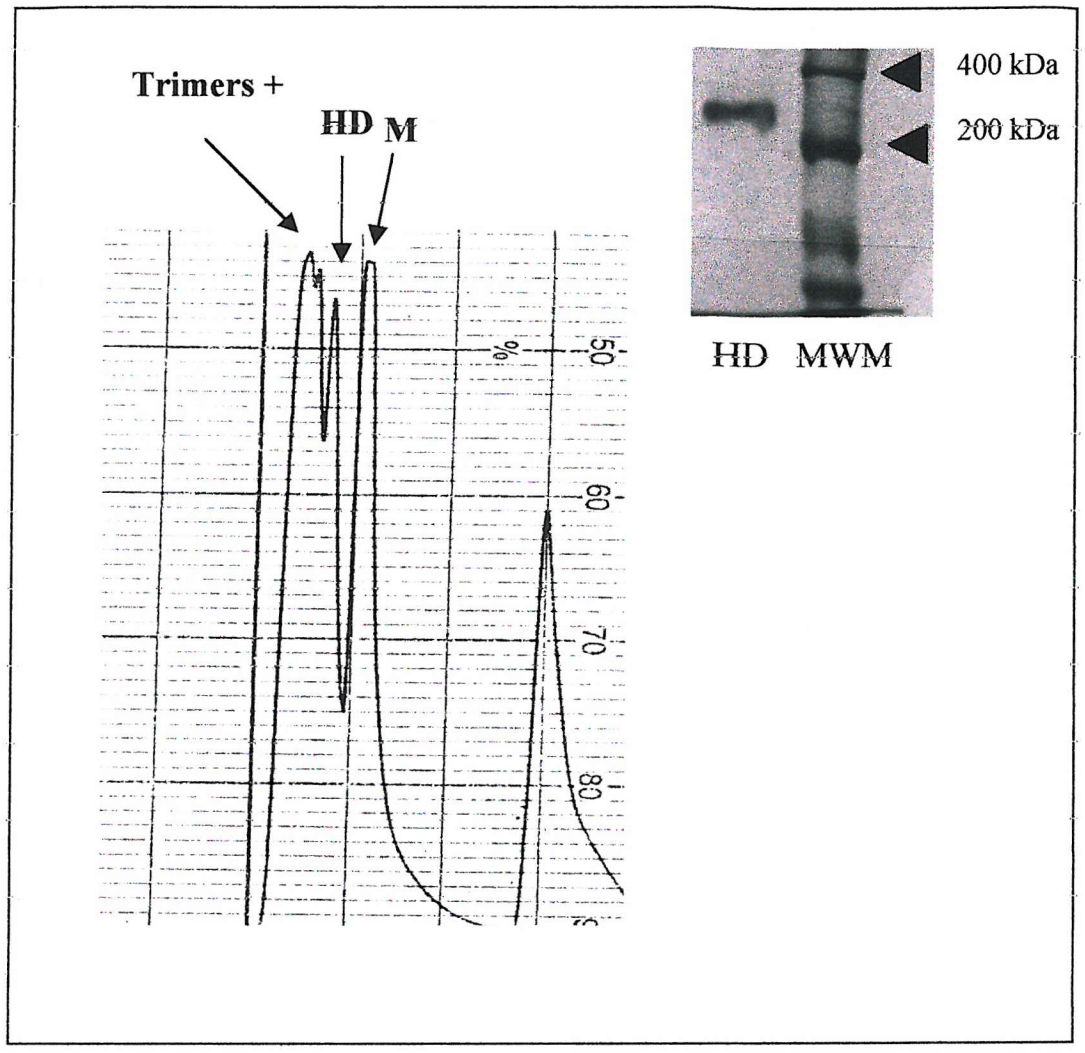

Fig.7.3.1 Production of homodimer derivatives. Homodimers were prepared as described, and dimerisation confirmed by HPLC analysis. A proportion of Ab remains as unreacted IgG (M). The coupling reaction produced both dimerised IgG (HD) as well as larger aggregates of trimers and greater (Trimers +). Following purification, dimers were analysed by SDS-PAGE to confirm purity (inset).

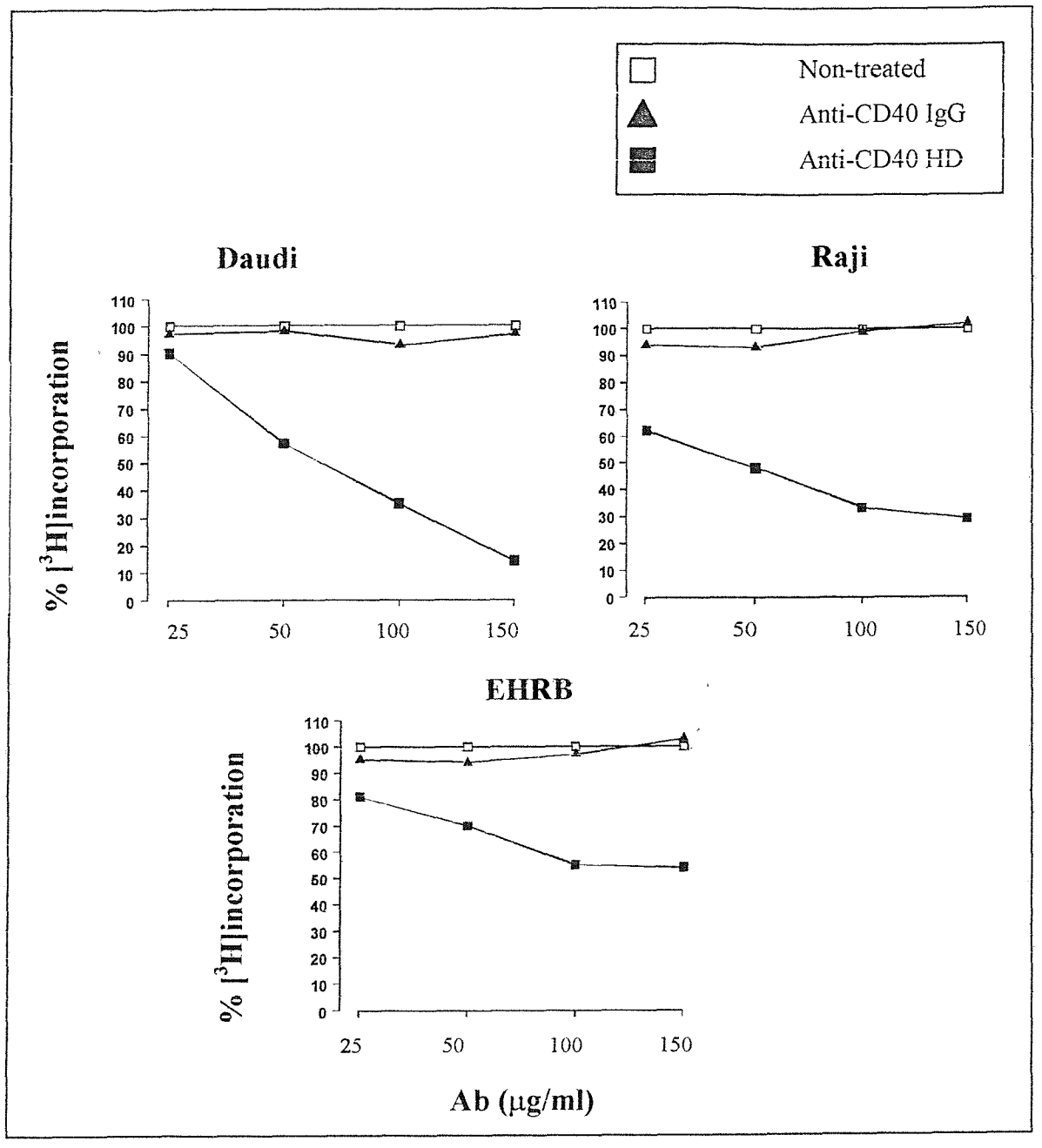

Fig.7.3.2 Anti-CD40 HD mediated growth arrest of Daudi, Raji, and EHRB. Cells (1x 10^6/ml) were cultured with monomeric or HD anti-CD40 IgG (concentrations as shown) for 24 hours. Cells were then pulsed for a further 16 hours with [^{3}H]thymidine (0.5 μCi/well). The DNA-incorporated radioactivity was then determined from 1 min counts on a β-counter. All determinants were performed in triplicate. Shown is the percentage of growth inhibition as compared to untreated cells (□) for those receiving monomeric anti-CD40 (▲) or HD anti-CD40 (■).

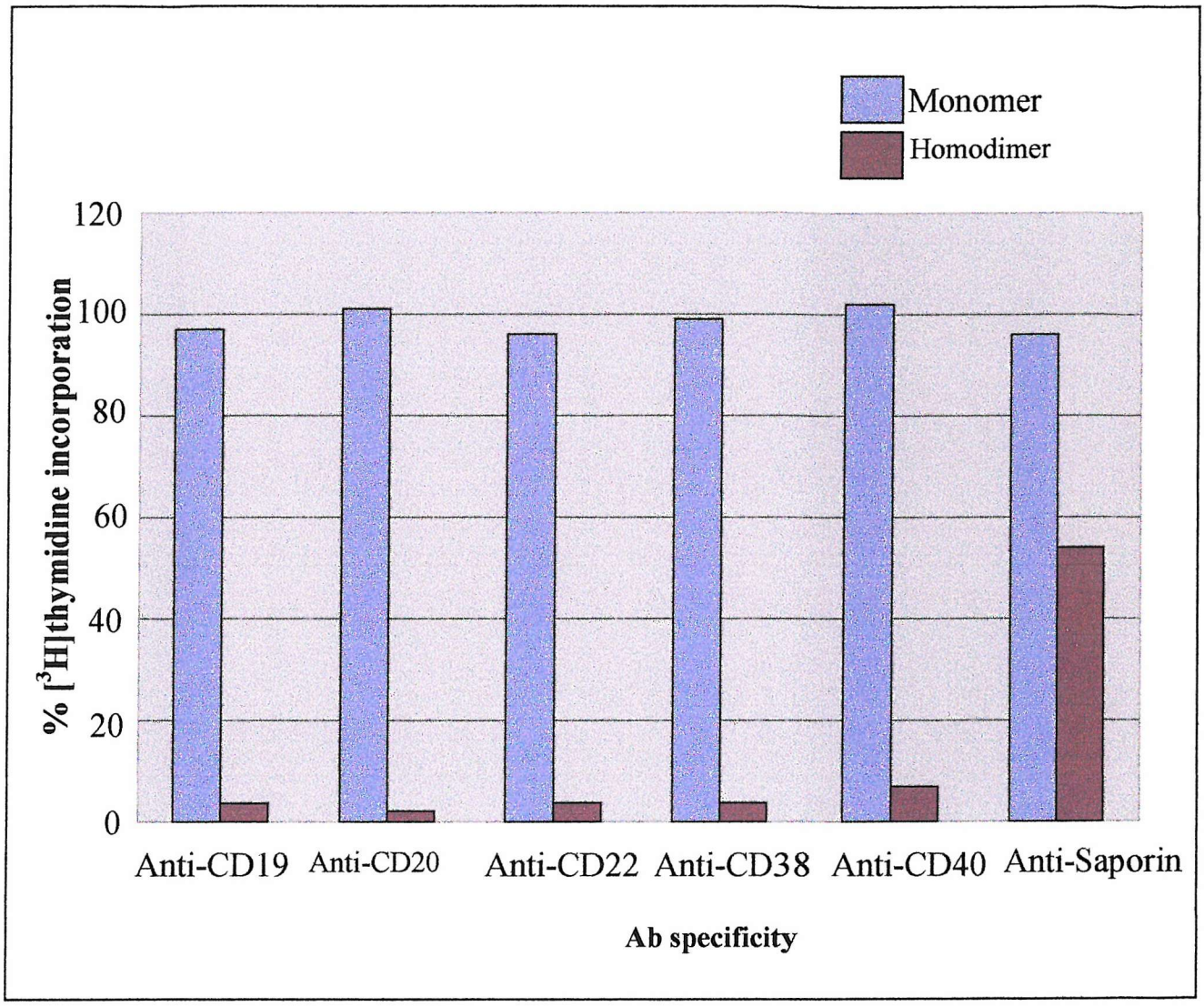

Fig.7.3.3 Growth inhibitory effects of HD on Daudi cells. Daudi tumor cells (1 x 10^6/ml) were cultured with monomeric or HD Ab (150 μg/ml) for 24 hours. Cells were then pulsed with [^{3}H]thymidine for a further 16 hours. Growth inhibition was calculated from the percentage of [^{3}H]thymidine incorporation in treated samples compared to untreated cells. All determinants were performed in triplicate. Ab specificity was as shown above. The non-binding, anti-saporin HD was used as a control.

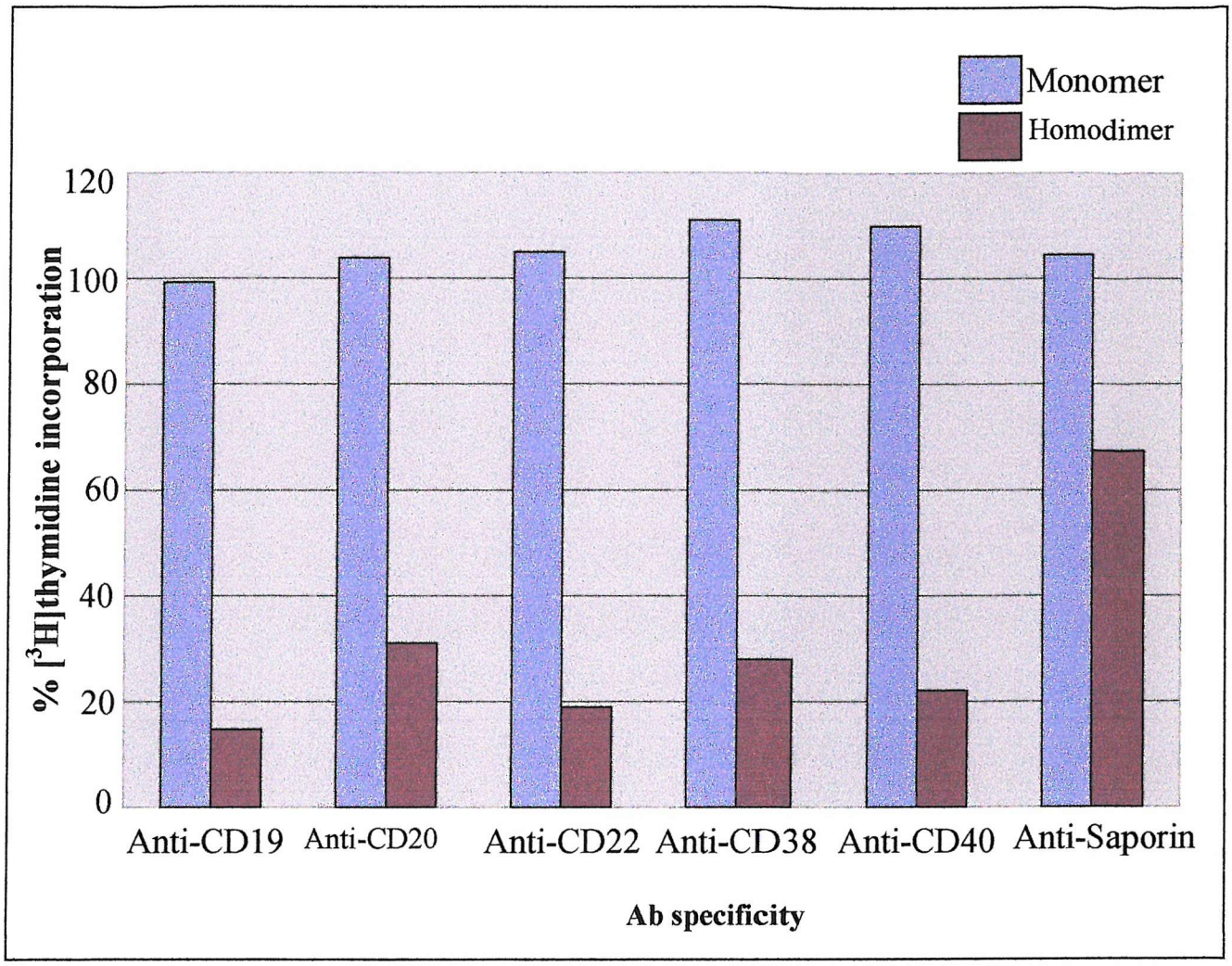

Fig.7.3.4 Growth inhibitory effects of HD on Raji cells. Raji tumor cells (1 x 10^6/ml) were cultured with monomeric or HD Ab (150 μg/ml) for 24 hours. Cells were then pulsed with [^{3}H]thymidine for a further 16 hours. Growth inhibition was calculated from the percentage of [^{3}H]thymidine incorporation in treated samples compared to untreated cells. All determinants were performed in triplicate. Ab specificity was as shown above. The non-binding, anti-saporin HD was used as a control.

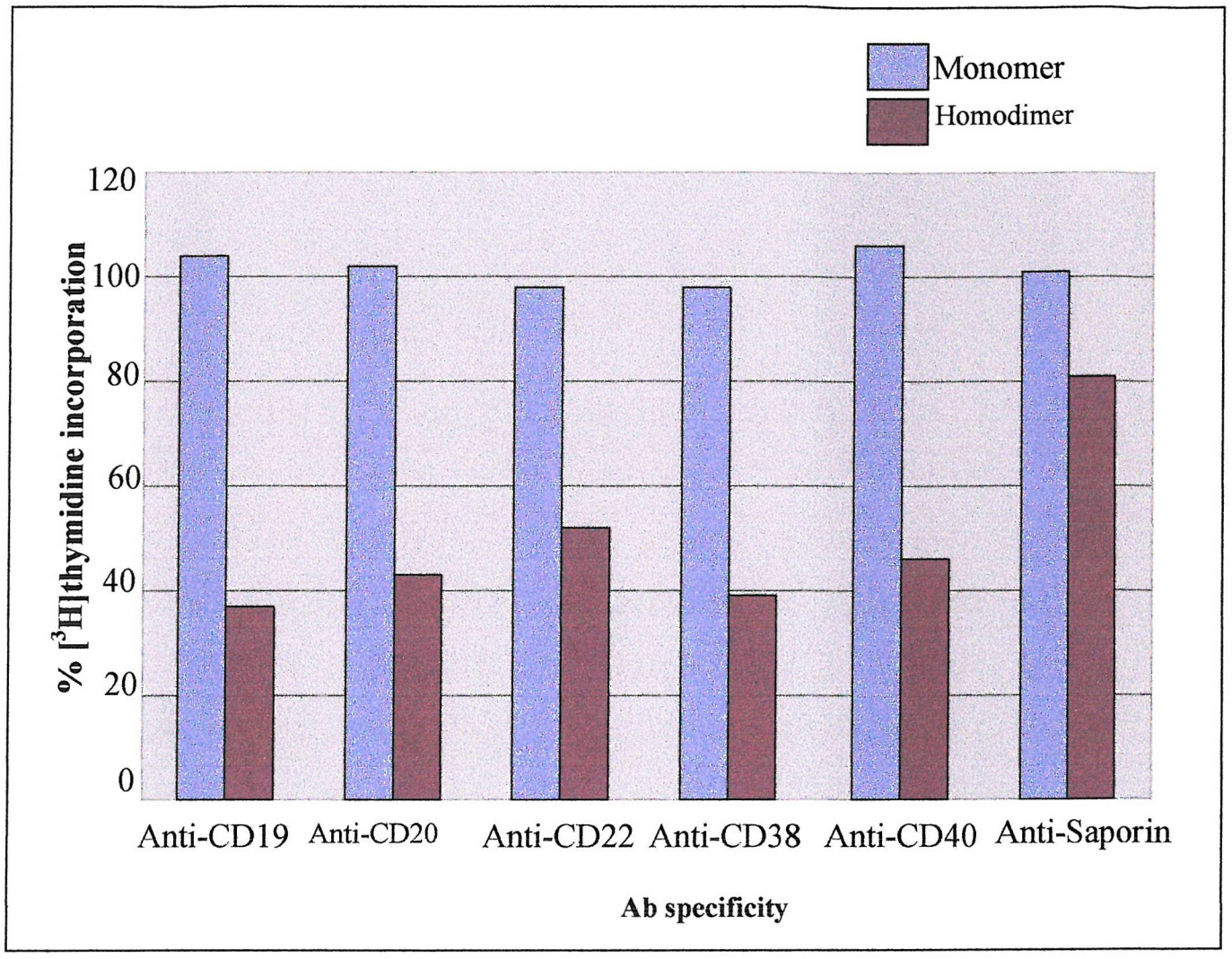

Fig.7.3.5 Growth inhibitory effects of HD on EHRB cells. EHRB tumor cells (1 x 10^6/ml) were cultured with monomeric or HD Ab (150 μg/ml) for 24 hours. Cells were then pulsed with [^{3}H]thymidine for a further 16 hours. Growth inhibition was calculated from the percentage of [^{3}H]thymidine incorporation in treated samples compared to untreated cells. All determinants were performed in triplicate. Ab specificity was as shown above. The non-binding, anti-saporin HD was used as a control.

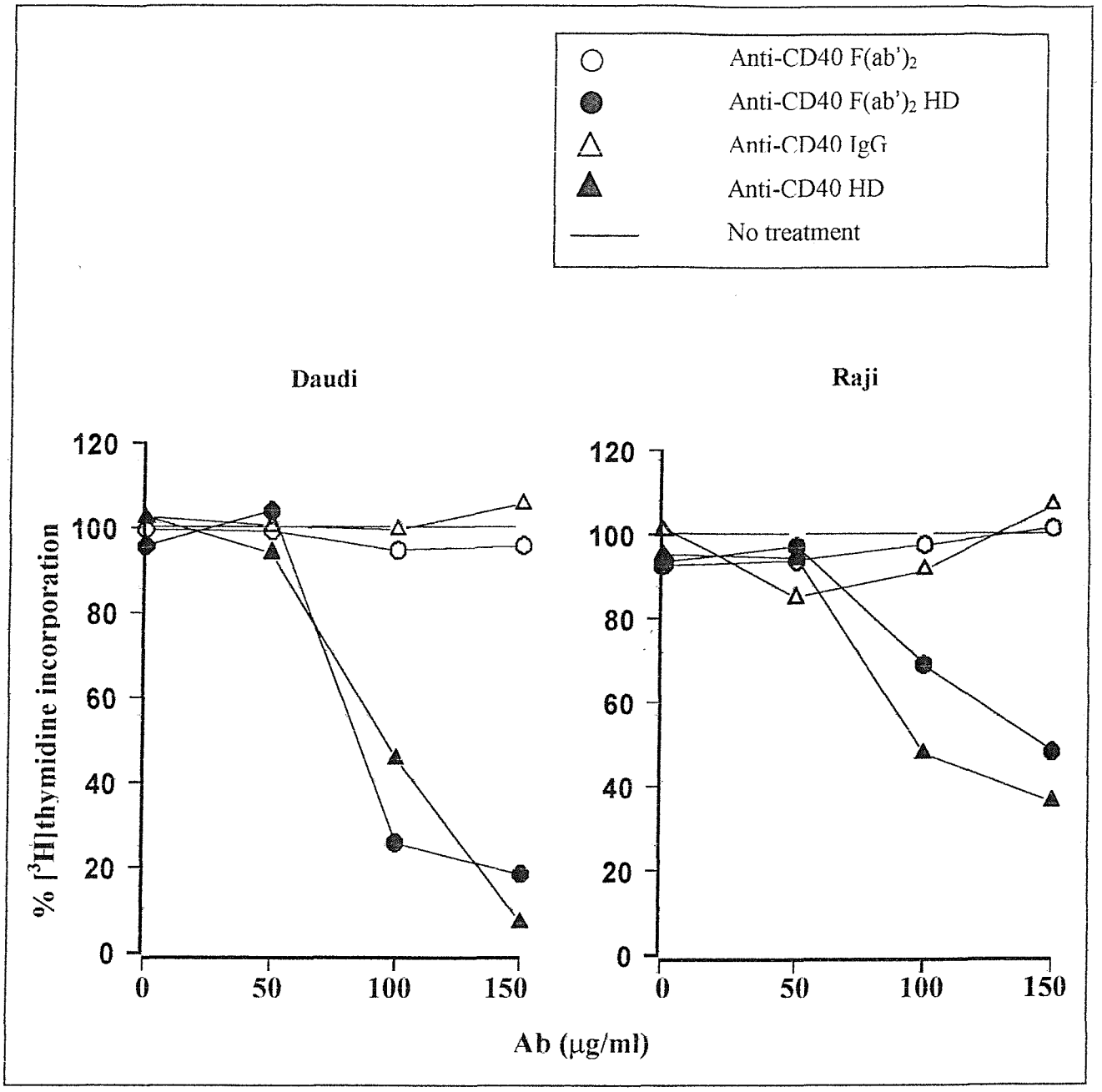

Fig.7.3.6 Growth inhibitory effects of anti-CD40 F(ab')$_2$ HD. Daudi and Raji tumor cells (1 x 10^6/ml) were cultured with monomeric or HD anti-CD40 IgG or F(ab')$_2$ (at concentrations shown) for 24 hours. Cells were then pulsed with [^{3}H]thymidine for a further 16 hours. Growth inhibition was calculated from the percentage of [^{3}H]thymidine incorporation in treated samples compared to untreated cells. All determinants were performed in triplicate.

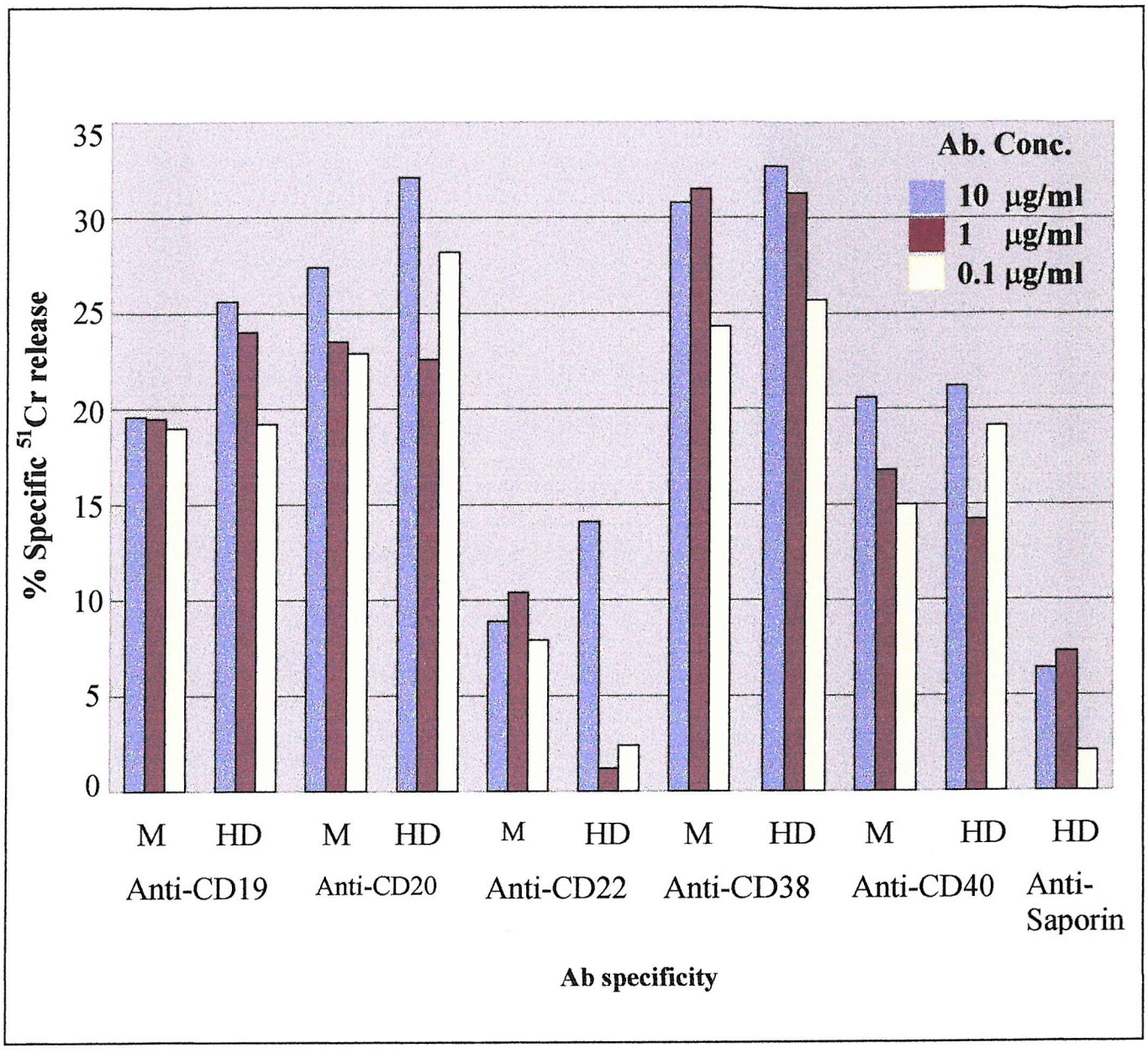

Fig.7.3.7 HD mediated ADCC of Daudi cells. Daudi cells (5 x 10^3/well) were incubated with monomeric or HD Ab in the presence of human effector cells, prepared from whole blood samples, at a ratio of 50:1, for 4 hours at 37^0C. Percent specific Cr^{51} release was then calculated, with maximum release determined from samples to which 1% Nonidet P-40 had been added. All determinants were performed in triplicate. The non-binding, anti-Saporin HD was used as a control.

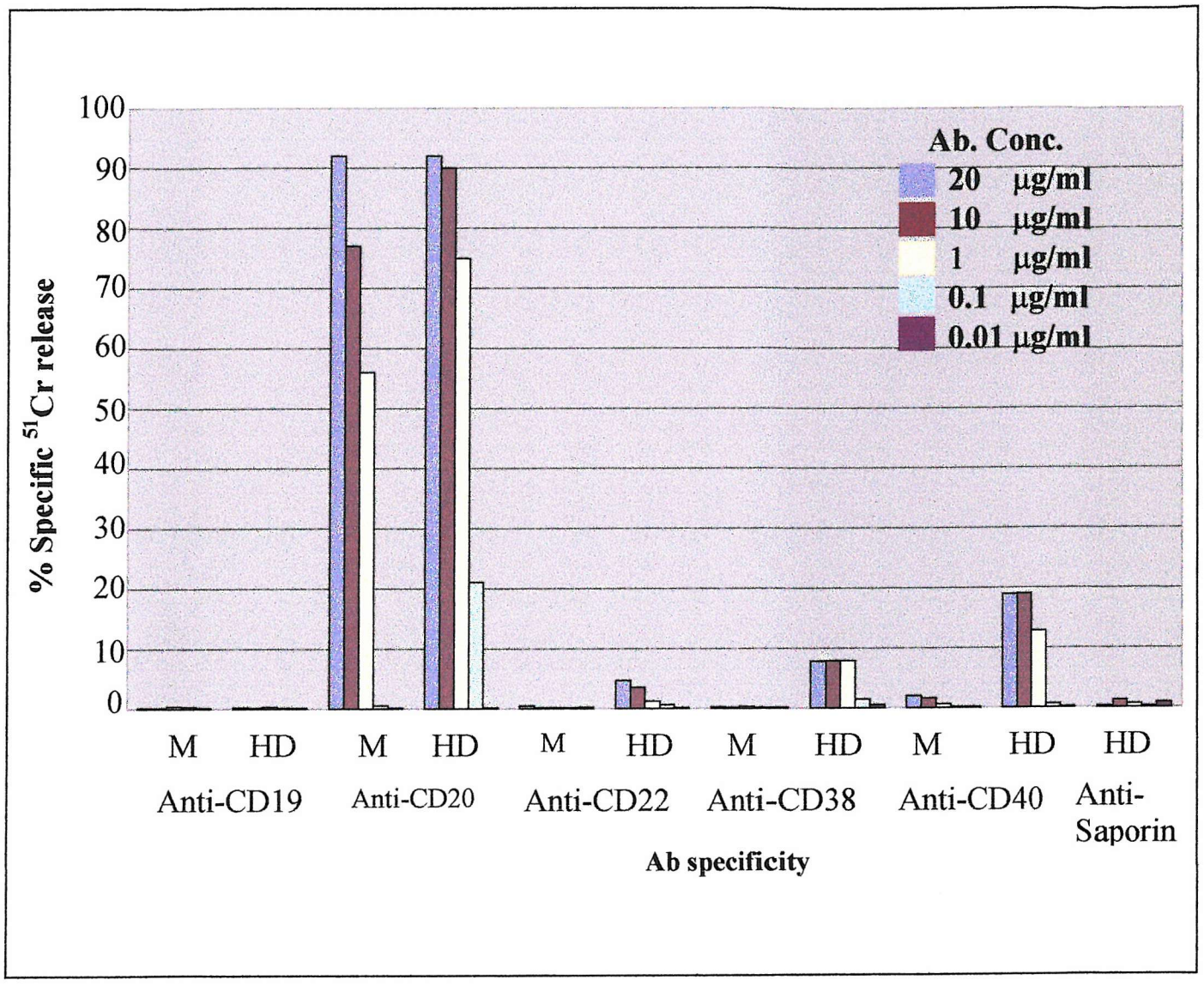

Fig.7.3.8 Complement lysis of Daudi cells. ^{51}Cr labelled Daudi cells (1 x 10^5), were mixed with monomeric or HD Ab in the presence of human serum (final dilution 1/5 with RPMI), at 37^0C for 45 min. Complement lysis was determined from the percentage specific ^{51}Cr release. Ab specificities were as above. The non-binding, anti-saporin HD was used as a control. Shown is the mean of triplicate samples.

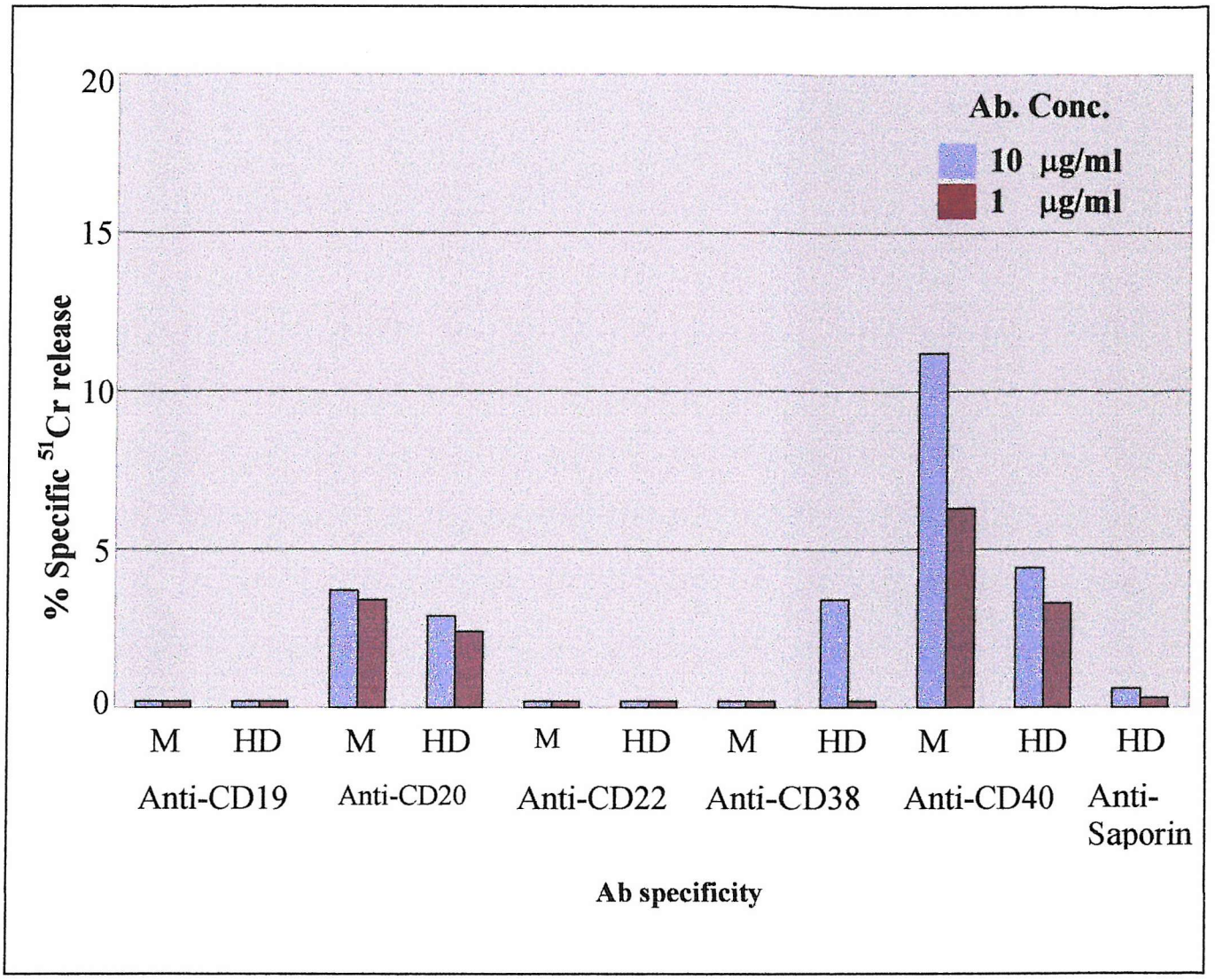

Fig.7.3.9 HD mediated ADCC of Raji cells. Raji cells (5 x 10^3/well) were incubated with monomeric or HD Ab in the presence of human effector cells, prepared from whole blood samples, at a ratio of 50:1, for 4 hours at 37^0C. Percent specific Cr^{51} release was then calculated, with maximum release determined from samples to which 1% Nonidet P-40 had been added. All determinants were performed in triplicate. The non-binding, anti-Saporin HD was used as a control.

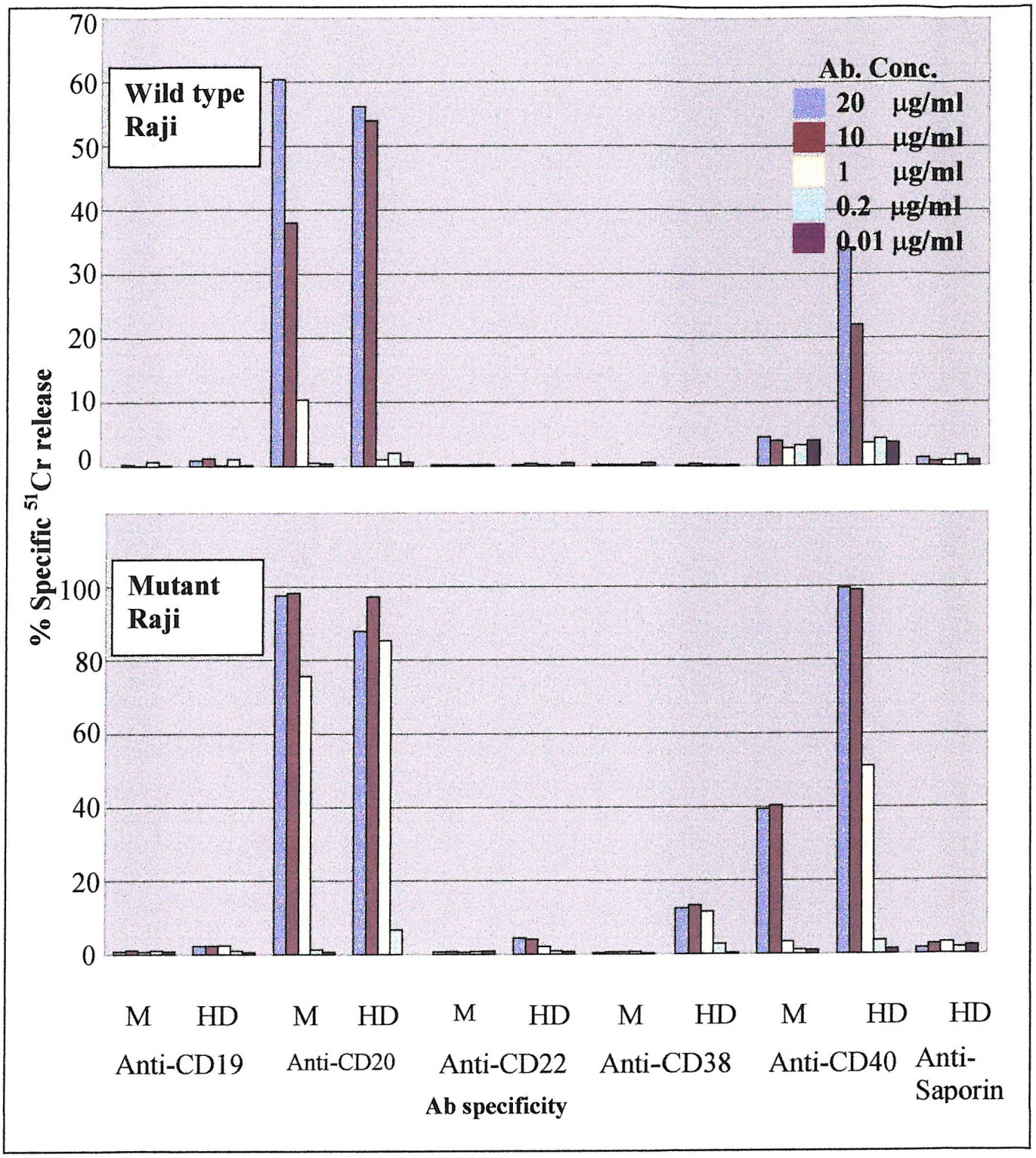

Fig.7.3.10 Complement lysis of Raji cells. ^{51}Cr labelled wild type or mutant Raji cells (lacking complement protection molecules) (1 x 10^5), were mixed with monomeric or HD Ab in the presence of human serum (final dilution 1/5 with RPMI), at 37^{0}C for 45 min. Complement lysis was determined from the percentage specific ^{51}Cr release. Ab specificities were as above. The non-binding, anti-saporin HD was used as a control. Shown is the mean of triplicate samples.

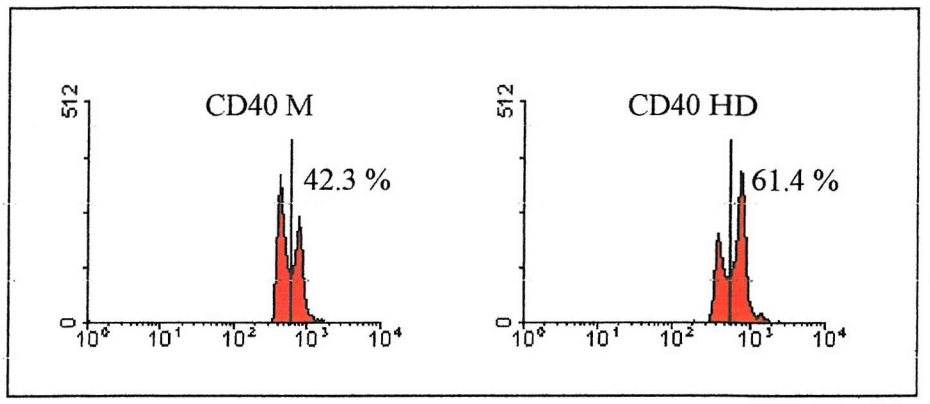

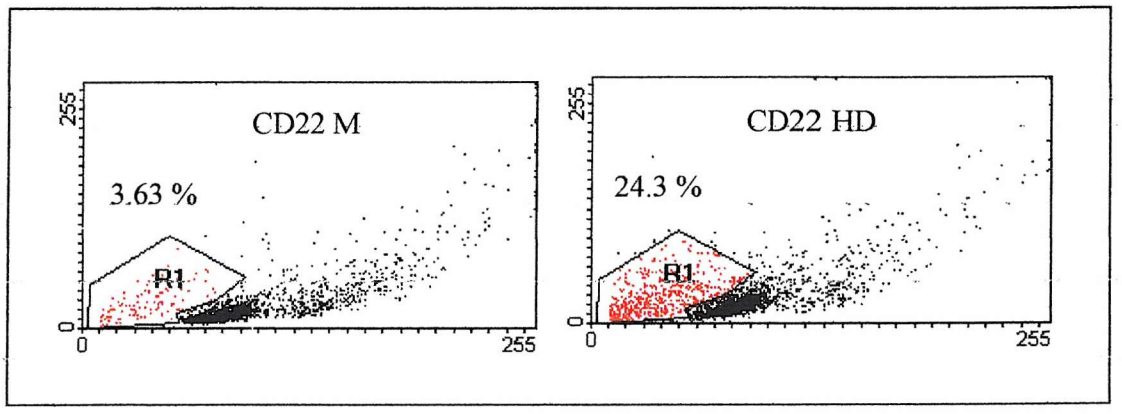

Fig. 7.3.11 Cell cycle status and apoptosis of Raji cells cultured with monomeric or HD anti-CD40 or anti-CD22 Ab. (A) Raji cells (0.5 x 10^6/ well) were cultured with monomeric or (HD) anti-CD40 Ab for 48 hours. Cells were harvested, washed, and labelled with 250 µl of hypo-PI at 4^0C overnight. Samples were then analysed on a FACScan, and the percentage of cells in each division of the cell cycle calculated. There is a clear increase in the percentage of cells in G2/M when cultured with HD Ab. The percentage of cells in G2/M phase from cells cultured with monmeric IgG is equivalent to that for untreated cells (not shown). **(B)** The percentage of dead or apoptotic cells following treatment with dimerised Ab was also determined. Shown is the typical scatter profile obtained for cells cultured with the anti-CD22 monomer or HD for 72 hours, showing a clear increase in the percentage of dead cells in the presence of the HD derivative (gated region). Again monomeric IgG did not increase the level of apoptosis over untreated cells (not shown).

Treatment		% Cells in G1
Untreated		39.66
Anti-saporin	M	41.65
	HD	47.39
Anti-CD19	M	40.28
	HD	49.54
Anti-CD20	M	39.60
	HD	47.50
Anti-CD22	M	36.01
	HD	50.38
Anti-CD38	M	41.98
	HD	54.02
Anti-CD40	M	37.86
	HD	56.91

Table 7.3.1 Cell cycle analysis of Daudi cells cultured with monomeric or HD Ab. Daudi cells (0.5 x 10^6/ well) were cultured with monomeric (M) or homodimerised (HD) Ab for 24 hours. Cells were harvested, washed, and labelled with 250 µl of hypo-PI at 4^0C overnight. Samples were then analysed on a FACScan, and the percentage of cells in each division of the cell cycle calculated. Shown are the percentage of cells in G1 at 24 hours.

Treatment		% Cells in G2/M
Untreated		43.50
Anti-Saporin	M	44.69
	HD	47.21
Anti-CD19	M	43.91
	HD	51.70
Anti-CD20	M	42.71
	HD	54.30
Anti-CD22	M	37.60
	HD	58.17
Anti-CD38	M	40.96
	HD	59.06
Anti-CD40	M	42.39
	HD	61.43

Table 7.3.2 Cell cycle analysis of Raji cells cultured with monomeric or HD Ab. Raji cells (0.5 x 10^6/ well) were cultured with monomeric (M) or homodimerised (HD) Ab for 48 hours. Cells were harvested, washed, and labelled with 250 µl of hypo-PI at 4^0C overnight. Samples were then analysed on a FACScan, and the percentage of cells in each division of the cell cycle calculated. Shown are the percentage of cells in G2/M at 48 hours.

Treatment		% Cells in G1 (24 hours)	% Cells in G2/M (48 hours)
Untreated		43.60	38.67
Anti-Saporin	M	45.96	37.03
	HD	48.11	38.19
Anti-CD19	M	47.57	37.63
	HD	48.62	39.24
Anti-CD20	M	43.93	38.02
	HD	43.12	37.39
Anti-CD22	M	43.89	37.48
	HD	47.38	37.33
Anti-CD38	M	42.88	38.14
	HD	43.58	40.24
Anti-CD40	M	46.16	33.58
	HD	46.92	36.72

Table 7.3.3 Cell cycle analysis of EHRB cells cultured with monomeric or HD Ab.
EHRB cells (0.5 x 10^6/ well) were cultured with monomeric (M) or homodimerised (HD) Ab for 48 hours. Cells were harvested, washed, and labelled with 250 µl of hypo-PI at 4^0C overnight. Samples were then analysed on a FACScan, and the percentage of cells in each division of the cell cycle calculated. Shown are the percentage of cells in G1 at 24 hours, and G2/M at 48 hours to allow direct comparison with the CC profiles of Daudi and Raji cells at these time-points.

Treatment		% Dead/ Apoptotic cells
Untreated		9.4
Anti-saporin	M	11.4
	HD	17.2
Anti-CD19	M	10.1
	HD	38.6
Anti-CD20	M	8.3
	HD	42.7
Anti-CD22	M	8.2
	HD	39.3
Anti-CD38	M	9.3
	HD	27.1
Anti-CD40	M	8.8
	HD	52.7

Table 7.3.4 Analysis of cell death in Daudi cells cultured with monomeric or HD Ab. Daudi cells (0.5 x 10^6/ well) were cultured with monomeric (M) or homodimerised (HD) Ab for 72 hours. Cells were then harvested, washed, and analysed on a FACScan. Fsc/Ssc analysis was performed to determine the relative percentage of dead or apoptotic cells. Shown are the percentage of dead cells following 72 hours incubation.

Treatment		% Dead/ Apoptotic cells
Untreated		3.28
Anti-saporin	M	3.76
	HD	5.99
Anti-CD19	M	2.64
	HD	14.36
Anti-CD20	M	2.64
	HD	9.92
Anti-CD22	M	3.63
	HD	24.36
Anti-CD38	M	3.88
	HD	9.64
Anti-CD40	M	2.84
	HD	10.48

Table 7.3.5 Analysis of cell death in Raji cells cultured with monomeric or HD Ab. Raji cells (0.5 x 10^6/ well) were cultured with monomeric (M) or homodimerised (HD) Ab for 72 hours. Cells were then harvested, washed, and analysed on a FACScan. Fsc/Ssc analysis was performed to determine the relative percentage of dead or apoptotic cells. Shown are the percentage of dead cells following 72 hours incubation.

Treatment		% Dead/ Apoptotic cells
Untreated		4.3
Anti-saporin	M	3.7
	HD	5.8
Anti-CD19	M	6.0
	HD	6.5
Anti-CD20	M	4.5
	HD	6.0
Anti-CD22	M	4.9
	HD	7.1
Anti-CD38	M	4.6
	HD	5.4
Anti-CD40	M	3.9
	HD	6.9

Table 7.3.6 Analysis of cell death in EHRB cells cultured with monomeric or HD Ab. EHRB cells (0.5 x 10^6/ well) were cultured with monomeric (M) or homodimerised (HD) Ab for 72 hours. Cells were then harvested, washed, and analysed on a FACScan. Fsc/Ssc analysis was performed to determine the relative percentage of dead or apoptotic cells. Shown are the percentage of dead cells following 72 hours incubation.

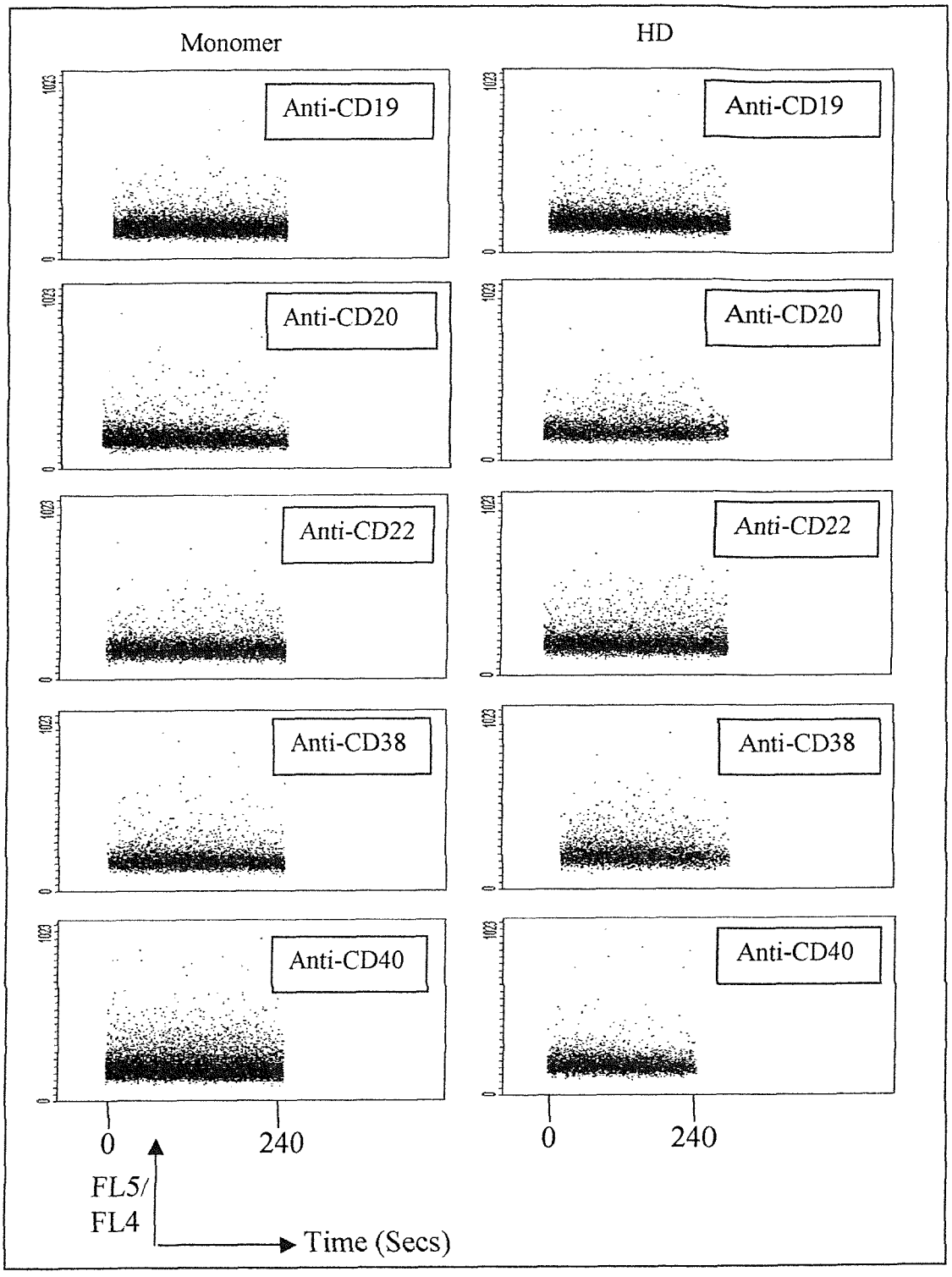

Fig.7.3.12 HD mediated calcium flux. Daudi cells (1 x 10^7/ml) were loaded with Indo-1-AM, warmed to 37^0C, incubated with monomeric or HD Ab (150 μg/ml) and immediately analysed on a FACS Vantage. Calcium flux was measured as the change in FL5/FL4 against time. Ab specificity was as indicated above.

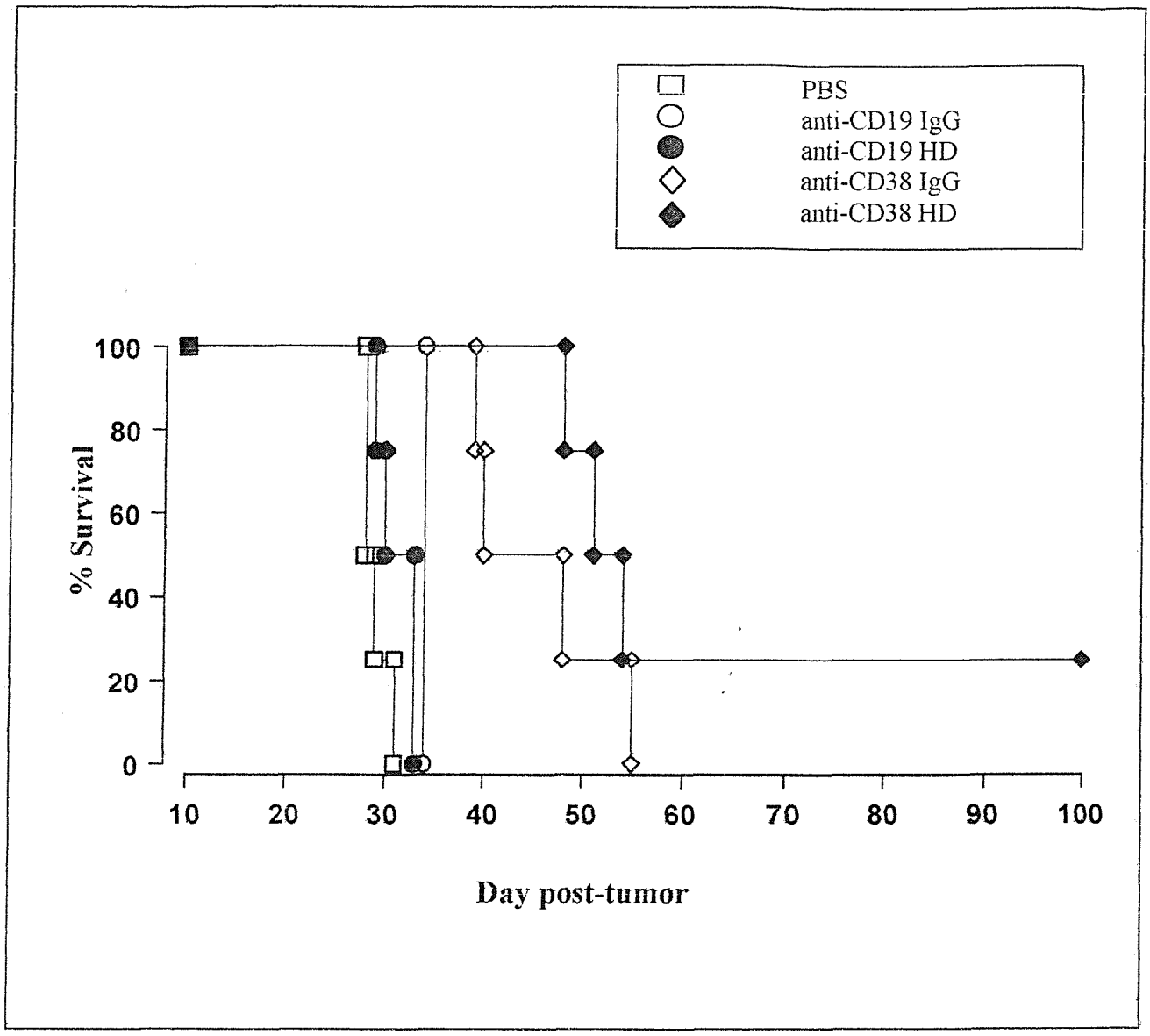

Fig.7.3.13 Anti-CD19 and CD38 HD therapy. Groups of four age and sex matched SCID mice were inoculated with 5 x 10^6 Daudi cells, i.v, day 0. Mice were then treated with either monomeric IgG or HD, 100 μg, i.v, day 7. Control animals received 200 μl PBS. Survival was recorded daily. Shown are the survival curves for animals receiving: PBS (□); anti-CD19 IgG (○); anti-CD19 HD (●); anti-CD38 IgG (◇); or anti-CD38 HD (◆).

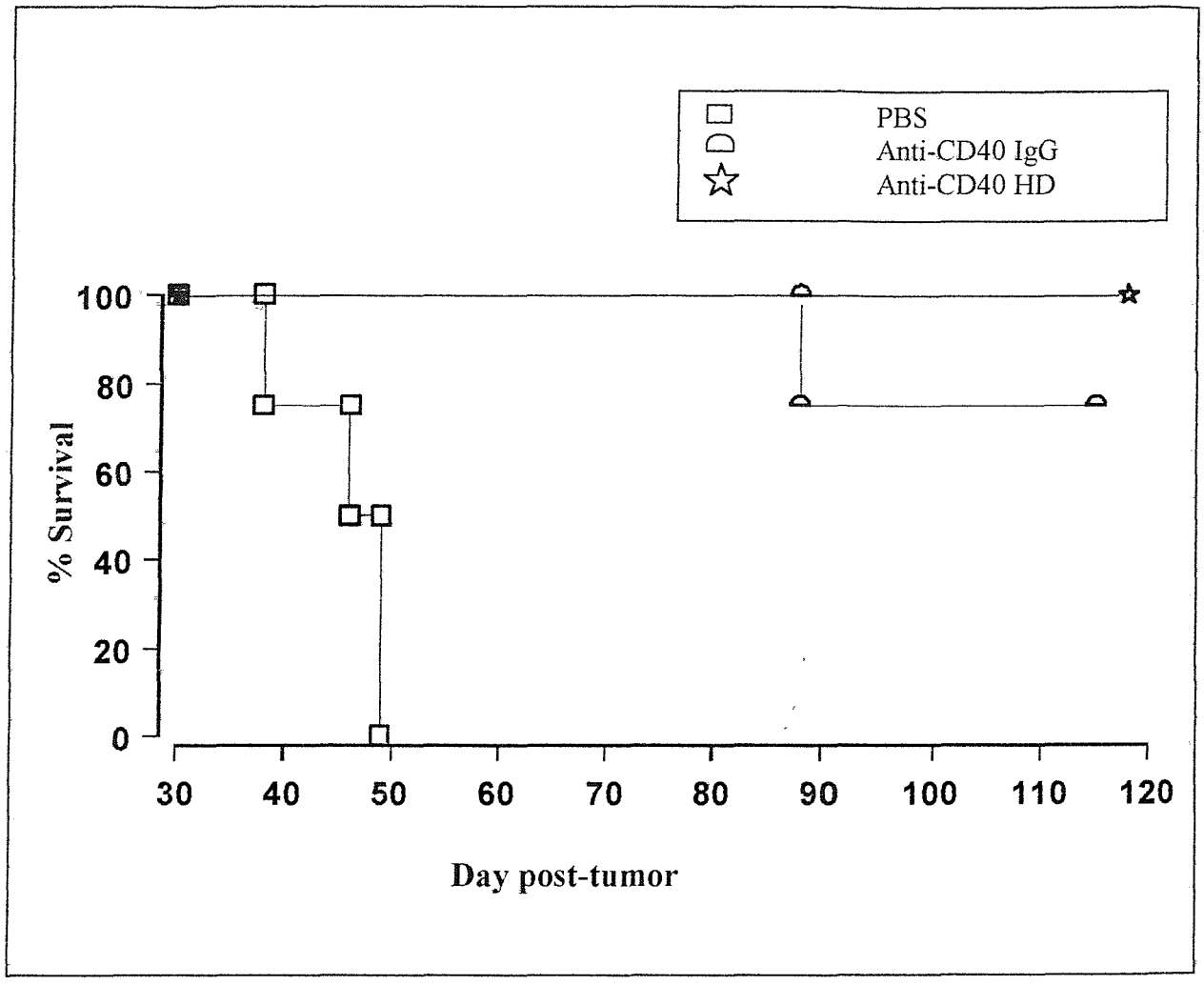

Fig.7.3.14 Anti-CD40 HD therapy. Groups of four age and sex matched SCID mice were inoculated with $5x10^6$ Daudi cells, i.v, day 0. Mice were then treated with either anti-CD40 IgG or anti-CD40 HD, 100μg, i.v, day 7. Control animals received 200μl PBS. Survival was recorded daily. Shown are the survival curves for animals receiving: PBS (□); anti-CD40 IgG (⌓); or anti-CD40 HD (☆).

7.4 Discussion

This chapter describes the production and activity of tetravalent, chemically cross-linked IgG HD. Such HD appear to display enhanced *in vitro* activity and function *in vivo* to clear tumor from inoculated animals. This activity is believed to account for the effectiveness of Ab therapeutic only at relatively high doses, through a small fraction of spontaneously formed HD molecules (227). These constitute only a relatively small proportion of the total Ig dose. By chemically synthesising HD derivatives we hoped to enhance activity of mAb that do not typically display anti-tumor properties. Due to the requirement for extensive *in vitro* analysis, and a lack of murine lymphoma culture lines, human Burkitt's lymphoma cell lines were chosen as a test model.

A panel of mAb which typically show no growth inhibitory effects against the Daudi, Raji and EHRB cell lines tested (personal communication; Dr Mark Cragg), were dimerised, and their subsequent anti-tumor activity analysed. These include IF5 (anti-CD20), AT13/5 (anti-CD38), HD37 (anti-CD19), and LOB7/6 (anti-CD40).

The HD constructs did display a capacity to inhibit the growth of Daudi, Raji and EHRB cell lines as determined by [^{3}H]thymidine incorporation assays. However, induction of growth inhibition required a relatively high concentration of HD (150 μg/ml). This is in contrast to the amount of Ab required to inhibit growth when we consider a conventional signaling Ab such as anti-μ (258), but does fit in with observations made by Ghetie et al (227). The requirement for such high Ab concentrations in order to elicit anti-growth effects, may well be related to the random nature of the chemical linkage process employed in the production of HD. It is probable that only a percentage of the engineered construct is active, and thus high doses are required to elicit a response. It is possible that HD produced by other methods, for example genetic engineering, may prove active at lower doses if more precise means of coupling are utilised.

HD derivatives displayed little enhanced activity in terms of ADCC but were potent activators of complement mediated tumor lysis. Complement activity was greatest with

HD to CD20 and CD40. Whilst the anti-CD20 mAb has previously been described as being extremely effective at triggering complement lysis (265), complement lysis with the anti-CD40 mAb (LOB7/6; IgG2a) has not been observed before. Not only does dimerisation increase the activity of previously unreactive mAb, but for those mAb, such as anti-CD20, which have been reported effective at triggering complement lysis in their native monomeric form, dimerisation resulted in enhanced activity generating higher levels of tumor lysis at lower Ab titres. This is most likely related to the role that the two (potentially juxtaposed) Fc regions play in this process. Greenman et al. (266) have previously demonstrated that the presence of two Fc tails in bisFabFc derivatives does not enhance levels of ADCC over a single Fc containing FabFc molecule. In contrast, Stevenson et al. (267) have demonstrated that bisFabFc molecules have a clear advantage in terms of complement based lysis of tumor cells over FabFc derivatives. This enhanced activity is most likely a representation of the increased numbers and juxtaposition of Fc regions. Thus, observations with the HD derivatives mirror those described for the bisFabFc/ FabFc derivatives – and is likewise, most probably a representation of the additional Fc region present in the HD as opposed to the monomeric IgG.

At suitably high levels HD do clearly induce an anti-growth response, the mechanism behind which appears to be in part related to cell cycle arrest and an increase in apoptosis. The nature of the arrest appears to vary between cell lines, with Daudi cells arresting in G1 and Raji cells arresting in the G2/M transition. Similar observations have been made by Ghetie et al. (227). Apoptosis, as demonstrated by the simple method of Fsc v Ssc analysis (with cells shrinking and condensing showing a reduced Fsc profile and increased Ssc profile respectively), is also increased in all cell lines studied. Confirmation of apoptosis at the time points examined was not readily detectable by PI staining (not shown). However, as cell shrinkage events are a primary event in apoptosis, and scatter changes are usually detectable before DNA fragmentation, this may not be too surprising. As changes in scatter are a reliable predictor of apoptosis, frequently giving identical levels of cell death as PI staining when the techniques are done in parallel (personal communication; Dr Mark Cragg) we can assume that the changes in scatter observed here are a genuine read out of cell death. Analysis at later time intervals (eg. 96

hours) may well allow detection of apoptosis by techniques such as PI staining, and remain to be done.

Despite potent growth inhibitory properties, the mechanism by which this activity is communicated remains unsolved. During classical signaling events observed following BCR ligation, the primary pathways involved operate through tyrosine phosphorylation which are necessary for the induction of growth inhibitory signals (268). Downstream consequences of tyrosine phosphorylation include release of IP_3 and calcium mobilisation. It is these changes in calcium levels that induce cellular responses such as growth inhibition (269). We therefore looked for such changes in cells following HD treatment. However, no increase in intracellular calcium levels were detectable. This may well be a reflection of the sensitivity of the cell lines used to the assays employed, or alternatively that HD constructs signaling does not involve calcium changes. Some preliminary studies looking at changes in tyrosine phosphorylation were also conducted with the anti-CD40 HD, but again no differences between the monomer, HD and untreated cells were observed (data not shown)

Interestingly, the activity of our HD constructs correlates with the known level of FcγR expressed on the cell lines, as determined by flow cytometric analysis using mAb AT10-FITC which recognises human FcγRII (data not shown). The growth inhibitory effects of the HD could in part be related to Fc cross-linking, which would help to explain the activity of the non-tumor binding, anti-saporin Ab. This did indeed display higher activity against the Raji and Daudi cell lines (which have relatively high levels of FcγR expression), and virtually no activity against the EHRB cell line (which has only low levels of FcγR). However, production of an anti-CD40 $F(ab')_2$ HD derivative demonstrated that even in the absence of Fc, HD derivatives are capable of substantial growth inhibition, suggesting that whilst Fc binding may contribute to these effects, it can not in itself, account for the effects observed.

The efficacy of our derivatives *in vivo* was also examined using a SCID xenograft model. Results indicate that at doses of 100 μg/animal, the constructs are able to provide significant protection. However, levels of protection did not appear greater than those observed with native mAb. Whilst HD have been shown to display a decreased serum half-life as compared to monomeric IgG of similar isotype (270), this does not appear to affect their activity in the SCID mice. We believe the efficacy of these mAb in the xenograft model to be in part due to the increased potency of cellular effector mechanisms such as ADCC and complement in this system, due for example, to the absence of serum Ig in SCID animals. Hence, it has proved difficult to resolve differences between HD and monomers *in vivo*, even by lowering the dose of treatment. However, it is clear that HD are highly effective at eradicating tumor from mice.

Whilst the primary mechanism involved in the action of HD appears to be growth inhibition and cell death the signaling pathways responsible for these events remain elusive. However, these data indicate that *in vitro* at least, the activity of mAb can be greatly increased through dimerisation, such that previously unresponsive Ab acquire anti-tumor properties. The action of these derivatives is retained *in vivo* and is not lost through disassociation of the two Ab molecules. HD have already proven effective against tumor (227) and bacteria (271), and as such, HD derivatives may offer an alternative therapeutic reagent in the treatment of lymphoma.

Chapter 8

General discussion and future aims

8.1 General overview and discussion

The use of Ab as a therapeutic modality in the treatment of cancer is becoming increasingly more popular. The precise specificity of mAb, coupled with the ability to produce them in almost limitless quantities (3) makes them attractive tools for immunotherapy. Following on from extensive *in vitro* and animal modelling studies, numerous clinical trials are now being established, and recent success with anti-CD20 and anti-CD52 mAb, amongst others, has revitalised the field (59, 60 and reviewed in 2). However, despite such successes, much of the cytotoxicity seen *in vitro* is not being translated in to clinical efficacy. An alternative to mAb based therapy, and one that is also gaining in recognition, is the use of BsAb. Such derivatives display dual specificity for both a tumor antigen and a cytotoxic trigger molecule on an immune effector species providing an intimate association between the two, thus, in theory, increasing cross-reactivity and tumor destruction (5). A range of candidate trigger molecules on effector cells (such as CD3 and CD16) have been examined closely, and several phase I and II clinical trials set up (86). BsAb targeting HER2/neu, a breast carcinoma antigen, and the FcγRI on PMN have proved especially promising. However, optimisation not only of the most appropriate effector molecules, but also of the most effective tumor antigen, and the relative contribution these two make to tumor regression, still requires much investigation. Moreover, whilst extensive *in vitro* studies have been conducted, little attention has been focused on *in vivo* animal trials, presumably due to the lack of suitable models. The aim of this work was to address this point in particular, and examine which tumor antigen(s) prove most suitable targets for therapy.

Here, we describe the application of BsAb in retargeting cellular effector mechanisms against two murine B cell lymphoma lines A31 and BCL_1 (219, 220). Two models have been employed. First, retargeting of autologous T cells via CD3 and CD2 antigens, and secondly, the retargeting of muG-CSF primed PMN via human FcγRI in a transgenic mouse model. In light of these findings, homodimerised IgG constructs

were also generated, to assess the potential for increasing direct anti-proliferative signals to tumor.

As T cell immunity has been shown to play a key role in controlling abnormal B cell proliferation, and T cells are known to have intimate associations with B cells during development and immune responses, they prove an attractive target for immunotherapy (83). Moreover, BsAb targeting T cells to tumor have already proved effective both *in vitro* and to some extent, *in vivo* (103, 105, 254). We examined the relative efficacy of retargeting T cells to a range of tumor associated antigens including tumor-Id, MHC II, CD19 and CD22. The ability of BsAb to effectively destroy tumor when targeted to these molecules was assesssed both *in vitro* and *in vivo*. A number of important points arose from our work. Firstly, somewhat surprisingly, the *in vitro* cytotoxicity of a derivative does not reflect its potential *in vivo*. Typically, BsAb directed against MHC II elicited the highest levels of RCC *in vitro* against both A31 and BCL_1 as determined by chromium-release assays. Other derivatives to CD19, Id and CD22 showed increasingly less effectiveness. The phenotype of the BCL_1 and A31 tumor models have been extensively characterised, and tumor antigen expression analysed by radio-labelling studies (231). Both tumor lines show similar levels of expression of these molecules, which have been identified for each antigen as approximately (in descending order): MHC II (1-2 x 10^5/cell): Id (9 x 10^4/cell); CD22 (6 x 10^4/cell): CD19 (4 x 10^4/cell); and CD40 (4 x 10^4/cell). Likewise, the capacity for antigenic modulation has also been assessed in this laboratory, and can be clearly ranked in the order (highest tendency first): CD22>Id>CD19>MHC II. Whilst BsAb performance weakly correlates to antigen density, it is the factor of modulation that seems most strongly influential. Hence, BsAb that target densely expressed, low modulating antigens (such as MHC II), generally are more effective in short-term cultured cytotoxicity assays than those targeting weakly expressed, highly modulating antigens (such as CD22). This observation holds true not only for T cell targeting BsAb (chapter 3), but also to those directed gainst FcγRI (chapter 4).

Here, BsAb to human FcγRI were used to retarget G-CSF primed transgenic murine PMN against the two lymphoma lines. Previous studies have shown FcγRI to be a

potent trigger molecule for ADCC on G-CSF primed PMN, demonstrating high levels of tumor lysis when targeted by mAb against MHC II molecules, but not other antigens (246). Others have further demonstrated that BsAb targeting MHC II are also highly effective *in vitro* (245). In light of these observations, one may expect an [FcγRI x MHC II] BsAb, applied in combination with G-CSF, to be especially therapeutic. Our studies indicate that *in vitro*, using isolated PMN as effectors in ADCC and RCC assays, MHC II does indeed prove, once again, to be the most suitable target for tumor lysis (chapter 4). However, where as antigen restricted killing was observed with PMN targeted by mAb, BsAb of all specificity were able to mediate some degree of tumor lysis, albeit at far lower levels than that observed with the [FcγRI x MHC II] BsAb. Killing was specifically triggered by FcγRI on PMN as effectors from non-transgenic mice (primed or unprimed), and unprimed receptor positive PMN, failed to lyse tumor in the presence of appropriate Ab.

Taken at face value, these observations indicate that MHC II may be the most suitable target antigen for BsAb therapy in these models, especially when targeted to FcγRI. This assumption is made on the basis that RCC is an important mechanism for tumor therapy. That processes of RCC and ADCC are important Ab effector mechanisms in immunotherapy has long been assumed. Studies have indicated a strong correlation between Ab isotype and *in vivo* activity, with those sub-classes most capable of triggering cytotoxic mechanisms eradicating tumor in animals. Moreover, isotype switch studies confirmed these beliefs, which were further substantiated by clinical data, whereby mAb of an appropriate isotype to engage human effector cell functions proved particularly efficacious at inducing remission (38, 39). However, a formal association between the capability of an Ab to trigger ADCC/RCC and its therapeutic efficacy has never been established. Whilst it is known that Fc, and therefore, by default, FcR are important to the therapeutic process, whether this means that ADCC/RCC is important is another issue. To some extent this question has been addressed before with mAb (231). However, we wished to more closely investigate the link between BsAb mediated RCC and therapeutic efficacy using the animal models described here.

A number of therapeutic trials were conducted against both the A31 and BCL_1 lymphoma models, initially with CD3-directed BsAb (chapter 3). An important consideration in therapeutic design is the reduced half-life of $F(ab')_2$ compared to IgG. Serum half-life studies with ^{125}I labelled mAb reveal $F(ab')_2$ to be cleared from circulation approximately 3 times more rapidly than IgG (chapter 3). This clearly has a substantial impact on therapeutic potential of $F(ab')_2$ BsAb when administered as a single dose. However, by increasing the frequency of inoculations we were able to compensate for the reduced circulatory life-span of the derivatives. Indeed, this factor has great bearing not only on the efficacy of derivatives in the animal models, but also on the clinical potential of BsAb.

A standard regime was established for all subsequent therapies, with mice receiving twice daily inoculations of BsAb for 5 days. A very similar profile of activity emerged for both lymphoma lines. BsAb to MHC II, CD19 or CD22 consistently failed to extend survival by more than a few days above that seen with control (PBS treated) groups. However, those derivatives containing an anti-Id Fab arm ([CD3 x Id] and [CD2 x Id]) performed exceptionally, greatly enhancing survival over controls. Consistently, at least 60 % of mice having received BCL_1 or A31 tumor and treated with [CD3 x Id] showed long-term remission, whilst 40 % given BCL_1 and 60 % of those given A31 and treated with [CD2 x Id] also showed LTS. Interestingly, an [Id x MHC II] BsAb with no T cell retargeting properties, also extended survival of treated animals by around 20 days (data not shown). Clearly, this data indicates that tumor antigen specificity is of great importance as only those derivatives targeting Id were able to protect animals from tumor challenge. Protection was not as dependent on the effector antigen targeted, with similar levels of protection observed irrespective of whether CD3 or CD2 was engaged. This, despite CD2 being a relatively poor target in *in vitro* assays.

The activity of the anti-Id BsAb was specifically due to *in vivo* bridging of a T cell to a tumor cell as non-conjugated parental $F(ab')_2$ was not effective at increasing survival. Neither was protection due to the presence of contaminating IgG as 1) BsAb were extensively purified using immunosorption techniques to remove Fc, and 2) anti-Id IgG itself has never been shown to cure either lymphoma line in our hands (231).

Development of the human FcγRI transgenic model (221), also provided an opportunity for assessing the activity of bispecific derivatives *in vivo*. This has been the first major study of the *in vivo* activity of FcγRI targeting BsAb in a fully immunocompetent murine model, and has given rise to a number of important observations (chapter 5).

Once again, the *in vitro* activity of the derivatives did not translate into corresponding *in vivo* activity. This observation was most dramatic for the [FcγRI x MHC II] BsAb, which although clearly the most potent at triggering PMN cytotoxicity *in vitro*, at best produced only around 10 days benefit to survival when used as a therapeutic agent. Similar levels of protection were observed for the anti-CD19 BsAb, which was far less active *in vitro*. Consisitently, the most therapeutically active BsAb were those targeting Id. Animals inoculated with either A31 or BCL_1 lymphoma lines were effectively cured when treated with these derivatives (over 80% entered LTS). Once again, this protection was dependent on effector engagement, as non-transgenic animals, or those without G-CSF priming (and thus with lower levels of receptor, fewer PMN, and with effector cells in a less activated state), were not protected by anti-Id BsAb. Additionally, anti-FcγRI or anti-Id $F(ab')_2$ alone, or as a mixture was not functional – only in a conjugated, bispecific form was protection achieved, demonstrating, as previously observed for T cell BsAb, that effectors and tumor require *in vivo* bridging to gain therapy.

Given that those BsAb that function best in RCC assays do not necessarily perform well *in vivo*, these observations seem to question the role RCC plays in therapy. However, tumor tracking experiments to ascertain the functional activity of BsAb *in vivo* (chapter 6) demonstrate that BsAb of all specificity were able to deplete tumor *in vivo*, at least during initial stages of therapy. This depletion was extremely rapid, occurring within 24 hours of treatment, and cleared over 99 % of tumor load compared to controls. This suggests that RCC is occurring in this system. However, it is insufficient to prevent subsequent development of disease. Only [FcγRI x Id] treated groups remained clear of tumor by day 15, where as all others presented splenic tumor of a similar volume to controls. Again, this initial depletion (with BsAb of all specificity), and subsequent anti-growth activity ([FcγRI x Id]) was specifically

dependent on FcγRI, as BsAb administered to non-transgenic mice in conjunction with muG-CSF failed to have any effect on tumor development.

These findings appear to fall in to direct contradiction with the observation that PMN are only able to lyse tumor through MHC II (246). However, such data was obtained using highly purified PMN in short-term *in vitro* assays. The situation may be very different *in vivo*, as cells other than PMN, for example macrophages, may be contributing to the initial phase of tumor clearance. Moreover, the cytokine milieu and inflammatory mediators present *in vivo* may produce an environment more conducive to killing by PMN, or indeed other phagocytes.

How then, may we explain the potency of the anti-Id BsAb over the other derivatives tested?

We believe that the mechanism of protection is intimately associated with direct signaling to the tumor. The capacity for anti-Id antibodies to induce anti-proliferative responses is well documented, and is believed to function by cross-linking the BCR, thus potentiating intracellular signals (258). BsAb may well employ similar mechanisms to induce their anti-tumor responses. In our system, effector cells drawn to the tumor by the BsAb may well serve to hyper-cross-link the BCR, thus stimulating signaling pathways. As evidence for intracellular signaling, we looked for changes in intracellular calcium levels following receptor ligation. Initially we tried to achieve this using isolated PMN in an attempt to directly simulate what may happen *in vivo*. However, these experiments proved extremely difficult, and so to imitate the association of an effector cell with the BsAb, a secondary Ab was employed to cross-link the anti-FcγRI arm of the derivatives. Under these conditions no change in calcium levels was observed in tumor cells incubated with BsAb alone (chapter 5). However, in the presence of the secondary reagent, a signal was observed with the anti-Id and anti-CD40 BsAb, but not the other derivatives. This data indicate that anti-Id BsAb at least have the potential to generate intracellular signals following cross-linking. Moreover, recent observations by Bast et al. (personal communication) have confirmed these findings using T cells as effectors. Calcium signals were observed in tumor following ligation with [CD3 x Id] BsAb in the presence of T cells. Thus it

appears likely that effector cell cross-linking can indeed signal a response in the B cell. However, whether in this system such signals lead to growth arrest or apoptosis *in vivo* has not been formally proven.

The question arises as to whether anti-Id BsAb targeted to **any** effector cell antigen would be therapeutic, and if not, why not?

Assuming long-term therapy is dependent on signaling, and this signaling is achieved by effector cell cross-linking of BCR, then it follows that any anti-Id BsAb should produce a similar response, providing the second arm of the derivative targets a reasonably highly expressed antigen on a sufficiently large effector population. To test this hypothesis, we have conducted therapy in a second transgenic model, expressing CD89 (FcαRI), with a [CD89 x Id] BsAb. This work was again in collaboration with Jan van de Winkel, and M. van Egmmond. Both the derivative and the transgenic model were produced, and assessed in Utrecht, although therapeutic trials were conducted at Tenovus. Investigations into the nature and role of FcαRI are now coming to fruition, especially following the generation of the transgenic murine model. Receptor expression and cytokine regulation in the transgenic mouse are similar to that in man, and the receptor is able to trigger phagocytosis of both tumor (272) and *Candida albicans* (213) *in vitro*, by PMN targeted with BsAb. Moreover, PMN targeted by the FcαR do not show the same antigen restriction as when targeted through FcγRI (212). In terms of *in vivo* targeting, this receptor has an additional advantage over FcγRI, in that it is constitutively expressed at high levels on circulating PMN, and therefore, does not require G-CSF supplementation. Preliminary experiments were conducted in F1 progeny of BALB/c x FCB/n FcαR positive transgenic mice. Therapy was conducted as before (chapter 4). Mice received muG-CSF (where appropriate) as for the FcγRI therapies (in order to activate and boost PMN numbers), 10^5 BCL_1 cells i.p, day 0, and were treated with anti-Id BsAb or mAb to a total of 50 μg, i.p, over 5 days. The results from the therapy are shown in Fig.8.1. Interestingly, levels of protection were not as great as those seen with either the [FcγRI x Id] or [T cell x Id] BsAb. Only 40 % of animals showed long-term protection over control cohorts. More surprisingly, BsAb only conferred protection in

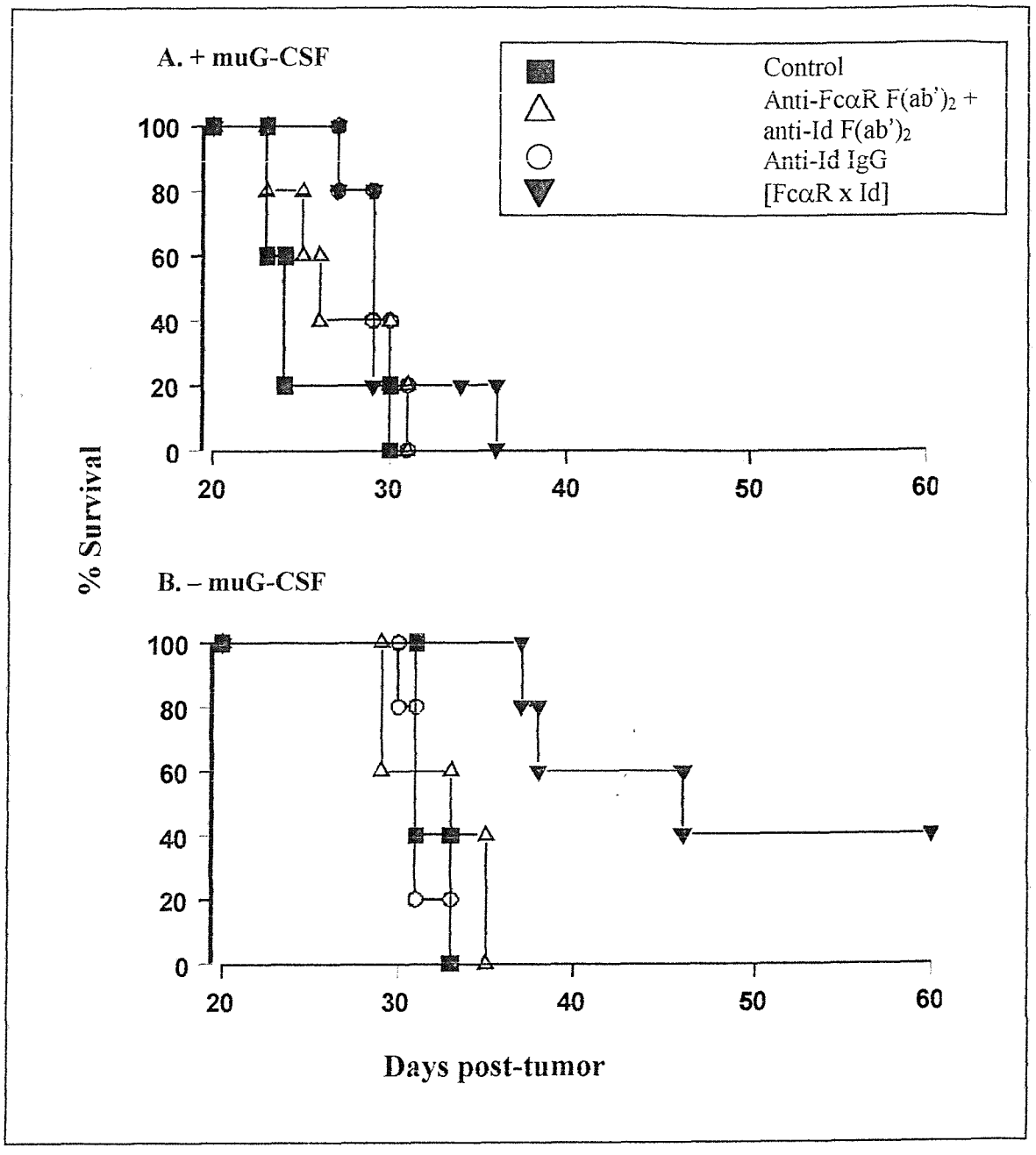

Fig.8.1 FcαR BsAb therapy. Groups of 5 FVB/n x BALB/c FcαR (CD89) positive F1 mice were inoculated with 10^5 BCL_1 tumor cells, i.p, day 0, and were treated with twice daily inoculations of 5μg Ab days 1 – 5 (50 μg total). Mice were either **(A)** primed with muG-CSF, 2 μg per day, s.c, starting day minus 4 through to day 5 or **(B)** left unprimed. Treatment was as follows: PBS (■); anti-FcαR $F(ab')_2$ + anti-Id $F(ab')_2$ (△); anti-Id IgG (○); [FcαR x Id] (▼). Survival was recorded daily.

unprimed animals. Levels of protection with BsAb were however, greater than those with mAb, and were dependent on direct effector to tumor cross-linking as unconjugated $F(ab')_2$ gave no protection.

It does appear that targeting to Id is able to provide protection when a range of different effector molecules are triggered by the second arm of the BsAb. However, certain molecules do seem to provide better targets than others, with FcγRI giving the highest degree of protection, out of those molecules tested. As the numbers of PMN, receptor levels and activation state are identical when targeting this receptor as compared to the FcαR, this indicates that FcγRI may be playing an additional role in the observed therapy (other than triggering cytotoxicity and performing the proposed function of BCR cross-linking).

One such role is participation in the activation of T cells. We have shown by depletion studies (chapter 6), that [FcγRI x Id] therapy is dependent on T cell immunity. How may targeting these two antigens (Id and FcγRI) lead to such a response?

Van Vugt et al. have shown that antigen internalisation via FcγRI leads to enhanced antigen presentation, following targeting to MHC II containing endocytic and lysosomal compartments, and that MHC II loaded with peptide in this fashion is able to stimulate antigen specific T cells (180). Regnault et al. (1998) have also demonstrated that FcγR antigen uptake can increase the efficacy of MHC I restricted antigen presentation (273). In this manner, it is plausible that APC, such as DC, that express a broad range of FcγR, can not only internalise and process antigen via FcγR, but also effectively present peptide to CTL via cross-priming mechanisms. Moreover, DC have been shown to effectively cross-prime apoptosing cells (263), and recent data by Nouri-Shirazi et al. (2000) has demonstrated that DC can capture and present tumor antigens to CTL, thus eliciting a specific anti-tumor response (274). Whilst less efficient cross-presentation by macrophages has also been reported (275) it seems likely that DC are the key regulators of these responses. It is possible therefore, that [FcγRI x Id] cross-links the BCR, thus delivering an apoptotic signal to the tumor, and that apoptosing tumor cells are internalised and processed by DC, possibly via FcγRI, and that peptides presented on MHC I during the process of cross-priming, are able to

induce a tumor specific T cell response. BsAb of other specificity may fail to induce immunity in this manner by simply inducing tumor phagocytosis, and not delivering an appropriate apoptotic signal. The FcαR may also prove a less attractive target than FcγRI, as it is not expressed by DC (212).

Whether the [CD3 x Id] and [CD2 x Id] BsAb also induce immunity is as yet undetermined. It is harder to assess the action of these derivatives, as T cell depletion studies are obviously not appropriate!

By whatever mechanism anti-Id BsAb are operating *in vivo*, it is also clear that they have a greater capacity for stimulation of the immunological processes responsible for tumor erradication than mAb. Evidence for this is most compelling for the anti-BCL_1 Id Ab (chapter 3 and 5). mAb against tumor Id do not provide protection at doses lower than 100 μg, and even at doses of 1 mg/ mouse provide only around days protection over controls. In contrast, BsAb are able to induce LTS with doses as low as 50 μg/mouse.

Further evidence for increased potency of bispecific derivatives comes from the study of tumor dormancy. Anti-Id mAb are able to inhibit proliferation of BCL_1 tumor, but frequently a residual population of dormant cells emerges (239). Frequently, tumor is able to escape from this state and re-grow. However, examination of animals treated with anti-Id bispecific show an absence of dormant populations. So far, none of the anti-Id BsAb treated animals in either the A31 or BCL_1 model have shown tumor re-growth. Direct testing for the presence of dormant cells by passage of splenocytes from cured to naïve animals and FACS analysis has also failed to reveal the presence of dormant tumor in BsAb treated animals (not shown). These findings are in accordance with others (105) and indicate that anti-Id BsAb may be able to eradicate the malignant clone completely.

Recently, French et al. (36) have demonstrated the potency of anti-CD40 mAb, which is highly effective at erradicating tumor and does so in a CD8 dependent fashion. Moreover, these animals are protected from subsequent tumor inoculations. However, somewhat surprisingly, BsAb to CD40 appear less active than anti-CD40 mAb. This

is true both when targeting FcγRI (chapter 5) or T cells (Alison Tutt, unpublished). Why this should be is uncertain. although points to a necessity for the Fc. Production of IgG BsAb, containing intact hybrid Fc regions may thus prove more efficacious.

However BsAb are functioning *in vivo*, whether by induction of effector-mediated cytotoxicity, transmembrane signaling, induction of host immune responses, or a combination of these processes, it is becoming increasingly apparent that target antigen selection is an important factor. Other target molecules on NHL that may prove suitable include CD20 and CD79α and CD79β.

CD20 is a B cell specific molecule, expressed on a range of malignancies. It is expressed at relatively high levels, does not undergo antigenic modulation, and whilst an exact function remains elusive, is believed to be involved in cell signaling and may form part of a calcium channel (276). Whilst ligation of CD20 on human B cells has been shown to induce apoptosis (277), unfortunately a mAb for murine CD20 does not exist. This makes analysis of CD20 as a target for immunotherapy in the syngeneic lymphoma models described, impossible at this time.

Much evidence points to targeting of the BCR as being therapeutically effective. However, whilst anti-Id BsAb are clearly the most efficacious, anti-Id derivatives suffer from being costly to produce, labour intensive, and susceptable to escape by Id-negative tumor variants. Targeting to IgM heavy chain (anti-μ) is not a viable option, due to the presence of high circulating levels of IgM that would sequester any therapeutic Ab away from the primary target. The CD79α and CD79β components of the BCR do not suffer from such problems. These molecules associate with surface Ig, and function as the signaling components of the BCR complex (as discussed in chapter 1). Thus, BsAb to CD79 α or β would be B cell specific, but more importantly, unlike anti-Id derivatives, would not be patient specific. Their function in signaling, which we propse to be critical to therapy, further promotes them as ideal candidates for tumor targeting.

Translating these observations in to a clinical perspective, the therapeutic data in chapters 3, 5 and 6, is highly encouraging. In terms of treating human patients, long-

term remission, whilst remaining the ultimate goal, is not the only realistic objective. An Ab providing partial remission, or significant depletion of tumor, would also be considered a success. Looking at the activity of these BsAb derivatives *in vivo*, especially those directed to FcγRI, a reduction of 99 % tumor load, if translated to the clinic, would be highly desireable. It may be that by extending the course of treatment with BsAb such as the [FcγRI x MHC II], to include repeated "top up" injections (administered in conjunction with muG-CSF), we could limit the growth (or re-growth) of tumor within these animals further still. Hence, although only the anti-Id derivatives gave LTS, the observation that cytokine primed PMN triggered through FcγRI can destroy tumor *in vivo* when targeted to other antigens, is an extremely solid platform off which to build.

Combination therapy with FcγRI BsAb and G-CSF in the clinic is highly feasible, and several extensive trials have been conducted. G-CSF is clinically approved both in the U.S and Europe, and has been demonstrated to be well tolerated, capable of extensive leukocytosis and neutrophilia, easily self-administered (s.c), and has few obvious side-effects. G-CSF has also been shown to increase levels of sialyl-Lewis (x) on PMN, an adhesion molecule for endothelial selectins, thus promoting PMN-endothelial cell interactions and migration (278). Already, BsAb targeting PMN via FcγRI to the breast carcinoma antigen HER2/neu are proving highly effective, as are T cell BsAb directed against ovarian, and other, cancer cells (5).

Once problems both in terms of production (manufacturing sufficient quantities of clinical grade material cost-effectively), and design (to increase half-life and decrease immunogenicity), are overcome, the application of BsAb to the clinic be further improved.

It is clear that BsAb IgG (hybrid-hybridoma derived conjugates), are not suitable for the clinic. Not only is it difficult to produce bulk quantities of pure material, but *in vivo*, such derivatives are considered too bulky for effective biodistribution, induce strong HAMA responses, and high levels of toxicity. Indeed, the presence of Fc that can bind and activate effector cells in the absence of tumor can dramatically reduce

the maximum tolerated dose of BsAb that can be administered to patients, several fold over that recorded for mAb (5).

Instead, $F(ab')_2$ BsAb produced by chemical conjugation, as used in this thesis, are more suitable for human therapy. The absence of Fc drastically reduces levels of non-specific activation and toxicity, and $F(ab')_2$ derivatives show better distribution due to their smaller size. However, production of such derivatives by conventional methods of proteolytic digestion of parental IgG, and subsequent reduction to generate individual F(ab') partners are not sufficiently cost effective for large scale production. A solution to the manufacturing of bulk quantities of pure BsAb required for the clinic lies in recombinant technology. Derivation of F(ab') from bacterial expression systems rather than IgG can greatly improve both yield and purity. Expression in *Escherichia coli* can generate high yields (279), and if such F(ab') fragments are humanised, to further reduce HAMA responses, they can be viable therapeutic tools.

Recent work in the field has concentrated on production of diabodies and single chain Fv fragments (BsscFv) to reduce BsAb size and increase biodistribution. Pre-clinical trials with such derivatives look promising. A [CD3 x Id] BsscFv has been demonstrated to show similar levels of binding and *in vitro* RCC as the equivalent bispecific IgG derivative, and has proven both stable and capable of inducing substantial tumor regression, *in vivo* (229). Likewise, a human [FcγRIII x HER2/neu] BsDb has been demonstrated to remain stable, and efficiently traffic to and remain at the site of tumor, *in vivo* (280). The major problem suffered by such constructs is greatly reduced serum half-life. This factor has been compensated for by increasing the number of inoculations, as in the therapys described in this thesis. However, in the future, alternative methods may become common place.

A key factor relating to catabolism of IgG is the ability to bind FcRn. This receptor originally identified for its role in transport of maternal IgG to the neonate, has since been demonstrated to have a role in maintaining homeostasis of serum IgG levels (118). Binding of IgG to FcRn is dependent on the Cγ2 and Cγ3 domains of the IgFc. Residues within these domains, identified as being important for controlling catabolic rate, and shown to be conserved between IgG of many species, have been mapped to

the known binding site of FcRn (11). Ghetie et al. have further demonstrated that mutagenesis of residues close to the FcRn:Fc interaction site of a recombinant murine Fcγl fragment, led to production of mutants with higher FcRn affinity (281). These mutants also displayed an extended serum half-life. The ability to extend the serum retention time of an Ab has important implications for clinical therapeutic trials. It is feasible that by engineering a "tag" containing those residues important to FcRn binding onto bispecific derivatives, the *in vivo* half-life of small Ab fragments, or $F(ab')_2$ could be extended considerably. In this way, derivatives suitably small enough to penetrate bulk tumor would no longer have to suffer from severely increased catabolism. An extended half-life would presumably require fewer doses of derivative to be given, thus reducing therapeutic costs – an important consideration for clinical application.

Alternative Ab derivatives that may extend therapeutic potential have also been sought. Given the apparent significance of targeting a signaling molecule, we aimed to increase therapeutic efficacy by increasing the signaling ability of mAb (chapter 7). This has previously been linked to homodimerisation of Ab (227). In our system, targeted against human Burkitt's lymphoma cell lines, HD constructs do appear to exert a number of anti-tumor effects, including growth arrest, complement mediated cell death, and apoptosis. Whilst Ab to some of the target antigens, such as CD20, are known to induce signaling, the Ab employed here all showed no activity as monomeric IgG. Hence, they make suitable candidates for examination. Dimerisation of Ab to CD19, CD20, CD22, CD38 and CD40 all improved their capacity to induce growth arrest and cell death.

HD of Ab has previously been shown to increase complement activity against bacteria. Wolff et al. (271) constructed human mAb homodimers specific for bacterial polysaccharides and demonstrated a 20 fold increase in protection against infection in rat models. They attributed this to increased complement activation due to the presence of two Fc regions. We too observed an increase in complement mediated cell death following Ab dimerisation. This was particularly evident for Ab to CD20 and CD40. Whilst the Ab to CD20 has previously been reported to be extremely effective at complement lysis (265), the finding that dimerised anti-CD40 was as potent, was

surprising. However, both mAb are of an appropriate isotype to induce complement fixation, namely mouse IgG2a. We also observed growth arrest and cell death in the presence of HD derivatives. Whilst complement activation has been linked to apoptosis (265) we are confident that such responses here, are not complement mediated. Serum used for cell culture is routinely heat-inactivated, thus removing the possiblility of complement-mediated cell death in culture assays.

Some concern was raised over the growth inhibitory properties of the non-binding, anti-saporin derivative following dimerisation. Whilst it is possible that anti-proliferative activity is semi-artifactual, in that HD simply cross-link Fc receptors, we do not believe this to be the case. This is in view of the observation that $F(ab')_2$ HD are able to function as actively as IgG derivatives (chapter 7). Ghetie et al. have shown similar responses from $F(ab')_2$ homodimers directed against CD19 antigen, indicating specific activity (227). In addition, whilst we observed no growth inhibition with monomeric IgG, others have found this not to be the case. Funakoshi et al. detected a direct anti-proliferative response when treating human cell lines with their anti-CD40 mAb (282). However, we have not observed anti-CD40 to inhibit growth, either in this system, or using murine lymphoma lines (231). We believe such discrepancies can at least in part be explained by the use of differing cell lines which no doubt respond differently to anti-CD40 mAb treatment, and also the fact that Funakoshi's group cross-linked their Ab to increase the anti-proliferative signals.

Whilst CC analysis indicates that HD are able to induce CCA and apoptosis in the lymphoma lines studied, the pathway(s) involved in these processes have not been determined, although appear not to involve intracellular calcium flux. Preliminary experiments with the anti-CD40 HD also showed no evidence for increases in tyrosine phosphorylation. However, observations are in-keeping with the notion that dimerisation of Ab can increase their signaling capabilty, and this in turn increases therapeutic potential. Indeed, HD are able to function effectively *in vivo* as demonstrated using tumor xenograft models (chapter 7).

From the work described in this thesis, and from the literature, there is increasing evidence that generation of a transmembrane signal by Ab is important in controlling tumor growth. This notion not only helps explain why Ab such as CD20 are able to

function effectively in the clinic, but may also explain the activity of derivatives such as BsAb, and why those targeting Id are so potent. Cross-linking of target antigen following effector recruitment may function to deliver a negative signal to the tumor, augmenting processes of RCC, and activating mechanisms of immunity (such as T cell reponses). For the future, BsAb designed against signaling molecules on the tumor, may prove most beneficial. Targeting to effector molecules may also be modified, so that rather than engaging cytotoxic trigger molecules, non-modulating antigens capable of sustained cross-linking may be preferred. In this way, red blood cells and platelets may be the "effectors" of the future. Cocktails of derivatives, and combination with established clinical practices, such as chemotherapy, may also improve efficacy.

8.2 Future work

The immediate focus of attention would be the observed induction of T cell immunity in the [FcγRI x Id] treated animals. It is becoming increasingly clear that not only can FcγRI enhance the uptake and presentation of antigen by APC, but also mediate effective immune responses against such antigens. Hence, we would initially wish to more closely investigate the mechanisms by which T cells contribute to therapy. Kinetics of the T cell response need to be established, and the relative contribution of both $CD4^+$ and $CD8^+$ cells established. T cells from cured mice could be adoptively transferred to naïve animals to see if they can protect against tumor challenge. Ultimately, we would wish to establish the specificity of the tumor specific CTL, and identify the nature of the antigenic peptide they are recognising. Establishment of tumor specific CTL lines, and elution of peptides from MHC I molecules can contribute to this understanding. We would also wish to establish the nature of the APC involved. Are DC key players, as hypothesised, or are other cells equally or more important ? Indeed, is the tumor itself presenting antigen to CTL ? We would also wish to investigate whether cytokines are important to the response, potentially by RT-PCR techniques, and whether again, the tumor cells are contributing in some manner. The splenic cytokine profile of animals given anti-Id BsAb may reveal clues as to the exact nature of the response, and may contribute to our understanding of the APC involved.

T cell BsAb should be re-examined in view of the findings with the [FcγRI x Id] BsAb, to determine whether similar responses are occuring in these mice. Tracking experiments should be performed to see if derivatives of all specificity can clear tumor in the short-term, and re-challenge experiments conducted to investigate whether these mice are also immune. Whilst complete depletion of T cells is not appropriate, depletion of individual sub-sets may allow us to determine if both $CD4^+$ and $CD8^+$ cells are equally important to the therapeutic response.

As we have suggested signaling to be of critical importance, studies to formally prove this point are of paramount importance. Whilst we have shown anti-Id BsAb capable of inducing intracellular calcium flux, following cross-linking, we would also seek to identify other signaling components. Analysis of PTK activity by PCR, and western blotting would be one such approach. Additionally, we would ideally like to show signaling in the presence of the effector cell, rather than by using a polyclonal Ab. It would also be of importance to determine whether cross-linking in this fashion does indeed lead to apoptosis in the tumor cells. Use of FACS based assays to look for caspase activity could be utilised, as well as performing TUNEL assays on splenocytes taken from mice under various conditions of treatment.

As discussed, production of derivatives targeting antigens such as CD79 α and β may yield a suitable alternative to Id. Obviously, as soon as a murine anti-CD20 becomes available we would aim to produce BsAb to that antigen as well. We would also like to construct BsAb to non-modulating antigens on cells such as platelets, that may be able to provide better cross-linking conditions. This would also allow us to examine more closely the role of the effector antigen in the anti-tumor response.

The relative contribution of the effector antigen could also be addressed more closely, using the FcαR transgenic model. We could initially question whether PMN retargeted through this molecule, display similar antigen restriction in terms of therapeutic outcome. Moreover, we could breed double transgenics (FcγR x FcαR) so as the efficacy of targeting the two receptors could be directly examined in the same mice. Anti-T cell BsAb could also be tested in this system. In this way, we can

directly compare the efficacy of targeting different effector cells to the BCR (eg. T cells and PMN), and different trigger molecules (eg. CD3, FcγRI, FcαR). The outcome of such experiments may direct the future development of BsAb derivatives significantly.

References

1. Taken from the Cancer Research Campaign web site, http://www.crc.org.uk/cancer/cancer_intro.html

2. Multani P.S. Grossbard M.L. (1998) Monoclonal antibody-based therapies for hematological malignancies. J. Clin. Oncol. 16: 3691

3. Kohler G. and Milstein C. (1975) Continuous cultures of fused cells secreting antibody of predefined specificity. Nature 256: 495

4. Glennie M.J. and Johnson P.W.M. (2000) Clinical trials of antibody therapy. Immunol. Today 21: 403

5. Segal D.M. Weiner G.J. and Weiner L.M. (1999) Bispecific antibodies in cancer therapy. Curr. Op. Immunol. 11: 558

6. Burnet F.M. (1970) The concept of immunological surveillance. Progr. Exp. Tum. Res. 13: 1

7. Franks L.M. and Teich N.M. (1991) Introduction to the cellular and molecular biology of cancer, 2nd Edition, Oxford University Press, Oxford, UK.

8. Khanna R. (1998) Tumor surveillance: missing peptides and MHC molecules. Immunol. Cell. Biol. 76: 20

9. Waldmann H. Gilliland L.K. Cobbold S.P. and Hale G. (1999) Immunotherapy. In *Fundamental Immunology*, 4th Edition, (Paul W.E. Ed.), pp.1511, Lippincott-Raven Publishers, Philadelphia, USA

10. Clark M. (2000) Antibody humanization: a case of the emperor's new clothes? Immunol. Today 21: 397

11. Clark M.R. (1997) IgG effector mechanisms. Chem. Immunol. 65: 88

12. Stewart A. and Schwartz R. (1994) Immunoglobulin V regions and the B cell. Blood 83: 717

13. Tarlinton D. (1998) Germinal centres: form and function. Curr. Op. Immunol. 10: 245

14. Goldsby R.A. Kindt T.J. and Osborne B.A. (2000) Kuby: Immunology, 4th Edition, pp.96, W.H. Freeman and Company, New York, USA

15. Stevenson G.T. (1993) Immunotherapy of tumors. In *Clinical aspects of Immunology*, 5th Edition, (Lachmann P.J. Peters K.D. Rosen F.S. and Walport M.J. Eds), pp.1799, Blackwell Scientific Publications, London , UK

16. Hombach J. Tsubata T. Leclerq L. Stappert H. and Reth M. (1990) Molecular components of the B cell antigen receptor of the IgM class. Nature 343: 760

17. Sakaguchi N. Kashiwamura S. Kinotot M. Thalmann P. and Melchers F. (1988) B lymphocyte lineage restricted expression of mb-1, a gene with CD3-like structural properties. EMBO. J. 7: 3457

18. Reth M. (1992) Antigen receptors on B-lymphocytes. Ann. Rev. Immunol. 10: 97

19. Brouns G.S. de Vries E. and Borst J. (1995) Assembly and intracellular transport of the human B cell antigen receptor complex. Intl. Immunol. 7: 359

20. Gold M.R. Matsuuchi L. Kelly R.B. and DeFranco A.L. (1991) Tyrosine phosphorylation of components of the B cell antigen receptors following receptor cross-linking. Proc. Natl. Acad. Sci. USA 88: 3436

21. Reth M. (1989) Antigen receptor tail clue. Nature 338: 383

22. Cambier J.C. (1995) Antigen and Fc Receptor Signaling: The awesome power of the immunoreceptor tyrosine based activation motif (ITAM). J. Immunol. 155: 3281

23. Tedder T.F. Zhou L.J. and Engel P. (1994) The CD19/CD21 signal transduction complex of B-lymphocytes. Immunol. Today 15: 437

24. Fearon D.T. and Carter R.H. (1995) The CD19/CR2/TAPA-1 complex of B-lymphocytes: Linking natural to acquired immunity. Ann. Rev. Immunol. 13: 127

25. Sato S. Miller A.S. Howard M.C. and Tedder T.F. (1997) Regulation of B-lymphocyte development and activation by the CD19/CD21/CD81/Leu 13 complex requires the cytoplasmic domain of CD19. J. Immunol. 159: 3278

26. Clark E.A. (1993) CD22, a B cell-specific receptor, mediates adhesion and signal transduction. J. Immunol. 150: 4715

27. Doody G.M. Justement L.B. Delibrias C.C. Mathews R.J. Lin J. Thomas M.L. and Fearon D.T. (1995) A role in B cell activation for CD22 and the protein tyrosine phosphatase SHP. Science 269: 242

28. O'Rourke L. Tooze R. and Fearon D.T. (1997) Co-receptors of B-lymphocytes. Curr. Op. Immunol. 9: 324

29. O'Keefe T.L. Williams G.T. Batista F.D. and Neuberger M.S. (1999) Deficiency in CD22, a B cell-specific inhibitory receptor, is sufficient to predispose to development of high affinity autoantibodies. J. Exp. Med. 189: 1307

30. Fujimoto M. Bradney A.P. Poe J.C. Steeber D.A. and Tedder T.F. (1999) Modulation of B lymphocyte antigen receptor signal transduction by a CD19/CD22 regulatory loop. Immunity 11: 191

31. Van Kooten C. and Banchereau J. (1996) CD40-CD40 ligand: a multifunctional receptor-ligand pair. Adv. Immunol. 61: 1

32. Cheng G. Cleary A.M. Ye Z.S. Hong D.I. Lederman S. and Baltimore D. (1995) Involvement of CRAF1, a relative of TRAF, in CD40 signaling. Science 267: 1494

33. Kehry M. (1996) CD40-mediated signaling in B-cells: Balancing cell survival, growth and death. J. Immunol. 156: 2345

34. Van Kooten C. and Banchereau J. (1997) Functions of CD40 on B cells, dendritic cells and other cells. Curr. Op. Immunol. 9: 330

35. Van Essen D. Kikutani H. and Gray D. (1995) CD40 ligand-transduced co-stimulation of T cells in the development of helper function. Nature 378: 620

36. French R.R. Chan H.T. Tutt A.L. and Glennie M.J. (1999) CD40 antibody evokes a cytotoxic T-cell response that eradicates lymphoma and bypasses T-cell help. Nat. Med. 5: 548

37. Fanger M.W. Shen L. Graziano R.F. and Guyre P.M. (1989) Cytotoxicity mediated by human Fc receptors for IgG. Immunol. Today 10: 92

38. Bruggemann M. Williams G.T and Bindon C.L (1987) Comparison of the effector functions of human immunoglobulins using a matched set of chimeric antibodies. J. Exp. Med. 166: 1351

39. Dyer M.J.S. Hale G. Hayhoe F.G.J. and Waldman H. (1989) Effects of CAMPATH-1 antibodies in vivo in patients with lymphoid malignancies: influence of antibody isotype. Blood 73: 1431

40. Burton D.R. and Woof J.M. (1992) Human antibody effector function. J. Adv. Immunol. 51: 1

41. Ross G.D. and Medof M.E. (1985) Membrane complement receptors specific for bound fragments of C3. Adv. Immunol. 37: 217

42. Kinoshita T. (1991) Biology of complement: The overture. Immunol. Today 12: 291

43. Esser A.F. (1991) Big MAC attack: Complement proteins cause leaky patches. Immunol. Today 12: 316

44. Morgan P. (1995) Complement regulatory molecules: Application to therapy and transplantation. Immunol. Today 16: 257

45. Juhl H, Helmig F, Baltzer K, Kalthoff H, HenneBruns D, and Krener B. (1997) Frequent expression of complement resistance factors CD46, CD55 and CD59 on gastrointestinal cancer cells limits the therapeutic potential of monoclonal antibody 17-1A. J. Surg. Oncol. 64: 222

46. Hughes M.H. and Cidlowski J. (1996) In *Apoptosis in normal development and cancer*, 1st edition, (Mels Stryer Ed.), pp.30. Taylor and Francis. London, U.K.

47. Kerr J.F.R. Wylie A.H. and Currie A.R. (1972) Apoptosis: A basic biological phenomenon with wide ranging implications in tissue kinetics. Br. J. Can. 26: 239

48. Kerr J.F.R. Winterford C..M. and Harmon B.V. (1994) Apoptosis. Its significance in cancer and cancer therapy. Cancer 73: 2013

49. Umansky S.R. (1996) Apoptosis: Molecular and cellular mechanisms (a review). Mol. Biol. 30: 285

50. Cohen G.H. (1997) Caspases: The executioners of apoptosis. Biochem. J. 326: 1

51. Wylie A.H. (1998) An endonuclease at last. Nature 391: 20

52. Arends M.J. Morris R.G. and Wylie A.H. (1990) Apoptosis: The role of the endonuclease. Am. J. Pathol. 136: 593

53. Fesus L. Thomazy V. and Falus A. (1987) Induction and activation of transglutaminase during programmed cell death. FEBS. 224: 104

54. Cordon-Cardo. C. (1995) Mutations of cell cycle regulators. Biological and clinical implications for human neoplasia. Am. J. Pathol. 147: 545

55. Yamada H. June C.H. Finkelman F. Brunswick M. Ring M.S. Lees A. and Mond J.J. (1993) Persistent calcium elevation correlates with the induction of surface immunoglobulin-mediated B cell DNA synthesis. J. Exp. Med. 177: 1613

56. Elledge R.M. and Lee W.H. (1995) Life and death by p53. Bioessays 17: 923

57. Greenblatt M.S. Benner W.P. Holstein M. and Harris C.C. (1994) Mutations in the p53 tumor suppressor gene: clues to cancer etiology and molecular pathogenesis. Can. Res. 54: 4855

58. Strasser A. (1995) Life and death during lymphocyte development and function. Curr. Op. Immunol. 7: 228

59. Maloney D.G. Grillo-Lopez A.J. White C.A. Bodkin D. Schilder R.J. Neidhart J.A. Janakiraman N. Foon K.A. Liles T-M. Dallaire B.K. Wey K. Royston I. Davis T. and Levy R. (1997) IDEC-C2B8 (rituximab) anti-CD20 monoclonal antibody therapy in patients with relapsed low-grade non-Hodgkin's lymphoma. Blood 90: 2188

60. Osterborg A. Dyer M.J.S. Bunjes D. Pangalis G.A. Bastion Y. Catovsky D. and Mellstedt H. (1997) Phase II multicentre study of human CD52 antibody in previously treated chronic lymphocytic leukemia. J. Clin. Oncol. 15: 1567

61. Brown S.L. Miller R.A. and Levy R. (1989) Anti-idiotype antibody therapy of B-cell lymphoma. Semin. Oncol. 16: 199

62. Vervoordeldonk S.F. Merle P.A. van Leeuwen E.F. van der Schoot C.E. von dem Borne A.E.G.K. and Slaper-Cortenbach C.M. (1994) FcγRII (CD32) on malignant

B cells influences modulation induced by anti-CD19 monoclonal antibody. Blood 90: 1632

63. Glennie M.J. and Stevenson G.T. (1982) Univalent antibodies kill tumor cells in vitro and in vivo. Nature 295: 712

64. Lane A.C. Foroozan S. Glennie M.J. Kowalski-Saunders P. and Stevenson G.T. (1991) Enhanced modulation of antibodies coating guinea pig leukemic cells in vitro and in vivo. J. Immunol. 146: 2461

65. Bonardi M. French R.R. Amlot P. Modena D. and Glennie M.J. (1993) Delivery of saporin to human B cell lymphoma using bispecific antibody – targeting via CD22 but not CD19, CD37 or Immunoglobulin results in efficient killing. Can. Res. 53: 3015

66. Glennie M.J. McBride H.M. Stripe F. Thorpe P.E. Worth A.T. and Stevenson G.T. (1987) Emergence of immunoglobulin variants following treatment of a B-cell leukemia with an immunotoxin composed of anti-idiotype and saporin. J. Exp. Med. 166: 43

67. Yokota T. Milenic D.E. Whitlow M. and Schlom J. (1992) Rapid tumor penetration of a single-chain Fv and comparison to other immunoglobulin forms. Can. Res. 52: 3402

68. Segal D. Qian J. Mezzanzanica D. Garrido M. Titus J. Andrew S. George A. Jost C. Perez P. and Wunderlich J. (1992) Targeting of anti-tumor responses with bispecific antibodies. Immunobiol. 185: 390

69. Qian J-H. Titus J.A. Andrew S.M. Mezzanzanica D. Garrido M.A. Wunderlich J.R. and Segal D.M. (1991) Human peripheral blood lymphocytes targeted with bispecific antibody release cytokines that are essential for inhibiting tumor growth. J. Immunol. 146: 3250

70. Roosnek E. and Lanzavecchia A. (1989) Triggering T-cells by otherwise inert hybrid anti-CD3/ anti-tumor antibodies requires encounter with the specific target cell. J. Exp. Med. 170: 297

71. Milstein C. and Cuello A.C. (1983) Hybrid hybridomas and their use in immunohistochemistry. Nature 305: 537

72. De Lau W.B.M. Heije K. Neefjes J.J. Oosterwegel M. Rozemuller E. and Bast B.E.J.E.G. (1991) Absence of preferential H/L chain association in hybrid hybridomas. J. Immunol. 146: 906

73. Nisonoff A. and Mandy W.J. (1962) Quantitative estimation of the hybridisation of rabbit antibodies. Nature 194: 355

74. Kostelny S.A. Cole M.S. and Tso J.Y. (1992) Formation of a bispecific antibody by the use of leucine zippers. J. Immunol. 148: 1547

75. Glennie M.J. McBride H.M. Worth A.T. and Stevenson. G.T. (1987) Preparation and performance of bispecific F(ab'γ)$_2$ antibody containing thioether-linked Fab'γ fragments. J. Immunol. 139: 2367

76. Kaprovsky B. Titus J.A. Stephany D.A. and Segal D. (1984) Production of target-specific effector cells using hetero-cross-linked aggregates containing anti-target cell and Fcγ receptor antibodies. J. Exp. Med. 160: 1686

77. Holliger P. and Winter G. (1997) Diabodies: small bispecific antibody fragments. Can. Immunol. Immunother. 45: 128

78. Holliger P. Brissinck J. Williams R.L. Thielemans K. and Winter G. (1996) Specific killing of lymphoma cells by cytotoxic T-cells mediated by a bispecific diabody. Prot. Eng. 9: 299

79. Coloma M.J. and Morrison S.L. (1997) Design and production of novel tetravalent bispecific antibodies. Nat. Biotechnol. 15: 159

80. Weiner G.J. Kostelny S.A. Hillstrom J.R. Cole M.S. Link B.K. Wang S.L. and Tso J.Y. (1994) The role of T-cell activation in anti-CD3 x anti-tumor bispecific antibody therapy. J. Immunol. 152: 2385

81. Brissinck J. Demanet C. Moser M. Leo O. and Thielemans K. (1991) Treatment of mice bearing BCL_1 lymphoma with bispecific antibodies. J. Immunol. 147: 4019

82. Simister M. Israel E. Alhouse J. and Story C. (1997) New functions of the MHC-class I related Fc receptor, FcRn. Biochem. Soc. Trans. 25: 481

83. Weiner G.J. and De Gast G. (1995) Bispecific monoclonal antibody therapy of B-cell malignancy. Leukemia and Lymph. 16: 199

84. Alegre M. Vandenabeele P. Flamand V. Moser M. Leo O. Abramowicz D. Urbain J. Fiers W. and Glodman M. (1990) Hypothermia and hypoglycemia induced by anti-CD3 monoclonal antibody in mice – role of TNF. JNCI. 79: 1393

85. Urba W.J. Ewel C. Kopp W. Smith J.W. Steis R.J. Ashwell J.D. Creekmore S.P. Rossio J. Sznol M. Sharfman W. Fento R. Janik J. Watson T. Beveridge J. and Longo D.L. (1992) Anti-CD3 monoclonal antibody treatment of patients with CD3 negative tumors – a phase IA/B study. Can. Res. 52: 2394

86. De Gast G.C. van de Winkel J.G.J. and Bast B.E.J.E.G. (1997) Clinical perspectives of bispecific antibodies in cancer. Can. Immunol. Immunother. 45: 121

87. Chen L. Linsley P.S. and Hellstrom K.E. (1993) Costimulation of T cells for tumor immunity. Immunol. Today 14: 483

88. Staerz U.D. Kanagawa O. and Bevan M.J. (1985) Hybrid antibodies can target sites for attack by T cells. Nature 314: 628

89. Perez P. Hoffman R.W. Shaw S. Bluestone J.A. and Segal D.M. (1985) Specific targeting of cytotoxic T cells by anti-T3 linked to anti-target cell antibody. Nature 316: 354

90. Klein S.C. van der Burg S.H. Boer L.H. Melief C.J.M. Kast W.M. de Gast B. and Bast E.J.E.G. (1997) Targeting of cytotoxic T cells against leukemic B cells by bispecific antibody (anti-CD3 x anti-CD19) does not distract the T cell away from its primary target. J. Immunol. 159: 5545

91. Qian D. and Weiss A. (1997) T cell antigen receptor signal transduction. Curr. Op. Cell. Biol. 9: 205

92. Van Leeuwen J.E.M. and Samelson L.E. (1999) T cell antigen-receptor signal transduction. Curr. Op. Immunol. 11: 242

93. June C.H. Ledbetter J.A. Linsley P.S. and Thompson C.B. (1990) Role of the CD28 receptor in T-cell activation. Immunol. Today 11: 211

94. Watts T. and DeBenedette M.A. (1999) T cell co-stimulatory molecules other than CD28. Curr. Op. Immunol. 11: 286

95. Lenschow D.J. Walunas T.L. and Bluestone J.A. (1996) CD28/B7 system of T cell costimulation. Ann. Rev. Immunol. 14: 233

96. Thompson C.B. and Alison J.P. (1997) The emerging role of CTLA-4 as an immune attenuator. Immunity 7: 445

97. Chen L. Ashe S. Brady W.A. Hellstrom I. Hellstrom K. E. Ledbetter J.A. McGowan P. and Linsley P.S. (1992) Co-stimulation of anti-tumor immunity by the B7 counter-receptor for the T lymphocyte molecules CD28 and CTLA-4.v Cell 71: 1093

98. Gerstmayer B. Hoffman M. Altenschmidt U. and Wels W. (1997) Costimulation of T-cell proliferation by a chimeric B7-antibody fusion protein Can. Immunol. Immunother. 45: 156

99. Freeman G.J. Freedman A.S. Segil J.M. Lee G. Whitman J.F. and Nadler L.M. (1989) B7, a new member of the Ig superfamily with unique expression on activated and neoplastic B cells. J. Immunol. 143: 2714

100. Pohl C. Denfeld R. Renner C. Jung W. Bohlen H. Sahlin U. Hombach A. van Lier R. Schwonzen M. Diehl V. and Pfreundschuh M. (1993) CD30 antigen specific targeting and activation of T cells via murine bispecific monoclonal antibodies against CD3 and CD28: Potential use for the treatment of Hodgkin's lymphoma. Int. J. Can. 54: 820

101. Mezzanzanica D. Garrido M. Neblock D.S. Daddona P.E. Andrew S.M. Zurawski V.R. Segal D. and Wunderlich J.R. (1991) Human T-lymphocytes targeted against an established human ovarian carcinoma with a bispecific $F(ab')_2$ antibody prolong host survival in a murine xenograft model. Can. Res. 451: 5716

102. Jung G. Ledbetter J.A. and Muller-Ebhard H.J. (1987) Induction of cytotoxicity in resting human T lymphocytes bound to tumor cells by antibody heteroconjugates. Proc. Natl. Acad. Sci. USA. 84: 4611

103. Renner C. Jung W. Sahin U. Denfeld R. Pohl C. Trumper L. Hartman F. Diehl V. van Lier R. and Pfreundschuh M. (1994) Cure of xenografted human tumors by bispecific monoclonal antibodies and human T cells. Science 264: 833

104. Nitta T. Yagita H. Azuma T. Sato K. and Okumura K. (1989) Bispecific $F(ab')_2$ monomer prepared with anti-CD3 and anti-tumor monoclonal antibodies is most potent in induction of cytolysis of human T cells. Eur. J. Immunol. 19: 1437

105. Demanet C. Brissinck J. Leo O. Moser M. and Thielemans K. (1994) Role of T-cell subsets in the bispecific antibody (anti-idiotype x anti-CD3) treatment of the BCL_1 lymphoma. Can. Res. 54: 2973

106. Ohmi Y. Shiku H. and Nishimura T. (1999) Tumor-specific targeting of T helper type 1 (Th1) cells by anti-CD3 x anti-c-ErbB-2 bispecific antibody. Can. Immunol. Immunother. 48: 456

107. Tutt A.L. Reid R. Wilkins B.S. and Glennie M.J. (1995) Activation and preferential expansion of rat cytotoxic (CD8) T cells in vitro and in vivo with a bispecific (anti-TCRα/β x anti-CD2) $F(ab')_2$ antibody. J. Immunol. 155: 2960

108. Woolridge J.E. Dahle C.E. and Weiner G. (1997) T-cell activation induced by anti-CD3 x anti-B cell lymphoma monoclonal antibody is enhanced by pre-treatment of lymphoma cells with soluble CD40 ligand. Can. Immunol. Immunother. 45: 174

109. Tutt A. Greenman J. Stevenson G.T. and Glennie M.J. (1991) Trispecific $F(ab')_3$ antibody derivatives for redirecting unprimed cytotoxic T cells. Eur. J. Immunol. 21: 1351

110. Tutt A. Stevenson G.T. and Glennie M.J. (1991) Trispecific F(ab')3 derivatives which utilise cooperative signaling via the TCR/CD3 complex and CD2 to activate and redirect cytotoxic T cells. J. Immunol. 147: 60

111. Raso V. and Griffin T. (1981) Hybrid antibodies with dual specificity for the delivery of ricin to immunoglobulin-bearing target cells. Can. Res. 41: 2073

112. Bonardi M.A. Bell A. French R.R. Gromo G. Hamblin T. Modena D. Tutt A.L. and Glennie M.J. (1992) Initial experience in treating human lymphoma with a combination of bispecific antibody and saporin. Int. J. Can. (suppl). 7: 73

113. Stevenson G.T. (1997) Chemical engineering at the antibody hinge. Chem. Immunol. 48: 126

114. Glennie M.J. Brennand D.M. Bryden F. McBride H.M. Stirpe F. Worth A.T. and Stevenson G.T. (1988) Bispecific F(ab'γ)$_2$ antibody for the delivery of saporin in the treatment of lymphoma. J. Immunol. 141: 3662

115. French R.R. Courtenay A.E. Ingamells S. Stevenson G.T. and Glennie M.J. (1991) Co-operative mixtures of bispecific F(ab')$_2$ antibodies for delivering saporin to lymphoma in vitro and in vivo. Can. Res. 51: 2353

116. French R.R. Penney C.A. Browning A.C. Stirpe F. George A.J. and Glennie M.J. (1995) Delivery of the ribosome inactivating protein, gelonin, to lymphoma cells via CD22 and CD38 using bispecific antibodies. Br. J. Can. 71: 986

117. Brambell F.W.R. Hemmings W.A. and Morris I.G. (1964) A theoretical model of gamma-globulin catabolism. Nature 203: 1352

118. Junghans R.P. and Anderson C.L. (1996) The protection receptor for IgG catabolism is the β2-microglobulin-containing neonatal intestinal transport receptor. Proc. Natl. Acad. Sci. USA. 93: 5512

119. Israel E.J. Taylor S. Wu Z. Mizoguchi E. Blumberg R.S. Bhan A. and Simister N.E. (1997) Expression of the neonatal Fc receptor, FcRn, on human intestinal epithelial cells. Immunology 92: 69

120. Ghetie V. Hubbard J.G. Kim J-K. Tsen M-F. Lee Y. and Ward S.E. (1996) Abnormally short serum half-lives of IgG in β2-microglobulin-deficient mice. Eur. J. Immunol. 26: 690

121. Mostov K.E. Friedlander M. and Blobel G. (1984) The receptor for transepithelial transport of IgA and IgM contains multiple immunoglobulin-like domains. Nature 308: 37

122. Kerr M.A. (1990) The structure and function of human IgA. Biochem. J. 271: 285

123. Mostov K.E. (1994) Transepithelial transport of immunoglobulins. Ann. Rev. Immunol. 12: 63

124. De Wit T.P.M. Morton H.C. Capel P.J.A. and van de Winkel J.G.J. (1995) Structure of the gene for the human myeloid IgA Fc receptor (CD89). J. Immunol. 155: 1203

125. Monteiro R.C. Cooper M.D. and Kubagawa H. (1992) Molecular heterogeneity of Fcα receptors detected by receptor-specific monoclonal antibodies. J. Immunol. 148: 1764

126. Abu-Ghazaleh R.I. Fujisawa T. Mestecky J. Kyle R.A. and Gleich G.J. (1989) IgA-induced eosinophil degranulation. J. Immunol. 142: 2393

127. Morton H.C. Van den Herik-Oudijk I.E. Voeebels P. Snijders A. Verhoeven A.J. Capel P.J.A. and van de Winkel J.G.J. (1995) Functional association between the human myeloid immunoglobulin-A Fc receptor (CD89) and FcR γ-chain: Molecular basis for CD89/ FcR γ-chain association. J. Biol. Chem. 270: 29781

128. Coico R.F. Tamma S.L. Bessler M. Wei C.F. and Thorbecke G.J. (1990) IgD-receptor-positive human T lymphocytes. I. Modulation of receptor expression by oligomeric IgD and lymphokines. J. Immunol. 145: 3556

129. Daeron M. (1997) Fc receptor biology. Ann. Rev. Immunol. 15: 203

130. Benhamou M. and Siraganian R.P. (1992) Protein-tyrosine phosphorylation: An essential component of FcεRI signaling. Immunol. Today 13: 195

131. Conrad D.H. (1998) Structure and function of CD23. In *The immunoglobulin receptors and their physiological and pathological roles in immunity*, (Van de Winkel J.G.J. and Hogarth P.M. Eds.), pp. 195, Kluwer Academic Publishers, UK

132. Ohno T. Kubagawa H. Sanders S. and Cooper M.D. (1990) Biochemical nature of an Fcμ receptor on human B-lineage cells. J. Exp. Med. 172: 1165

133. Shibuya A. Sakamoto N. Shimizu Y. Shibuya K. Osawa M. Hiroyama T. Eyre H.J. Sutherland T.R. Endo Y. Fujita T. Miyabayashi T. Sakano S. Tsuji T.

Nakayama E. Phillips J.H. Lanier L.L. and Nakauchi H. (2000) Fcα/μ receptor mediates endocytosis of IgM-coated microbes. Nat. Immunol. 5: 441

134. Berken A. and Benacerraf B. (1965) Properties of antibodies cytophilic for macrophages. J. Exp. Med. 123: 119

135. Anderson C.L. and Abraham G.N. (1980) Characterisation of the Fc receptor for IgG on a human macrophage cell line U937. J. Immunol. 125: 2735

136. Anderson C.L. (1982) Isolation of the receptor for IgG from human monocyte cell line (U937) and from human peripheral blood monocytes. J. Exp. Med. 156: 1794

137. Qiu W.Q. de Bruin D. Brownstein B.H. Pearse R. and Ravetch J.V. (1990) Organisation of the human and mouse low-affinity FcγR genes: Duplication and recombination. Science 248: 732

138. Deo Y.M. Graziano R.F. Repp. R. and van de Winkel J.G.J. (1997) Clinical significance of IgG Fc receptors and Fcγ receptor-directed immunotherapies. Immunol. Today 18: 127

139. Unkeless J.C. Scigliano E. and Freedman V.H. (1988) Structure and function of human and murine receptors for IgG. Ann. Rev. Immunol. 6: 251

140. Gosselin E.J. Wardwell K. Gesselin D.R. Alter N. Fisher J.L. and Guyre P.M. (1992) Enhanced antigen presentation using human FcγR (monocyte/ macrophage)-specific immunogens. J. Immunol. 149: 3477

141. Porges A.J. Redecha P.B. Doebele R. Pan L.C. Salmon J.E. and Kimberly R.P. (1992) Novel FcγRI family gene products in human mononuclear cells. J. Clin. Invest. 90: 2102

142. Van de Winkel J.G.J. Ernst L.K. Anderson C.L. and Chiu I-M. (1991) Gene organisation of the human high affinity receptor for IgG, FcγRI (CD64). J. Biol. Chem. 266: 13449

143. Guyre P.M. Graziano R.F. Vance B.A. Morganelli P.M. and Fanger M.W. (1989) Monoclonal antibodies that bind distinct epitopes on FcγRI are able to trigger receptor function. J. Immunol. 143: 1650

144. Erbe D. Collins J.E. Shen L. Graziano R.F. and Fanger M.W. (1990) The effect of cytokines on the expression and function of Fc receptors for IgG on human myeloid cells. Mol. Immunol. 27: 57

145. Valerius T. Repp R. de Wit T.P.M. Berthold S. Platzer E. Kalden J.R. Gramatzki M. and van de Winkel J.G.J. (1993) Involvement of the high-affinity receptor for IgG (FcγRI; CD64) in enhanced tumor cell cytotoxicity of neutrophils during granulocyte colony-stimulating factor therapy. Blood 82: 931

146. Gosselin E.J. Brown M.F. Anderson C.L. Zipf T.F. and Guyre P.M. (1990) The monoclonal antibody 41H16 detects the leu 4 responder form of human FcγRII. J. Immunol. 144: 1817

147. Brooks D.G. Qiu W.Q. Luster A.D. and Ravetch J.V. (1989) Structure and expression of human IgG FcγRII (CD32): Functional heterogeneity is encoded by the alternatively spliced products of multiple genes. J. Exp. Med. 170: 1369

148. Stuart S.G Simister N.E Clarkson S.B Kacinski B.M. Shapiro M. and Mellman I. (1989) Human IgG Fc receptor (hFcRII; CD32) exists as multiple isoforms in macrophages, lymphocytes and IgG-transporting placental epithelium. EMBO J. 8: 3657

149. Anderson C.L. Ryan D.H. Looney R.J. and Leary P.C. (1987) Structural polymorphism of the human monocyte 40 kilodalton Fc receptor for IgG. J. Immunol. 138: 2254

150. Clark M.R. Clarkson S.B. Ory P.A. Stollman N. and Goldstein I.M. (1989) Molecular basis for a polymorphism involving Fc receptor II on human monocytes. J. Immunol. 143: 1731

151. Warmerdam P.A.M. van de Winkel J.G.J. Vlug A. Westerdaal N.A.C. and Capel P.J.A. (1991) A single amino acid in the second Ig-like domain of the human FcγRII is critical for human IgG2 binding. J. Immunol. 147: 1338

152. Van de Winkel J.G.J. and Capel P.A. (1993) Human IgG Fc receptor heterogeneity: Molecular aspects and clinical implications. Immunol. Today 14: 215

153. Hibbs M. Selvaraj P. Carpen O. Springer T. Kuster H. Jouvin M. and Kinet J. (1989) Mechanisms for regulating expression of a membrane isoform of FcγRIII (CD16). Science 246: 1608

154. Anderson P. Caliguira M. O'Brien C. Manley T. Ritz J. and Sahlossman S.F. (1990) FcγRIII (CD16) is included in the ζ NK receptor complex expressed by human natural killer cells. Proc. Natl. Acad. Sci. USA. 87: 2274

155. Huizinga T.W.J. van der Schoot E. Jost C. Klaassen R. Kleijer M. von dem Borne A.E.G. Roos D. and Tetteroo P.A.T. (1988) The PI-linked receptor FcγRIII is released on stimulation of neutrophils. Nature 333: 667

156. Huizinga T.W.J. Dolman K.M. van der Linden J.M. Kleijer M. Nuijens J.H. von dem Borne A.E.G. and Roos D. (1990) Phosphatidylinositol linked FcγRIII mediates exocytosis of neutrophil granule proteins, but does not mediate initiation of the respiratory burst. J. Immunol. 144: 1432

157. Kimberly R. Ahlstorm J. Click M. and Edberg J. (1990) The GPI-linked FcγRIII on PMN mediates transmembrane signaling events distinct from FcγRII. J. Exp. Med. 171: 1239

158. Salmon D. Kapur S. and Kimberly R. (1987) Opsonin independent ligation of FcγR – the 3G8 bearing receptors on neutrophils mediate the phagocytosis of concavalin A treated erythrocytes and non-opsonised escherichia-coli. J. Exp. Med. 166: 1798

159. Salmon J.E. Brogle N.L. Edberg J.C. and Kimberly R.P. (1991) FcγRIII induces actin polymerisation in human neutrophils and primes phagocytosis mediated by FcγRII. J. Immunol. 146: 997

160. Galon J. Gauchat J.F. Mazieres N. Spagnoli R. Storkus W. Lotze M. Bonnefoy J.Y. Fridman W.H. and Sautes C. (1996) Soluble Fcγ receptor type III (CD16)

triggers cell activation through interaction with complement receptors. J. Immunol. 157: 1184

161. Kurosaki T. and Ravetch J.V. (1989) A single amino acid in the glycosyl phosphatidylinositol attachment domain determines the membrane topology of FcγRIII. Nature 342: 805

162. Salmon J.E. Edberg J.C. and Kimberly R.P. (1990) Fcγ receptor III on human neutrophils: Allelic variants have functionally distinct capacities. J. Clin. Invest. 85: 1287

163. Ory P.A. Clark M.R. Kwoh E.E. Clarkson S.B. and Goldstein I.M. (1989) Sequences of complementary DNAs that encode the NA1 and NA2 forms of FcγRIII on human neutrophils. J. Clin. Invest. 84: 1688

164. Huizinga T.W.J. Kleijer M. Tetteroo P.A.T. Roos D. and von dem Borne A.E.G. (1990) Biallelic neutrophil NA-antigen system is associated with a polymorphism on the phospho-inositol-linked Fcγ receptor III (CD16). Blood 75: 213

165. Fridman W.H. Teillaud J-L. Bouchard C. Teillaud C. Astier A. Tartour E. Galon J. Mathiot C. and Sautes C. (1993) Soluble Fcγ receptors. J. Leuk. Biol. 54: 504

166. Indik Z.K. Park J-G. Hunter S. and Schreiber A.D. (1995) The molecular dissection of FcγR mediated phagocytosis. Blood 86: 4389

167. Sanchez-Mejorada G. and Rosales C. (1998) Signal transduction by Fc receptors. J. Leuk. Biol. 63: 521

168. Van den Herik-Oudijk I.E. Ter Bekke M.W.H. Tempelman M.J. Capel P.J.A. and van de Winkel J.G.J. (1995) Functional differences between two Fc receptor ITAM signaling motifs. Blood 86: 3302

169. Van de Winkel J.G.J. and Anderson C.L. (1991) Biology of human immunoglobulin G Fc receptors. J. Leuk. Biol. 49: 511

170. Shen L. Graziano R.F. and Fanger M.W. (1989) The functional properties of Fcγ RI, II, and III on myeloid cells: a comparative study of killing of erythrocytes and tumor cells mediated through the different Fc receptors. Mol. Immunol. 26: 959

171. Graziano R.F. Looney R.J. Shen L. and Fanger M.W. (1989) Fcγ receptor-mediated killing by eosinophils. J. Immunol. 142: 230

172. Shen L. Guyre P.M. and Fanger M.W. (1987) Polymorphonuclear leukocyte fubction triggered through the high affinity Fc receptor for monomeric IgG. J. Immunol. 139: 534

173. Mitchel M.A. Huang M-M. Chien P. Indik Z.K. Pan X.Q. and Schreiber A.D. (1994) Substitution and deletion in the cytoplasmic domain of the phagocytic receptor FcγRIIA: effect on receptor tyrosine phosphorylation and phagocytosis. Blood 84: 1753

174. Indik Z.K. Pan X.Q. Huang M.M. McKenzie S.E. Levinson A.I. and Schreiber A.D. (1994) Insertion of cytoplasmic tyrosine sequences into the nonphagocytic receptor FcγRIIB establishes phagocytic function. Blood 83: 2072

175. IndikZ.K. Hunter S. Huang H-M. Pan X.Q. Chien P. Kelly C. Levinson A.I. Kimberly R.P. and Schreiber A.D. (1994) The high affinity Fcγ receptor (CD64) induces phagocytosis in the absence of its cytoplasmic domain: The γ subunit of FcγRIIIA imparts phagocytic function to FcγRI. Exp. Hematol. 22: 599

176. Kwiatkowska K. and Sobota A. (1999) Signaling pathways in phagocytosis. Bioessays 21: 422

177. Munn D.H. McBride M. and Cheung N.K. (1991) Role of low-affinity Fc receptors in antibody-dependent tumor cell phagocytosis by human-monocyte derived macrophages. Can. Res. 51: 1117

178. Fanger N.A. Wardwell K. Shen L. Tedder T.F. and Guyre P.M. (1996) Type I (CD64) and type II (CD32) Fcγ receptor-mediated phagocytosis by human blood dendritic cells. J. Immunol. 157: 541

179. Liu C. Goldstein J. Graziano R.F. He J. O'Shea J.K. Deo Y. and Guyre P.M. (1996) FcγRI-targeted fusion proteins result in efficient presentation by human monocytes of antigenic and antagonistic T cell epitopes. J. Clin. Invest. 98: 2001

180. Van Vugt M.J. Kleijmeer M.J. Keler T. Zeelenberg I. van Dijk M.A. Geuze H.J. and van de Winkel J.G.J. (1999) The FcγRIa ligand binding chain triggers MHC class II antigen presentation independently of its associated FcR γ-chain. Blood 94: 808

181. Rouzer C.A. Scott W.A. Hamil A.L. and Cohn Z.A. (1980) Dynamics of leukotriene C production by macrophages. J. Exp. Med. 152: 1236

182. Rouzer C.A. Scott W.A. Kempe J. and Cohn Z.A. (1980) Prostaglandin synthesis by macrophages requires specific receptor-ligand interaction. Proc. Natl. Acad. Sci. USA. 77: 4729

183. Willis H.E. Browder B. Feister A.J. Mohanakumar T. and Ruddy S. (1988) Monoclonal antibody to human IgG Fc receptors. J. Immunol. 140: 234

184. Simms H.H. gaither T.A. Fries L.F. and Frank M.M. (1991) Monokines released during short term Fcγ receptor phagocytosis up-regulate polymorhonuclear leukocytes and monocyte-phagocyte function. J. Immunol. 147: 265

185. Krutmann J. Kirnbauer R. Kock A. Schwarz T. Schopf E. May L.T. Sehgal P.B. and Luger T.A. (1990) Cross-linking Fc receptors on monocytes triggers IL-6 production. J. Immunol. 145: 1337

186. Debets J.M.H. van de Winkel J.G.J. Ceuppens J.L. Dieteren I.E.M. and Burman W.A. (1990) Cross-linking of both FcγRI and FcγRII induces secretion of TNF by human monocytes, requiring high affinity Fc-Fcγ receptor interactions. J. Immunol. 144: 2099

187. Ericson S.G. Zhao Y. Gao H. Miller K.L. Gibson L.F. Lynch J.P. and Landreth K.S. (1998) IL-6 production by human neutrophils after Fc-receptor cross-linking or exposure to G-CSF. Blood 91: 2099

188. Tax W.J.M. Tamboer W.P.M. Jacobs C.W.M. Frenken L.A.M. and Koene R.A.P. (1997) role of polymporphic Fc receptor FcγRIIA in cytokine release and adverse affects of murine IgG1 and anti-CD3/ T cell receptor antibody (WT31). Transplantation 63: 106

189. Sulica A. Metes D. Gherman M. Whiteside T.L. and Herberman R.B. (1996) Divergent effects of FcγRIIIa ligands on the functional activities of human natural killer cells in vitro. Eur. J. Immunol. 26: 1199

190. Muta T. kurosaki T. Misulovin Z. Sanchez M. Nussenzweig M.C. and Ravetch J.V. (1994) A 13-amino-acid motif in the cytoplasmic domain of FcγRIIB modulates B-cell receptor signalling. Nature 368: 70

191. D'Ambrosio D. Hippen K.L. Minskoff S.A. Mellman I. Pani G.Siminovitch K.A. and Cambier J.C. (1995) Recruitment and activation PTP1C in negative regulation of antigen receptor signaling by FcγRIIB1. Science 268: 293

192. Chacko G.W. Tridandapani S. Damen J. Liu L. Krystal G. and Coggeshall K.M. (1996) Negative signaling in B-lymphocytes induces tyrosine phosphorylation of the 145 kDa inositol polyphosphate 5-phosphatase, SHIP. J. Immunol. 157: 2234

193. Coggeshall K.M. (1998) Inhibitory signaling by B cell FcγRIIb. Curr. Op. Immunol. 10: 306

194. Hippen K.L. Buhl A.M. D'Ambrosio D. Nakamura K. Persin C. and Cambier J.C. (1997) FcγRIIB1 inhibition of BCR-mediated phosphoinositide hydrolysis and Ca^{2+} mobilization is integrated by CD19 dephosphorylation. Immunity 7: 49

195. Daeron M. Malbec O. Latour S. Arock M. and Fridman W.H. (1995) Regulation of high-affinity IgE receptor-mediated mast cell activation by murine low-affinity IgG receptors. J. Clin. Invest. 95: 577

196. Clynes R.A. Travers T.L. Presta L.G. and Ravetch J.V. (2000) Inhibitory Fc receptors modulate in vivo cytotoxicity against tumor targets. Nat. Med. 6: 443

197. Salmon D. Kimberley R.P. Gibofsky A. and Fotino M. (1984) Defective mononuclear phagocyte function in systemic lupus erythematosus – dissociation of Fc receptor- ligand binding and internalisation. J. Immunol. 133: 2525

198. Lamour A. Baron D. Soubrane C. Cartran J. Khayat D. Adeler Y. le Goff P. and Youinou P. (1995) Anti-FcγRIII autoantibody is associated with soluble receptor in rheumatoid arthritis and synovial fluid. J. Auto. Immunity. 8: 249

199. Clynes R. and Ravetch J.V. (1995) Cytotoxic antibodies trigger inflammation through Fc receptors. Immunity 3: 21

200. Sylvestre D.L. and Ravetch J.V. (1994) Fc receptors initiate the Arthus reaction: redefining the inflammatory cascade. Science 265: 1095

201. Hazenbos W.L. Gessner J.E. Hofhuis F.M. Kuipers H. Meyer D. Heijnen I.A. Schmidt R.E. Sandor M. Capel P.J. Daeron M. van de Winkel J.G. and Verbeek J.S. (1996) Impaired IgG-dependent anaphylaxis and Arthus reaction in FcγRIII (CD16) deficient mice. Immunity 5: 181

202. Edwards J. Blades S. and Cambridge G. (1997) Restricted expression of CD16 in synovium and dermis: implications for tissue targeting in rheumatoid arthritis. Clin. Exp. Immunol. 108: 401

203. Manger K. Repp R. Spriewald B.M. Rascu A. Geiger A. Wassmuth R. Westerdaal N.A. Wentz B. Manger B. Kalden J.R. and van de Winkel J.G.J. (1998) FcγRIIa polymorphism in caucasian patients with systemic lupus erythematosus: association with clinical symptoms. Arthritis Rheum. 41: 1181

204. Titus J.A. Perez P. Kaubisch A. Garrido M.A. and Segal D.M. (1987) Human K/ natural killer cells targeted with hetero-cross-linked antibodies specifically lyse tumor cells in vitro preventing tumor growth in vivo. J. Immunol. 139: 3153

205. Hombach A. Jung W. Pohl C. Renner C. Sahin U. Schmits R. Wolf J. Kapp U. Diehl V. and Pfreundschuh M. (1993) A CD16/ CD30 bispecific antibody induces lysis of Hodgkin cells by unstimulated natural killer cells in vitro and in vivo. Int. J. Can. 55: 830

206. Van Spriel A.B. van Ojik H.H. and van de Winkel J.G.J. (2000) Immunotherapeutic perspective for bispecific antibodies. Immunol. Today 21: 391

207. Slamon D. Clark G. Wong S. Levin W. Ulrich A. and McGuire W. (1987) Human breast cancer – correlation of relapse and survival with amplification of the HER-2/neu oncogene. Science 235: 177

208. Stovckmeyer B. Valerius T. Repp R. Heijnen I.A.F.M. Buhring H-J. Deo Y.M. Kalden J.R. Gramatzki M. and van de Winkel J.G.J. (1997) Pre-clinical studies with FcγR bispecific antibodies and GCSF primed neutrophils as effector cells against Her-2/neu overexpressing breast cancer. Can. Res. 57: 696

209. Heijnen I.A.F.M. Rijks L.J.M. Schiel A. Stockmeyer B. van Ojik H.H. Dechant M. Valerius T. Keler T. Tutt A. Glennie M.J. van Royen E.A. Capel P.J.A. and van de Winkel J.G.J. (1997) Generation of HER-2/neu specific cytotoxic neutrophils (PMN) in vivo. J. Immunol. 159: 5629

210. Ball E. Guyre P.M. Mills L. Fisher J. Dinces N.B. and Fanger M.W. (1992) Initial trial of bispecific antibody-mediated immunotherapy of CD15-bearing tumors: cytotoxicity of human tumor cells using a bispecific antibody comprised of anti-CD15 (MoAb PM18) and anti-CD64/ FcγRI (MoAb 32). J. Hematotherapy. 1: 85

211. Goldstein J. Graziano R.F. Sundarapandiyan K. Somasundaram C. and Deo Y.M. (1997) Cytolytic and cytostatic properties of an anti-human FcγRI (CD64) x epidermal growth factor bispecific fusion protein. J. Immunol. 158: 872

212. Valerius T. Stockmeyer B. van Spriel A.B. Graziano R.F. van den Herik-Oudijk I.E. Repp. R. Deo Y.E. Lund J. Kalden J.R. Gramatzki M. and van de Winkel J.G.J. (1997) FcαRI (CD89) as a novel trigger molecule for bispecific antibody therapy. Blood 11: 4485

213. Van Spriel A.B. van den Herik-Oudijk I.E. van Sorge N.M. Vile H.A. van Strijp J.A. and van de Winkel J.G.J. (1999) Effective phagocytosis and killing of *Candida albicans* via targeting FcγRI (CD64) or FcαRI (CD89) on neutrophils. J. Infect. Dis. 179: 661

214. Gullberg U. Andersson E. Garwicz D. Lindmark A. and Olsson I. (1997) Biosynthesis, processing and sorting of neutrophil proteins: insight into neutrophil granule development. Eur. J. Haematol. 58: 137

215. Hampton M.B. Kettle A.J. and Winterbourn C.C. (1998) Inside the neutrophil phagosome: oxidants, myeloperoxidase, and bacterial killing. Blood 92: 3007

216. Owen C.A. and Campbell E.J. (1999) The cell biology of leukocyte-mediated proteolysis. J. Leuk. Biol. 65: 137

217. Stvrtinova V. Jakubovsky J. and Hulin I. (1995). *Inflammation and Fever.* Academic Electronic Press.

218. Illidge T.M. Cragg M.S. McBride H.M. French R.R. and Glennie M.J. (1999) The importance of antibody-specificity in determining successful radioimmunotherapy of B-cell lymphoma. Blood 94: 233

219. Slavin S. and Strober S. (1977) Spontaneous murine B cell leukemia. Nature 272: 624

220. Cobb L.M. Glennie M.J. McBride H.M. Breckon G. and Richardson T.C. (1986) Characterisation of a new B cell lymphoma. Br. J. Can. 54: 807

221. Heijnen I.A.F.M. van Vugt M.J. Fanger N.A. Graziano R.F. de Wit T.P.M. Hofhuis F.M.A. Guyre P.M. Capel P.J.A. Verbeek J.S. and van de Winkel J.G.J. (1996) Antigen targeting to myeloid-specific human FcγRI/CD64 triggers enhanced antibody responses in transgenic mice. J. Clin. Invest. 97: 331

222. Elliot T. Glennie M.J. McBride H.M. and Stevenson G.T. (1987) Analysis of the interaction of antibodies with immunoglobulin idiotypes on neoplastic B lymphocytes: implications for immunotherapy. J. Immunol. 138: 981

223. Glennie M.J. Tutt A.L. and Greenman J. (1993) In *Tumor Immunobiology: A practical Approach* (Gallagher G. Rees R.C. Reynolds C.W. Eds.), pp. 225, IRL Press at Oxford University Press, Oxford, U.K.

224. Holborrow E.J. and Johnson G.D. (1967) Immunofluorescence. In Handbook of Experimental Immunology. (Weir D.M. Ed.), pp.580. Blackwell Scientific Publications, Oxford, UK.

225. Nicoletti I. Migliorati G. Pagliacci M.C. Grignani F. and Riccardi C. (1991) A rapid and simple method for measuring thymocyte apoptosis by propidium iodide staining and flow cytometry. J. Immunol. Methods. 139: 271

226. Dive C. Gregory C.D. Phipps D.J. Evans D.L. Milner A.E. and Wyllie A.H. (1992) Analysis and discrimination of necrosis and apoptosis by multiparameter flow cytometry. Bioch. Biophys. Acta. 1133: 275

227. Ghetie M. Podar E. Ilgen A. Gordon B.E. Uhr J. and Vitetta E. (1997) Homodimerisation of tumor-reactive monoclonal antibodies markedly increases their ability to induce growth arrest or apoptosis of tumor cells. Proc. Natl. Acad. Sci. USA. 94: 7509

228. Lammeli U.K. (1970) Cleavage of structural proteins during assembly of the head of bacteriophage T4. Nature 227: 680

229. De Jonge J. Heirman C. de Veerman M. Van Meirvenne S. Moser M. Leo O. and Thielemans K. (1998) In vivo retargeting of T cell effector function by recombinant bispecific single chain Fv (anti-CD3 x anti-idiotype) induces long-term survival in the murine BCL_1 lymphoma model. J. Immunol. 161: 1454

230. George A.J.T. McBride H.M. Glennie M.J. Smith L.J. and Stevenson F.K. (1991) Monoclonal antibodies raised against the idiotype of the murine B cell lymphoma, BCL_1, act primarily with heavy chain determinants. Hybridoma 10: 219

231. Tutt A.L. French R.R. Illidge T.M. Honeychurch J. McBride H.M. Penfold C.A. Fearon D.T. Parkhouse R.M.E. Klaus G.G.B. and Glennie M.J. (1988) Monoclonal antibody therapy of B cell lymphoma: signaling activity on tumor cells appears more important than recruitment of effectors. J. Immunol. 161: 3176

232. Krop I. de Fougerolles A.R. Hardy R.R. Allison M. Schlissel M.S. and Fearon D.T. (1996) Self renewal of B-1 lymphocytes is dependent on CD19. Eur. J. Immunol. 26: 238

233. Torres R.M. Law C.L. Santosargumedo L. Kirkham P.A. Grabstein K. Parkhouse R.M.E. and Clark E.A. (1992) Identification and characterisation of the murine homolog CD22, a lymphocyte-B-restricted adhesion molecule. J. Immunol. 149: 2641

234. Tomonari K. (1988) A rat antibody against a structure functionally related to the mouse T-cell receptor/ T3 complex. Immunogenetics 28: 455

235. Coulie P.G. Uyttenhove C. Wauters P. Manobios N. Klausner R.D. Samelson L.E. and Van Snick J. (1991) Identification of a murine monoclonal antibody specific for an allotypic determinant on mouse CD3. Eur. J. Immunol. 21: 1703

236. Demanet C. Brissinck J. De Jonge J. and Thielemans K. (1996) Bispecific antibody-mediated immunotherapy of the BCL_1 lymphoma: increased efficacy with multiple injections and CD28 induced co-stimulation. Blood 87: 4390

237. Stevenson G.T. Glennie M.J. Hamblin T.J. Lane A.C. and Stevenson F.K. (1988) Problems and prospects in the use of lymphoma idiotypes as therapeutic agents. Int. J. Can. (suppl.) 3: 9

238. Vitetta V.S. and Uhr J.W. (1994) Monoclonal antibodies as agonists: an expanded role for their use in cancer therapy. Can. Res. 54: 5301

239. Marches R. Racila E. Tucker T.F. Picker L. Mongini P. Hsueh R. Scheuermann R.H. and Uhr J.W. (1996) Tumor dormancy and cell signaling III: role of hyper-cross-linking of IgM, CD19 and CD40 on the induction of cell cycle arrest and apoptosis in B lymphoma cells. Ther. Immunol. 2: 125

240. Midorikawa Y. Yamashita T. and Sendo F. (1990) Modulation of the immune response to transplanted tumors in rats by selective depletion of neutrophils *in vivo* using a monoclonal antibody: abrogation of specific transplantation resistance to chemical carcinogen-induced syngeneic tumors by selective depletion of neutrophils *in vivo*. Can. Res. 50: 6243

241. Hasbold J. Johnson-Leger, C. Atkins C.J. Clark E.A. and Klaus G.G.B. (1994) Properties of mouse CD40: cellular distribution of CD40 and B cell activation by monoclonal anti-mouse CD40 antibodies. Eur. J. Immunol. 24: 1835

242. Repp R. Valerius T. Sendler A. Gramatzki M. Iro H. Kalden J.R. and Platzer E. (1991) Neutrophils express the high affinity receptor for IgG (FcγRI; CD64) after in vivo application of rhG-CSF. Blood 78: 885

243. Gosselin E.J. Wardwell K,. Rigby W. and Guyre P.M. (1993) Induction of MHC-class II on human polymorphonuclear neutrophils by GM-CSF, IFN-γ and IL-3. J. Immunol. 151: 1482

244. Lieschke G.J. and Burgess A.W. (1992) Drug therapy: granulocyte colony-stimulating factor and granulocyte-macrophage colony-stimulating factor (I and II). N. Engl. J. Med. 327: 28

245. Heijnen I.A.F.M. Broekhuizen R. Glennie M.J. and van de Winkel J.G.J. (1997) Phagocytosis and lysis of murine B cell lymphoma by transgenic myeloid effector cells via an FcγRI x MHC class II bispecific. Can. Immunol. Immunother. 45: 166

246. Elsasser D. Valerius T. Repp R. Weiner G.J. Deo Y. Kalden J.R. van de Winkel J.G.J. Stevenson G.T. Glennie M.J. and Gramatzki M. (1996) HLA class II as a potential target antigen on malignant B cells for therapy with bispecific antibodies in combination with granulocyte colony-stimulating factor. Blood 87: 3803

247. Ely P. Wallace P.K. Givan A.L. Graziano R.F. Guyre P.M. and Fanger M.W. (1996) Bispecific-armed, interferon γ-primed macrophage-mediated phagocytosis of malignant Non-Hodgkin's lymphoma. Blood 87: 3813

248. Mourad W. Geha R.S. and Chatila T. (1990) Engagement of major histocompatability complex class-II molecules induces sustained, lymphocyte function associated molecule-1 dependent cell-adhesion. J. Exp. Med. 172: 1513

249. Altomonte J.I. Pucillo C. Damante G. and Maio M. (1993) Cross-linking of HLA class II antigens modulates the release of tumor necrosis factor-α by the EBV-B lymphoblastoid cell line JY. J. Immunol. 151: 5115

250. Matsumoto Y. Saiki I. Murata J. Okuyama H. Tamura M. and Azuma I. (1991) Recombinant human granulocyte colony-stimulating factor inhibits the metastasis of hematogenous and non-hematogenous tumors in mice. Int. J. Can. 49: 444

251. Stoppacciaro A. Melani C. Parenza M. Mastracchio A. Bassi C. Baroni C. Parmiani G. and Colombo M.P. (1993) Regression of an established tumor genetically modified to release granulocyte colony-stimulating factor requires granulocyte-T cell cooperation and T cell produced interferon-γ. J. Exp. Med. 178: 151

252. Bridges S.H. Kruisbeek A.M. and Longo D.L. (1987) Selective in vivo anti-tumor effects of monoclonal anti-I-A antibody on B cell lymphoma. J. Immunol. 139: 4242

253. Cemerlic D. Dadey B. Han T. and Vaickus L. (1991) Cytokine influence on killing of fresh chronic lymphocytic-leukemia cells by human leukocytes. Blood 77: 2707

254. Cochlovius B. Kipriyanou S.M. Stasser M.J. Christ O. Schuhmacher J. Strauss G. Moldenhauer G. and Little M. (2000) Treatment of human B cell lymphoma xenograft with a CD3 x CD19 diabody and T cells. J. Immunol. 165: 888

255. Schoenberger S.P. Toes R.E. van der Voort E.I. Offringa R. and Melief C.J. (1988) T-cell help for cytotoxic T lymphocytes is mediated by CD40-CD40L interactions. Nature 393: 480

256. Grafton G. Goodall M. Gregory C.D. and Gordon J. (1997) Mechanisms of antigen receptor dependent apoptosis of human B lymphoma cells probed with a panel of 27 monoclonal antibodies. Cell. Immunol. 182: 45

257. Cobbold S.P. Martin G. and Waldmann H. (1990) The induction of skingraft tolerance in MHC-mismatched or primed recipients: primed T cells can be

tolerised in the periphery with CD4 and CD8 antibodies. Eur. J. Immunol. 20: 2747

258. Cragg M.S. Zhang L. French R.R. and Glennie M.J. (1999) Analysis of the interaction of monoclonal antibodies with surface IgM on neoplastic B-cells. Br. J. Can. 79: 850

259. Brunswick M. June C.H. Finkelman F.D. Dintzis H.M. Inman J.K. and Mond J.L. (1989) Surface immunoglobulin-mediated B-cell activation in the absence of detectable elevations in intracellular ionized calcium: a model for T-cell-independent B-cell activation. Proc. Natl. Acad. Sci. USA. 86: 6724

260. Holte H. Blomhoff H.K. Beiske K. Funderud S. Torjesen P. Gaudernack G. Stokke T. and Smeland E.B. (1989) Intracellular events associated with inhibition of B cell activation by monoclonal antibodies to HLA class II antigens. Eur. J. Immunol. 19: 1221

261. Klaus G.G. Choi M.S. and Holman M. (1994) Properties of mouse CD40. Ligation of CD40 activates B cells via a Ca (++) dependent, FK506-sensitive pathway. Eur. J. Immunol. 24: 3329

262. Clark E.A. Shu G.L. Luscher B. Draves K.E. Banchereau J. Ledbetter J.A. and Valentine M.A. (1989) Activation of human B cells. Comparison of the signal transduced by IL-4 to four different competence signals. J. Immunol. 143: 3873

263. Albert A.L. Sauter B. and Bhardwaj N. (1998) Dendritic cells acquire antigen from apoptotic cells and induce class I-restricted CTLs. Nature 392: 86

264. Cragg M.S. French R.R. and Glennie M.J. (1999) Signaling antibodies in cancer therapy. Curr. Op. Immunol. 11: 541

265. Cragg M.S. Howatt W.J. Bloodworth L. Anderson V.A. Morgan B.P and Glennie M.J. (2000) Complement mediated cell death is associated with DNA fragmentation in the presence of serum. Cell. Death. Differentiation 7: 28

266. Greenman J.G. Hogg N. Nikoletti S. Slade C. Stevenson G. and Glennie M. (1992) Comparative efficiencies of bispecific $F(ab'\gamma)_2$ and chimeric/human IgG

Ab in recruiting cellular effectors for cytotoxicity via Fcγ receptors. Can. Immunol. Immunother. 34: 361

267. Stevenson G.T. Pindar A. and Slade C.J.(1989) A chimeric antibody with dual Fc regions (*bis*FabFc) prepared by manipulations at the IgG hinge. Anti-Can. Drug. Design. 3: 219

268. Yao X. Flashwinkel H. Reth M. and Scott D.W. (1995) Immunoreceptor tyrosine-based activation motif is required to signal pathways of receptor-mediated growth arrest and apoptosis in murine B-lymphoma. J. Immunol. 155: 652

269. McConkey D. Orrenius S. and Jondal M. (1990) Cellular signaling in programmed cell death (apoptosis). Immunol. Today 11: 120

270. Wolff E.A. Schreiber G..J. Cosand W.L. and Raff H.V. (1993) Monoclonal Ab homodimers: enhanced anti-tumor activity in nude mice. Can. Res. 55: 2560

271. Wolff E.A. Esselstyn J. Maloney G. and Raff H.V. (1992) Human monoclonal Ab homodimers. Effect of valency on in vitro and in vivo antibacterial activity. J Immunol 148: 2469

272. Van Egmond M. Hanneke van Vuuren A.J. and van de Winkel J.G.J. (1999) The human Fc receptor for IgA (FcαRI; CD89) on transgenic peritoneal macrophages triggers phagocytosis and tumor cell lysis. Immunol. Lett. 68: 83

273. Regnault A. Lankar D. Lacabanne V. Rodriguez A. Thery C. Rescigno M. Saito T. Verbeek S. Bonnerot C. Ricciardi-Castagnoli P. and Amigorena S. (1999) FcγR-mediated induction of dendritic cell maturation and MHC class-I restricted antigen presentation after immune complex internalisation. J. Exp. Med. 189: 371

274. Nouri-Shirazi M. Banchereau J. Bell D. Burkeholder S. Kraus E.T. Davoust J. and Palucka K.A. (2000) Dendritic cells capture killed tumor cells and present their antigens to elicit tumor-specific immune responses. J. Immunol. 165: 3797

275. Norbury C.C. Hewlett L.J. Prescott A.R. Shastri N. and Watts C. (1995) Class I MHC presentation of exogenous soluble antigen via macropinocytosis in bone marrow macrophages. Immunity 3: 783

276. Chang K.L. Arber D.A. and Weiss L.M. (1996) CD20: a review. Appl. Immunohistochem. 4: 1

277. Shan D. Ledbetter J.A. and Press O.W. (1998) Apoptosis of malignant human B cells by ligation of CD20 with monoclonal antibodies. Blood 91: 1644

278. Ohsaka A. and Saionji K. (1998) In vivo administration of granulocyte colony-stimulating factor increases the surface expression of sialyl-Lewis(x) in neutrophils on healthy volunteers. Acta Haematol. 100: 187

279. Carter P. Ridgway J. and Zhu Z. (1995) Toward the production of bispecific antibody fragments for clinical applications. J. Hematother. 4: 463

280. Adams G.P. Schier R. McCall A.M. Crawford R.S. Wolf E.J. Weiner L.M. and Marks J.D. (1998) Prolonged in vivo tumor retention of a human diabody targeting the extracellular domain of human HER2/neu. Br. J. Can. 77: 1405

281. Ghetie V. Popov S. Borvak J. Radu C. Matesoi D. Medesan C. Ober R.J. Ward E.S. (1997) Increasing the serum persistance of an IgG fragment by random mutagenesis. Nat. Biotech. 15: 637

282. Funakoshi S. Longo D.L. Beckwith M. Conley D.K. Tsarfaty G. Tsarfaty I. Armitage R.J. Fanslow W.C. Spriggs M.K. and Murphy W.J. (1994) Inhibition of human B cell lymphoma growth by CD40 stimulation. Blood 83: 2787